CLEAN DEVELOPMENT MECHANISM POTENTIAL OF COMPRESSION IGNITION DIESEL ENGINES USING GASEOUS FUELS IN DUAL FUEL MODE

A Thesis

Submitted in Partial Fulfilment of the Requirements for the Award of the Degree of

DOCTOR OF PHILOSOPHY

By

BIBHUTI BHUSAN SAHOO

CENTRE FOR ENERGY
INDIAN INSTITUTE OF TECHNOLOGY GUWAHATI
GUWAHATI-781 039, INDIA

NOVEMBER, 2010

Dedicated to my Parents . . .

Smt. Sukumari Sahoo

and

Shri Rasananda Sahoo

Your lives of faith, family, and farming
sowed the seeds of my future

DECLARATION

I hereby certify that the material presented in this thesis is entirely my own account of my research and contains as its main content work except where otherwise stated, which has not previously been submitted for a degree or diploma at this institute or any tertiary education institution.

Bibhuti Bhusan Sahoo
Centre for Energy
Indian Institute of Technology Guwahati
Guwahati – 781 039, India.

November 2010.

CERTIFICATE

It is certified that the work contained in the thesis entitled **Clean Development Mechanism Potential of Compression Ignition Diesel Engines Using Gaseous Fuels in Dual Fuel Mode** by **Bibhuti Bhusan Sahoo**, a student in the Centre for Energy, Indian Institute of Technology Guwahati, India, for the award of the degree of **Doctor of Philosophy** has been carried out under our supervision and this work has not been submitted elsewhere for the degree.

Dr. U. K. Saha
Associate Professor
Department of Mechanical Engineering
Indian Institute of Technology Guwahati
Guwahati – 781039, India.

Dr. N. Sahoo
Associate Professor
Department of Mechanical Engineering
Indian Institute of Technology Guwahati
Guwahati – 781039, India.

ABSTRACT

The climate change problem results from the concentration of greenhouse gases (GHGs) in the atmosphere. The purpose of the Clean Development Mechanism (CDM) is to promote clean development in developing countries, and is based on the idea of emission reduction 'production'. These reductions are 'produced' and then subtracted against a hypothetical 'baseline' of emissions. The fossil gasoline and diesel petroleum fuels used in internal combustion (IC) engines are one of the contributors to the global environmental degradation for their GHG emissions. Diesel engines contribute on important part of the world's transportation and industrial infrastructure, especially in heavy-duty equipment such as trucks, buses, construction and farm equipments, locomotives, ships etc. In the recent times, there are issues related to their GHG emissions such as, carbon dioxide (CO_2), methane (CH_4), and carbon monoxide (CO). The use of alternative fuels is one of the most effective means of resolving this problem. Gaseous fuels receive more prominence in the domain of alternative fuels because of the possibilities of cleaner combustion. However, they are not suitable for compression ignition (CI) concept diesel engine when used alone due to their low cetane numbers and high auto-ignition temperatures. Hence, the CI engine of the 'dual fuel' approach plays a significant role in the efficient utilization of a wide range of gaseous fuels. During a dual fuel operation, a carbureted air-gas mixture is sucked and compressed like in a conventional diesel engine. The compressed air-gas mixture is fired by a small liquid fuel injection, pilot, which ignites spontaneously at the end of compression process.

Biogas and syngas are the two alternative gaseous fuels examined in the present investigation. In general, Biogas is produced by 'anaerobic digestion' process where the organic materials break down by bacteria under lesser air environments. Since these engines use fossil diesel, even a small amount, have the shortcomings of emitting of air pollutants. Thus, an alternative renewable diesel fuel substitute, bio-diesel, was applied for biogas ignition. The biogas and bio-diesel dual fuel technology is more concerned at the rural need. Syngas, the second studied alternative gaseous fuel, is composed of two diatomic molecules CO and H_2 that provide the building blocks upon which an entire field of fuel science and technology is based. In principle, it can be produced from any hydrocarbon feedstock such as NG, naphtha, residual oil, petroleum coke, coal and biomass. Syngas, used in this study, was simulated by mixing H_2 and CO, two main constituent of syngas compositions. By varying the H_2/CO contents, the simulated composition can represent the range of syngas encountered from different sources.

The review of the earlier work by various researchers have clearly suggested that the engine operating and design parameters, namely load, speed, compression ratio, pilot fuel injection

timing, pilot fuel mass inducted, intake manifold conditions, and type of gaseous fuel, have effects on the performance, combustion and emission characteristics of dual fuel diesel engines. However, the systematic investigations of individual parameters relevant to engine characterization have not been reported exhaustively in the literature. The second law analysis or evaluation of available energy determines the maximum possible performance of a thermodynamic system. In addition, impact of process change in the system in terms of system losses is also assessed. These findings help in reducing the availability loss to improve the performance of the engine in terms of efficiency and power output. However, there were only few literatures accessed on availability analysis of dual fuel engines. Therefore, the present contribution is focused to perform a systematic experimental investigation including the thermodynamic behavior of diesel engine under dual fuel mode.

To accomplish the above problems of diesel engines, few additional components such as gas mixer and gas carburetor were designed, developed and incorporated into the base engine setup for executing the dual fuel operation. Experiments were conducted on a modified engine test unit so as to run biogas and syngas under dual fuel operations. The base diesel engine is a single-cylinder, constant-speed, water-cooled and direct-ignition diesel engine with a rated power of 5.2 kW at 1500 rpm. For an equal power output from each of the diesel and dual fuel engine operation, the performance results were evaluated. This type of comparison approach can decide the feasibility of a dual fuel engine usage in place of a conventional diesel engine. The engine was operated at different load levels ranging from idle (no-load) condition to a maximum of 100% load in steps of 20%. The biogas used in the present investigation was composed of about 48% CH_4 and 42% CO_2 by volume. In this study, the results of the CI engine in dual fuel mode using biogas and varying pilot fuel quality were discussed. Jatropha oil bio-diesel was also utilized as pilot fuel to achieve full diesel substitution. In syngas operation, a total of four different types of syngas fuels were tested in dual fuel mode. The type of syngas fuel was determined by varying volumetric ratio of H_2 and CO content. The volumetric fraction of H_2 content in fuel-gas was varied to 100, 75, 50 and 0% of the total H_2 and CO contained syngas. The dual fuel mode experimental and thermodynamic analysis results obtained were also compared with available literatures. Finally, the CDM potential of biogas and syngas as alternative fuels for use in a CI diesel engine under dual fuel mode was investigated individually. The total carbon concentrations from the tested dual fuel modes were calculated based on ppm emissions per kW hour and compared relative to the diesel mode to check their potential towards CDM.

Keywords:
CDM, Compression ignition, Dual fuel, Pilot ignition, Biogas, Syngas, Bio-diesel, Load, Pilot quality, H_2:CO-ratio, Performance, Efficiency, Combustion, Emission, Availability, Exergy

ACKNOWLEDGEMENTS

A person cannot go through life without the help and guidance from others. One is invariably indebted may be of Physical, Mental, Psychological or Intellectual in nature, knowing or unknowingly. To enlist all of them is not easy. To repay them even in words is beyond my capability. The present work is an imprint of many persons who have made significant contribution to its materialization. It is a pleasure to thank the many people who made this thesis possible.

I have been very fortunate with my supervisors. With recondite honour, I offer my sincerest gratitude to my research supervisors, Dr. Ujjwal K. Saha and Dr. Niranjan Sahoo, Department of Mechanical Engineering, Indian Institute of Technology Guwahati, India, who have supported me throughout my thesis with their patience and knowledge whilst allowing me the room to work in my own way. They wrote a research proposal that allowed me to hit the ground running, which is always a nice way to start. With their enthusiasm, their inspiration, and their great efforts to explain things clearly and simply, they helped to overcome all the hurdles during my research path. They taught me how to question thoughts and express ideas. They also provided refreshing insight, critical questions and an ironic common sense that was exhilarating. Throughout my thesis-writing period, they provided encouragement, sound advice, good teaching, good company, and lots of good ideas. Their valuable time spent in correcting my thesis is also gratefully acknowledged. I would have been lost without them. I would like to cherish, throughout my life, the memory of my association with them as a student.

I wish to express my heartfelt gratitude to Prof. P. Mahanta, Head of Centre for Energy, for providing excellent experimental and computational facilities I have needed to produce and complete my thesis. I appreciate his willingness to discuss technical matters and share his deep insight into engine phenomena. Special thanks must go to him for providing me enough guidance towards the inclusion of 'clean development mechanism' investigation of internal combustion engines in my thesis content. His critical comments on the subject matter and his willingness to answer my queries at all levels are exceptional.

I have had the pleasure of association with members of Doctoral Committee, Prof. S. C. Mishra, Prof. A. Dewan, Dr. V. S. Moholkar and Dr. C. Somayaji with whom I have had many fruitful discussions, academic and otherwise. Their encouragement is greatly acknowledged.

I would like to thank Mr. P. Kalita and Mrs. L. Barbora, Scientific Officer, Centre for Energy whom I used to trouble a lot regarding the financial help for procurement of model materials and other laboratory requirements. They have also provided me a lot of technical comments, suggestions and assistance during my research work. My sincere and special thanks to Mrs. A. Rajbanshi and Mr. D. Huzuri for extending all the necessary help in looking into all official documents during the course of my research work.

An experimental research programme generally poses a lot of hurdles at various stages. In my daily work I have been blessed with friendly and cheerful fellow lab mates who have made

this adventure at Energy Efficiency Laboratory at IIT Guwahati truly a time I will never forget. The outcome of my research work is due to fruitful technical discussion, never-ending support and motivation of my colleagues, Mr. B. K. Debnath and Mr. P. Prusty. They provided technical assistance in configuring the instrumentation used in this research and helped me gather the data. I am extremely thankful to both of them for everything without which the research work would have been incomplete.

I would like to place on record the financial grant offered by DST, New Delhi and CCSTDS, Chennai, which enabled me to attend and present a technical paper in ASME Internal Combustion Engine 2009 Spring Technical Conference at Milwaukee, Wisconsin, USA during 3-6 May, 2009.

The machinists and technicians in the Mechanical Engineering department have assisted for engine problems and fabrication and fitting of the equipments for the dual fuel conversions. Thanks to Mr. N. K. Das, Mr. J. Saikia, Mr. M. Sarma, Mr. D. Khaklary, Mr. M. K. Baishya and Mr. D. Chetri. Many thanks to the 'Biogas Training and Development Center' at the institute and assistance from the staffs, Dr. J. Suhrawardy, Mr. J. Kalita, Mr. U. Guharoy, Ms. D. Yadav, Mr. N. Sharma, Mr. D. Kalita and Mr. G. Das, who have provided the required biogas to complete my biogas related experimental work.

Special thanks to Dr. G. S. Paul, Mrs. M. Sharma, Mr. S. Chatterjee, Mr. B. Buragohain, Mr. R. Patil, Dr. R. Das, Mr. A. Satheesh, Mr. M. Eswaran, Mr. R. P. Chopade, Mr. D. K. Biswal, Mr. R. Das, Mr. H. Sarangi, Mr. B. Nayak, Mr. R. Kumar, and Mr. S. S. Mohapatra with whom I shared a large part of my institute stay as a close friend. I thank all of them for sharing their valuable time, enlivening moments during my stay in and around the institute. I sincerely apologize for any omission in mentioning any individual's name who has helped me directly or indirectly in completing the present work.

The unconstrained patience shown by my family members, to whom I kept on saying that 'I will finish next month' for past one year, throughout the period of my research work is inexpressible and I wish to thank them for their continual love and support. I truly could not ask for better parents. They have given me all the opportunities in the world, the freedom to pursue the ones I desired, and the encouragement to follow through. I feel proud of my wife Bijayini and my sweet little daughter Arriva who provided me sharing and caring support all along. I am blessed to have Bina, Reena and Jharana as sisters; Madhaba and Ambuja as brothers-in-law; and Arpita, Ashirbad and Anubhav as nibling. I am indebted to them for all the sacrifices made to make my effort a success. I express my gratitude to my parents-in-law and in-laws Suni and Dipu who have aided and encouraged me throughout this endeavor.

Last but not least, thanks be to God for my life through all tests in the past four and a half years. You have made my life more bountiful. May your name be exalted, honored, and glorified.

November 2010

Guwahati, INDIA ***Bibhuti Bhusan Sahoo***

CONTENTS

NOMENCLATURE

Abbreviations

A/F	mass air-fuel ratio
ATDC	after top dead centre
BDC	bottom dead centre
BTDC	biogas training and development centre
BHP	brake horse power, (hp)
BSEC	brake specific energy consumption, (kJ/s-kW)
bsfc	brake specific fuel consumption, (kg/BP-hr)
BSU	Bosch smoke unit
BMEP	brake mean effective pressure, (bar)
BP	brake power, (kW)
BTDC	before top dead centre
BTE	brake thermal efficiency, (%)
C	centigrade
CA	crank angle, (degree)
cc	cubic centimetre
CDF	conventional dual fuelling
CDM	clean development mechanism
CER	certified emission reduction
CH_4	methane
CHP	combined heat and power
CI	compression ignition
CN	cetane number
CNG	compressed natural gas
CO	carbon monoxide, (ppm)
CO_2	carbon dioxide, (%)
CR	compression ratio
db	decibel
deg.	Degree
DG	diesel genset
DI	direct injection
EPA	environment protection agency
ET	emission trading
EU	European Union
FD	fossil diesel
GHG	greenhouse gas
GWP	global warming potential
HC	hydrocarbon, (ppm)
HCCI	homogeneous charge compression ignition
HDFI	high-pressure diesel fuel injection
HHV	higher heating value, (MJ/kg)

HRR	heat release rate, (J/deg. CA)
IC	internal combustion
ICE	internal combustion engine
IDI	indirect injection
IMEP	indicated mean effective pressure, (bar)
IP	indicated power, (kW)
IT	injection timing, (deg. CA)
J	Joule
JI	joint implementation
JME	jajoba methyl ester
JOME	jatropha oil methyl ester
K	Kelvin
kW	kilo Watt
kJ	kilo Joule
LFCR	Liquid fuel consumption rate (kg/hr)
LHV	lower heating value, (MJ/kg)
lph	liters per hour
M	mega
min	minute
mm	millimeter
MPRR	maximum pressure rise rate, (bar/deg. CA)
MRPR	maximum rate of pressure rise, (bar/deg. CA)
ms	millisecond
N	Newton
NG	natural gas
NO_x	oxides of nitrogen, (ppm)
Pa	Pascal
PM	particulate matter
ppm	parts per million
PSI	Pound per square inch
REGR	reformed exhaust gas recirculation
rev	revolutions
RHR	rate of heat release, (J/deg. CA)
RME	rape methyl ester
rpm	revolutions per minute
s	second
SEC	specific energy consumption, (kJ/s-kW)
sfc	specific fuel consumption, (kg/BP-hr)
SI	spark ignition
SO_x	oxides of sulphur
TDC	top dead centre
TO	throttle opening
UBHC	unburned hydrocarbon, (ppm)
UNFCCC	United Nations Framework Convention on Climate Change

Notations

$\dot{m}_d$	diesel mass flow rate, (kg/s)
$\dot{m}_g$	gas mass flow rate, (kg/s)
$\dot{m}_{Lf}$	liquid fuel mass flow rate in liquid fuel mode, (kg/s)
$\dot{m}_p$	pilot mass flow rate, (kg/s)
P	cylinder pressure, (bar)
Q_n	apparent net heat-release rate, (J/deg. CA)
V	instantaneous volume of the cylinder, m^3
Z	diesel displacement rate
γ	ratio of specific heats
η_{th}	thermal efficiency, (%)
θ_{IGN}	crank angle at ignition (CA)
θ_{INJ}	crank angle at dynamic injection (CA)
θ_R	ignition delay period (CA)
C_p	specific heat, (kJ/kg-K)
$\dot{m}$	mass flow rate, (kg/hr)
P_0	ambient pressure, (bar)
P_{eg}	exhaust gas pressure out from engine, (bar)
R_{eg}	exhaust gas constant, (kJ/kg-K)
T_0	ambient temperature, (K)
T_1	cooling water inlet temperature, (K)
T_2	cooling water outlet temperature, (K)
T_3	calorimeter water inlet temperature, (K)
T_4	calorimeter water outlet temperature, (K)
T_5	exhaust gas temperature from engine, (K) or, calorimeter exhaust gas inlet temperature, (K)
T_6	calorimeter exhaust gas outlet temperature, (K)

Greek symbols

θ	crank angle
^{o}	degree
η	efficiency
%	percentage
λ	excess air ratio

Subscripts

cw	cooling water
d	diesel
eg	exhaust gas
in	input
im	inlet manifold
g	gas
gn	gas nozzle
gc	gas carburetor
Lf	liquid fuel
p	pilot
w	water

LIST OF FIGURES

LIST OF TABLES

Chapter – 1

INTRODUCTION

Overview

Internal combustion engines are a major consumer of fossil fuels, and combustion of fossil fuels inevitably produces emissions of the greenhouse gas carbon dioxide (CO_2). The compression-ignition (CI) diesel engines, like other fossil fuel-based technologies, contribute to greenhouse gas (GHG) emissions. The stricter emission regulations impel an 'urgent' appeal to reduce emissions from diesel engines. Use of alternative fuels is one of the approaches to improve carbon sequestration from diesel engines. Gaseous fuels receive more prominence in the domain of alternative fuels because of the possibilities of cleaner combustion. The high self-ignition temperature characteristic of gaseous fuels makes its direct use in CI engines difficult, and hence, it can be utilized with the dual fuel approach. During a dual fuel operation, a carbureted gas-air mixture inducts through the inlet manifold and compresses like in a conventional diesel engine. This compressed mixture is then fired by a pilot spray of diesel or diesel-like fuel which provides ignition centers. Aiming to this technology, the present work examines two gaseous fuels viz., biogas and syngas, in a CI diesel engine under dual fuel operation. In addition, the usage of petroleum fossil diesel is minimized in by replacing bio-diesel as pilot ignition source. The dual fuel operations are performed by varying the various engine parameters. Additionally, the thermodynamic energy and exergy analyses are executed for the dual fuel modes. The entire experimental and thermodynamic results of dual fuel modes are analyzed and compared to that of base diesel engine. The 'Clean Development Mechanism' (CDM) allows net global GHG to be reduced at a much lower global cost by financing emission reduction projects in developing countries. Towards this, the CDM potential of the biogas and syngas dual fuel operations is investigated and discussed. In this Chapter, the brief history of CDM, dual fuel concept with benefits, emission regulations for diesel engines, and various alternative fuel options for diesel engines are reviewed. The structure of the present thesis is also outlined at the end.

1.1 Motivation

In the recent times, the significant increase in the carbon dioxide (CO_2) concentration in the atmosphere may cause global warming due to the greenhouse gas (GHG) effect in the coming decades. Carbon dioxide is one of six major GHGs recognized by the *International Panel on Climate Change*. The other five greenhouse gases are, methane (CH_4); nitrous oxide (N_2O); hydrofluorocarbons (HFCs); perfluorocarbons (PFCs); and sulfur hexafluoride (SF). Greenhouse gases do not absorb solar radiation around its wavelength of peak intensity in the visible spectrum, but do absorb the infrared radiation scattered from the earth's surface. Thus, they alter the radiation balance of the earth, and also, contribute to an increase in global atmospheric temperatures due to enhanced absorption of infrared radiation. The consequences of this global warming are thought to include changes in climate patterns, a re-balancing of eco-systems, additional melting of the polar ice-caps and rising sea-levels due to thermal expansion of the oceans (MacLean and Lave, 2003). In this context, the United Nations have started a mitigation process at the 'Earth Summit' in Rio de Janeiro in 1992 with the UN Framework Convention on Climate Change (UNFCCC). The process was later continued by yearly Conference of the Parties sessions starting in 1995. In 1997 at the third such session the Kyoto Protocol to the UNFCCC was signed and/or acceded by a total of 120 countries and ratified by 96 countries representing 37% of the GHG emissions of the Annex I Parties (http://www.unfccc.de/; Hyvarinen, 2000).

The Kyoto Protocol carries legally binding GHG emission targets for the so-called Annex I (to the UNFCCC) parties, or more precisely, Annex B (to the Protocol). These countries are obliged to reduce their overall GHG emission level by at least 5% below 1990 levels during the commitment period 2008–2012. The Kyoto Protocol allows Annex B parties to meet these commitments partly by achieving emission reductions abroad. Because, reducing GHG emissions at an emission source in another country may be cheaper than doing so domestically. There are three cross-border emission reduction mechanisms that Annex B can apply in order to reduce the cost of their commitments: Emissions Trading (ET), Joint Implementation (JI) or Clean Development Mechanism (CDM). As defined in Article 12 of the Protocol, the CDM allows a country with an emission-reduction or emission-limitation commitment for Annex B parties to implement an emission-reduction project in developing countries. Such projects can earn saleable certified emission reduction (CER) credits, each equivalent to one tonne of CO_2, which can be counted towards meeting Kyoto targets.

Internal combustion (IC) engines consume fossil petroleum fuels, and during combustion, they produce the greenhouse gas CO_2 emissions. The CO_2, CH_4 and N_2O GHGs may be converted into global warming potentials (GWP) with units of kg CO_2-equivalent (kg CO_2-e) by using the following conversions: 1 kg CO_2 = 1 kg CO_2-e GWP; 1 kg CH_4 = 21 kg CO_2-e GWP; and 1 kg N_2O = 310 kg CO_2-e GWP (IPCC, 1996). Impact of greenhouse gases from the transport is approximately 20% of the total greenhouse, the use of gasoline fuels in road transport is the most important– 52%, diesel fuels contribute 26% and aircraft–19% (MacLean and Lave, 2003). Diesel technology is a unique combination of energy efficiency, power, reliability, and durability. Diesel engines play a vital role in various important sectors such as, transport, farm and construction equipments, power electric generators, locomotives, river barges and other marine work vessels. However, they are under attack now-a-days due to their emissions of soot and NO_x. Also, they are under scanner for their emissions of GHGs like CO_2 and CH_4. In addition, diesel engines have to meet much stricter tailpipe-emission standards. On October 6, 2003, the National Auto Fuel Policy has been announced, which envisages a phased program for introducing Euro 2–4 emission and fuel regulations by 2010. The implementation schedule of EU emission standards in India is summarized in Table 1.1 (http://www.dieselnet.com/standards/). Table 1.2 shows the USA–EPA and Bharat Stage III non-road emission regulations for diesel engines (less than 8 kW power output).

Table 1.1 Indian Emission Standards Implementation (4-Wheel Vehicles) (http://www.dieselnet.com/standards/)

Standard	Reference	Date	Region
India 2000	Euro 1	2000	Nation wide
Bharat stage II	Euro 2	2001	NCR*, Mumbai, Kolkata, Chennai
		04/2003	NCR*, 10 Cities†
		04/2005	Nationwide
Bharat stage III	Euro 3	04/2005	NCR*, 10 Cities†
		04/2010	Nationwide
Bharat stage IV	Euro 4	04/2010	NCR*, 10 Cities†

* National Capital Region (Delhi)

† Mumbai, Kolkata, Chennai, Bangalore, Hyderabad, Ahmedabad, Pune, Surat, Kanpur and Agra

Table 1.2 Non-road small diesel engine emission regulations (http://www.dieselnet.com/standards/)

Emission regulation	Power (kW)	NO_x + HC (g/kWh)	CO (g/kWh)	Particulates (g/kWh)	Date
USA – EPA (Tier 3)	< 8	7.5	8.0	0.4	2008
Bharat Stage III	< 8	7.5	8.0	0.8	April 2011

During recent years, various techniques have been developed to reduce CO_2 emissions and to improve carbon sequestration of these reciprocating engines. Such approaches include the use of hybrid vehicles, fuel cells and alternative fuels, or adoption of operational modifications. There are pros and cons with respect to each approach but all share the common theme of replacing the fossil fuel. The GHG emissions from diesel engines are due to the use of fossil diesel fuel. Therefore, the reduction, or even complete replacement of diesel usage can solve the problem. This 'Switch mode of fuel' technology specifies the use of 'diesel alternative fuel' in diesel engines. The term 'alternative fuel' is any fuel suggested for use in a vehicle other than petrol or diesel. A more general classification of alternative fuels separating them into three groups: *The first group* includes petroleum fuels with non-petroleum additives (alcohols, ethers, etc.) which are close to traditional petroleum fuels in performance properties; *The second group* includes synthetic liquid fuels with properties close to traditional petroleum fuels but obtained in processing of gaseous, solid, or liquid feedstock (natural gas, coal, oil shales, etc.), particularly in processing natural gas into synthesis gas and then into methanol or hydrocarbons with the so-called GTL (Gas to Liquid) technology; *The third group* includes non-petroleum fuels (alcohols, bio-fuels, biogas, land-fill and sewage gas, natural and associated gases, hydrogen, etc.) which differ significantly from traditional petroleum fuels in physicochemical and performance properties (Lapidus *et al.,* 2005). Table 1.3 shows a selected list of fossil fuels and bio-fuels used in diesel engine transport applications. The present work is related to the reductions of GHG emissions from diesel engines by employing third group of alternative fuels, 'gaseous fuels'. With the development of diesel engines based on gaseous fuel operation, the fossil diesel combustion will be replaced by gaseous fuel combustion either partially or completely. The lower usage of diesel fuel will obviously improve the GHG emissions from diesel engines.

Table 1.3 Approximate compositions and properties of selected fossil fuels and bio-fuels that are used in transport applications (Calais and Sims, 2000)

Fuel	Approximate average formula	Average molecular weight	Approx. C:H ratio	Energy density (MJ/L)	Energy density (MJ/m^3)	CO_2 emissions (g/MJ)
NG	~$CH_{3.85}$	18.2	1:3.85	---	38.2	51.3
LNG	~$CH_{3.85}$	18.2	1:3.85	25.0	---	51.3
CNG	~$CH_{3.85}$	18.2	1:3.85	---	38.2	51.3
LPG	~$C_3H_{7.8}$	49	1:2.6	25.7	---	60.2
Petrol	~$C_{5.4}H_{10.7}$	80	1:2	35.2	---	65.8
Automotive diesel	~$C_{15.2}H_{22.2}$	212	1:1.9	38.6	---	65.8
Methanol	~CH_3OH	32.04	1:4	15.8	---	60.8
Ethanol	~CH_3CH_2OH	46.07	1:3	23.4	---	64.3
RME biodiesel	~$C_{13}H_{29}O$	201	1:2.29	33.3	---	85.0

1.2 Dual Fuel Concept

Gaseous fuels receive more prominence in the domain of alternative fuels because of the possibilities of cleaner combustion. When burnt, it produces virtually no SO_x and relatively little NO_x, the main constituents of acid rain, and substantially less CO_2, a key culprit in the greenhouse debate, than most oil products and coal (Henham and Makkar, 1998; Hill and Douville, 2000). But, gaseous fuels usually have low cetane numbers (CN) and higher auto-ignition temperature as compared to standard diesel oil. These characteristics of fuel-gas make its direct use in CI engines difficult. Hence, the CI engine of the 'dual fuel' type plays an increasingly significant role in the efficient utilization of a wide range of gaseous fuels as alternatives fuels and the reduction of exhaust emissions from transport vehicles (Liu and Karim, 1995). Some researchers have reported that to achieve the required reductions of GHGs, the dual fuel technology must be considered in diesel engines (Stewart *et al.,* 2007). The 'dual fuel' diesel engines are based upon diesel technology. The primary fuel is gaseous fuel but they are designed to operate interchangeably with diesel or diesel like liquid fuel as 'pilot' ignition source. The dual fuel engines are classified broadly into two categories depending on the amounts of utilization of the gaseous and liquid fuel. The most of the dual fuel engines use injection of small amounts of liquid fuel to provide ignition to a lean mixture of gas and air. The bulk of energy comes from the gaseous fuel (also called primary fuel)

components. The second category is associated with addition of some gaseous fuel to air in a fully operational diesel engine for high operational loads.

Diesel engines with appropriate relatively simple conversion are made to operate on dual fuel approach. During this operation, a carbureted gas-air mixture inducts through the inlet manifold and compresses like in a conventional diesel engine. This compressed mixture does not auto-ignite due to lack of good ignition quality of gaseous fuel. Hence, it is fired by a pilot spray of diesel-like fuel that has low self-ignition temperature. The ignition centers formed by the pilot spray lead to the flame propagation through the inducted homogeneous air-gas mixture (Prakash, 2001; Kumar *et al.,* 2003b; Sahoo *et al.,* 2009a). A dual fuel engine uses fuels of different flammability. In case of shortage of gas, this engine can be switched from dual fuel to diesel fuel mode easily. The biggest advantage in the dual fuel method is that it can utilize a small quantity of diesel-like pilot fuel to ignite fuel-gas. Although there is only a small amount of pilot (for example, say, about 5% to 20% of diesel), its burning energy is much higher than the spark ignition energy. This makes the ignition-lag period and even all the burning period shorter than a spark-ignited dual fuel system. Hence, it solves the severe post combustion, high exhaust temperature, and severe heat charge in a gas fuelled CI engine. As a whole, a dual fuel engine as an ideal multi-fuel engine that operates effectively on a wide range of fuels including the flexibility of operating as a conventional diesel engine.

The disadvantage of dual fuel engine is the necessity to have liquid diesel fuel available for ignition (Mansour *et al.,* 2001). Of course, this problem can be avoided by using diesel-like alternative bio-diesel fuels as the pilot ignition source. Some of the important benefits of dual fuelling are as described in the following.

- Existing diesel engines run with cleaner and cheaper gaseous fuels with little or no modification.
- Fuel flexibility and fail safe operation: if gas is interrupted, full diesel operation can be recovered immediately.
- Higher compression ratios, and thus, better thermal efficiency than spark ignition dual fuel operation.
- Very long service intervals of injectors with the diesel ignition system.
- The lean burn combustion of dual fuel diesel engines contributes to reduced misfire and combustion temperature. Therefore, pilot fuel combined with clean gaseous fuel provides lubrication to valves and rings, and hence, longer maintenance service intervals than the diesel mode of operation.
- Reductions of exhaust emissions: specifically, NO_x, CO_2 and particulates.

1.3 Fuel Selection

The world is in need of a sustainable, efficient, carbon-neutral fuel source. Carbon dioxide is released to the atmosphere due to burning of solid waste and wood, and also, in decomposition of organic matter. Methane emissions also result from the decomposition of organic wastes in an oxygen-deprived environment. Hence, efficient energy generation and proper waste management are necessary to maintain living standards and to protect our environment (Mohammadi *et al*., 2006).The 'anaerobic digestion' is a process which limits the emission of CO_2 and CH_4 into the environment since the digestion of these wastes takes place in a closed environment, and the process generated a gas called 'biogas'. As a gaseous fuel, biogas can be used for production of heat and power and it does not affect the net carbon dioxide in the environment. Biogas can be produced from renewable sources such as, cow dung and other animal waste and also from plant matter such as leaves and water hyacinth. It is readily available and affordable for people around the world. The availability of fuel was exploited throughout the UK as well as Germany, particularly during World War II when fuel was scarce. The composition of biogas varies with the source, but usually it has 50–70% CH_4, 25–50 % CO_2, 1–5 % H_2, 0.3–3 % nitrogen (N_2) and traces of hydrogen sulfide (H_2S) (Bedoya *et al.,* 2009). However, the biogas, yielded by different biogas digestion tanks, is of different pressure, specific gravity and specific volume (Jiang *et al*., 1989). As an ICE fuel, biogas has an extremely low volumetric energy density, low flame velocity and lower flammability limits due to its high CO_2 content. When used as SI engine fuel and due to the high self-ignition temperature of biogas, the chances of SI knocks is reduced. This characteristic of biogas makes its direct use in CI engines difficult. However, it can be utilized in a CI engine with the dual fuel approach (Porpatham *et al.,* 2007, 2008; Sudheesh and Mallikarjuna, 2010). It is also suggested by von Mitzlaff (1988) that biogas-diesel dual mode may be applied to conventional direct-injection CI engines with minor modifications.

Hydrogen is a strong contender as an environment friendly fuel for IC engines because burning of this carbon-less gas releases only water vapor into the atmosphere. Further, IC engines are also capable of burning the carbon monoxide gas as it is not contaminated. Syngas is ideally a mixture of H_2 and CO produced by gasifying a solid fuel feedstock (such as coal or biomass). In its simplest form, syngas is composed of two diatomic molecules CO and H_2 that provide the building blocks upon which an entire field of fuel science and technology is based. Over the years, the gaseous mixture of CO and H_2 has had many names depending on how it was formed; producer gas, town gas, water gas, synthesis gas, and

syngas etc. to name a few. In principle, syngas can be produced from any hydrocarbon feedstock such as NG, naphtha, residual oil, petroleum coke, coal and biomass (Spath and Dayton, 2003). Mixtures of H_2 and CO could serve as an alternative spark ignition (SI) fuel due to their high anti-knock behavior (Shudo and Takahashi, 2004; Shudo, 2006). However, addition of H_2 to CO tends to increase combustion temperatures and hence, increases nitric oxide (NO) emissions under stoichiometric SI combustion (Li and Karim, 2005). Hence, the use of H_2 and CO mixtures is more appropriate in lean burn conditions where combustion temperatures are moderated by excess air like in a CI diesel engine. Also, these mixtures could serve in dual fuel mode that operates under CI using a pilot injection of diesel fuel (Boehman and Le Corre, 2008). Again, in their published work, Garnier *et al.* (2005) have suggested the use of syngas in diesel engines with dual fuel mode for mechanical and electrical applications. Various other researchers have tried to explore this environmentally clean and low cost fuel in gas turbines and reciprocating engines to produce electricity.

Although dual fuel engines utilize cleaner primary gaseous fuels, since they use a small amount of fossil diesel for the pilot ignition purpose, have the shortcomings of emitting of air pollutants, such as NO_x and CO_2 (Nakanishi *et al*., 2000; Park *et al.,* 2002). So some diesel like fuel such as, bio-diesel can be used as an alternative energy resource for fuel-gas ignition source. Bio-diesel, any diesel fuel that is derived from biomass or animal fat, is a renewable diesel fuel substitute. Their uses reduce dependence on foreign petroleum fossil fuels, mitigate GHG emissions, reduce air pollution, and produce local jobs (Noguchi *et al*., 1996; Ajav *et al.,* 1998; Kumar *et al*., 2003a; Agarwal, 2007). Some experimental works have shown that bio-diesel and vegetable oils as pilot fuels can improve engine performance (Nwafor, 2000b; Kumar *et al.,* 2001; Selim *et al.,* 2008). Bio-diesel also reported as a possible substitute or extender for conventional diesel because of their similar characteristics (Otera, 1993; Sharma and Singh, 2008).

1.4 Objectives of the Present Investigation

The major objective of this thesis is to explore the concept of reducing greenhouse gas emissions from diesel engines by exploiting gaseous fuels in place of fossil diesel consumption. In this direction, systematic experimental investigations were carried out in a single-cylinder, constant-speed, direct-injection and compression-ignition diesel engine operating biogas/ syngas with diesel/ bio-diesel as pilot ignition source under dual fuel mode. The necessary equipments were designed, fabricated and added to the base diesel engine to

run under dual fuel mode. The dual fuel engine was operated from 0 to 100% load with several variations in the design and operating parameters. The engine mechanical performance was studied on the basis of thermal efficiency, volumetric efficiency, brake specific energy consumption, exhaust gas temperature, maximum diesel substitution rate and gas flow rate. Further, combustion analysis was carried out from various parameters such as cylinder peak pressure, pressure–crank angle diagrams, net heat release rate, maximum rate of pressure rise, and ignition delay. Again, the important emission characteristics were examined by dry concentrations of NO_x, CO, CO_2 and HC. In order to establish the basis for comparison of dual fuel results, a baseline test with 100 % diesel fuel was also conducted.

The concept of 'availability' (also called 'exergy') is introduced by the second law of thermodynamics. The availability of a thermodynamic system is the maximum useful mechanical work that can be produced when the system is brought to thermal, mechanical and chemical equilibrium with its environment through reversible processes. The combination of experimental and thermodynamic investigation will represent a perfect analysis characterization of a new technology. The thermo-mechanical availability analysis of the diesel and dual fuel operations were investigated from their retrieved experimental resulted data. Specifically, the effects of engine operations on all exergy transfer terms, such as fuel chemical exergy, work, cooling water, exhaust gas, exergy efficiency and irreversibility, are explored with the help of both first and second law of thermodynamics. Finally, the all important issue of GHG carbon emissions from the dual fuel operations were analyzed through CDM potential investigation of the alternative biogas and syngas fuels.

In summary, the main objectives of the present investigations reported in the thesis using biogas/ syngas as gaseous fuel in a CI diesel engine under dual fuel mode are as follows:

- Optimization of engine operating and design parameters such as load, pilot fuel quality and gaseous fuel type for minimum emissions and maximum efficiency from the dual fuel operations.
- Maximum replacement of fossil petroleum diesel fuel by employing bio-diesel as pilot ignition in dual fuel mode.
- Energy and Exergy analysis of dual fuel engine operations for a perfect analysis characterization of a new technology.
- CDM potential investigation of gaseous fuels utilized in the CI diesel engine under dual fuel mode of operation.

1.5 Thesis Organization

The first chapter of this volume set the background for the work where the dual fuel concept in compression ignition diesel engines is introduced. The selection of alternative fuels from various categories and their importance of use in the dual fuel concept diesel engines are emphasized. **Chapter 2** provides background concerning the operations of dual fuel diesel engines with various gaseous fuels. The performance of these engines relies more heavily upon the various engine design and operating parameters. The work carried out by previous researchers regarding the effects of these engine parameters on the performance, combustion and emission characteristics of engines are reviewed. The use of bio-diesel even for a pilot fuel is promoted by several researchers. The importance of thermodynamic analysis for the present work is also briefed. **Chapter 3** describes the details of laboratory rig including working principles of various engine instrumentation employed for the engine testing. The experimental procedures along-with experimental data calculation uncertainties are also described. The modified design and fabrication details of dual fuel operations are also discussed in this section. **Chapters 4 and 5** represent the results of biogas dual fuel investigation. The details of experimental work with a complete coverage to performance, combustion and emission characteristics for various dual fuel operations with biogas are presented here. In addition, the thermodynamic analysis which covers both first law and second law of thermodynamics applied to the biogas dual fuel engine operations. Likewise, **Chapters 6 and 7** stand for the outcomes of syngas dual fuel operations. **Chapter 8** represents the authentic of biogas and syngas operations as alternative fuels in diesel engines under dual fuel mode. Finally, a concluding **Chapter 9** summarizes the findings and results of this work and suggests future developments.

Chapter – 2

LITERATURE REVIEW AND SCOPE OF RESEARCH

Overview

Internal combustion engines which consume fossil petroleum fuels for their combustion produce the greenhouse gas emissions like carbon dioxide, methane, nitrous oxide, and other carbon emissions like carbon monoxide. The dual fuel mode approach is one of the methods to reduce diesel engine made green house gas emissions which can also benefits the clean development mechanism. Based on this, two promising gaseous fuels, biogas and syngas have been chosen for this study to assess their potential towards the clean development mechanism. With introducing simple modification to the existing diesel engines, biogas can be used as a gaseous alternative fuel. Again, syngas is a methane based fuel and hence, in addition to diesel engines, this alternative fuel can be used in existing natural gas engines easily. This chapter represents a review of literature on dual fuel diesel engine, the 'gas diesel engine', operation with various available gaseous fuels. More emphasis is given to the related dual fuel operations based on biogas and syngas fuels. It also includes maximum possible replacement of conventional fossil diesel fuel even by using bio-diesel, an alternative bio-fuel, for the pilot purpose in a dual fuel operation. The chapter looks deeply into the effects of engine design and operating parameters on performance, combustion and emission characteristics of dual fuel diesel engines run on gaseous fuels. Different techniques employed to obtain efficient dual fuel operation and reduced emissions by various researchers are described. In this chapter, several dual fuel experiments carried out by various researchers are analyzed from energy and exergy point of view. Basic thermodynamic properties of the systems are determined by energy analysis utilizing main operating conditions. Exergy destructions within the dual fuel system and exergy losses to environment are investigated to determine thermodynamic inefficiencies in the system and to assist in guiding future improvements in the plant. Finally, the objectives derived from the performance and thermodynamic analyses of previous literatures are summarized.

2.1 The Gas Diesel Engine

2.1.1 History

The concept of compression-ignition in reciprocating engines is fundamentally developed by Rudolf Diesel. His initial idea was to build an engine that followed as closely as possible the cycle proposed by Sadi Carnot cycle in 1824 (Sonntag and van Wylen, 1991). In 1892, a patent was issued to R. Diesel for an engine in which compressed air temperature exceeds the ignition temperature of fuel (Milton, 2001). This patented CI engine runs on coal dust and later on coal gas (Abd Alla *et al.,* 1999). Subsequently, more successful commercial applications have been made using the dual fuel concept. So the operation of diesel engines on gaseous fuels is neither new nor recent.

- The earliest experiments on dual fuel system were performed by Cave in 1929, and Helmore and Sokes in 1930, in which burning hydrogen was induced as a secondary fuel in diesel engines. When hydrogen burn completely, there was reduction of liquid fuel load and saving of 20% diesel fuel (Liu, 1995). However, at that time, the dual fuel engine was not used commercially due to its mechanical complexity and rough running caused by auto-ignition and knocking at relatively low compression ratios.

- In 1939, the first commercial dual fuel engine, fuelled by town gas or other types of gaseous fuels, was produced by the National Gas and Oil Engine Co. in Great Britain. This type of engine was relatively simple in operation and mainly employed in some areas where cheap stationary power production was required. During the Second World War, scientists in Great Britain, Germany and Italy paid more attention to the possible application of dual fuel engines in civil and military areas due to the shortage of liquid fuels. Some vehicles with diesel engines were successfully converted to dual fuel running. Different kinds of gaseous fuels, such as coal gas, sewage gas or methane, were employed in conventional diesel engines (Karim, 1987).

- After the Second World War, due to economical and environmental reasons, dual fuel engines have been further developed and employed in a very wide range of applications from stationary power production to road and marine transport, such as in long and short haul trucks and buses. Some conversions from the original compression ignition diesel engines to dual fuel operation were made by manufacturers utilizing a double plunger system or two pumps in the injection system of the engine to handle the small quantity of diesel fuel required for ignition (Thyagarajan and Babu, 1985; Sridhar, 2003).

2.1.2 Engine modification

In general, gaseous fuels have low cetane numbers and therefore, not suitable for CI engines when used alone. Fraser *et al.* (1991) and Naber *et al.* (1994) have determined the ignition delay of methane experimentally and found the local temperatures in excess of 1200K for ignition within 2ms. However, the temperature at the end of the compression stroke of even a modern DI diesel engine is rarely above 1000K (Hodgins *et al.,* 1996). Since these fuels are unable to be ignited in the required time by CI alone, hence an alternative means of charge ignition is needed. As described by Liu (1995), this can be achieved by the following ways:

- Converting the engine to spark ignition.
- Retaining the diesel injection system and adding the gaseous fuel to the inlet manifold (Conventional Dual fuelling, CDF).
- Retaining the diesel injection system and adding the gaseous fuel directly into the cylinder (High-Pressure Direct Injection, HDFI or 'co-injection')

The technique used for dual fuel operation in this work is CDF as it requires little or, eventually no modification for CI engines conversion. A schematic layout of a CDF version diesel engine is shown in Figure 2.1. In a CDF operation, the diesel engine induces and compresses a mixture of air and gaseous fuel that is prepared in the external mixing device, called mixer or mixing chamber. The amount of pilot fuel supplied by the normal diesel fuel injection system, for this air-gas mixture ignition, is between 10-20% of the operation on diesel alone at normal working loads. The pilot amount differs with the point of engine operation and its design parameters. During a part load engine operation, the fuel gas supply is reduced by means of a gas control valve. However, a simultaneous reduction of the air supply decreases the air quantity induced. Hence, the compression pressure and the mean effective pressure of the engine are decreased. This, eventually, leads to a drop in power and efficiency. The drastic reductions in the compression conditions even become too weak for the mixture to effect self-ignition. Therefore, dual fuel engines are not to be throttled /controlled on the air-side. Ideally, there is a need for optimum variation in the liquid pilot fuel quantity used any time in relation to the gaseous fuel supply to provide the best engine performance over the whole desired load range (Mansour *et al.,* 2001). Usually, the main goal, for both emissions and economic reasons, is to minimize the use of the diesel fuel and maximize its replacement by the cheaper gaseous fuel throughout the whole engine load range. The dual fuel engines operate effectively on a wide range of different gaseous fuels while maintaining the capacity for operation as a conventional diesel engine. Normally, the

change over from dual fuel to diesel operation and vice versa is made automatically, even under loading conditions (Henham and Makkar, 1998).

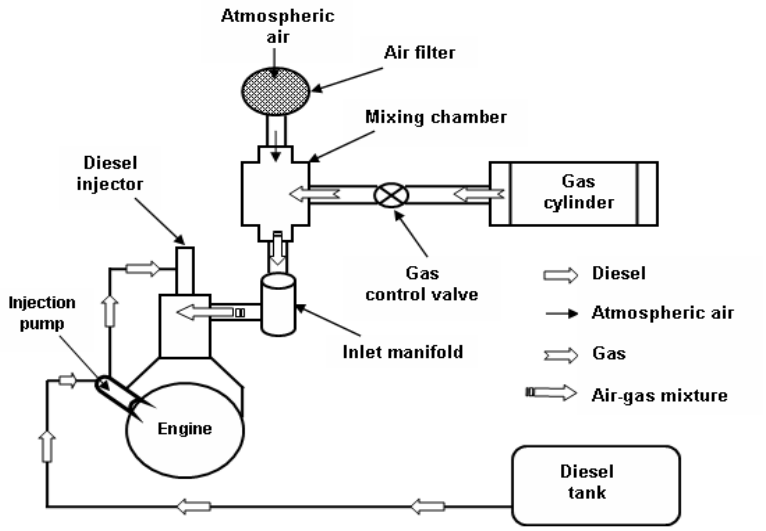

Figure 2.1 Schematic diagram of CDF system

2.1.3 The combustion process

The combustion processes in CI engines running on pure diesel fuel can be divided into four stages as shown in Figure 2.2. They are, A-B: period of ignition delay; B-C: premixed (rapid pressure rise) combustion; C-D: controlled (normal) combustion; and D-E: late combustion. Point 'A' is the start of fuel injection and 'B' for start of combustion. However, the combustion processes in gas-fumigated dual fuel engines using pilot injection have been identified to take place in five stages as shown in Figure 2.3. They are the pilot ignition delay (AB), pilot premixed combustion (BC), primary fuel ignition delay (CD), rapid combustion of primary fuel (DE) and the diffusion combustion stage (EF) (Nwafor 2003).

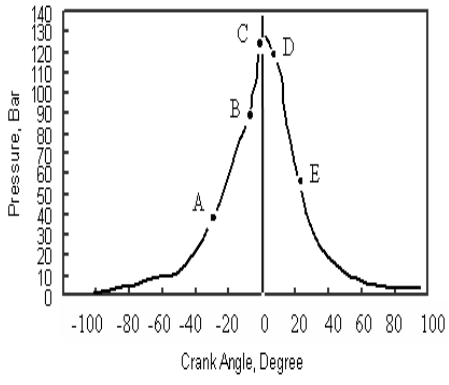

Figure 2.2 Details of combustion processes in diesel engine (Nwafor, 2003)

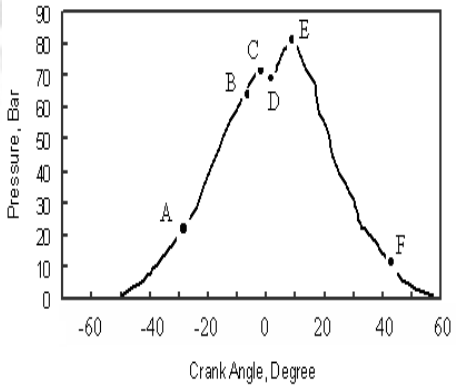

Figure 2.3 Dual fuel pilot injection pressure crank angle diagram (Nwafor, 2003)

Ignition delay (AB) of injected pilot fuel exists longer than the pure diesel fuel operation. This is due to the reduction in oxygen concentration resulting from gaseous fuel substitution for air. The pressure rise (BC) is moderately low as compared to pure diesel fuel operation due to the ignition of small quantity of pilot fuel. Again, there is a finite time lag between the development of the first and second pressure rises due to a longer ignition delay of gas-air mixture, a result of the high self-ignition temperature. However, this ignition delay is short as compared with the initial delay period due to the pilot fuel injection. The pressure decreases slowly (CD) until the actual combustion of the fumigated gas starts. The phase of combustion (DE) is very unstable because it started with flame propagation that has been initiated by the spontaneous ignition of pilot fuel. The pressure rise here does not cause any operating problem since it occurs in an increasing cylinder volume. Diffusion combustion stage (EF) starts at the end of rapid pressure rise and continues well into the expansion stroke. This is due to the slower burning rate of gaseous fuel and the presence of diluents from the pilot fuel. Some gas-air mixture may escape combustion under this phase due to low oxygen concentration, valve overlap, flame quenching on the walls or the effects of crevices. The success of this phase primarily depends on the length of ignition delay. There is a negative heat release in diesel fuel operation prior to main start of combustion which could be possibly due to the cooling of the injected liquid fuel. This effect is not apparent with the dual fuel combustion processes as pre-oxidation of the gaseous fuel starts before pilot fuel injection.

2.2 Dual Fuel Diesel Engine – Prospects

The dual fuel concept allows the low cetane number gaseous fuels to be used in CI diesel engines. However, limitations specific to performance of dual fuel engines create a new set of issues that need to addressed for the success of this concept. When, some of the engine operating and design parameters namely, load, speed, compression ratio, pilot fuel injection timing, pilot fuel mass, inlet manifold condition, composition of gaseous fuel candidates vary, the performance of the dual fuel gaseous engines are affected. Numerous studies have been done by many researchers to examine the effect of the above mentioned parameters on the emission, performance and combustion characteristics of dual fuel engines. The investigated engine, primary gaseous fuel and the pilot differ among the researchers. The type of test engine and fuels (both gas and pilot) experimented by several researcher(s) for their dual fuel operations are given in the following table.

Table 2.1 Summary of engine type and dual fuel used in the experimental investigation by various researcher(s)

Researcher(s)	Test Engine	Pilot Fuel	Primary Fuel
Abd Alla *et al.* (2000, 2002)	Single-cylinder, four-stroke, water-cooled engine (Ricardo E6)	Diesel	CH_4, C_3H_8
Abu-Jrai *et al.* (2007, 2009); Tsolakis *et al.* (2005)	Lister-Petter TR1 engine, 773 cm^3, naturally aspirated, air-cooled, single-cylinder, DI, CR: 15.45:1	Diesel	Reformed exhaust gas recirculation (H_2+CO)
Badr *et al.* (1999)	Two-cylinder, 4-stroke, water-cooled, DI, Bore: 105 mm, stroke: 152.5 mm, normally aspirated dual fuel engines	Diesel	CH_4
Bari (1996)	Two-cylinder, 4-stroke cycle diesel engine (16.8 kW at 1500 rpm, Model-2105 Nang Chang Company, China), water-cooled, naturally aspirated with double swirl CC	Diesel	Biogas
Banapurmath *et al.* (2008)	Kirlosker Make, single-cylinder, 4-stroke, constant-speed, rated power 5.2 kW (7 HP) at1500 rpm, eddy-current dynamometer type	Diesel, Honge oil, HOME	Producer gas
Banapurmath *et al.* (2009)	Kirlosker Make, single-cylinder, 4-stroke, constant-speed, rated power 5.2 kW (7 HP) at1500 rpm, eddy-current dynamometer type	Diesel, Honge, Rice bran, Neem	Producer gas
Boehman and Le Corre (2008); Garnier *et al.* (2005)	Single-cylinder, direct-injection, air-cooled stationary diesel engine, injection timing (20 ^{0}BTDC, fixed)	Diesel	Syngas
Henham and Makkar (1998)	Two-cylinder, 4-stroke, water-cooled, IDI, Lister Petter LPWS2 diesel engine	Gasoil	Biogas
Krishnan *et al.*(2004)	Single-cylinder DI, CI engine	Diesel	NG
Kusaka et al.(2000)	Water cooled, 4-stroke, and 4-cylinder conventional DI diesel engine	Diesel	NG
Lekpradit *et al.* (2008)	Cummins diesel engine, 4-stroke, 4-cylinders, constant-speed at 1500 rpm, capacity: 3.9 L	Diesel	Producer gas
Mansour *et al.*(2001)	Naturally aspirated, V-8 Deutz FL8 413F 4-cycle diesel engine	Diesel	NG

Masood *et al.* (2007)	Kirloskar AV-1 Make, 4-stroke, single-cylinder, CI engine with variable CR, rated power 3.7 kW at 1500 rpm	Diesel	Hydrogen
Nwafor (2000a; 2002; 2003; 2007), Nwafor and Rice (1994)	Petter model AC1 single-cylinder, air-cooled, high-speed, IDI, 4-stroke diesel engine	Diesel	NG
Nwafor (2000b)	Petter model AC1 single-cylinder, air-cooled, high-speed, IDI, 4-stroke diesel engine	RME, neat rapseed oil	NG
Papagiannakis and Hountalas (2003;2004)	Single-cylinder, naturally aspirated, 4-stroke, air-cooled, high-speed, Lister LV1 DI diesel engine with a bowl in piston CC	Diesel	NG
Ramadhas *et al.* (2006; 2008)	Canon Make, 4-stroke, DI, naturally aspirated, single-cylinder, CI engine, rated speed 1500 rpm	Diesel	Wood, Coir pith
Roy *et al.* (2009)	Single-cylinder, 4-stroke, water-cooled, DI, shallow-dish CC, Rated speed: 1000 rpm, CR: 16	Diesel	Producer gas
Selim *et al.* (2008)	Ricardo E6 single-cylinder variable compression IDI diesel engine	JME	NG, LPG
Selim (2001)	Ricardo E6 single-cylinder variable compression IDI diesel engine	Diesel	CNG
Selim (2004)	Ricardo E6 single-cylinder variable compression IDI diesel engine	-do-	CH_4, CNG, LPG
Selim (2005)	Ricardo E6 single-cylinder variable compression IDI diesel engine	-do-	CH_4, LPG
Singh *et al.* (2007a)	A naturally aspirated multi-cylinder DG with matching alternator	FD	Producer gas
Singh *et al.* (2007b)	A naturally aspirated multi-cylinder DG with matching alternator	Bio diesel	Producer gas
Stewart *et al.* (2007)	Lister–Petter 4×90, DI, four-stroke, naturally aspirated diesel engine	Diesel	CH_4, C_3H_8, C_4H_{10}
Tippayawong *et al.* (2007)	4-stroke, naturally aspirated, water-cooled, CI engine, rated power 5.5 kW at 2400 rpm, torque 25 N-m at 1900 rpm	Diesel	Biogas
Uma *et al.* (2004)	DI, six-cylinder, vertical, 4-stroke engine with mechanical injector	Diesel	Producer gas

2.2.1 Effect of load

(a) Combustion

The effect of load on combustion noise for the diesel and dual fuel engine at an engine speed of 1200 rpm was examined by Selim (2001). The pressure rise rate (combustion noise) for the diesel engine increased slightly when the load was increased. For the dual fuel mode, the combustion noise also increased when the load increased and was always higher than that for the diesel fuel case. Combustion noise for the diesel case was about 4 bar/^oCA and it only fluctuates slightly around this value. For the dual fuel engine, it increased from 4 bar/^oCA at a load of 4.5 N-m to 15.5 bar/^oCA at 18.5 N-m. Increasing the load at constant speed resulted in an increase in the mass of gaseous fuel admitted to the engine, since the pilot mass injected was kept constant at all loads. This increase in the mass of methane then caused an increase in the ignition delay period of pilot diesel which then auto-ignites and starts burning the gaseous fuel at a higher rate of pressure rise. This type of results was also noticed by Nielsen *et al.* (1987) on a NG inducted dual fuel engine.

An experiment was conducted by Papagiannakis and Hountalas (2004) to observe the combustion characteristics of a NG-diesel dual fuel operation at 20, 40, 60, and 80% of full load. At part engine load, cylinder pressure under dual fuel operation diverged from the respective values under normal diesel operation. The lower cylinder pressures observed under dual fuel operation during the compression stroke were the result of the higher specific heat capacity of the NG-air mixture. The total heat release rate under dual fuel operation was slightly higher compared to the one under normal diesel operation revealing late combustion of the gaseous fuel. However, the effect on the cylinder pressure was small since it was in the expansion stroke. At high engine load, the cylinder pressure traces under dual fuel operation diverged again from the respective values under diesel mode during the compression stroke and the initial stages of combustion. It is revealed that the total rate of heat release under dual fuel operation was higher compared to the one under normal diesel operation. The effect is stronger at low engine speed, indicating later combustion of the gaseous fuel and this obviously has an effect on the 'bsfc'. The combustion duration was higher under dual fuel operation at low engine load but dropped with the increase of load. Especially, at low engine loads, the combustion duration, even tends to become lower compared to diesel mode.

The effect of load changes, at a fixed engine speed of 1500 rpm, on three different gaseous fuels (methane, propane and butane) was investigated by Stewart *et al.* (2007). Equivalence

ratio was held constant for each case. It was noticed that, as load increased, more of the cycle energy was supplied from the diesel fuel. This implied a larger pilot injection mass supply to promote a more stable and smoother combustion process. Heat release rate data for propane and butane showed that these fuels exhibit decreasing and then increasing peak heat release rates that occur later in the cycle. This indicates the occurrence of some change to the basic combustion process. As the carbon number of the primary fuel increased, the initial heat release rate reduced and the diffusion stage increased. This is important because it imposes a limit upon the fuel type, used for primary fuel substitution.

(b) Efficiency

At low engine loads, the 'bsfc' for dual fuel operation was considerably higher compared to the diesel mode (Papagiannakis and Hountalas, 2004). It shows a poor utilization of the gaseous fuel, mainly, due to the lower temperature and air-fuel ratio inside the combustion chamber of the engines, resulting in a slower combustion rate as observed from the results of the heat release rate analysis (Heywood, 1988; Hountalas, 1994). On the other hand, at high load, the improvement of gaseous fuel utilization led to a relevant improvement of the 'bsfc' under dual fuel operation, which tend to converge to the case under normal diesel operation. However, its value continues to be higher compared to the under normal diesel operation. Similar results were also found by Uma *et al.* (2004) where they observed that SEC increased with decreasing load for both diesel and dual fuel modes. This implies the considerable efficiency loss at low-load condition. SEC in dual fuel mode was higher than the diesel mode throughout the tested load condition. Increased SEC indicates the efficiency reduction in the dual fuel mode. This is due to reduced heating value of the producer gas-air mixture and drop in the pressure of the gas entering the air inlet and lower flame velocity. The results are similar to the earlier studies (Parikh *et al*., 1989; Sridhar *et al*., 2001) which also reported de-rating of diesel engine in dual fuel mode. Singh *et al.* (2007a) have found a minor reduction in engine output about 1-2% for the lower calorific value of air-producer gas mixture (Table 2.2). However, using producer gas with bio-diesel as CI engine fuel, Singh *et al.* (2007b) found higher thermal efficiency than diesel/producer gas mixture.

In a dual fuel mode of operation, the maximum brake thermal efficiency was of 19.9% at 70% load using coir-pith and 21% at 70% load using wood chips as compared to 25% in diesel mode (Ramadhas *et al.,* 2006). With further increase in engine load, the thermal efficiency of the coir-pith dual fueled engine started decreasing drastically as shown in Fig.

2.4. This is due to the lower calorific value of producer gas, which contains more combusted mixture that enters into the engine. SEC in dual fuel mode was higher than that of diesel mode at all load conditions which was an indication of the efficiency reduction in the dual fuel mode. Similar results were also found by the authors by using rubber seed oil and producer gas in the same engine setup (Ramadhas *et al.,* 2008). Due to lack of adequate combustion time between two fuels, diesel and producer gas, Sridhar et al. (2005) found lower thermal efficiency and hence, higher exhaust temperature under dual fuel mode operation than diesel mode. With the presence of producer gas, Banapurmath *et al.* (2009) estimated the maximum thermal efficiency for diesel, honge, rice bran and neem oils as 31, 28, 27 and 26%, respectively.

Table 2.2 Effect of fuel and load on engine output, SEC, brake thermal efficiency and sound pressure (Singh et al., 2007a)

Engine Load (%)	**63**	**63**	**84**	**84**	**98**	**98**
Mode of operation	FD	Dual fuel	FD	Dual fuel	FD	Dual fuel
RPM of engine	1487	1490	1493	1483	1486	1489
Engine output (kW)	14.08	14.00	19.34	18.93	22.59	22.00
LFCR (kg/hr)	3.586	1.336	4.517	1.445	5.370	4.183
SEC (MJ/kW-hr)	11.07	19.55	10.15	15.39	10.35	11.61
η_{bth} (%)	32.53	18.41	35.45	23.38	34.77	31
PGFR (m^3/hr)	----	50	----	53	----	17
LFR (%)	----	62.74	----	68.00	----	22.24
Sound pressure (db)	100.5	96.90	101.50	102.15	99.50	100.40

FD: Fossil-diesel, LFR: Liquid fuel replacement (%), PGFR: Producer gas flow rate (m^3/hr), LFCR: Liquid fuel consumption rate (kg/hr), SEC: specific energy consumption (MJ/KW-hr)

(c) ***Emissions***

The formation of nitric oxide (NO) is favored by high oxygen concentration and high charge temperature (Benson and Whitehouse, 1973; Heywood, 1988; Lavoie, 1970). The NO_x concentration is affected considerably by the presence of gaseous fuel-air mixture. Papagiannakis and Hountalas (2004) found lower NO_x levels under NG/diesel operation as compared to the diesel mode at the same engine speed and load conditions. At low loads, the NO_x emission under dual fuel operation was slightly lower (Figure 2.5). This is mainly as a

result of the lower rate of premixed controlled combustion of the gaseous fuel, which results in lower charge temperature inside the combustion chamber. At higher load, the NO_x level under dual fuel operation was considerably lower compared to the 100% diesel operation. The NO_x levels in producer gas/diesel dual fuel mode were also found lower at all tested loading conditions by Uma *et al.* (2004), Sridhar *et al.* (2005) and Banapurmath *et al.* (2009).

The rate of CO formation is a function of the unburned gaseous fuel availability and mixture temperature which controls the rate of fuel decomposition and oxidation (Benson and Whitehouse, 1973; Heywood, 1988; Kouremenos, 1997). The CO emissions under dual fuel operation were significantly higher as shown in Fig. 2.6. At low engine speed, CO level under dual fuel operation decreased with the increase of engine load. This is the result of the improvement of gaseous fuel utilization especially during the second phase of combustion. At high engine speed, the increase of engine load did not affect the level of CO due to the availability of less combustion time (Papagiannakis and Hountalas, 2004). Similar dual fuel operation results for CO emissions at different load conditions were found by Ramadhas *et al.* (2006, 2008). They also found higher CO_2 emission for the dual fuel mode operation than diesel mode at all operating loads due to the presence of CO and CO_2 in producer gas (Fig. 2.7). To reduce CO emissions, injector design, compression ratio, ignition advance, combustion chamber design etc. will have to be optimized Uma *et al.* (2004).

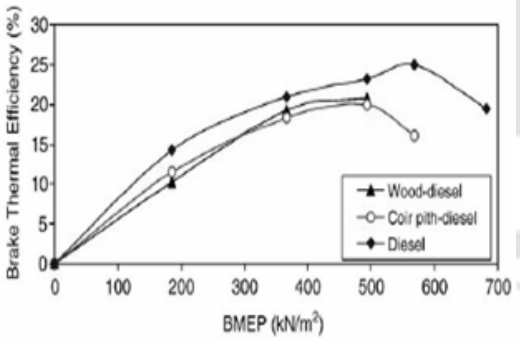

Figure 2.4 Brake thermal efficiency of the engine w.r.t. BMEP (Ramadhas et al., (2006)

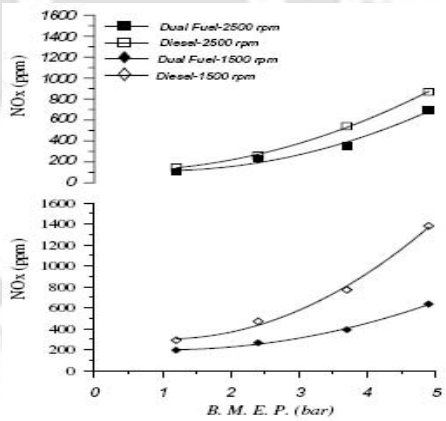

Figure 2.5 Variation of NO_x under normal diesel and dual fuel operation versus load (Papagiannakis and Hountalas, 2004)

At low engine load, HC emissions under dual fuel mode were found considerably higher compared to the diesel mode by Papagiannakis and Hountalas (2004) as shown in Fig. 2.8. This is mainly due to the lower charge temperature and air-fuel ratio, resulting in slower combustion and allowing small quantities of fuel to escape the combustion process. With the

increase of engine load, there was a sharp decrease of HC emissions under dual fuel mode. This is the result of the increase of burned gas temperature that helps to oxidize the HCs efficiently. But for all cases examined by the authors, the HC emissions were found considerably higher under dual fuel mode compared to diesel mode. On the other hand, the experimental results of Uma *et al.* (2004) showed that HC emissions in producer gas/diesel mode were little higher than diesel mode. Banapurmath *et al.* (2009) also reported higher HC and CO emissions for dual fuel mode using producer gas with three injected fuels namely, honge oil, rice bran and neem oil than diesel operation. The soot emissions under dual fuel operation were found considerably lower compared to the diesel mode for all cases examined by Papagiannakis and Hountalas (2004) as shown in Fig. 2.9. Under normal diesel mode, soot emissions increased with increase in load. On the other hand, under dual fuel mode and for all cases examined, the soot emissions did not follow the same trend since a reduction of soot emissions was observed with increase in load. This is expected since the increase of engine load is accomplished by increasing the amount of gaseous fuel that forms no soot while the increasing charge temperature contributes to its oxidation (Agarwal and Assanis, 1998; Hountalas and Papagiannakis, 2000; Karim, 1980; Karim and Khan, 1968; Liu and Karim, 1997; Papagiannakis and Hountalas, 2003). During a producer gas/rice bran oil dual fuel operation, Singh *et al.* (2007a) observed that at 84% load with 18.4:1 CR the percentage reductions in concentration of pollutants like CO, CO_2, NO, NO_2 were 55.5, 19.7, 82 and 83% respectively, while HC concentration increased by 67.2%. While, with experiments on same engine setup, Singh *et al.* (2007b) reported that addition of producer gas/bio-diesel reduced the NO_x emissions significantly but it increased the concentration of other pollutants.

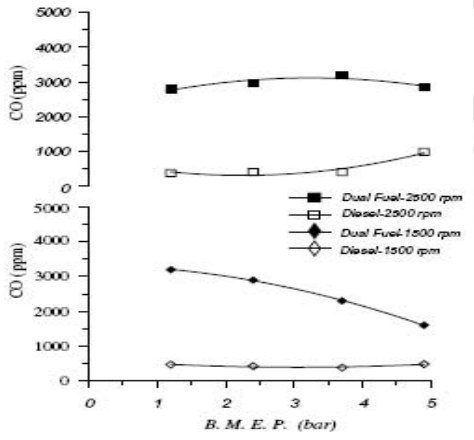

Figure 2.6 CO under normal diesel and dual fuel operation versus load (Papagiannakis and Hountalas, 2004)

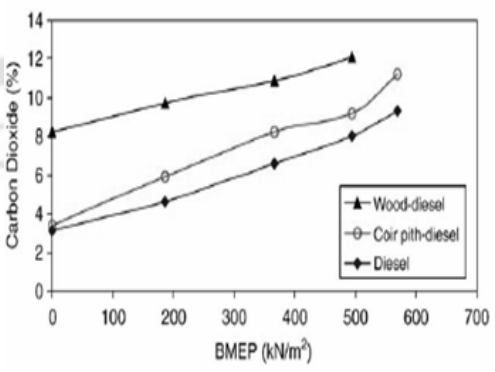

Figure 2.7 Carbon dioxide emissions of the engine w.r.t. BMEP (Ramadhas *et al.,* 2006)

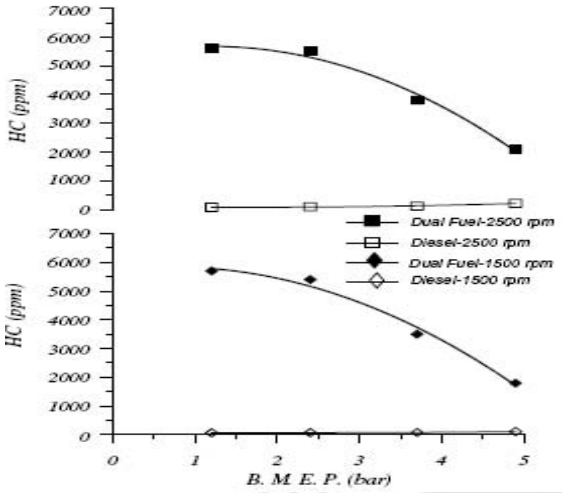

Figure 2.8 UBHC under normal diesel and dual fuel operation versus load (Papagiannakis and Hountalas, 2004)

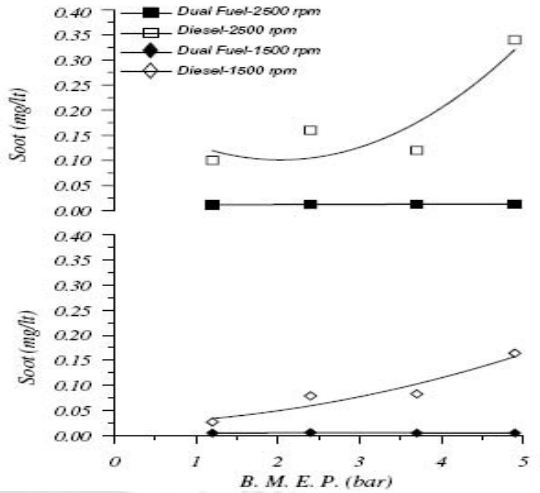

Figure 2.9 Soot emissions under normal diesel and dual fuel operation versus load (Papagiannakis and Hountalas, 2004)

2.2.2 Effect of speed

(a) Combustion

Selim (2001) has examined the effect of engine speed on combustion noise for diesel and dual fuel modes. Generally, as the engine speed increases, the pressure rise rate $(dP/d\theta)$ decreases for both mode of operation. In diesel mode, the pressure rise rate dropped from about 5.5 bar/^oCA at speed of 990 rpm to around 2.93 bar/^oCA at 1890 rpm. However, for the dual fuel mode the pressure rise rate was higher than that for the diesel case, almost at all engine speeds, and it followed a similar trend to the diesel mode. It dropped from 6.6 bar/^oCA at 980 rpm to 2.95 bar/^oCA at 1880 rpm. The author also found similar results for all three gaseous fuels used for another investigation (Selim, 2004). The author observed that the pressure rise rate was highest with methane, followed by LPG and NG at almost all engine speeds. The investigations by Selim *et al.* (2008), using jojoba methyl ester as a pilot fuel to NG, also found similar results regarding pressure rise rate. It was also shown in an IDI diesel engine by Imoto *et al.* (1997) that the combustion noise of dual fuel mode was decreased for an increased engine speed.

(b) Efficiency

Under unsteady conditions, Mansour *et al.* (2001) observed a small power and torque losses in dual fuel version as compared to the diesel mode, except around the speed of 2400 rpm. This difference is due to the system response time of gaseous fuel injection in the admission collector. When the engine speed elevated to 2450 rpm, the torque and brake power in dual

fuel version becomes slightly higher than in the diesel mode. Selim (2004) has investigated the effects of engine speed for three gaseous fuels in a dual fuel operation. During these experiments, the constant parameters were the pilot fuel injection timing 35 ^{0}BTDC, mass of pilot fuel 0.37-0.47 kg/h and compression ratio 22. It was seen that, the LPG produced the lowest torque output and thermal efficiency as compared to methane or the NG mixture. The torque output and efficiency was highest for methane gas. The thermal efficiency improved with increase in engine speed. Similar results were shown by Selim *et al.* (2008) by using of jojoba methyl ester as a pilot fuel to NG and LPG. However, in a biogas premixed charge diesel dual fuelling engine, the authors found almost no performance deterioration at all test speeds (Duc and Wattanavichien, 2007).

Tippayawong *et al.* (2007) have evaluated the effect of short-term as well as long-term operation on performance and wear of a biogas/diesel dual fuel mode. In a short-term performance, biogas/diesel mode was found to give acceptable operation up to 1800 rpm, with diesel replacement rate over 90% by mass. Dual fuel operation exhibited higher power output than that under normal diesel operation, especially at low speed but the magnitudes were not markedly different (Fig. 2.10). This is attributed to the fact that gaseous fuel evaporates more readily than liquid fuel, which is more pronounced at lower speed. The difference was reduced with an increase in speed. Dual fuel operation proved to have higher efficiency than that of diesel mode. In the long dual fuel operation time, the power tended to fluctuate slightly (Fig. 2.11). This is attributed to carbon deposition on the inlet and exhaust port, as well as to several eruptive supplies of biogas from the reactor. Unusual wear on critical components was not detected except a small degree of carbon deposits building up inside the combustion chamber which could be solved by periodic maintenance and service.

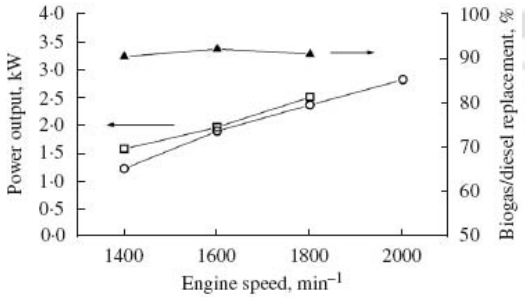

Figure 2.10 Comparison between short-term engine power out from diesel (○) and dual fuel (□) operations, and fraction of biogas replacement (▲) in dual fuel operation (Tippayawong *et al.*, 2007)

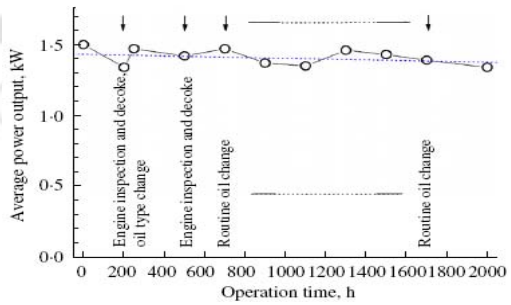

Figure 2.11 Variation of average electrical power generated with operation time (Tippayawong *et al.*, 2007)

(c) Emissions

The effect of engine speed of a jojoba methyl ester (JME) pilot ignited CNG and LPG dual fuel operation on the CO emissions was shown by Selim *et al.* (2008) in Figs. 2.12 and 2.13 respectively. CO level was highest for JME/LPG mode followed by JME/CNG, then diesel/LPG and minimum for diesel/CNG case. Similar trend was noticed for HC emissions as shown in Fig. 2.13. When the engine speed was increased, both CO and HC emissions were reduced due to improved mixing process for the combustible mixture. Regarding NO_x emission, Papagiannakis and Hountalas (2004) reported that the increase of engine speed under dual fuel operation resulted in a decrease of NO_x values compared to diesel operation.

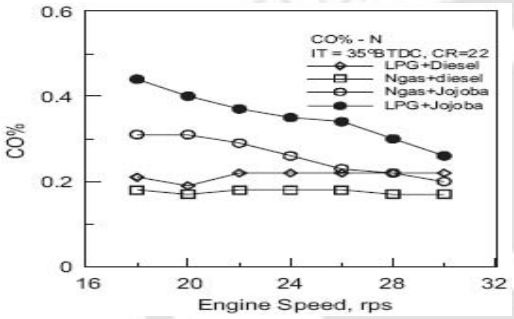

Figure 2.12 Effect of speed on CO emissions for different dual fuels (Selim *et al*., 2008)

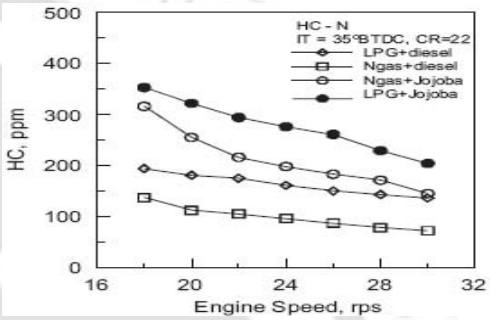

Figure 2.13 Effect of speed on HC emissions for different dual fuels (Selim *et al.,* 2008)

2.2.3 Effect of pilot fuel injection timing

The injection timing of pilot fuel is an important factor that influences the performance of dual fuel engines. For a fixed total equivalence ratio, advancing the injection timing increase the peak cylinder pressure because more fuel is burned before TDC and the peak pressure moves closer to TDC. Retarding the injection timing decreases the peak cylinder pressure because more of the fuel burns after TDC. This is because, the pilot fuel combustion is delayed and thus, the temperature of the mixture is not enough to propagate the flame in the whole air-gas mixture, and consequently, incomplete combustion of the mixture takes place. The charge temperature increases with advancing the injection timing of pilot fuel and the associated higher energy release rates of the mixture. Similarly, the rates of pressure rise during the combustion of gaseous fuel increases with advancing injection timing of pilot fuel.

(a) Combustion

Selim (2001) has compared the effect of pilot diesel injection timing on the combustion noise of a dual fuel engine to 100% diesel mode was shown in Fig. 2.14. For the late injection of pilot, (20 to 25°BTDC), the combustion noise was comparable for diesel and dual fuel cases.

However, when the injection advance increased (25 to 40°BTDC), the dual fuel engine produced a higher rate of pressure rise $(dP/d\theta)$. With the presence of gaseous fuel in the mixture, any advance in pilot fuel injection results longer ignition delay period and increase in pressure rise rate. Similar results were established by the author using NG, CH_4 and LPG as gaseous fuels in (2004), for a LPG/diesel dual fuel operation in (2005) and again by Selim *et al.* (2008) using jojoba methyl ester as a pilot fuel for NG and LPG. Experimental results of Nwafor (2000a) showed that diesel fuel operation produced the shortest delay periods at both operated test speeds. At high loads and combustion temperatures, the ignition delay reduced and combustion was dominated by the system temperature. At low loads, with longer delay periods, greater proportion of pilot fuel took part in premixed combustion, thus increased the tendency of diesel to knock. Very poor atomization resulted a relatively long delay period, due to the slow development of very fine droplets. Dual fuel operation with advanced timing showed the highest exhaust temperatures. For a fixed total equivalence ratio, amount of pilot fuel, intake temperature and advancing the injection timing has a great effect on the maximum charge temperature in the cylinder. Abd Alla *et al.* (2002) have reported that any advances in the injection timing increased the tendency to knocking early for medium and high engine loads (Fig. 2.15) due to increase of maximum charge temperature.

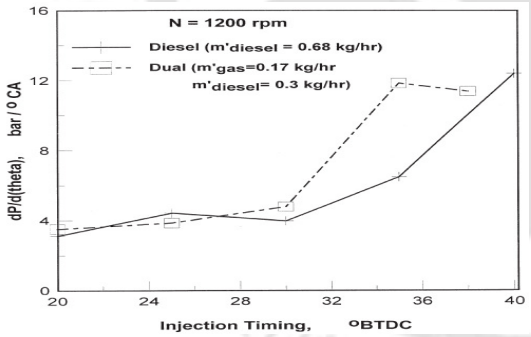

Figure 2.14 Effect of pilot fuel injection timing on pressure rise rate for the diesel and dual fuel engine (Selim, 2001)

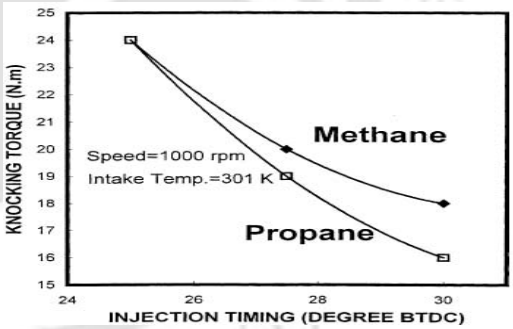

Figure 2.15 Effect of injection timing on knocking torque for a dual fuel engine fuelled with methane and propane (Abd Alla *et al.,* 2002)

Fuel conversion efficiency (defined by the ratio of the brake power to the total rate of energy input into the engine) is calculated from the measured total diesel and natural gas flow rates multiplied by their respective lower heating values. When brake power and engine speed were held constant for all injection timings, the particular heat release pattern that provides for greater work per unit mass of fuel translated into higher fuel conversion efficiency

(Krishnan *et al.,* 2004). As injection timing was retarded from 35 to 15°BTDC, the start of heat release was delayed and the overall heat release process was shifted away from TDC. Also, the duration and peak heat release were increased. These effects contributed to the loss in fuel conversion efficiency between 35 and 15°BTDC. As injection timing was advanced from 40 to 60°BTDC, the duration of heat release did not change significantly even though the start of heat release delayed. The delayed start of heat release has led to a decrease in fuel conversion efficiency for timings advanced beyond 45°BTDC. The onset of combustion was seen to be earlier for injection timings between 30 and 45°BTDC. For timings advanced beyond 45°BTDC or retarded beyond 30°BTDC, combustion began progressively closer to TDC. However, combustion duration did not follow the same trend. For instance, although combustion has started at about the same time for both 15 and 60°BTDC, the combustion duration for the former was seen to be much longer than that of the latter. Hence, the prolonged combustion time for 15°BTDC progressed into the expansion stroke, thereby reduced the fuel conversion efficiency compared to 60°BTDC.

(b) Efficiency

The effect of advanced injection timing on the performance of NG used dual fuel combustion was examined by Nwafor (2000a). The injection was first advanced by 5.5° (i.e. 35.5°BTDC). After the engine ran for about 5 minutes at this timing, it stopped. With subsequent attempts, the author failed to start the engine. However, after changing the injection to 33.5°BTDC, the engine ran smoothly, but seemed to incur penalty on fuel consumption especially at high load levels. Table 2.3 compares fuel consumption measurements for the two speeds i.e., 3000 rpm and 2400 rpm of investigation. The governor injected more pilot fuel than when run on standard time units. The poor performance of gas engines at low load levels is due to the effect of gas residuals and low cylinder temperature. It is also due to the reduction in combustion efficiency caused by reduced flame propagation speed and increased compression work resulting from the large amount of air-gas inducted. The diesel fuel operation produced the highest BTE at both the speeds. Standard timing dual fuel mode showed little improvement over the advanced system at 3000 rpm. However, at 2400 rpm the dual fuel mode standard and advanced timing showed similar trends at low and intermediate load levels.

Table 2.3 Effect of advanced injection timing on performance of NG (Nwafor, 2000a)

Engine load (N)	Diesel fuel operation (kg/h)	Standard timing. Pilot fuel consumed (kg/h)	Standard timing. Gas consumed (l/min)	Advanced timing. Pilot fuel consumed (kg/min)	Advanced timing. Gas consumed (l/min)
Engine speed = 3000 rev/min					
6.61	0.539	0.368	10.0	0.408	10.0
13.18	0.642	0.402	11.0	0.456	11.0
17.72	0.696	0.442	12.4	0.478	12.5
23.78	0.818	0.447	14.0	0.496	14.0
29.33	0.894	0.470	16.0	0.509	16.0
33.87	0.975	0.493	17.0	0.535	17.0
38.92	1.045	0.529	18.0	0.594	18.0
44.47	1.154	0.563	19.0	0.642	19.0
49.52	1.266	0.570	20.2	0.631	20.2
Engine speed = 2400 rev/min					
8.63	0.463	0.333	8.0	0.349	8.0
13.68	0.509	0.299	12.0	0.319	12.0
18.73	0.592	0.278	14.0	0.298	14.0
24.79	0.680	0.279	15.2	0.295	15.2
29.83	0.735	0.303	16.0	0.324	16.0
35.89	0.829	0.312	17.0	0.366	17.0
41.44	0.887	0.328	17.5	0.383	17.5
46.80	1.013	0.344	18.0	0.456	18.0
53.56	1.132	---	---	---	---

Advancing the pilot fuel injection timing produces higher combustion temperatures of air-gas mixture. This leads to increase in the brake power and, consequently, thermal efficiency of the engine. This was shown for methane and propane gases dual fuel operations by Abd Alla *et al.* (2002). Similar trend of results were also found from dual fuel operation of a CI engine by Banapurmath *et al.* (2008) for the honge oil/producer gas and Lekpradit *et al.* (2008) for diesel/producer gas. Banapurmath *et al.* (2008) have estimated the thermal efficiency for the dual fuel engine at injection timings of 19, 23 and 27°BTDC as 18.25%, 19.25% and 20.5% respectively. In the their experimental work Lekpradit et al. (2008) have even found higher thermal efficiency for the dual fuel engine with advanced injection timing than the diesel mode with standard injection timing. Selim (2004) has investigated the effects of pilot fuel injection timing for a dual fuel diesel engine. The highest torque output for methane and natural gas occurred when the injection timing was 25°BTDC, while for LPG it occurred at 30°BTDC. The torque output and hence, the thermal efficiency was highest at certain

timings, and it decreased at earlier or later timing. Selim *et al.* (2008) have shown the decrease in power output with advance in jojoba methyl ester pilot fuel injection timing. The advance in fuel injection timing caused the maximum pressure rise rate and maximum pressure to increase during the compression stroke which tends to decrease the mean effective pressure and power output. Krishnan *et al.* (2004) have tried different pilot injection timings in a single cylinder CI engine. The overall set of experiments involved engine testing at a constant speed of 1700 rpm, full load (42 kW, 1220 kPa bmep) engine operation at fixed pilot quantity and inlet conditions. As injection timing was advanced from 15 to 45°BTDC, fuel conversion efficiency was increased from 38% to about 43%. Upon further advance of the injection timing, the efficiency decreased to about 40% at 60°BTDC.

(c) Emissions

The effects of injection timings of 25, 27.5 and 30°BTDC on the emissions of an IDI diesel engine were investigated by Abd Alla *et al.* (2002). Advancing the pilot fuel injection timing reduced the UBHC emissions. This is due to a longer ignition delay of the mixture with the increased timing advance. The longer ignition delay allows a full spray penetration and development, creating a larger amount of the pilot fuel-air-gaseous fuel mixture (or flame propagation region) prior to ignition. The higher combustion rates of this larger premixed regions yields higher combustion temperatures and thus, lowers the UBHC emissions. With bigger injection advance, better overall combustion and the activity of the partial oxidation reactions reduced the CO emissions. It also widened the lower combustion limit boundary of the overall lean mixture effectively. For a fixed total equivalence ratio, amount of pilot fuel and intake temperature, advancing the injection timing has a great effect on the maximum charge temperature in the cylinder. For any total equivalence ratio, as the injection was retarded, the maximum charge temperature decreased. The net effect is a reduction in NO_x.

The standard timing dual fuel mode produced the highest cylinder wall temperatures while the advanced injection timing system showed the lowest values (Nwafor, 2000a). The HC emissions of the gas-fuelled engine were higher than that in pure diesel fuel operation. Dual fuel standard timing showed higher concentration of HC in the exhaust at low load levels over the advanced injection mode. However, this system showed decreased HC emission levels at high load level operation. HC emissions increase due to several factors, including quenching, lean combustion, wall wetting, cold starting and poor mixture preparation. For both test conditions, the HC levels were relatively high in dual fuel operations and stay

reasonably high throughout the load range. Nwafor (2007) has reported effect on emissions of CO and CO_2 for the advanced injection timing. The advanced injection timing has shown a significant reduction in CO emissions compared to standard dual fuel operation. The diesel fuel operation produced the lowest CO emissions at low loading conditions and increased with load (Fig. 2.16). The advanced injection timing gave a net reduction in CO production at high loading conditions. The highest CO_2 concentrations in the exhaust were recorded when running on pure diesel fuel (Fig. 2.17). Standard injection timing at both speeds offered a net reduction in CO_2 emissions as compared to the pure diesel mode.

Lekpradit *et al.* (2008) observed lower CO and highest NO_x emissions when they advanced the injection timing of a diesel/producer gas dual fuel engine. Krishnan *et al.* (2004) have found some interesting emission results for their dual fuel operations. They noticed that, the NO_x emissions for the maximum efficiency timing (45°BTDC) were much higher than those for very retarded (15°BTDC) or very advanced (60°BTDC) timings. Along with NO_x reduction, efficiency also decreased when injection advanced or retarded from 45°BTDC. However, it was interesting that the efficiency for 60°BTDC was about 3% greater than that for 15°BTDC and NO_x emissions were lower as well. Thus, it is clearly more beneficial to advance the pilot injection timing to reduce NO_x emissions and maintain minimal loss in fuel conversion efficiency. For the timings retarded beyond 25°BTDC, both HC and CO emissions were found to decrease especially between 20 and 15°BTDC timings.

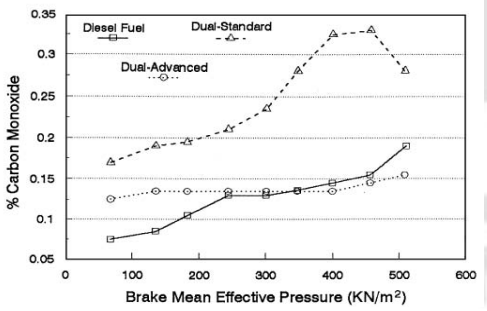

Figure 2.16 Injection advanced effect on carbon monoxide emissions at 3000 rpm (Nwafor, 2007)

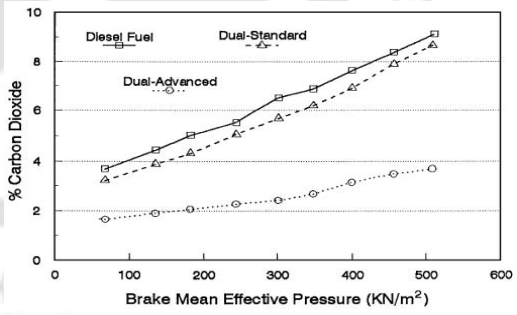

Figure 2.17 Injection advanced effect on carbon dioxide emissions at 3000 rpm (Nwafor, 2007)

2.2.4 Effect of pilot fuel mass

The pilot fuel quantity is one of the most important variables that have a controlling influence on the performance of dual fuel engines, especially at light loads. It is known that most diesel

fuel injection systems experience poor atomization and combustion when the amount of fuel injected per cycle is reduced below 5 to 10% of the maximum design level.

(a) Combustion

The effect of pilot fuel-gas ratio on knock characteristics of dual fuel engine was examined by Nwafor (2002). The author measured the ignition delay of dual fuel operation longer as compared to that of diesel mode. Similar results were also presented by the author for natural gas in an unmodified CI engine (Nwafor and Rice, 1994). The increase in speed increased the ignition delay when running on pure diesel fuel, hence the quantity of premixed pilot fuel that took part in combustion increased. Increasing the pilot fuel and thus, reducing primary fuel in dual fuel engines reduced the knocking phenomena. Abd Alla *et al.* (2000) have also indicated that use of higher pilot fuel quantity to enhance the combustion process at low loads leads to increase the tendency to knock at high loads. Increasing the pilot fuel mass also resulted in higher maximum combustion pressure (Selim, 2004 and Selim *et al.,* 2008). The authors noticed that, for the dual fuel engine, the maximum pressure was always higher than the diesel mode due to the combustion and extra heat release from gaseous fuels. The maximum pressure rise rate is generally reduced when the pilot fuel quantity is increased. This is because of the increase in flame volume resulting from the increase in pilot fuel mass, which burns the gaseous fuel smoothly and at a lower rate of combustion. However, when the pilot fuel mass increased beyond a certain amount, the ignition delay period of the pilot diesel increased and hence, the pressure rise rate for the gas-air mixture increased (Selim, 2001). Badr *et al.* (1999) have noticed that the increase in pilot quantity lowers the flame spread limits due to number of contributing factors. These include: greater energy release on ignition, correspondingly improved pilot fuel injection characteristics, larger pilot-mixture envelope size, larger ignition centres, higher rate of heat transfer to the unburned gaseous mixture and increased contribution of hot residual gases.

(b) Efficiency

The employment of a large pilot fuel quantity produces higher power output (Abd Alla *et al.,* 2000). The increase of pilot fuel quantity led to successful flame propagation and consequently increased the output power. Supporting to this result, the experimental investigations of Selim (2001) showed that increasing the pilot diesel fuel mass resulted increase in the engine torque due to the increase in the amount of heat released from burning more fuel. Further, Selim (2004) has examined the effects of pilot fuel quantity on a dual fuel

engine operation of NG, LPG and CH_4. During these experiments the following parameters are kept constant: engine speed 1300 rpm, pilot fuel injection timing 35°BTDC and compression ratio 22. Increasing the pilot diesel fuel for the three gaseous fuels resulted in greater energy release on ignition, improved pilot injection characteristics and larger size of pilot mixture envelope. These factors tend to increase the power output and thermal efficiency of the dual fuel engine (Abd Alla *et al.,* 2000). The experimental works from Selim *et al.* (2008) have also found increase in output with increase in the jojoba pilot fuel mass.

(c) Emissions

The variations of the exhaust gas concentrations of methane and CO with equivalence ratio for different pilot fuel quantities was investigated by Badr *et al.* (1999)**.** They observed that there is a limiting equivalence ratio beyond which the CO and the unconverted CH_4 emissions become virtually unaffected by the pilot quantity. This is indicative of the equivalence ratio limit for successful flame propagation from the pilot ignition centers. Abd Alla *et al.* (2000) have investigated the effect of three pilot fuel quantities, 0.15, 0.20 and 0.25 kg/h, on the emissions of an IDI diesel engine fuelled with gaseous fuel. At very light loads, with a small pilot fuel quantity, the concentrations of UBHCs were measured relatively high. This is because, in an excessively lean mixture, the flame originating from the pilot ignition does not propagate throughout the whole combustion chamber; only partial oxidation occurs, and thus, UBHC as well as CO emissions are relatively higher. At higher loads, when the gaseous fuel concentration in the air charge was above the lean combustion limit, the flame was able to propagate through most of the combustion chamber unaided, and varying the pilot fuel quantity has little effect. The change in oxidation reactions from unsuccessful to successful flame propagation reduced the HCs and CO emissions slightly. In dual fuel engines, the effective size of the combustion zone, which relates to the size of the pilot fuel zone, is another important factor, besides to the mechanism of oxidation of nitrogen that determines the quantity of NO_x produced. For the same total equivalence ratio, increasing the pilot fuel quantity increased the charge temperature which tends to increase the production of NO_x. For relatively high loads, the combustion of gaseous fuel was more complete and less affected by the pilot fuel quantity, and thus, has a mild effect. Similarly, for a given pilot fuel quantity when higher gaseous fuel concentrations in the cylinder charge were employed, the significant increases in the size of the combustion zone led to correspondingly increased

higher production of NO_x. Hence, it is concluded that the use of large pilot fuel quantities and high charge equivalence ratios resulted in a significant increase in the production of NO_x.

2.2.5 Effect of engine compression ratio

(a) Combustion

Selim (2004) has examined the effects of compression ratio of a dual fuel engine: First, on knock onset and ignition failure and secondly, on the maximum pressure rise rate. For LPG, reduction in the compression ratio resulted in retarding the occurrence of knock onset in the dual fuel engine (from 8.1 to 17.6 to 20 N-m) and also extended the ignition limits greatly (from 7.85 to 17 to 18.5 N-m). This is due to the early knocking at high compression ratios associated with higher pressures and temperatures and lower self ignition temperatures of LPG. For extended ignition limits and knock free operation of the dual fuel engine, the compression ratio has to be reduced to lower values. The NG mixture and methane also showed similar trend to LPG with the only difference at the compression ratio of 22. As LPG has the lowest self ignition temperature (about 400°C), it started knocking and also, ignition failed at lower engine torque compared to the other two gases namely, methane (about 650°C) and CNG (about 500°C). It is noticed that increasing the compression ratio generally increases the combustion noise due to the higher self ignition of the gaseous fuels at higher pressures and temperatures. The author found that, as the compression ratio was reduced, the combustion noise was also reduced, and the ignition limits were extended. Using jojoba methyl ester as a pilot, Selim *et al.* (2008) also reported similar results for CNG and LPG.

(b) Efficiency

The effect of compression ratio on the output brake power and 'bsfc' was shown by Selim et al. (2008). Increasing the compression ratio increased the power output as the expansion ratio was increased (Fig. 2.18). The authors also observed that, except for lower compression ratios, the 'bsfc' was almost comparable for all the fuels studied.

(c) Emissions

The effect of compression ratio on the CO emission studied by Selim *et al.* (2008) is shown in Fig. 2.19. The CO and HC emission was highest for JME/LPG case followed by JME/CNG, then diesel/LPG and minimum for diesel/CNG case. With increase in compression ratio, the CO and HC emission was reduced. This is attributed by the improved mixing process for the combustible mixture.

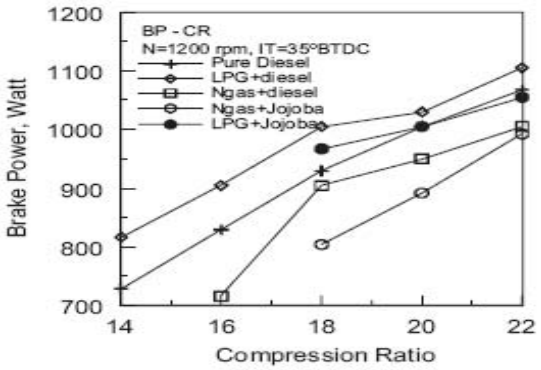

Figure 2.18 Effect of compression ratio on brake power output for different dual fuels (Selim *et al*., 2008)

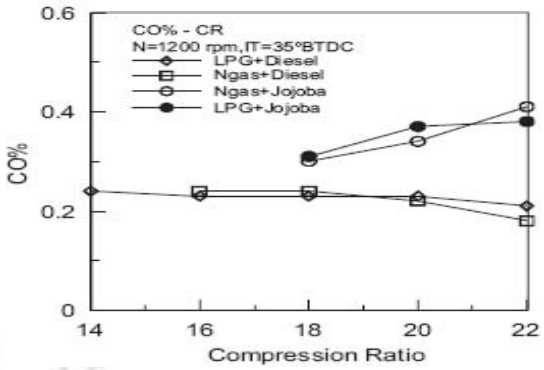

Figure 2.19 Effect of compression ratio on CO emissions for different dual fuels (Selim *et al*., 2008)

2.2.6 Effect of intake manifold conditions

(a) Combustion

In order to improve exhaust emissions at part load, Kusaka *et al.* (2000) have modified the intake charge condition including intake temperature and exhaust gas recirculation (EGR). They installed a heat exchanger in the intake system and a Pt-catalyst was used in the exhaust system to reduce unburned natural gas emission. The 'baseline' condition was taken as: intake temperature of 20°C and EGR 0%. In the case of intake heating of 165°C, the start of heat release rate occurred earlier than that of other conditions due to higher cylinder temperature. On the other hand, the combination of 50% EGR and intake heating of 210°C retarded the start of heat release as compared to that of intake heating of 165°C without EGR. Ignition reaction proceeds faster by intake heating, while the inert gases included in re-circulated exhaust gas impede progress of ignition reactions. It was also seen that EGR can favorably control the rate of pressure rise.

(b) Efficiency

The use of a heat exchanger with EGR has resulted higher temperature than without EGR. This is because the heat transfer from the exhaust gas to charge by mixing is more effective than that by a heat exchanger. Thus, high EGR ratio combined with the use of heat exchanger achieved higher cylinder temperature, which activated NG mixture oxidation. However, when the result of 50% EGR was compared with 60% EGR, the engine performance was not improved. This is because higher EGR ratio combined with intake heating reduced oxygen concentration in the cylinder, resulting in deteriorated combustion (Kusaka *et al.,* 2000).

(c) Emissions

The exhaust emissions characteristics under various intake conditions were reported by Kusaka *et al.* (2000). The EGR with intake heating reduced HC levels compared to the 'baseline' condition. NO_x was drastically increased in the case of intake heating without EGR. However, when EGR was combined with intake heating, NO_x was reduced drastically. Generally, a dual fuel engine is operated with high EGR ratio because it produced little soot, leading to reduced NO_x emission. This is because of the fact that the inert gas, which has a large heat capacity, lowers combustion temperature, and also, EGR reduces the oxygen concentration in the cylinder. From these above points of view, EGR combined with intake heating reduced NO_x and HC emissions without deteriorating thermal efficiency.

2.2.7 Effect of type of gaseous fuel

(a) Combustion

The in-cylinder pressure behavior of a dual fuel engine for gasoil (or diesel) only, gasoil/NG (60% substitution), and gasoil/gas mixture ($NG:CO_2$::1:1) were presented by Henham and Makkar (1998). At 2000 rpm, peak pressure raised from 70 to 83 bar at 60% NG substitution and dropped to 77 bar for gas mixture of $NG:CO_2$ (1:1), whereas, at 2800 rpm, it was moved up from 57 to 70 bar at 60% NG substitution and went down to 67 bar for gas mixture of $NG:CO_2$ (1:1). The authors indicated that the exhaust temperature was affected more by NG substitution up to 45%. At 58% NG substitution, exhaust temperature increased with increasing CO_2 in gas mixture, from 382°C to 402°C. As the amount of gaseous fuel increased, the maximum combustion pressure and pressure rise rate increased for the dual fuel operations (Selim, 2004, Masood *et al.,* 2007). Increasing the load at constant speed resulted in an increase in the mass of gaseous fuel admitted to the engine, since the pilot mass injected was kept constant at all loads. This increase in the mass of gaseous fuel caused an increase in the ignition delay period of the pilot diesel. Then, the pilot fuel auto-ignited and started burning the gaseous fuel at a higher rate of pressure rise. LPG produced the highest pressure rise rate and knocking combustion as compared to methane and the NG mixture prior to knocking because of its high tendency to self ignite. The maximum pressure for the LPG case also appeared to be the highest, followed by methane and then NG mixture. This is due to the early ignition of the LPG that produces higher maximum pressure BTDC.

Papagiannakis and Hountalas (2003) have examined the effect of dual fuel engine combustion characteristics to the variation of mass ratio of gaseous fuel (NG) at different

loading conditions. At part load condition, increasing the NG mass ratio over 50%, the cylinder pressure after ignition increased at a slower rate as compared to diesel mode (Fig. 2.20). The initial heat release rate for mass ratios up to 50% was almost the same while for higher values it was lower, revealing less premixed combustion. The effect of NG combustion on the total heat release gets evident only at high mass ratios around 80%. At 80% load, the cylinder pressure traces under dual fuel operation strongly diverged from the respective values under diesel mode as NG mass ratio increased (Fig. 2.21). The second peak of heat release observed due to combustion of NG did not affect strongly the pressure curve since it was in the expansion stroke. For all cases examined, the cylinder pressure under dual fuel mode decreased when increasing the amount of NG. The maximum combustion pressure was strongly affected by the presence of gaseous fuel. As the quantity of gaseous fuel increased keeping load constant, the peak cylinder pressure decreased significantly. But, the slope remained almost same regardless of load. Ignition delay increased with increase in the percentage mass of NG. The increase is due to the reduction of charge temperature close to the point of fuel injection and high overall specific heat capacity (Karim, 1980 and Heywood, 1988). Under dual fuel operation, there was an increase of combustion duration with increasing NG mass ratio. For a diesel/producer gas dual fuel operation, Roy et al. (2009) have investigated that 20% H_2 content in producer gas operation took 4–5°CA less than to the case with 13.7% H_2 content operation in both normal and two stage combustion. In another experimental work, diesel/syngas (with 10% H_2) mode shortened the ignition delay and duration of combustion in dual fuel operation (Boehman and Le Corre, 2008).

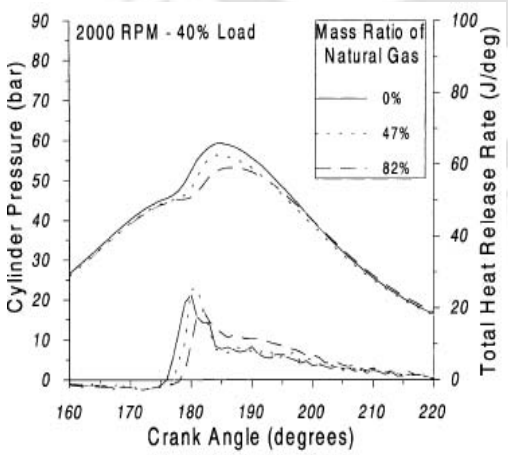

Figure 2.20 Experimental cylinder pressure and heat release traces under normal diesel and dual fuel operation at 40% of engine load (Papagiannakis and Hountalas, 2003)

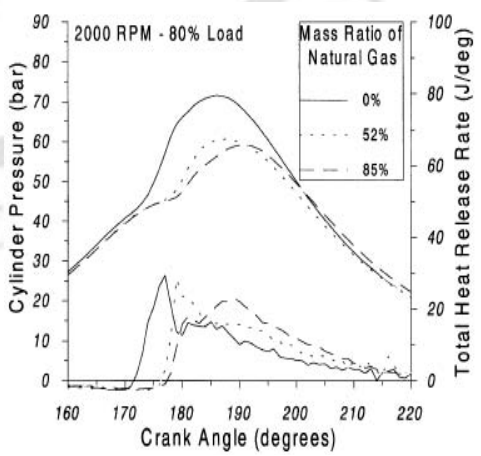

Figure 2.21 Experimental cylinder pressure and heat release traces under normal diesel and dual fuel operation at 80% of engine load (Papagiannakis and Hountalas, 2003)

(b) Efficiency

Laboratory investigation was carried out by Bari (1996) to see the effect of CO_2 on the performance of biogas/diesel duel fuel engine. At certain percentage of diesel substitution by NG (15, 30, 50 and 75 %), the pure CO_2 is introduced with the NG. The speed and power were maintained at constant level by varying the quantity of diesel flow. When the percentage of CO_2 in biogas was increased, the biogas supply to produce the same power also increased. The CO_2 in the mixture dissociated into CO and oxygen, because the flame temperature of diesel was very high to initiate dissociation. CO is comparatively fast burning gas than other alternative fuels (Chigier, 1981), thus the burning rate of the total gas-air mixture accelerates for the presence of CO. The amount of oxygen found by dissociation of CO_2 increased the concentration of oxygen in the gas air mixture. Therefore, it reduced the ignition delay as well as enhanced the combustion of unburned carbon particles. Under the above conditions, the engine performance was found comparatively better with lower 'bsfc' and diesel flow rates. When the percentage of CO_2 becomes higher in the gaseous mixture, CO_2 remained undissociated. This undissociated CO_2 acts as inert gas. Addition of such inert gas affects the burning velocity of gas-air mixture (Zhanghou, 1990). Therefore, it resulted incomplete combustion and increased 'bsfc'. Bari (1996) has suggested that, biogas containing more than 40% CO_2 needs scrubbing, because of the harsh running of the engine.

Henham and Makkar (1998) have conducted tests on the dual fuel diesel engine at various proportions of gas mixture comprising of NG and CO_2. The gasoil was substituted by NG at four constant levels (22%, 37%, 45% and 58%). Then, taking each constant level of NG as 100%, it was mixed with CO_2 to vary the composition of gas mixture. The overall efficiency dropped with NG substitution at all constant levels. On mixing NG with CO_2 efficiency was not much affected up to 37% NG substitution. With higher NG substitution, efficiency decreased with increasing CO_2 in gas mixture. At 58% NG substitution level, efficiency decreased from 28.2% to 26.2%. With higher gas substitution a greater proportion of air was replaced by gas. Hence, volumetric efficiency of the engine was lowered and it resulted in less power. Using similar type of simulated biogas in a SI engine, the researchers have found lower power and thermal efficiency for the dual fuel mode (Huang and Crookes, 1998). Papagiannakis and Hountalas (2003) have examined the dual fuel engine performance characteristics by varying the mass ratio of NG. At part load under dual fuel operation, the 'bsfc' was considerably higher as compared to the diesel mode, mainly as a result of the low combustion rate of gaseous fuel. A similar trend was observed at high load under dual fuel

operation, but in this case the slope of 'bsfc' increment with NG mass ratio was lower compared to the one at part load. Considering the fact that although the LHV of NG is higher compared to the diesel fuel used, its 'bsfc' was even higher. This reveals a poor utilization of the gaseous fuel due mainly to the lower temperature inside the combustion chamber and the late start of ignition because of the higher ignition delay (Hountalas, 2000).

Selim (2004) has investigated the effects of the amount of gaseous fuel in a dual fuel diesel engine. For all the three tested gaseous fuels, the torque was increased with increasing the amount of gaseous fuel. The author observed that the torque and thermal efficiency for the dual fuel engine using pure methane was higher than that of the NG mixture which was higher than LPG. This is due to the higher LHV for methane (50 MJ/kg) compared to the NG (47.7 MJ/kg) mixture and LPG (46.1 MJ/kg). The dual fuel engine, for all fuels used, however, suffers from low thermal efficiency at part load, and then it increased with increasing load by increasing the mass of gaseous fuel admitted. In their experimental results, Stewart *et al.* (2007) have found a reduction of 20% energy consumption for propane at both half- and three-quarters-load cases. This is attributed to the enhanced reactivity of the fuel. Methane was found to increase the BSEC for all cases. However, maximum gas substitution levels were obtained while using methane. Roy *et al.* (2009) have investigated the effect of variation in the H_2 content of the producer gas with diesel for dual fuel operation. For 20% H_2 content in producer gas, they found a broader window of fuel-air equivalence ratio (0.42–0.79) with the highest indicated thermal efficiency of 37–38% or more. Where as for 13.7% H_2 content the optimum window of equivalence ratio was narrower (0.52–0.68) for a similar level of indicated thermal efficiency. This suggests that the 20% is superior to the 13.7% H_2 content producer gas dual fuel operation. For a hydrogen/diesel dual fuel operation, Masood *et al.* (2007) have also retrieved maximum brake thermal efficiency from the engine with 100% hydrogen. Also, they found that hydrogen performs better at high compression ratios.

(c) Emissions

Papagiannakis and Hountalas (2003) have described the dual fuel engine exhaust emission characteristics by varying the mass ratio of NG. At part load, as the NG mass ratio increased, soot concentration decreased sharply. With high engine load and at higher mass ratios, soot decreased sharply as compared to diesel mode. This is due to the higher gas temperature that promotes soot oxidation rate contributing to a further decrease of soot concentration. Taking these into consideration for dual fuel operation, use of a high percentage of NG is an efficient way to reduce soot concentration. Practically, the gaseous fuel produces no soot. It is widely

recognized that the high oxygen concentrations and high charge temperatures favor the formation of nitric oxide (NO) (Kouremenos *et al.,* 1997; Kouremenos *et al.,* 1999; Lavoie *et al*., 1970; Rakopoulos *et al*., 1995). At high engine load and low mass ratios of NG, there was a sharper decrease of NO concentration compared to part load conditions with increase in gaseous fuel percentage. The reduction of NO concentration is due to several factors; the less intense premixed combustion, the reduction of gas temperature due to increase of the specific heat capacity, the slower combustion, and the reduction of oxygen concentration due to presence of the NG mass ratio which replaces an equal amount of air in the cylinder charge. At low load, with increase of gaseous fuel percentage, the low charge temperature combined with a slower burning rate led to increase in HC emissions. At high engine load, there was an increase of HC emissions with increasing gaseous fuel mass ratio. This is due to the increase of burnt gas temperature, which promotes the oxidation of UBHC. Under dual fuel operation, the filling of the crevice volumes with unburned mixture of air and gaseous fuel during compression and combustion while the cylinder pressure continues to rise, is an important source dominating the formation of HC emissions. At part load, increasing the amount of gaseous fuel increased the CO level sharply. This is due to the slow combustion rate of gaseous fuel, which maintains the charge temperature at low levels resulting to a reduction of the oxidation process of CO. At high engine load, CO emissions increased with increasing NG mass ratio. However, beyond a certain value of gaseous fuel mass ratio they started to decrease, as a result of the high gas temperature and faster combustion rate. In general, CO emission values under dual fuel operation are considerably higher compared to diesel mode.

In an experiment Henham and Makkar (1998) found that the emission of CO was affected mainly by NG substitution and not so much by the proportion of CO_2 in the gas mixture. The increase in CO emission as compared to that with gasoil mode was caused by the lower air-fuel ratio. In a syngas/diesel operation, when diesel substitution level was increased, the CO_2 and NO_x emissions were increased as well (Garnier *et al.,* 2005). Increase in CO_2 emissions were expected because of a significant part of CO_2 (12%) presence in syngas. However, dual fuel engines use a fuel with a higher carbon-to-hydrogen ratio and therefore, they produce lower CO_2 emissions per unit volume and energy of fuel used (Stewart *et al.,* 2007). For the case of primary fuel CH_4, the authors reported a 20% reduction of CO_2 based on g/kWh. The use of high H_2 content producer gas in a diesel/producer gas mode reduced the HC and CO emissions (Roy *et al.,* 2009). The authors reported about 10–25% lower HC and CO leves with 20% H_2 content producer gas than that with 13.7% H_2 content. But the NO_x emissions

with 20% H_2 content producer gas were found very high. Similar traces of results for emissions are also investigated by Masood *et al.* (2007) for their diesel/hydrogen dual fuel experiments. Li and Karim (2005) have changed the fuel composition for hydrogen–methane mixtures through the addition of some H_2 to CH_4. They observed that there were significant changes in the NO_x emissions only for lean mixture operation while, very much less changes were encountered for stoichiometric mixture operation. However, CO dual fuel mode produced higher NO_x emissions than those with methane or the hydrogen–methane mixtures tested over a wide range of equivalence ratio. In a syngas-diesel operation, NO_x emissions were found to be increased due to the presence of hydrogen in the syngas which caused the increase of adiabatic flame temperature (Boehman and Le Corre, 2008). The effects of different H_2/CO ratios on a diesel engine by introducing simulated reformed exhaust gas recirculation (REGR) into the engine suction have been reported by Tsolakis *et al.* (2005). The combustion of REGR with maximum H_2 and minimum CO contents resulted in the highest reduction of NO_x emissions. In all the examined cases, the use of REGR have resulted reduced NO_x and smoke emissions. Similar type of test results were also observed by Abu-Jrai *et al.* (2007, 2009) by varying H_2/CO ratios in the same engine.

2.2.8 Effect of pilot fuel quality

Energy conversion alone is inadequate to satisfy long-term energy demands and to gain independence from petroleum based fuels. Therefore, all potential fuel alternatives are to be recognized and examined. Fossil fuel combustion is the main culprit in environmental pollution, whilst the impacts of vegetable oil fuel systems are on the whole less adverse and more localized than those of fossil fuels (Nwafor, 2000b). Bio-diesel, an alternative diesel fuel, is made from renewable biological sources such as vegetable oil and animal fats. It is biodegradable, non-toxic and possesses low emission profiles. Also, the uses of bio-fuels are environmentally beneficial. The name bio-diesel was introduced in the United States during 1992 by the National Soy Diesel Development Board (presently National Bio-diesel Board). Chemically, bio-diesel is referred to as the mono-alkyl-esters of long-chain-fatty acids derived from renewable lipid sources. Bio-diesel is the name for a variety of ester based oxygenated fuel from renewable biological sources. It can be used in CI with little or no modifications (Goldemberga and Coelhob, 2004).

The use of rape methyl ester (RME) and neat rapeseed oil as pilot fuels to NG was investigated by Nwafor (2000b). The thermal efficiency of the engine with diesel fuel and the RME pilot was similar and lower than the values obtained for neat rapeseed oil at both speeds

of investigations. The neat rapeseed oil pilot system exhibited the longest delay period at light loads. HC emissions with diesel fuel and rapeseed oil systems were similar at the speed of 3000 rpm. Selim *et al.* (2008) have used jojoba methyl ester (JME) as pilot fuel to NG and LPG in a dual fuel diesel engine. They found that using JME the engine made to knock later at high output at high compression ratio of 22. The combustion noise was lower for JME for wider ranges of loads, at different compression ratios. Using JME in the dual fuel engine reduced both the average pressure rise rate. Some results also suggested that bio-diesel and vegetable oils as pilot fuels can improve engine performance (Kumar *et al.,* 2001; Nwafor, 2000b; Selim *et al.,* 2008). In an another research, using the supercharged mixing system combined with bio-diesel as pilot fuel, thermal efficiency and substitution of pilot fuel were increased, whereas methane and CO emissions were reduced (Bedoya *et al.,* 2009). Bio-diesel also reported as a possible substitute or extender for conventional diesel because of their similar characteristics (Otera, 1993; Sharma and Singh, 2008). However, their use in dual technology has not been documented extensively.

Based on above successful investigations, in this work, jatropha oil methyl ester (JOME) was used as pilot fuel. A jatropha plant grows almost anywhere, even on gravely, sandy and saline soils with low water requirement. Jatropha oil, a non-edible oil, exhibits higher calorific value and cetane number compared to others like karanja oil, rapeseed oil, rice bran oil, and cottonseed oil etc. Jatropha oil is converted into JOME by the transesterification process. This involves making the triglycerides of jatropha oil to react with methyl alcohol in the presence of a catalyst (NaOH/KOH) to produce glycerol and fatty acid ester. Bio-diesel having higher cetane numbers than petroleum diesel leads to a shorter ignition delay and in turn it leads to a non-intuitive decrease in NO_x emissions (Tat, 2003). The properties of diesel and methyl ester of jatropha oil are given in Table 2.4. The above literature studies, by different researcher(s), have revealed the effect of engine parameters and type of gaseous fuel on the performance of different dual fuel diesel engines are summarized in Table 2.4.

Table 2.4 Properties of diesel and methyl ester of jatropha oil
(Naeser and Bennet, 1980; Basker, 1993)

Sl No.	Properties	Diesel	JOME
1	Density (kg/m^3)	840	880
2	Calorific value (kJ/kg)	42,490	38,450
3	Viscosity (m^2/sec)	4.59×10^{-6}	5.65×10^{-6}
4	Cetane number	45-55	50
5	Flash point (°C)	50	170
6	Carbon residue (%)	0.1	0.5

Table 2.5 Comparison of results by researcher(s) on the performance of dual fuel diesel engines

Researcher(s)	Performance of dual fuel diesel engines
Effect of engine load	
Papagiannakis and Hountalas (2004); Hountalas (1994)	Compared to the normal diesel operation: inferior 'bsfc' at the same engine operating conditions, lower peak cylinder pressure at a given load condition, longer combustion duration at low load. Lower NO_x, drastic decrease in soot emissions, but higher CO and HC emissions.
Selim (2001); Nielsen *et al*. (1987)	Increased combustion noise with increase in load, always higher than that of the diesel fuel case.
Singh *et al*. (2007a)	A minor reduction in engine output (1-2%) compared to the diesel case. Reduced CO, CO_2, NO and NO_2 while HC and exhaust gas temperature increased.
Singh *et al*. (2007b)	Higher brake thermal efficiency with bio-diesel/producer gas than diesel/producer gas dual fuel operation. Significant reduction in NO_x emission from producer gas/bio-diesel dual fuel operation.
Stewart *et al*. (2007)	Increase in the carbon number of the primary fuel reduced the initial rate of heat release and hence, the diffusion stage of combustion was increased. This limits the primary fuel substitution.
Uma *et al*. (2004) ; Parikh *et al*. (1989) ; Sridhar *et al*. (2001) ; Singh *et al*.(2007a)	Decreased engine performance at part load conditions for both diesel and dual fuel modes. Higher CO emissions at all operated load conditions and little higher HC emissions compared to diesel case. But, dual fuel operation reduced NO_x and SO_2 without increasing particulate emissions.
Ramadhas *et al*. (2006, 2008)	Decreased engine performance with increase in emissions at part load conditions both at diesel and dual fuel mode. Higher CO emission from the dual fuel mode than that of diesel mode under all load conditions.
Banapurmath *et al*. (2009)	Lower brake thermal efficiencies of engine with dual fuel operation with all the injected fuels than diesel fuel operation. The magnitude of engine derating was in the order of 30 %. Lower smoke and NO emissions while HC and CO emissions were higher than diesel operation.
Effect of engine speed	
Mansour *et al*. (2001)	A light power and torque losses with regard to the diesel mode, except around the speed of 2400 rpm. Slightly higher equivalence ratios for a given speed condition. Slightly higher maximum combustion pressure for all engine speeds than the diesel fuelling level.
Papagiannakis and Hountalas (2004)	The increase of engine speed under dual fuel operation results in a further decrease of NO_x values compared to normal diesel operation.
Selim (2001, 2004); Imoto *et al*. (1997); Selim *et al*. (2008)	Decreased pressure rise rate with increase in engine speed and higher than that for diesel case.
Selim (2004); Tippayawong *et al*. (2007)	Increasing the engine speed increased the brake power output, led to a decrease in the 'bsfc' and consequently improved the thermal efficiency.
Selim *et al*. (2008)	Reduced CO and HC emission with increase in speed. Higher power output for an increase in speed.

Effect of pilot fuel injection timing	
Abd Alla *et al*. (2002)	Improved thermal efficiency with advance injection timing but early knocking at medium and high loads. Increase in NO_x, reduction in CO and UBHC emissions with advance injection.
Krishnan *et al*. (2004)	Increased fuel conversion efficiency within injection timing of 15 ^{0} to 45 ^{0}BTDC and decreased afterwards. Decreased peak heat release rates with retard injection timing. Higher NO_x for timing 45 ^{0}BTDC than those for very retarded (15 ^{0}BTDC) or very advanced (60 ^{0}BTDC) timings.
Nwafor (2000a)	Lower thermal efficiency with both advanced and standard timing compared to diesel case. Longer delay periods for standard dual timing at high loads than the advanced injection timing operation. Higher HC emissions and exhaust temperatures with advanced timing.
Selim (2001, 2005)	Higher MPRR than that for the diesel mode for the injection advance increase (25 to 40 ^{0}BTDC). Comparable MPPR for both diesel and dual fuel cases with late injection (20 to 25 ^{0}BTDC).
Selim (2004); Selim *et al*. (2008)	Reduced torque output and the thermal efficiency with advanced pilot fuel injection timing. But, it increased the maximum pressure and MPRR.
Banapurmath *et al*. (2008)	Moderate improvement in the brake thermal efficiency with advanced injection timing.
Lekpradit *et al*. (2008)	Higher brake thermal efficiency for dual fuel engine with advanced injection timing than the diesel engine on standard timing injection. Lower CO and highest NO_x emissions for the advanced injection timing.
Effect of mass of pilot fuel inducted	
Abd Alla *et al*. (2000)	Improved thermal efficiency by increasing the amount of pilot fuel but leads to early knocking at high loads. Increase in NO_x, reduction in CO and HC by increasing the amount of pilot fuel.
Badr *et al*. (1999)	Exhaust emissions of the CO and CH_4 were unaffected by the pilot quantity within a limiting equivalence ratio.
Nwafor (2002)	Reduced the knocking phenomena with increased pilot fuel and reducing primary fuel.
Selim (2001)	Increased engine torque with increase in the pilot fuel mass. Lower maximum pressure and MPRR for a pilot fuel mass of 0.52 kg/hr, and it increased for a lower or higher amount.
Selim (2004); Selim *et al*. (2008)	Increased torque output and thermal efficiency with increase in the quantity of pilot fuel. Higher maximum combustion pressure but reduced MPRR with increase in the pilot fuel mass.
Effect of engine compression ratio	
Selim (2004)	Earlier knocking when a high compression ratio is used in the dual fuel engine. Increasing the compression ratio generally increases the combustion noise.
Selim *et al*. (2008)	Reduced combustion noise for a reduction in the compression ratio with extended in the ignition limits. Increased the power as the expansion ratio increases for an increase in the compression ratio. Reduced CO and HC emission with increase in compression ratio.
Effect of engine intake manifold conditions	
Kusaka *et al*. (2000)	Improved thermal efficiency and reduced HC and NO_x emissions for the EGR with intake heating. EGR controls the rate of pressure rise. Deterioration of combustion characteristics with excessive EGR ratio (>50%).

Effect of type of gaseous fuel	
Bari (1996)	Not much deterioration in the 40% CO_2 in biogas engine performance as compared to the engine with NG (96% methane). Whereas, improved the 30% CO_2 in biogas engine performance as compared to the same running with NG.
Henham and Makkar (1998)	Overall efficiency falls with gas mixture substitution and adding CO_2, and this is more at higher speed. Possible 60% gasoil substitution without knock. Exhaust temperature affected more by NG substitution than by CO_2 addition except at maximum NG substitution. CO affected mainly by NG substitution and less by gas quality. More rapid pressure rise on combustion.
Papagiannakis and Hountalas (2003)	At high load, lower increment of 'bsfc' slope with NG mass ratio as compared to the one at part load. Decreased cylinder pressure with increase in the amount of NG. Increased combustion duration with increase in NG mass ratio. Sharp decrease in soot concentration, lower NO, and high HC and CO emissions with increase in NG mass ratio.
Selim (2004)	Increasede MPRR and maximum pressure with increase in the mass of gaseous fuel.
Masood *et al*. (2007)	Increased thermal efficiency with increased percentage of fuel-gas. At 100% load, lower HC and CO with high NO_x emissions for an increase in hydrogen substitution for all compression ratios.
Roy *et al*. (2009)	A broader window of fuel-air equivalence ratio and higher engine power using high H_2 content producer gas. Lower combustion duration, lower HC and CO emissions, and higher NO_x for high H_2 content producer gas dual fuel operation.
Effect of pilot fuel quality	
Nwafor (2000b)	Similar and lower 'bsfc' for NG dual fuel mode with diesel and the rapeseed oil pilot injection than when running on rape methyl ester pilot injection.
Selim *et al*. (2008)	Using jojoba methyl ester (JME) made the engine to knock later at high output than pilot diesel ignition. At different compression ratios, lower combustion noise for JME for wider ranges of loads. Reduced both average pressure rise rate as well as its standard deviation using JME.
Kumar *et al*. (2001); Nwafor (2000b); Selim *et al*. (2008)	Improved engine performance with bio-diesel and vegetable oils as pilot fuels as compared to diesel pilot ignition.
Bedoya et al. (2009)	Increased thermal efficiency and pilot fuel substitution level by using the supercharged mixing system combined with biodiesel as pilot fuel. Reduced methane and CO emissions.
Banapurmath *et al*. (2008)	Reduced thermal efficiency, higher smoke, CO, NOx, and HC, and lower liquid fuel substitution with bio-diesel and vegetable oils as pilot fuels as compared to diesel pilot ignition.
Ramadhas *et al.* (2008)	Higher rubber seed oil pilot fuel consumption than that of diesel pilot case. Higher CO emission of rubber seed oil-producer gas operation than diesel-producer gas operation under all load conditions.
Singh *et al.* (2007b)	Higher brake thermal efficiency using producer gas/bio-diesel than diesel/producer gas mode. Reduced NO_x emission of producer gas/bio-diesel mode but it increased the other pollutants.

2.3 Availability Analysis of IC Engines

The concept of 'availability' (also called 'exergy') is introduced by the second law of thermodynamics. The availability of a thermodynamic system is defined as the maximum useful mechanical work that can be produced when the system is brought to thermal, mechanical and chemical equilibrium with its environment through reversible processes. It is an extensive property of the system and depends on both the state of the system and on the properties of the environment. The state of the environment is referred to as the dead state, defined by the environmental temperature, pressure and composition. A standard reference environment normally adopted in the availability analysis (Moran, 1982) is shown in Table 2.6. In availability analyses of thermal systems, it is customary to divide the availability content of a system into two parts:

i. *The thermo-mechanical availability*: It refers to the maximum useful mechanical work extractable as the system comes into thermal and mechanical equilibrium with the surrounding atmosphere. The mass of the system is not permitted to pass or chemically react with the environment. The thermal and mechanical equilibrium are achieved when both the temperature and pressure of the system are equal to that of the environment. This specific state of the system is called the restricted dead state.

ii. *The chemical availability*: One part of the chemical availability of a system concerns only the system's species that are also present in the environment, known as diffusion availability. Whereas, the other part, called reactive availability, concerns the amount of work developed by allowing species of the system to chemically react with substances of the environment in order to form also environmental species (Chavannavar and Caton, 2006). The system achieves the chemical equilibrium when any of its components unable to interact in any way with those of the environment in order to produce work.

Table 2.6: Standard reference environment (Moran, 1982)

$T_0 = 298.15\ K$	$P_0 = 1.01325\ bar$
Substance	*Molar fraction*
N_2	0.7567
O_2	0.2035
H_2O	0.0303
CO_2	0.0003
Other (e.g. Ar)	0.0092

Whether it is an IC engine or not, the application of traditional first law theory to a thermodynamic system fails to give the best insight into the engine's operation (Flynn *et a.,* 1984; Moran, 1982; VanGerpen and Shapiro, 1990). Therefore, the second law analysis should be coupled to the first law. The second law analysis provides the knowledge of when and where the available energy is lost or destroyed in the engine system. Evaluation of available energy determines the maximum possible performance of a thermodynamic system (Caton, 2000a). In addition, impact of process change in the system in terms of system losses is also assessed. These findings help in reducing the availability loss to improve the performance of the engine in terms of efficiency and power output (Kumar *et al.,* 2004). In an IC engine operation, availability analysis reveals the capability of working medium to produce useful mechanical work: (a) destroyed due to thermodynamic irreversibilities, such as combustion, heat transfer, mixing, throttling, friction, etc., and (b) lost due to undesirable availability transfers, such as heat transfer to the cylinder walls and loss of thermal energy to the exhaust (Rakopoulos and Giakoumis, 2006). These system losses data are used to develop an explanation of why engine performance is changed by the variation of design and operating parameters like speed, load and type of fuel etc.

Availability analysis from the second law application is not a new technique (Bruges, 1959). This type of analysis has used for many years for evaluating stationary systems (Brzustowski and Golem, 1976–77; Shapiro and Kuehn, 1980) and automotive engines (Flynn *et al.,* 1984; Primus *et al.,* 1984; Primus and Flynn, 1985; Al-Najem and Diab, 1992; Rakopoulos and Giakoumis, 1997; Kopac and Kokturk, 2005; Sahoo *et al.,* 2009b). Alkidas (1988) presented availability balance equations for a diesel engine on an overall basis. Various Cummins Engine Company researchers (Flynn *et al.,* 1984; Primus, 1984; Primus and Flynn, 1985; McKinley and Primus, 1988) presented a quantification of engine irreversibility. They reported the throttling and thermal mixing losses along with the well established combustion irreversibility. In contrast, Van Gerpen and Shapiro (1990) performed a detailed theoretical analysis for the closed part of the cycle bringing in focus the controversial term of chemical availability. A different type of study, the combined energy and exergy analysis can be used to determine an optimum engine condition. In this context, the energy efficiency was found maximum at a speed of 2040 rpm whereas maximum exergy efficiency found at a speed of 2580 rpm for a SI engine operation (Kopac and Kokturk, 2005). In another study, Sahoo *et al.* (2009b) have selected the optimum engine speed of a diesel engine for a given throttle opening position under a single loading condition using second law analysis.

A thermodynamic cycle simulation was used to obtain the availability characteristics as functions of speed and load for a SI engine (Caton, 2000b). The availability destroyed (as a percentage of the fuel availability) by the combustion process resulted in the range between 5 and 25%. This fraction found lowest for the highest speed and load. The author also investigated the effects of compression ratio (CR) and expansion ratio (ER) on second law parameters for a SI engine (Caton, 2007; 2008). This study examined the cases of part load and wide open throttle condition at different CRs and ERs. In another work, Chavannavar and Caton (2006) studied the destruction of availability at constant pressure, volume, and temperature combustion processes for isooctane vapor-air mixtures. The results of this work showed that the availability destruction decreased with increasing reactant temperatures.

Recently, Rakopoulos and co-workers are carrying out their significant effort on availability analysis research in IC engines using of various alternative fuels including syngas. Rakopoulos and Kyritsis (2001) have developed a method for computing both combustion irreversibility and working medium availability in a diesel engine cylinder. They calculated the combustion irreversibility analytically as a function of fuel reaction rate using the second law analysis and a chemical equilibrium hypothesis. The same authors (Rakopoulos and Kyritsis, 2006) also studied the availability balance computationally using a zero-dimensional model during combustion of hydrogen-enriched natural and landfill gases. From the second law view point, combustion of hydrogen showed qualitatively different from the combustion of hydrocarbon fuels. Rakopoulos and Michos (2008) have developed a multi-zone combustion model for prediction of SI engine performance and NO emissions. The availability analysis of the same engine was also presented with varying load using syngas as fuel (Rakopoulos *et al.,* 2008). The computed NO emissions from the multi-zone model for various engine loads found to be in good agreement with the respective experimental ones.

Continuing with the dual fuel availability analysis, to study the part load conditions of a NG-diesel engine, a quasi-two-zone combustion model has been developed by Hosseinzadeh and Saray (2009). The combustion phenomenon of the dual fuel engine was studied by increasing pilot fuel quantity. It was found that increasing the pilot fuel quantity increased the work availability and reduced chemical availability of unburned fuels. Also, the results indicated that, increasing the pilot fuel quantity by about 12% resulted in an increase of 23% in availability destruction and 29% in the second law efficiency as compared to the baseline dual fuel engine. This enhancement is due to a better combustion progress and increased

indicated work for a high amount of pilot fuel quantity. The effects of hydrogen addition on the exergy balance in a lean burn NG SI engine was presented computationally in the reference (Ozcan, 2010). A thermodynamic engine cycle simulation was extended to perform the exergy analysis. A zero-dimensional, two-zone computational model of the engine operation was used for the closed part of the cycle. The results showed with increasing hydrogen content, the irreversibility produced during combustion decreased, and the second-law efficiency sharply increased at near the lean limit.

Fuel consumption in an IC engine is affected by a number of factors; equipment type, engine speed and load, type of loading etc. When an engine is operated at its rated power at any load condition, further throttle opening adds nothing to its performance. Hence, for an engine fuel economy, the engine and road speeds are to be matched to the throttle opening. 'Gear Up and Throttle Down' is a fuel saving technique in which a substantial amount of fuel can be saved by shifting vehicle to a faster gear and slowing the engine speed by reducing the throttle openings to maintain the desire engine speed. Towards this, an experiment was conducted in a multi-cylinder DI diesel engine to determine the optimum engine speed of a diesel engine for a given throttle opening (TO) position under a single loading condition (Sahoo *et al.,* 2009b). This was done by analyzing the experimental data through the second law of thermodynamics which provides histograms of calculated availability and irreversibility terms. The authors varied the engine speed at different engine loads with different TO positions. At 70% load, the engine speeds were recorded as 2000, 3500, and 4500 rpm for the variations of 50, 75, and 100% TO respectively (Fig. 2.22). At 70% load, the shaft availability was calculated maximum as 30.2% at 50% TO compared to 27.1 and 23.2% for 75 and 100% TO respectively. Also, 50% TO position showed the condition of maximum exergy efficiency and minimum 'bsfc'. The exergy efficiencies were found as 45, 44.5, and 40.6% (Fig. 2.23) where as the bsfc were 0.27, 0.31 and 0.38 kg/kWhr for 50, 75, and 100% TO respectively. Hence, combining all the findings, at 70% load, 2000 rpm was determined as the true optimum engine speed at 50% TO position. Similar type of analysis with 90% and 100% load revealed their optimum speeds as 2300 rpm at 75% TO and 3250 rpm at 100% TO positions respectively. For variations in the vehicle road speed, an appropriate gear can be engaged to the engine crankshaft without changing the above optimum operating condition which can reduce the fuel consumption and improve the engine fuel economy.

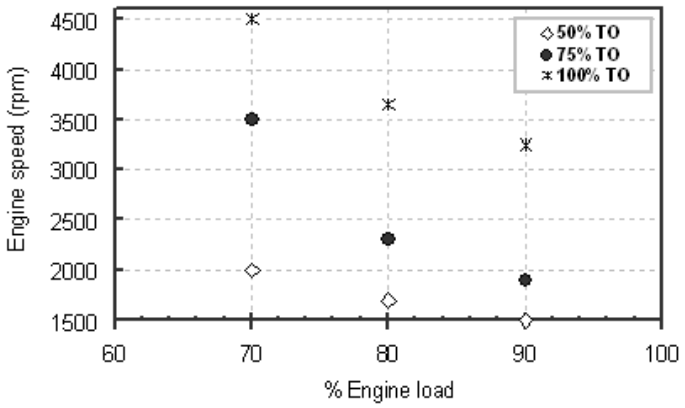

Figure 2.22 Variations of engine speed at different engine load (Sahoo *et al.,* 2009b)

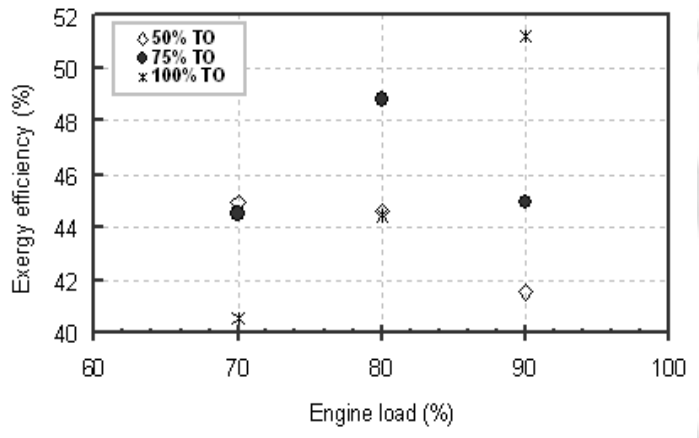

Figure 2.23 Comparison of exergy efficiency at different load (Sahoo *et al.* 2009b)

2.4 Scope of the Work

The comprehensive literature survey has indicated the presence of a significant amount of work on the use of natural gas in compression ignition diesel engines. Much of the methods used for natural gas can also be used for biogas as a result of similarities in properties of gas. From the already published works, most researchers concentrated on SI engines. The authors' research work concerns the use of biogas in dual fuel diesel engines. Including this, much of the literature reviewed on biogas has used simulated biogas for their dual fuel applications. However, there were very little attempts to use actual biogas in diesel engines. The issues that stand out are the diesel engine performance behavior of actual biogas combustion under dual fuel operation. Again, there is a significant number of small or low-power single-cylinder engines currently operated worldwide for irrigation and small scale power generation. Most of these small engines are used in rural or remote areas where they encounter problems of

liquid fuels shortage. The technical issues of these small single cylinder diesel engines that can efficiently utilize biogas are yet to be systematically addressed.

Syngas is ideally a mixture of H_2 and CO produced by gasifying a solid fuel feedstock (such as coal or biomass). In its simplest form, syngas is composed of two diatomic molecules CO and H_2 that provide the building blocks upon which an entire field of fuel science and technology is based. Over the years, the gaseous mixture of CO and H_2 has had many names depending on how it was formed; producer gas, town gas, water gas, synthesis gas, and syngas etc. to name a few. Generally, the volumetric H_2/CO ratios of syngas fuels vary greatly depending on the source and the processing technique. The different combinations of H_2/CO ratio in syngas affect the efficiency, combustion and emissions of an IC engine when used in dual fuel mode. In the previous literatures, several researchers have conducted tests on various types H_2 and CO composition syngas fuels. In these published works, there was more information regarding the type and composition of used gaseous fuels while very little detailed information about engine geometry was mentioned. This makes more difficult to evaluate or analyze the reported results because the engine performance, combustion and exhaust gas emissions depend not only on the properties of the gaseous fuels but also on the characteristics of engines tested. In addition, almost all past investigations were conducted with different engines test benches with controlled engine cooling water and lube oil temperatures to a predetermined value. However, this is contrary to real operational conditions. Including this, as found from the previous literatures, the use of only CO gas as a fuel for CI engines under dual fuel mode is not explored.

The second law analysis provides the knowledge of when and where the available energy is lost or destroyed in the engine system. Evaluation of available energy determines the maximum possible performance of a thermodynamic system. In addition, impact of process change in the system in terms of system losses is also assessed. These findings help in reducing the availability loss to improve the performance of an engine in terms of efficiency and power output. The availability analysis has been used for many years for evaluating stationary systems and automotive engines. However, too little has been done towards the thermodynamic analysis of dual fuel IC engines.

Therefore, to solve the above mentioned problems from previous literatures, the present contribution is focused to perform a systematic experimental investigation including the

thermodynamic behavior of a CI diesel engine under dual fuel mode. The following objectives have been addressed in the present investigation:

- **Optimization of engine operating and design parameters.**
  It is found from several published literatures that the dual fuel operations behave differently to the changes in operating and design parameters. Load is an important operating parameter for dual fuel operations because the engine performance at part load varied remarkably to the medium and high load cases. Again, the characteristics of a dual fuel engine such as, efficiency, ignition delay and emissions vary much to the changes in the fuel composition. Therefore, in this work, various engine parameters such as load, pilot fuel quality and gaseous fuel type, are optimized for minimum emissions and maximum efficiency from the dual fuel operations.
- **Maximum replacement of fossil petroleum diesel fuel.**
  During dual fuel operations fossil diesel, even a small amount, used for pilot ignition of gaseous fuels, have the shortcomings of emitting of air pollutants. Hence, to reduce dependence on foreign petroleum fossil fuels and mitigate GHG emissions, a diesel like fuel, bio-diesel, is employed in this work as the fuel-gas ignition source.
- **Energy and exergy analysis for dual fuel engine operation.**
  The performance characteristics of dual fuel modes are quite different to the diesel mode. To have the knowledge of energy losses whereabouts the combined energy and exergy analyses are added to this research program. Whether the dual fuel mode efficiency able to surpasses the diesel mode efficiency? The availability analysis will able to determine this for both the systems. In addition, impact of changes in the design and operating parameters of the dual fuel system in terms of system losses can also be assessed. These findings will help in reducing the availability loss to improve the performance of the engine in terms of efficiency and power output.
- **CDM potential of CI diesel engines using gaseous fuels under dual fuel operation.**
  The principal aim of this research program is to pull through diesel engines from their greenhouse gas emissions of CO_2 and CH_4. To satisfy this, the two utilized alternative gaseous fuels have to qualify their potential towards clean development mechanism under dual fuel mode. Hence, this important investigation of the biogas and syngas dual fuel operations is to be executed to meet the aim of this research work.

2.5 Summary

The review of the earlier work have clearly suggested that several engine operating and design parameters have effects on the performance, combustion and emission characteristics of dual fuel diesel engines. However, the systematic investigations of individual parameters relevant to engine characterization have not been reported exhaustively. The evaluation of available energy is capable of assessing the impact of process change in the system in terms of system losses. This finding helps in reducing the losses to improve the performance of the engine in terms of efficiency and power output. However, there were only few literatures accessed on availability analysis of dual fuel engines. Therefore, the present contribution is focused to perform a systematic experimental investigation including the thermodynamic behavior of diesel engine under dual fuel mode. To accomplish the objective, a small CI diesel engine has been chosen for the experimental work. The details of laboratory setup required for the dual fuel operations are described in the following Chapter.

Chapter – 3

EXPERIMENTAL SETUP AND PROCEDURES

Overview

Diesel engines emit carbons in their exhaust which contribute the global greenhouse gases. Researchers have suggested that dual fuel mode with gaseous fuels should be employed to mitigate greenhouse gas emissions from diesel engines. To solve this problem, the present contribution decides to perform a systematic experimental investigation using gaseous fuels under dual fuel mode of operation. It is decided to optimize the engine parameters such as load, pilot quality and gaseous fuel type in this study. The conventional dual fuel (CDF) system is one of the methods is employed in this work. The CDF is a technique which requires little or, eventually no modification for CI engines conversion. In this method, the diesel injection system is retained for pilot ignition spray to the inducted air-gas mixture. The total experiments are conducted on a single-cylinder, four-stroke, constant-speed, and direct-injection CI diesel engine. This chapter elaborates the engine specification, the instruments used to perform measurements, the fuel supply systems, and the assisting software packages. It also provides details of experimental rig developed for conducting engine performance tests under dual fuel operation of two gaseous fuels viz., biogas and syngas, in a compression ignition diesel engine. The gas installation circuits assisting with various measuring instruments are added to the base diesel engine for the dual fuel operations. The necessary equipments are designed, fabricated and also modified. The diesel engine conversion methodology for dual fuel mode is presented in two parts. The first part discusses on biogas as primary fuel with diesel or jatropha bio-diesel as pilot ignition. While the second part deals with syngas-diesel dual fuel tests. This chapter is concluded with experimental testing procedures, experiment repeatability, computational procedure for various performance parameters and the experiment measurement uncertainty for both diesel mode and dual fuel mode operations.

3.1 The Engine Test Bed

The engine used in the present investigation is a single-cylinder, constant-speed, four-stroke, direct-injection, water-cooled diesel engine. It is designed for operating with diesel fuel with a conventional fuel injection system and loaded with an eddy-current type dynamometer. The injection nozzle has three holes of 0.3mm diameter with a spray angle of 120°. The engine is provided with a hemispherical combustion chamber. Cooling of the engine is accomplished by circulating water through the jackets of the engine block and cylinder head. The setup is installed with necessary equipment and instruments for combustion pressure and crank angle measurements. A piezoelectric pressure transducer is mounted flush with the cylinder head surface to measure the cylinder pressure. These signals are interfaced with computer through engine indicator for pressure-crank angle $(P-\theta)$, pressure-volume $(P\text{-}V)$ plots and engine indicated power. The liquid fuels are supplied to the engine injection pump from fuel tank under gravity feed. The air flow to the engine is monitored by passing the intake air through an air box with orifice meter and manometer. Type K thermocouples are installed on different locations of engine setup and connected to a data logger for measuring various temperatures. Provision is also made for interfacing air flow, fuel flow, temperatures and load measurements with personal computer. The software package is fully configured for $P-\theta$, $P-V$ plot and performance curves at various operating points. The salient features of the diesel engine chosen for this study are shown in Table 3.1. The base engine test bed is represented schematically in Fig. 3.1.

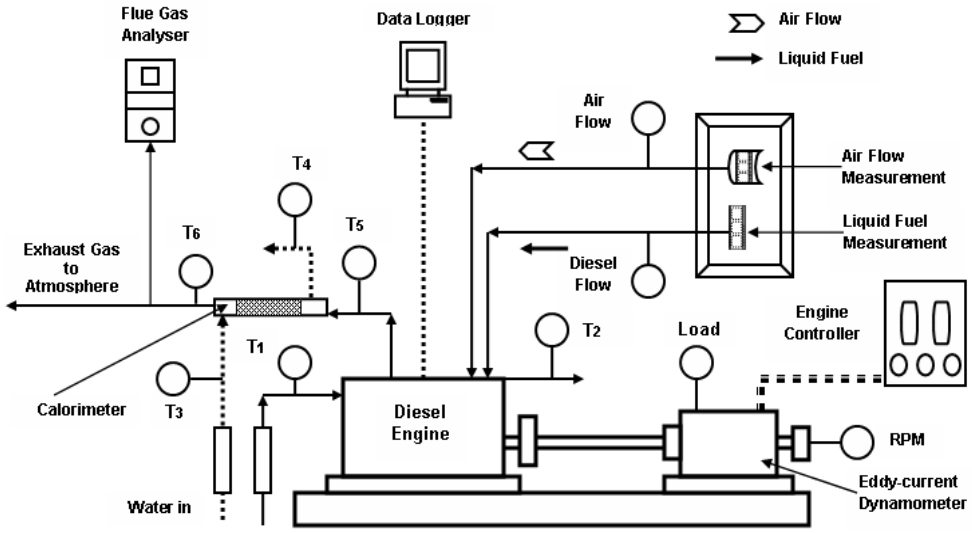

Figure 3.1 Schematic diagram of the base diesel engine with equipment

Table 3.1 Details of base diesel engine configuration

System specifications	
Parameter	*Specification*
Make and model	Kirloskar, Model TV1
Engine type	Single-cylinder, 4-stroke, DI diesel engine
Rated power (diesel)	5.2 kW (7 BHP) @1500 rpm
Type of cooling	Water cooled
Bore × Stroke	87.5 × 110 mm
Swept volume	0.661 Liter
Compression ratio	17.5:1
Speed	1500 rpm, constant
Injection pressure	210 bar
Injection timing (diesel)	23°BTDC
Combustion chamber	Hemispherical bowl-in piston type
Dynamometer	Eddy-current (Make: Saj, Model: AG10)
Governor	Mechanical governing (centrifugal)
Air flow	Orifice meter and manometer (100–0–100mm)
Fuel flow	Fuel measuring unit, range 0–450 ml
Speed indicator and sensor	Digital, non-contact type speed sensor
Load indicator	Model AX–271, 0–50kg, 230V AC
Load sensor	Load cell, type strain gauge, range 0–50kg
Temperature indicator	Type digital, multipoint
Temperature sensor	K type thermocouple
Rotameters	Engine cooling 40–400 lph, calorimeter 10–100 lph
Engine software	'Enginesoft' engine performance analysis software
Pressure transducer	
Make, type of sensor and maximum pressure	PCB make, Piezo electric (15000 psi)
Resolution and response time	0.1 psi, 2 micro seconds
Crank angle sensor	360 degree encoder with a resolution of 2 degree
System constants	
Orifice diameter	20 mm
Dynamometer arm length	185 mm
C_d for orifice	0.6
Specific Heat of Exhaust (C_p)	1.1 kJ/ kg-K
Air density	1.17 kg/m^3

3.2 Fuel Supply System

3.2.1 Gaseous fuel

Two gaseous fuels, biogas and syngas, were employed in the present experimental work. These gases were introduced individually to the engine manifold for their dual fuel operation. The primary gaseous fuel, biogas, was collected from Biogas Development Training Centre (BDTC), IIT Guwahati from a Samriddhi model type digester. Biogas was generated by the anaerobic digestion of cow manure and cook waste matter. The biogas was composed of about 48% CH_4 and 42% CO_2 by volume. The gas was collected in handy type storage balloons made of rubber sheet and then transported to the laboratory. The storing capacity of the balloon was $0.8m^3$ of gas at ambient conditions. The biogas from these balloons was supplied to the engine cylinder through a gas carburetor fitted in between balloon outlet and inlet manifold. The second gaseous fuel used for the experiment was 'syngas'. It is mainly a mixture of two energy content molecules, hydrogen (H_2) and carbon monoxide (CO). In this work, syngas was simulated with adding two gas compositions, H_2 (99.99% purity) and CO (99.95% purity), from two separate high pressure cylinders. The simulated syngas supplied to the engine cylinder through individual pressure regulator, flow meter, gas mixture and gas carburetor etc. before inducing into the intake manifold. The fuel-gas quality was determined by the H_2 and CO content, expressed in percentage (%) by volume.

3.2.2 Liquid fuel

In the present investigation two liquid fuels were used; first, standard diesel fuel for reference as baseline (also cited in the texts as: 'diesel mode', 'only diesel case', '100% diesel mode', etc.) comparison. Further, diesel and jatropha oil methyl ester (JOME) as pilot fuels for dual fuel operation. The liquid fuels were supplied to the engine injection pump from the fuel tank under gravity feed. One minute fuel consumption measurements were performed on a volumetric basis using graduated glass burette. The burette was filled with liquid fuel just prior to metering from the fuel tank. These measurements were converted to gravimetric basis by measuring fuel density and, recorded in the computerized control system. Baseline measurements were taken with 100% diesel for the experimented diesel engine. Then, for biogas dual fuel experiments, diesel and JOME, and for syngas dual fuel operation only diesel as pilot ignitions were supplied to the engine for ignition purpose. The amount of pilot fuel was varied by adjusting the fuel cut-off valve position.

3.3 Instrumentation on the Engine Setup

3.3.1 Engine performance measurement

The amount of load on the engine by the eddy-current dynamometer was varied by a manually controlled knob with a digital load indicator. The engine performance was measured from the computerized system for a given load setting. The various performance parameters measured were BP, FP, BMEP, 'bsfc', efficiencies, air and fuel flow rates, A/F ratio, heat balance, etc. The FP is obtained by determining IMEP from $P-\theta$ traces through the 'Enginesoft' engine performance analysis software. The formulae used for the calculations of the results are illustrated in *Appendix A*. The performance analysis procedure for dual fuel operation is also included.

3.3.2 Air and gas flow measurement

The air flow to the engine was monitored by passing the intake air through an air box with orifice meter and manometer. The air flow was calculated and recorded in the computerized engine control panel system. During the diesel/syngas operation, the flow rates of two individual gases (H_2 and CO), and the air-syngas mixture were measured separately using pre-calibrated rotameters. Because the biogas stored in the balloon was at ambient pressure conditions, the free flow into the engine cylinder through in the gas carburetor was not possible. To make biogas suction exist, a calculated weight was placed over the balloon to maintain a little higher pressure of the gas condition inside the balloon to that of ambient condition. Biogas consumption rate was measured via timing a complete $0.8m^3$ amount of biogas consumption from gas balloon used during the dual fuel operation.

3.3.3 $P-\theta$ measurement

For combustion diagnostics, the in-cylinder pressure was measured using a piezo sensor of PCB Make mounted on the engine cylinder. The specifications of the hermitically sealed sensor were: Model – HSM111A22, resolution – 0.69 kPa, rise time = 2 micro second, discharge constant = 500 second, natural frequency of the crystal = 400 kHz. The crank angle measurement was sensed by a 360 degree incremental encoder with push-pull interface. The encoder operates on an electro-optical scanning principle. They transform mechanical movements into electrical signals which are then acquired on a PC (Personal Computer) at time interval of two-degree crank angle.

3.3.4 Temperature measurement

Type K thermocouples connected to a data logger are installed in various engine positions to measure individual temperatures such as; in/out engine cooling water flow, in/out calorimeter water flow, exhaust gas out from the engine (i.e., inlet to calorimeter), and exhaust gas out from calorimeter.

3.3.5 Emission measurement

The flue gas compositions were analyzed using a multi-component analyzer based on infrared and chemical cell technique. The apparatus was calibrated using certified gases before reading the emissions. Exhaust gas sample was drawn from the exhaust manifold through a probe during the steady engine operation under a specified set of operating conditions. These samples were monitored in a flue gas analyzer system for the direct reading of CO, CO_2, NO, NO_2, and hydrocarbon (HC) emissions. The resolution, accuracy and range of these gas measurements for Quintox Make Kane flue gas analyzer are indicated in Table 3.2.

Table 3.2 Specifications of Quintox flue gas analyzer

Emission	Resolution	Accuracy	Range
CO_2	0.1%	±5% of reading and ±0.1% volume	0 – 20%
CO	1 ppm	±20 ppm < 400 ppm 5% of reading < 2,000 ppm ±10 of reading > 2,000 ppm	0 – 10,000 ppm
NO	1 ppm	±5% ppm < 100 ppm ±5% of reading > 100 ppm	0 – 5,000 ppm
NO_2	1 ppm	±5 ppm < 100 ppm ±10 ppm < 500 ppm ±5% of reading > 500 ppm	0 – 1,000 ppm
HC	1 ppm	±5% of reading and ±12 ppm volume	0 – 2,000 ppm (Propane)

3.4 Engine Conversion Methodology

3.4.1 Biogas operation

For any gaseous fuel dual fuel operation, it is essential to supply a homogeneous air-gas mixture into engine cylinders for combustion and, also to vary the fuel-gas flow according to engine performance requirement. A mixing device called 'gas carburetor' or simply 'carburetor' or 'mixing device' provides a homogeneous fuel gas-air mixture. To achieve this, a gas carburetor was designed particularly for it and added to the intake manifold as a means to introduce biogas. Considering practical approaches, a T- joint with the gas pipe protruding type mixing device was designed and fabricated according to recommendations of von Mitzlaff (1988). The 'gas pipe' or 'gas nozzle' is cut oblique with the opening facing the engine inlet. The protruding section increases the active pressure drop for the gas to flow into

the mixing device. The design calculations to evaluate diameter of the gas nozzle inlet is based on the parameters include, rated power, cubic capacity, rated speed, volumetric efficiency, manifold diameter, diesel substitution, gas calorific value and velocity of gas. To improve mixing further a turbulence grid was introduced in the gas carburetor. The details of the gas carburetor design (Fig. 3.2 and 3.3) are presented in *Appendix B*. The schematic of biogas dual fuel conversion is shown in Fig. 3.4. The same gas carburetor was used for syngas-diesel dual fuel operation. This typical laboratory arrangement of gas storage and supply devices for biogas dual fuel operation is shown in Fig. 3.5.

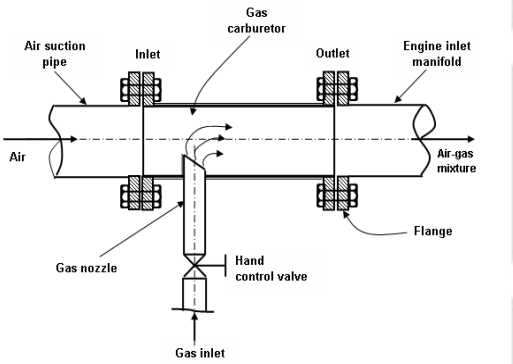

Figure 3.2 Schematic of gas carburetor

Figure 3.3 Fabricated gas carburetor

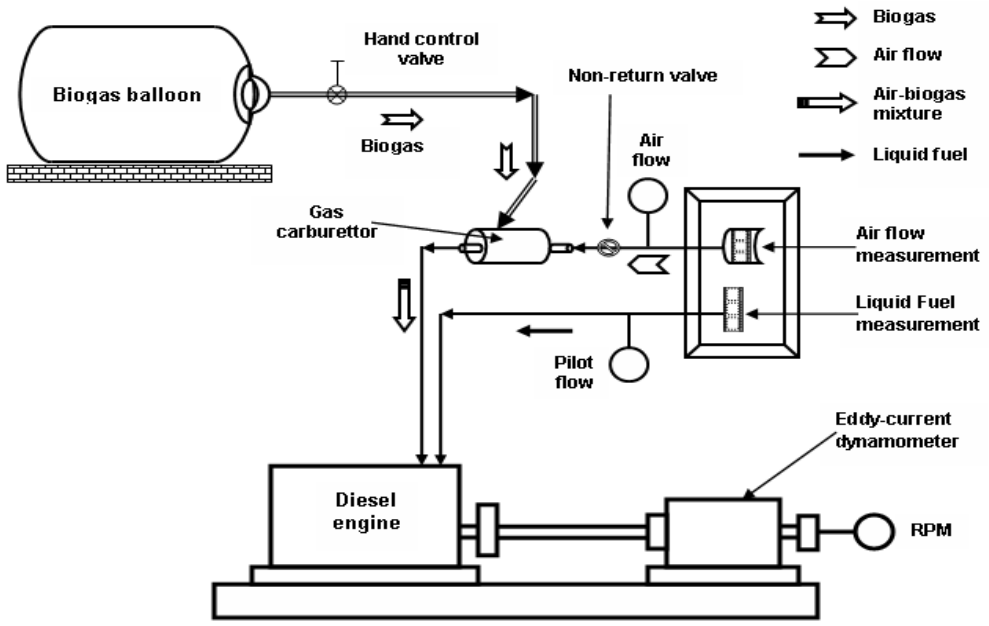

Figure 3.4 Schematic of the biogas dual fuel conversion

Figure 3.5 Laboratory arrangements of biogas dual fuel operation

3.4.2 Syngas–diesel operation

A few additional components such as gas mixer, non-return valve, pressure regulator and gas carburetor etc. were incorporated into the base diesel engine setup to operate it on dual fuel mode. The schematic of gas installation circuit added to the base diesel engine for syngas dual fuel operation is shown in Fig. 3.6. The detail of the laboratory setup for syngas-diesel dual fuel operation is shown in Fig. 3.7. The design and fabrication work added for dual fuel mode are explained in the following paragraphs.

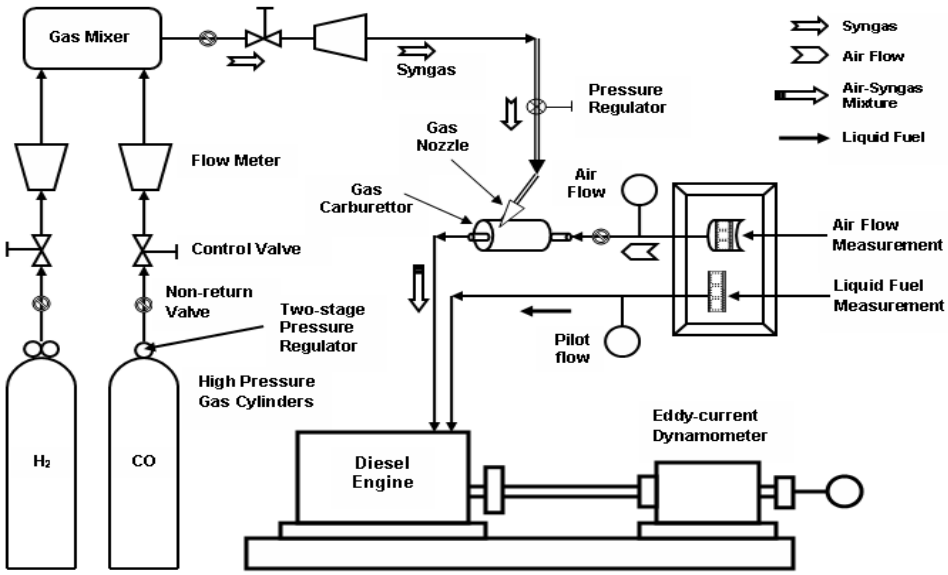

Figure 3.6 Schematic diagram of the syngas–diesel dual fuel conversion

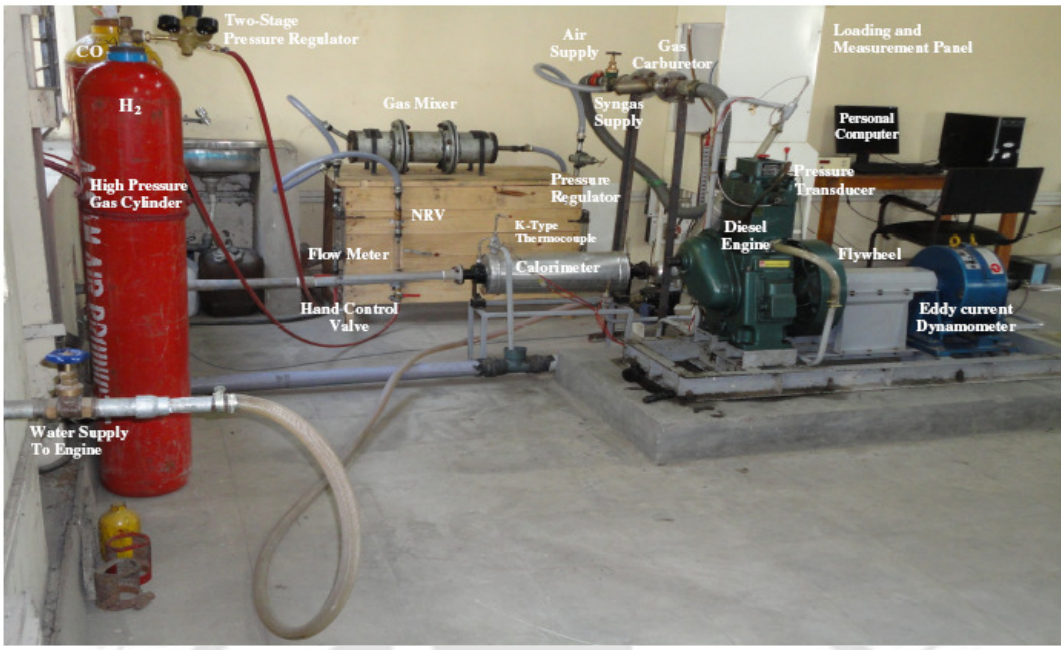

Figure 3.7 Laboratory setup for syngas–diesel dual fuel operation

i. A gas-mixing apparatus, called 'gas mixer' or 'gas reservoir', was fabricated in order to prepare simulated syngas (Fig. 3.8 and 3.9). The volume of the gas mixer was determined in such way that it can accommodate at least ten (10) times of engine swept volume requirement. This volume ensures a decent well mixed simulated syngas quantity along with reduced high inlet pressure gas availability for the dual fuel operation. Again, to achieve better mixing of H_2 and CO, the turbulence was generated by feeding individual gas at an angle into the gas mixer. Hydrogen gas was fed from the top inlet of mixer as it will move upwards due to its property of lightness. The case CO gas was reversed to that of H_2 gas supply. Inside the gas mixer the pressure of syngas was reduced by providing wire mesh in the path of gas flow. The pressure of simulated syngas from the mixer was then brought to ambient condition by controlling through a single stage pressure regulator. Finally, the syngas and air mixed homogeneously in the gas carburetor before entering the engine cylinder for combustion.

ii. In order to feed the CI engine with a homogeneous syngas-air mixture, the earlier designed gas carburetor for biogas operation was used. The gas carburetor was fastened in between engine intake manifold and air suction side. The inlet pressure of syngas into the carburetor from gas mixer was kept at atmospheric condition as that of air by a single stage pressure regulator. This ensures a homogeneous air-syngas mixture because the required venturi of the carburetor was created by this design approach.

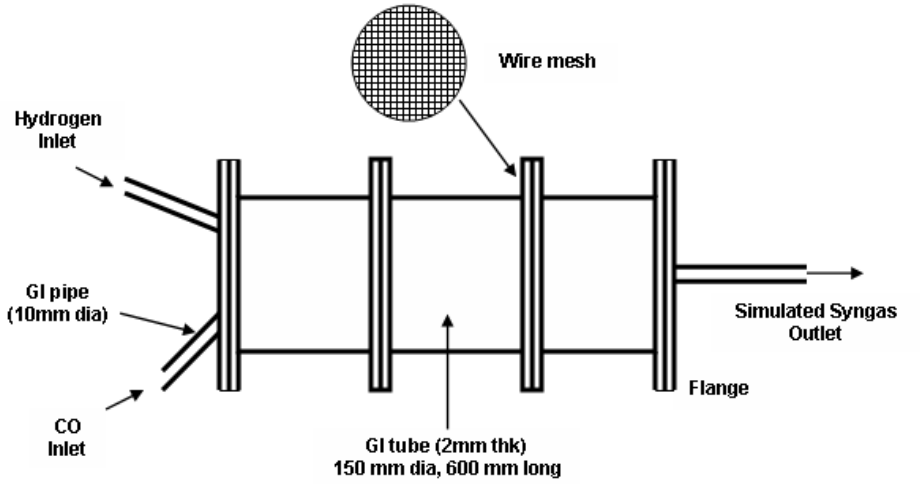

Figure 3.8 Schematic of gas mixer

Figure 3.9 Fabricated gas mixer

3.5 Experimental Procedures

3.5.1 Baseline tests

To establish a basis for comparison of results and to ensure the consistency of the experimental observations, baseline performance tests were carried out with the engine operating on diesel fuel only. The engine load ranges from a minimum of 0.1 kg to a maximum of 16 kg load. The engine tests were conducted for the entire load range i.e., 0 to 100% in steps of 20% at constant speed of 1500 rpm. First, engine was warmed up and run for few minutes at 1500 rpm under no-load condition to reach stable operating conditions. The water flow was adjusted to 250 and 70 liters per hour for the engine cooling and calorimeter respectively according to the engine supplier instructions. Then, as per

experimental design a load level was set for engine operation. Once the engine reaches the steady-state condition, the engine was ready to present the baseline results. For this, the following data were recorded manually:

1) Engine jacket water (in/out), calorimeter water (in/out) and exhaust gas temperature,
2) The difference in liquid level in the manometer for air flow, and
3) Volume of diesel fuel consumption by the engine in one minute.

After setting the above inputs manually to the computer software program, the data were converted to engineering units and were updated and displayed on a monitor at every second. The engine efficiency data were displayed in the form of BP, BMEP, IP, IMEP, bsfc, efficiencies, air and fuel flow rate, A/F ratio, heat balance, etc. The crank angle measurement was sensed by an optical sensor and then was acquired on a PC at time interval of two-degree CA. The engine peak cylinder pressure and $P-\theta$ diagram were recorded for each tested load. For emission measurements, exhaust gas samples were drawn from the exhaust manifold into flue gas analyzer through a probe during the steady engine operation. The emission readings were recorded directly from the flue gas analyzer for the sample. This experimental measurement procedure was repeated for 0%, 20%, 40%, 60%, 80% and 100% engine loading. The load variations on the engine were conducted at 1500 ± 50 rpm. The load was varied in steps by means of the eddy-current dynamometer with the help of a manually controlled knob with a digital load indicator provided in the engine controller.

3.5.2 Biogas dual fuel tests

For the biogas dual fuel operation, biogas flow was opened up slowly from gas balloon and allowed biogas to reach gas carburetor. The homogeneous air-gas mixture from carburetor was then sucked into the cylinder to take part in the dual fuel combustion via engine manifold. The amount of biogas was increased manually till engine shows signs of misfire. This limits the maximum biogas flow for the dual fuel operation. During the process, engine speed increased due to added extra chemical energy from biogas. To maintain a constant level power and speed from both diesel and dual fuel modes, the quantity of diesel or JOME was varied by adjusting liquid fuel cut-off valve. The original and modified design of fuel cut-off valve is shown in Fig. 3.10 and 3.11 respectively. Finally, the cut-off valve was locked manually at the rated engine speed of 1500 rpm. This means that the engine operated with minimum pilot consumption at these operating conditions. Now, at a steady-state dual

fuel operation, again the same input manual parameters, as described for baseline tests, were inserted into the computer software program for efficiency and combustion results. For emission results, exhaust gas sample was examined by flue gas analyzer.

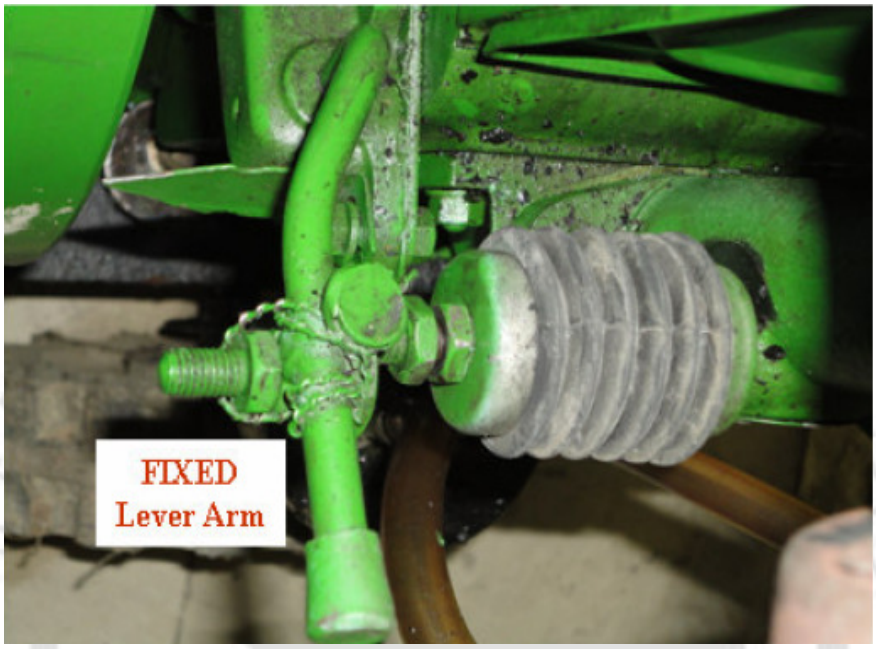

Figure 3.10 Original fuel cut-off design

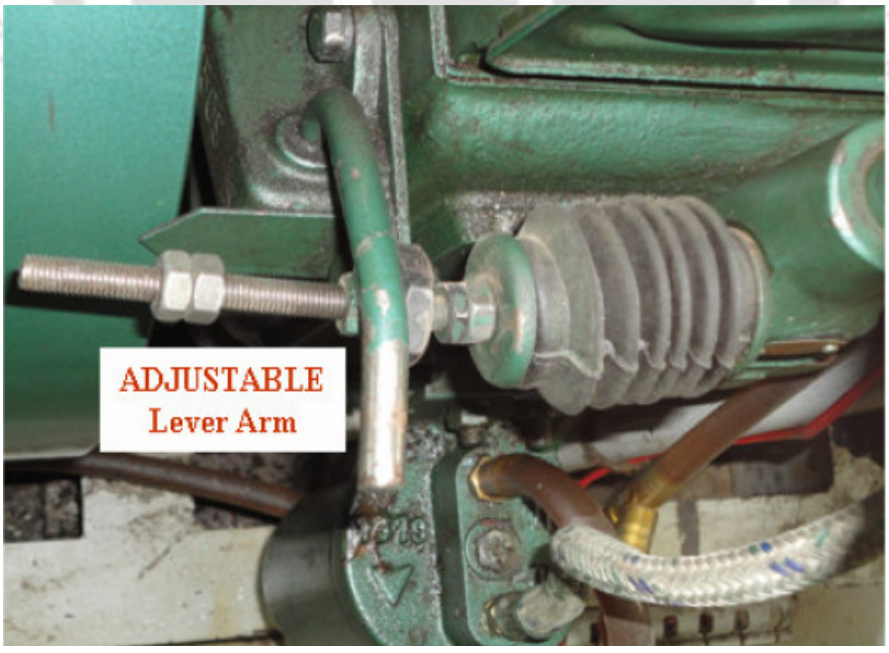

Figure 3.11 Modified fuel cut-off design

3.5.3 Syngas–diesel dual fuel tests

For the syngas dual fuel operation, the H_2 and CO gases were supplied from respective high pressure cylinder to an outlet pressure of about 1 to 2 bar using two-stage pressure relief valves. To avoid any possible fire hazard due to burning of H_2 in presence of possible oxygen or air availability in the gas mixer, CO gas was supplied initially into the mixer followed by highly flammable H_2 gas. The simulated syngas was prepared by mixing individual components of H_2 and CO on a calculated volumetric ratio in the gas mixer. For an example, volumetric ratio of H_2:CO is 1:1 for H_2:CO ratio of 50:50 syngas. The proportion of H_2 and CO in syngas was controlled throughout the dual fuel operation by adjusting the individual gas flow rate. The required flow rates of H_2, CO and syngas, were achieved by manual adjustment of the control valves, and are measured separately using calibrated flow meters. For stable operating conditions, at a set engine load, the syngas fuel valve was opened slowly and allowed the fuel-gas to enter from mixer to gas carburetor. The homogeneous air-gas mixture from carburetor was then sucked into the cylinder to take part in the dual fuel combustion. The syngas flow was increased till engine shows signs of misfire. This decided the maximum gas flow for the dual fuel operation. During the process, engine speed increased due to added extra chemical energy from gaseous fuel. To maintain the constant engine operating speed of 1500 rpm and also, to keep same power output as of 100% diesel mode, supply of diesel to the engine was reduced by adjusting diesel cut-off valve. Finally, the cut-off valve was locked manually at the rated engine speed. Now, for a steady-state dual fuel operation, again the same input manual parameters, as described for baseline tests, were inserted into the computer software program for efficiency and combustion results. For emission results, exhaust gas sample was analyzed for NO_x, HC, CO and CO_2 emissions from the flue gas analyzer.

Once the entire above test readings were sorted out, the normal diesel oil operation of the engine was restored by shutting gas flow and adjusting liquid fuel cut-off valve to original position. The engine was then in a position for another set of operating conditions and its experimental results starting from baseline readings. This above experimental measurement procedure was repeated as per the experimental design. At the end of whole experimental design, gas flow rate was ceased completely and the engine was made to run at a steady-state condition using only diesel at no-load condition before shut down.

3.5.4 Experiment repeatability

Experimental design was used for univariate data collection and analysis of results. The performance parameters were measured thrice as per experimental design for both diesel and dual fuel modes and averaged for each operating point. The recorded average experimental data were employed for analysis purpose.

3.5.5 Analysis procedure

The formulae used in the various performance and combustion parameter calculations of baseline and dual fuel modes were illustrated in Appendix A. The dependant variables calculated from these were analyzed and compared.

3.5.6 Uncertainty analysis

The uncertainties associated with both the diesel and dual fuel mode engine performance calculations were estimated using sequential perturbation techniques (Kline and McClintock, 1953; Moffat, 1982). The details of each measured independent parameter and also, each performance parameter overall relative measurement errors were summed up in *Appendix C*. It includes contributions from individual uncertainties in measurement mass of diesel flow (1%), air flow (0.5%); biogas and water flow (2%); lower heating value calculation (1%); engine load and speed (0.5%); and temperature $(3^0 C)$. Based on the above, the calculated engine performance was believed to be accurate within $\pm\ 3\%$. However, the emission levels were recorded with an error of 5%.

3.6 Summary

In this Chapter, the basic requirements and procedures adopted to carry out diesel and dual fuel mode of operations has been described. Various assisting measuring instruments including exhaust gas analyzer were instrumented to the engine setup. The necessary equipments are designed, fabricated and added to the base diesel engine for the dual fuel modes. The important engine modification like the liquid fuel cut-off valve redesign has been arranged. The repeatability of experimental results, the procedure of both diesel and dual fuel engine operations, and the uncertainties associated with the collected experimental data, for the whole engine operations have been discussed. For the sake of convenience, the details of diesel and dual fuel mode procedures are elaborated separately.

Chapter – 4

BIOGAS DUAL FUEL ENGINE EXPERIMENTS

Overview

Gaseous fuels promise to establish cleaner combustion in internal combustion engines. When used in diesel engines, these alternative fuels contribute to the clean development mechanism. Before assuring clean development mechanism potential of biogas, the first kind of fuel examined in this work, an experimental investigation is conducted in a diesel engine under dual fuel mode. The necessary arrangements and modifications are completed for the base diesel engine to work under dual fuel mode ahead of the experiments. Following to the experimental procedure, this chapter presents the average outcomes of performance, combustion and exhaust gas emission parametric quantity variations of an engine fuelled with biogas under different loading conditions. The performance of a single-cylinder, four-stroke, direct-injection, constant-speed and compression-ignition diesel engine operating under dual fuel mode conditions is monitored. In this study, the experimental observations of the compression-ignition engine under biogas dual fuel mode with varying pilot fuel quality are also discussed. Jatropha oil methyl ester (JOME) or jatropha bio-diesel is utilized as pilot fuel to achieve a full diesel substitution. Engine performance under these conditions has been compared in regards to alternative operation with diesel as pilot fuel. Including this, for a same power output from both the diesel and dual fuel engine operations, the performance characteristics results are also equated. The engine mechanical performance is studied on the basis of thermal efficiency, volumetric efficiency, brake specific energy consumption, exhaust gas temperature, maximum diesel substitution rate and gas flow rate. Further, combustion analysis is carried out from parameters such as, cylinder peak pressure, pressure–crank angle diagrams, net heat release rate, maximum rate of pressure rise, and ignition delay. In addition, the dry concentrations of engine emissions such as NO_x, CO, CO_2 and HC are registered. This work is aimed to quantify the behavior of pilot fuel variables of interest under the biogas dual fuel operation.

4.1 Experimental Design

In this work, the type of dual fuel mode was decided by the pilot fuel quality (diesel/bio-diesel) keeping biogas as the primary fuel unchanged. The important properties of fuels utilized in the experiments are presented in Table 4.1. The lower heating value, density and flame velocity of biogas were calculated theoretically from its methane composition values. In order to establish the basis for comparison of dual fuel results as per experimental design (Table 4.2), a baseline test with 100% diesel fuel was also conducted. For a safe operation, as per engine supplier instructions, the diesel engine was run to a maximum of about 90% of its power rating and the corresponding load was considered as the 100% benchmark load for the experimental design. The engine tests were conducted from 0 to 4.6 kW shaft output (0% or idle or no-load condition to a maximum of 100% in steps of 20%) for both baseline and dual fuel experiments. The mass flow rates of diesel, biogas and pilot fuels consumed during the engine tests are presented in Table 4.3.

Table 4.1 Important properties fuels used in biogas dual fuel experiment

Properties	Diesel	JOME	Biogas
Chemical formula	$C_{12}H_{26}$	N/A	48% CH_4; 42% CO_2 by volume
Density (kg/m^3) at 1 atm, 15 ^{0}C	850	880	1.27*
Calorific value (MJ/kg)	42	38	15.74*
Flame velocity (m/s) (Kumar et al., 2003b) (Swami Nathan et al., 2010)	0.3	N/A	0.25
Cetane number (Kumar et al., 2003a)	45-55	50	---
Auto-ignition temperature (K) (Swami Nathan et al., 2010) (Kumar et al., 2010)	553	573	923
Stoichiometric A/F (kg/ kg)	14.92*	N/A	5.36*
Energy density (MJ/Nm^3)	2.82*	N/A	2.87*

* calculated value

Table 4.2 Experimental design matrix for biogas dual fuel data collection

Mode of operation	System components	Designation of operation	Engine operation
Diesel	Fuel: Standard Diesel	Baseline Test/ Diesel mode	Speed: 1500 ± 50 rpm Load: 0, 20, 40, 60, 80, 100% Injection timing: 23°BTDC
Dual fuel	Primary: Biogas Pilot: Diesel	Biogas-diesel	- do -
Dual fuel	Primary: Biogas Pilot: JOME	Biogas-JOME	- do -

Table 4.3 Fuel consumption data for various engine operations

Engine load (%)	Mass flow rate of liquid fuel (kg/hr)	Mass flow rate of biogas (kg/hr)
	Diesel mode	
0	0.83	---
20	0.91	---
40	1.06	---
60	1.26	---
80	1.53	---
100	1.98	---
	Biogas-diesel	
0	0.51	2.18
20	0.56	2.34
40	0.56	2.54
60	0.56	2.9
80	0.61	3.39
100	0.66	4.69
	Biogas-JOME	
0	0.73	2.03
20	0.66	2.34
40	0.67	2.54
60	0.68	3.05
80	0.69	3.58
100	0.8	5.54

4.2 Performance Parameters

At an individual tested engine loads, both shaft power and torque outputs were kept equal in magnitude for both diesel (baseline) and dual fuel operations. From Fig. 4.1, it can be seen that the brake power and torque increased gradually with an increase in load. It is obvious because, at constant engine speed, as load increases both torque and power output increase. For a safe operation, the diesel engine was run to maximum power output and torque of 4.5 kW and 3.0 kg-m respectively, which are about 90% of maximum engine ratings.

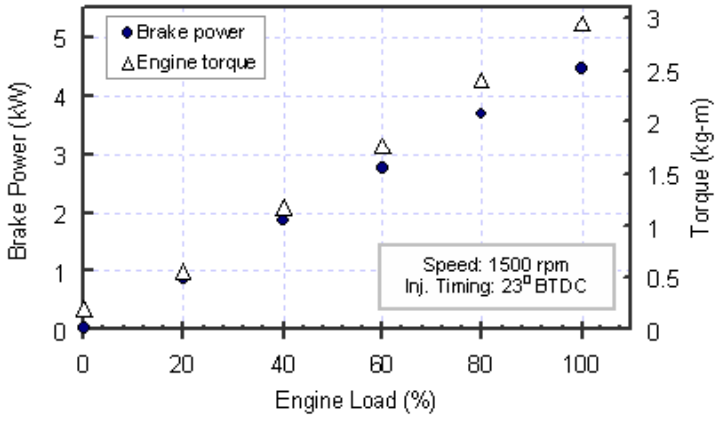

Figure 4.1 Variation of shaft output and torque with engine load

The brake thermal efficiencies of both the dual fuel operations were lower than that of diesel mode as shown in Fig. 4.2. A considerable reduction in thermal efficiency (about 19% to 40%) was observed under dual fuel modes as compared to diesel mode for the entire load range. This is mainly due to the lower heating value of biogas. At lower loads of 0 to 40%, there were maximum reductions of about 30 to 40% for both the dual fuel modes. This is due to the poor mixing of air-biogas and inadequate combustion rate of this mixture in the lower temperature zone of 0 to 40% loads. The trend of dual fuel mode efficiency matches closely to that of diesel mode when the load was increased. The thermal efficiency was found maximum at slightly lean mixture condition of 80% engine load for all the tested fuel conditions. Among all the test modes, the best efficiency point is achieved at this load. Mixtures richer or leaner than this point caused incomplete combustion or slow the burning rate, and hence led to a drop in thermal efficiency. The maximum thermal efficiencies with the dual fuel mode were 16.8% and 16.1% for diesel and JOME pilot ignition respectively. While a maximum of 20.9% thermal efficiency was found for the diesel mode. At the higher temperature zone of 100% load, the higher self ignition temperature property bearer biogas combusted better to give an improved efficiency at the minimum oxygen operation. At this condition, the dual fuel modes have an equal efficiency reductions range at 80% load as compared to diesel mode. At best efficiency point, the efficiency with the biogas-JOME mode was observed only 4% lower as compared to biogas-diesel mode. There were no substantial differences in thermal efficiency found in between both dual fuel modes. This is because of the matched properties of calorific value and density for both the pilot fuels. Including this, the presence of oxygen molecules in the bio-diesel helped a better combustion in the engine combustion chamber.

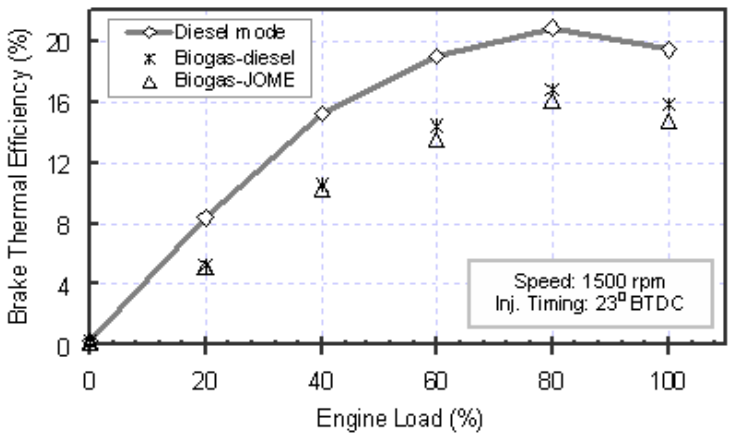

Figure 4.2 Variation of brake thermal efficiency with load

The lubrication regime of the mating surface affects the efficiency, durability and exhaust emissions of the engine. In general, most friction occurs at, or near, top dead centre where low piston velocity is low, and where the temperature is higher, due to the proximity of the combustion chamber (Masjuki *et al.,* 1999). Biogas contains lower energy than that of diesel oil. So, the biogas dual fuel mode generates lower combustion pressure and hence, their expansion ratio is less. Including this, biogas dual fuel mode produced less combustion temperature compared to diesel mode. Again, low viscous biogas does not mix with lubricating oil during engine operation. All these factors collectively reduced the friction power (FP) consumption of the both the dual fuel operations as compared to diesel mode (Fig. 4.3). Jatropha bio-diesel contains oxygenated moieties and double bonds. This improved the overall lubricity of bio-diesel over diesel fuel and resulted lower friction coefficient (Bhale *et al.,* 2008). This led to lower FP consumption of about 0.5 to 1.5 kW for biogas-JOME mode over biogas-diesel operation. This is one of the advantages of using bio-diesel as pilot over diesel fuel. In addition, as a whole, the dual fuel operations are able to save about 0.5 to 2 kW of FP than that of diesel mode. This benefits a dual fuel mode over a diesel mode. In general, the IMEP method to calculate FP is based on the concept of force balance. Therefore, this method can be prone to large errors if the cylinder pressure measurements are inaccurate. Looking at the quantity of FP saved (about 0.5 to 1.5 kW), it seems that these values are at the higher side due to errors in the calibration of the pressure transducer which causes substantial difference in the calculated IMEP and hence FP. Also, the uncertainty of the pressure transducer used in this work is 2% as per the Supplier's manual.

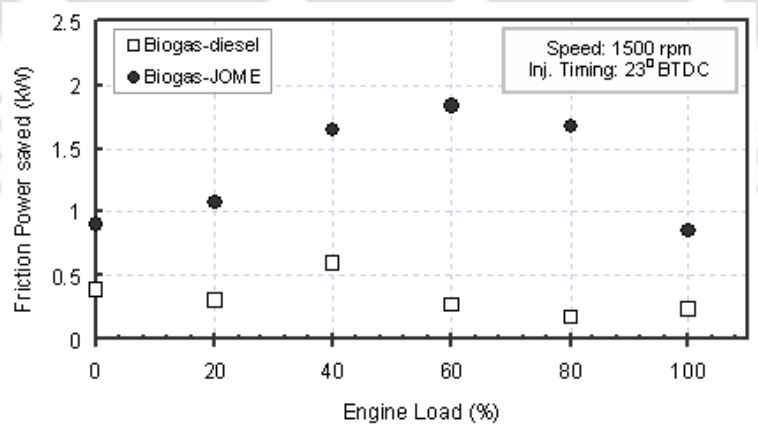

Figure 4.3 Comparison of friction power saved during dual fuel operations with load

Brake specific energy consumption (BSEC) of a dual fuel mode was calculated from the data of fuel consumption rate and LHV of pilot liquid fuel (diesel or JOME) and biogas. The BSEC of the engine was higher at part loads (up to 40%) irrespective of the fuel used shown in Fig. 4.4. This is due to the poor combustion efficiency of biogas fuelled dual fuel modes. The BSECs of both the dual fuel modes were higher than that of diesel mode for the entire

load range. The pilot fuel had less influence, and there were no differences in the BSEC with the type of pilot fuel used. This indicates that JOME can be used as an alternative to diesel fuel as the pilot ignition for a dual fuel operation. The presence of carbon dioxide in the biogas cut down the burning velocity and thereby resulted in incomplete combustion that increased the BSECs of both the dual fuel modes. In the process, both the dual fuel modes established higher exhaust gas temperatures (about 40 to 70^0 C) than that of diesel mode (Fig 4.5). The maximum exhaust temperatures for diesel and JOME pilot ignited dual fuel modes were found as 880 K and 895 K respectively as compared to 846 K of diesel mode.

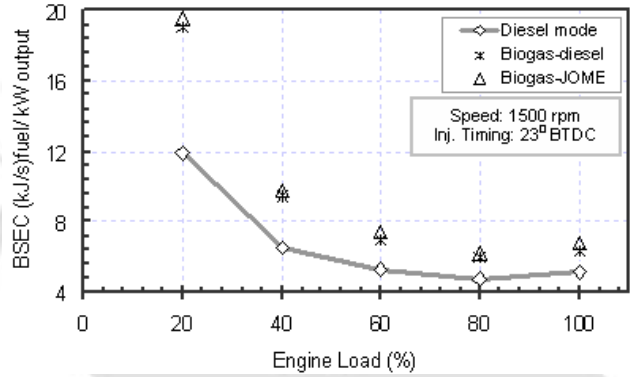

Figure 4.4 Variation of brake specific energy consumption with load

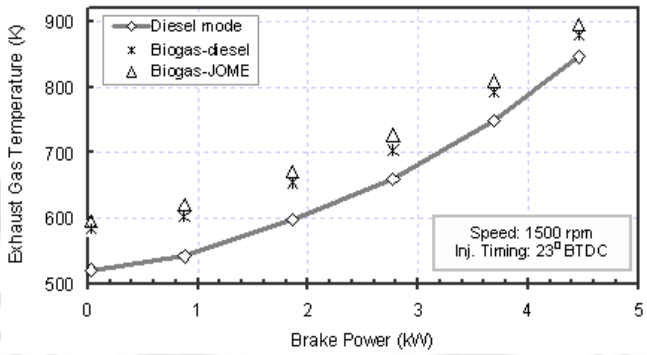

Figure 4.5 Variation of exhaust gas temperature with load

The variation of volumetric efficiency with power output is shown in Fig. 4.6. The volumetric efficiencies with dual fuel operations were found lower than diesel mode. The higher temperature of the retained exhaust gas (Fig. 4.5) preheats the incoming fresh air and lowered the volumetric efficiency (Kumar *et al.,* 2003a). In addition, at higher power outputs higher biogas substitution displaces a greater proportion of air. Hence, the volumetric efficiency of dual fuel operations decreased further to result its minimum value at the maximum power output condition. Among the dual fuel operations, biogas-JOME fuelling mode produced reduced volumetric efficiency than the other mode due to the lower LHV of

JOME and hence, higher biogas flow rate during its operation. However, the differences in volumetric efficiencies between these two dual fuel modes were not substantial. The maximum and minimum volumetric efficiencies found for diesel mode was about 85% and 81% at 0 and 100% respectively. These values were 82 and 78%, and 82 and 77%, for diesel and JOME pilot ignition dual fuel modes respectively.

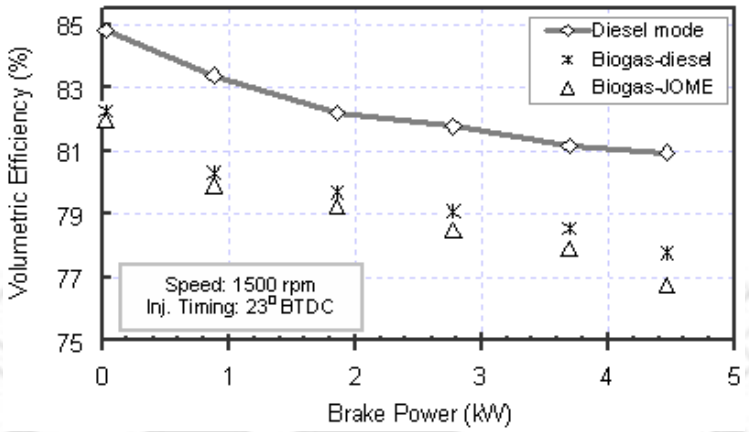

Figure 4.6 Volumetric efficiency variation with load

Comparing both the dual fuel operations, the biogas flow rates under biogas-JOME mode were found little higher than the other mode for the entire load range (Fig. 4.7). At maximum load, due to the presence of oxygen in the bio-diesel, biogas-JOME mode was able to accommodate more volume of biogas combustion still in the rich mixture zone. Under diesel-biogas mode, a possible diesel fuel replacement of 22, 36, 45, 54, 60 and 69% was determined at 0, 20, 40, 60, 80 and 100% engine load respectively (Fig. 4.7). On the other hand, the biogas-JOME operation showed a maximum of 22 to 66% bio-diesel substitution for the same loading combinations. However, considering the fossil fuel replacement, the biogas-JOME mode was able to save 100% diesel oil. At lower loads of 0 to 40%, due to a lower overall engine temperature, the inability of easy auto-ignition of biogas enabled a low gas flow into the combustion chamber. In the process, it provided less energy for the dual fuel operation. Therefore, to provide a higher temperature zone to the biogas for its auto-ignition and also, to maintain a constant power output at individual loads, a larger amount of liquid pilot fuel was supplied at lower loads. However, this lowered the pilot fuel replacement at lower loads. Due to its high self ignition temperature (about 580°C), biogas burned better at higher load temperature zone. Hence, the liquid fuel replacements improved at higher loads and also, showed its maximum value at 100% load for the dual fuel modes.

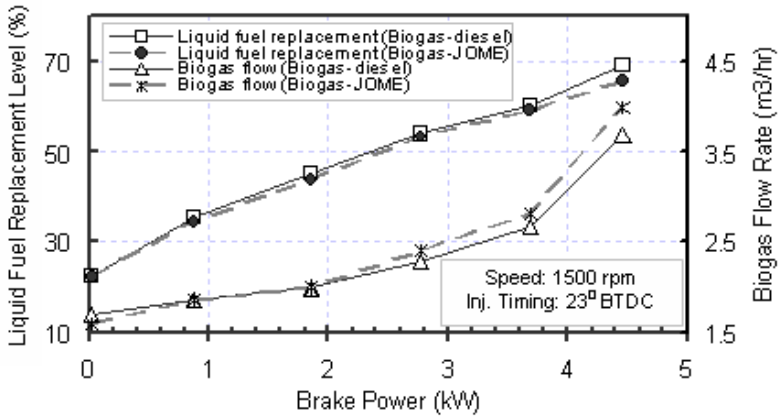

Figure 4.7 Variation of liquid fuel substitution and gas flow rate with load

4.3 Combustion Parameters

The comparison of pressure-crank angle variations for each of the tested fuel modes are shown in Figs. 4.8 through 4.10 for different engine loads. This is also to recall here that the biogas was supplied till the sign of misfire during both the dual fuel operations. Therefore, the above Figs. (4.8 to 4.10) have confirmed the smooth and normal combustion under dual fuel operations i.e., there was no sign of knock. It can be seen that the maximum pressure attended in the cycle was less for both the biogas dual fuel modes. A significant quantity of CO_2 present in biogas absorbed the heat release and thereby brought down the engine pressure and temperature. Also, the prolonged ignition delay of dual fuel modes (Fig. 4.11) caused the peak pressure attainment to shift by about 14^0 CA towards expansion stroke than the diesel mode. This led to lower amplitude of peak pressures for both the dual fuel modes. The occurrence of cylinder peak pressure mainly depends on the combustion rate in the initial stages, which is influenced by the fuel taking part in uncontrolled heat release phase.

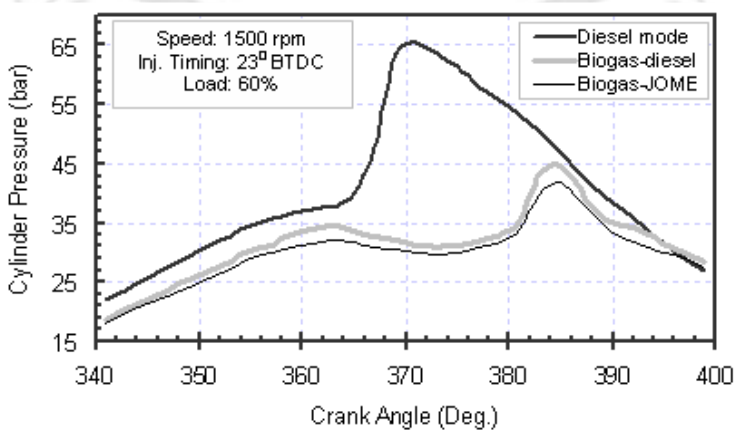

Figure 4.8 Variation of cylinder pressure with crank angle at 60% load

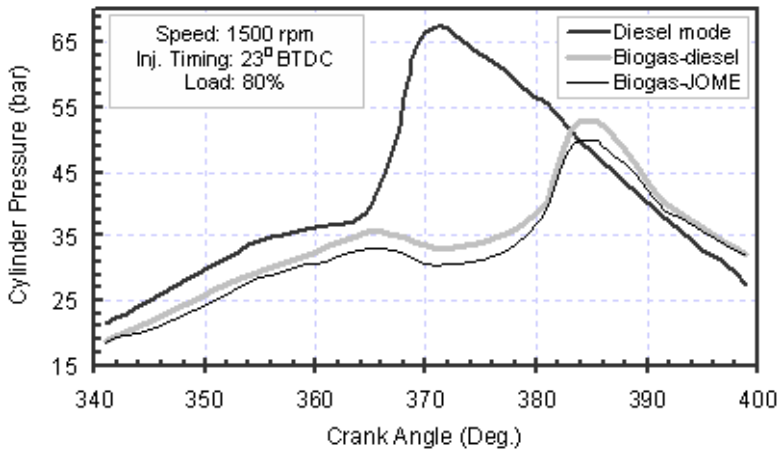

Figure 4.9 Variation of cylinder pressure with crank angle at 80% load

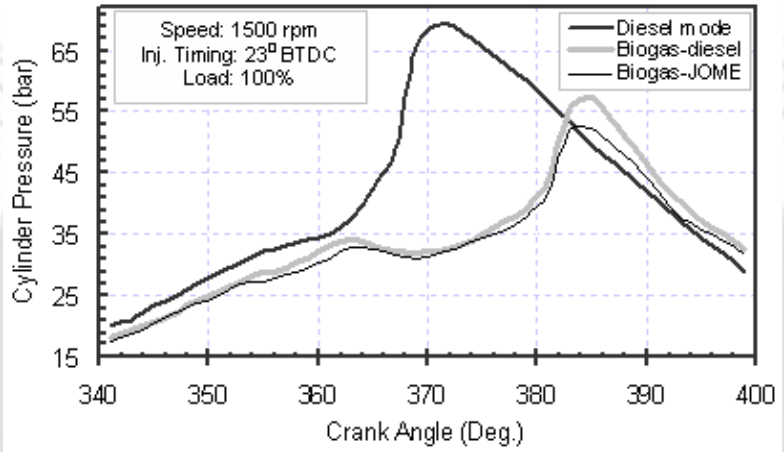

Figure 4.10 Variation of cylinder pressure with crank angle at 100% load

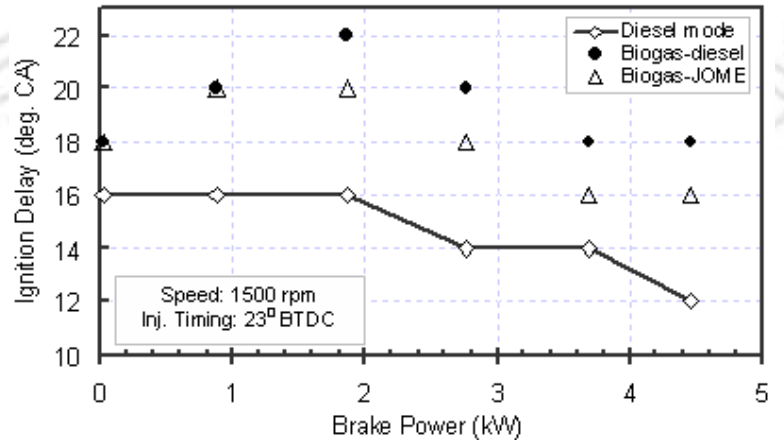

Figure 4.11 Variation of ignition delay with power output

In general, when load increases, the addition of fuel chemical energy per cycle increases the cylinder peak pressure (Fig. 4.12). Normal diesel operation showed the highest peak pressure of 69.5 bar at maximum load. The effect of lower burning velocity and lower energy input

per cycle of biogas reduced the peak pressure for dual fuel operations. This also resulted in a slower rate of pressure rise. At 100% load, the highest peak pressure found as 57.2 bar for biogas-diesel mode followed by 52.3 bar for biogas-JOME mode. Looking at the Fig. 4.12 it can be realized that the trends of increase in peak pressure under the dual fuel operations are mild within 0 to 40% load. This is due to the poor combustion of biogas at lower load operating conditions. However, beyond 40% load, these trends showed an intense degree of pressure rise in the higher temperature operating zones. Comparing in between the dual fuel modes, the bio-diesel ignited dual fuel mode produced a little lower peak pressure than that of diesel ignited mode. This is mainly because of the lower chemical energy capacity of JOME than the diesel fuel.

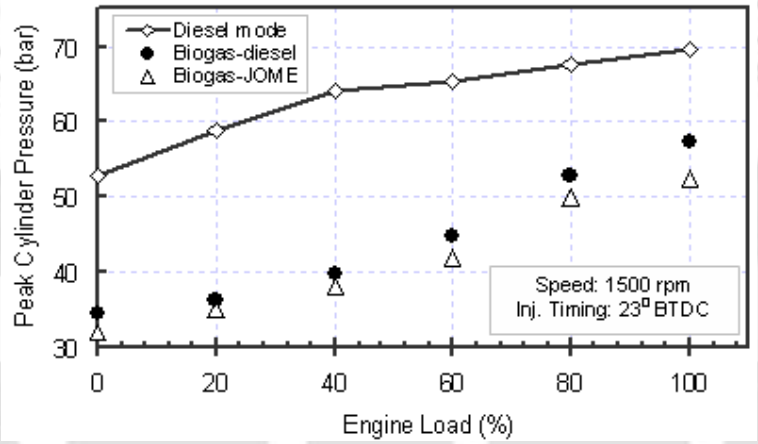

Figure 4.12 Comparison of peak cylinder pressure with load

When the load increased, there was an increase in maximum rate of pressure rise (MRPR) or combustion noise of all the fuel modes examined (Fig. 4.13). As the engine output increased, the mass of fuel-gas admission increased. Ignition of more gaseous mass caused the higher pressure rise rate and noise. The diesel mode showed a highest MRPR due to its higher energy content in fuel. For the dual fuel modes, the MRPR was highest for biogas-diesel followed by biogas-JOME mode. This may be postulated to higher ignition delay of the liquid pilot fuel and dual fuel mode as well (Selim *et al.,* 2008). The jatropha bio-diesel has a lower ignition delay period as compared to the diesel fuel (Sahoo and Das, 2009). Therefore, as expected, biogas-diesel combustion showed a longer delay due to the presence of pilot diesel as shown in Fig. 4.11. Thus, it confirmed the lower combustion noise for the JOME pilot ignited dual fuel mode as compared to the diesel ignited mode. The increase in ignition delay of the fuels decreased the net thermal efficiency, and energy generated from burning

fuel. Hence, it increased the likelihood of emitting some of the combustion energy as exhaust gas in the form of higher exhaust gas temperature as illustrated in Fig. 4.5. Of course, from engine material and assembly destructive viewpoint, both dual fuel modes have established the safe operation in the base diesel engine as their MRPR were below to that of diesel mode.

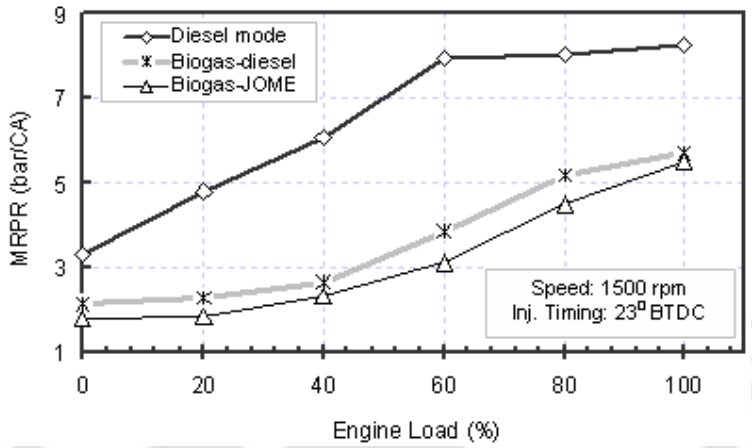

Figure 4.13 Comparison of MRPR with load

The maximum heat release rate with an uncertainty of 0.5 % of both the dual fuel modes was lower than that of diesel mode (Fig. 4.14 to 4.16). The longer ignition delay of pilot fuel progressed to the delay in the biogas combustion and this reduced the heat release rate of the dual fuel modes. At low combustion temperature conditions of 0 to 40% loads, the reductions in heat release rates of the dual fuel modes were higher. This is because of the presence of CO_2 and methane (which has a high self ignition temperature) in biogas. However, as load increased, the dual fuel operation heat release rates was improved due to the accumulation of a relatively higher of biogas supply for the combustion in the high temperature operating conditions. At 100% load, the maximum heat release rate of biogas-diesel and biogas-JOME modes were found as 144 J/deg. CA and 136 J/deg. CA as compared to 162 J/deg. CA for the diesel mode. Because of the higher ignition delay, the occurrence of maximum heat release rates observed late in the expansion stroke for both the dual fuel modes in comparison with the neat diesel mode. Hence, the heat releases during the late combustion phase for both the dual fuel operations were higher than that of the diesel mode. This lowered the expansion ratio for both the dual fuel modes and hence, produced lower power output for the dual fuel modes. From the Figs. 4.14 to 4.16, it can be viewed that there is a negative net heat release rate under dual fuel operations. This is probably due to the presence of some H_2 in the biogas composition which form water molecules or moisture during the biogas combustion. Bio-

diesel ignited dual fuel operation produced little higher negative heat release rate than that of other mode due to the higher biogas consumption. Among the dual fuel modes, due to its lower heat content, JOME ignited dual fuel mode resulted lower heat release than that of diesel ignited pilot mode.

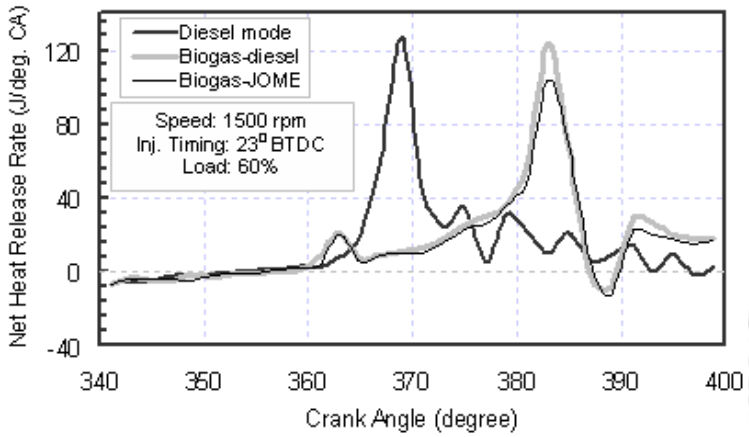

Figure 4.14 Variation of net heat-release rate as a function of crank angle at 60% load

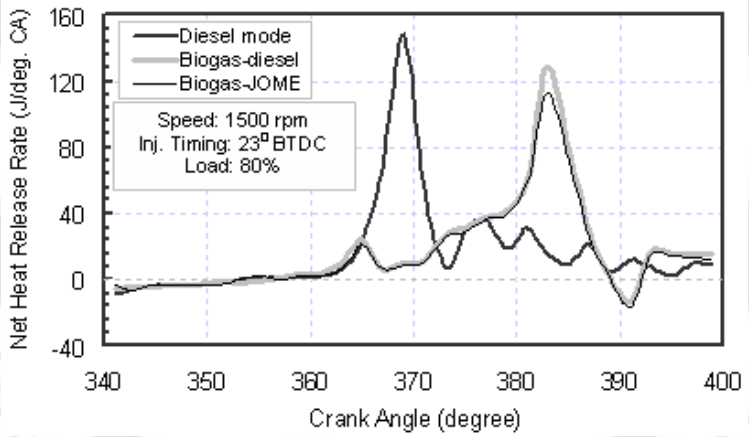

Figure 4.15 Variation of net heat-release rate as a function of crank angle at 80% load

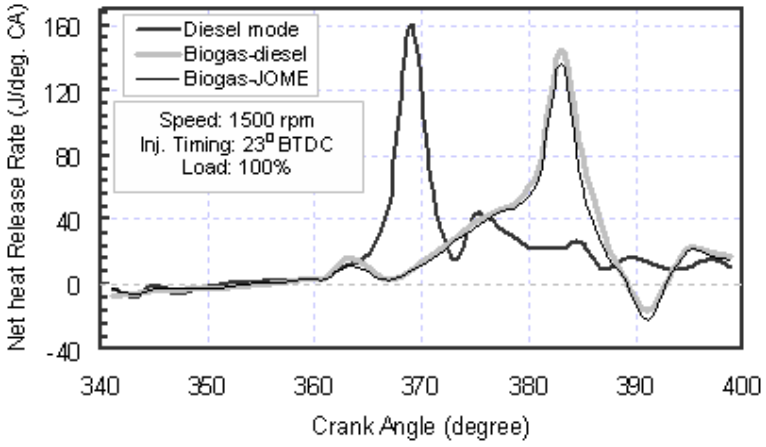

Figure 4.16 Variation of net heat-release rate as a function of crank angle at 100% load

4.4 Emission Characteristics

With an adequate presence of CO_2 (42% by volume) in its composition, the stoichiometric flame speed of biogas (about 25 cm/s) is lower than that of diesel fuel (about 30 cm/s). Hence, the flame front can not propagate fast enough and far enough to consume the entire air-biogas mixture within the combustion time period available. At low loads, these factors led to higher HC and CO emissions for the biogas fueling dual fuel modes. Figure 4.17 shows the average response of CO emissions for the tested fuel modes. When increasing the load beyond 40%, a fall in CO level was observed. During a dual fuel mode operation, biogas energy share was increased with rise in load i.e. the pilot share decreased. In general it is seen that CO falls when the diesel share reduces (Swami Nathan *et al.,* 2010). At rich fuel-air mixture zone of 100% load, the reduction of oxygen availability again benefited the phenomenon of incomplete combustion. This caused the CO level to increase again after the overall air-fuel ratio condition of 1.2 of about 80 to 85% load for the dual fuel modes. After half load, pure diesel mode showed higher CO emissions compared to both the dual fuel operations. At maximum load, there was a decrease of about 50% CO emissions for biogas-diesel mode (73 ppm) as compared to the diesel mode (139 ppm). At equal load, CO emissions increased nearly 16% for biogas-JOME mode when compared the biogas-diesel mode. To develop an equal power output, the lower calorific value carrier jatropha bio-diesel has led to the injection of higher amount of fuel under its dual fuel mode as compared to diesel ignited mode. This increased the higher CO emissions for JOME ignited dual fuel mode. However, after half load, the levels of CO emissions from both the dual fuel operations were well below than the pure diesel mode and the USA-EPA non-road regulation limits.

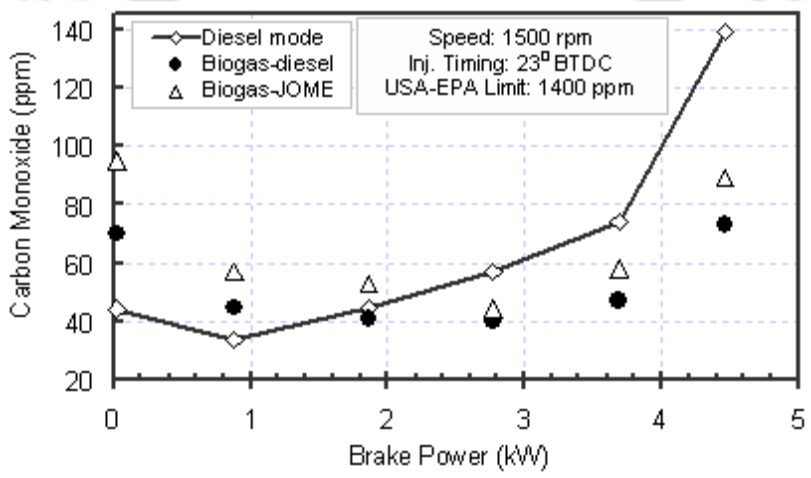

Figure 4.17 Variation of carbon monoxide emission with power output
[Uncertainty: 5 %]

When load was increased, the concentration of CO_2 emissions increased during both diesel mode and dual fuel operations for the entire load range as shown in Fig. 4.18. For an increase in load, the combustion temperature increased and thus, oxygen in the intake air easily oxidized with carbon components in the fuel to produce higher CO_2. However, diesel mode CO_2 emission was lower as compared to both the dual fuel modes. The biogas used in this work contains a huge amount of CO_2 (about 42% by volume) in its composition. It is well known that CO_2 is an inert gas which just appears in the engine exhaust gas without combustion. Thus, at any loading condition, the CO_2 emissions for biogas fuelled dual fuel modes were higher than the diesel mode. As the load was increased from 0 to 100%, a higher amount of biogas took part in the combustion, and hence, a significant increase in the CO_2 emission recorded under dual fuel operations at higher loads. At 100% load, the maximum CO_2 emissions found as 8 and 9% for diesel and JOME ignited dual fuel modes respectively as compared to 6% of diesel mode.

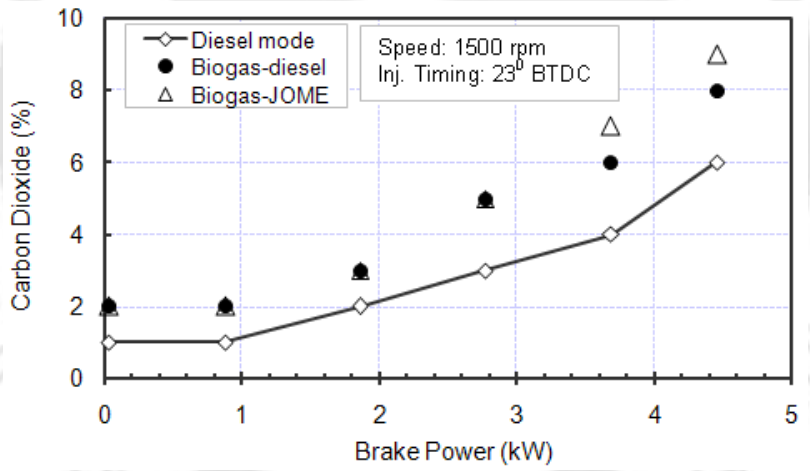

Figure 4.18 Variation of carbon dioxide emission with power output
[Uncertainty: 5 %]

The NO_x emission depends upon combustion chamber temperature which in turn depends on the applied load (Heywood, 1988). Therefore, with increase in load there is always an increase in NO_x emission. From the experiments, it was found that NO_x emissions increased with increase in load for all the fuels tried on the engine (Fig. 4.19). However, due to the effect of CO_2, low energetic dual fuel operation produced much lower NO_x compared to diesel mode. This was due to poor air-fuel mixing rates which reduces charge temperature. The maximum NO_x concentration was found 156 ppm for neat diesel operation at 100% load. This value further reduced to 49 ppm and 42 ppm for diesel and JOME pilot ignited dual fuel

modes respectively. Therefore, the benefits of reduced emissions of both CO (after half load) and NO_x concentrations were achieved under the dual fuel operation. HC emission levels for diesel mode reached to minimum value with a little lean mixture region of about 80% engine load as shown in Fig. 4.20. When the mixture becomes very lean, due to incomplete combustion, HC rises. For a dual fuel operation, when load was increased, the increment in the amount of biogas energy share increased the HC level. This was probably because of the unburned portion of the charge which is thought to be composed of biogas becomes richer (Swami Nathan *et al.,* 2010). It is to recall here that, the dual fuel operation was executed to a maximum biogas level up to engine misfire. Hence, at higher loads, for the maximum biogas combustion, there was a sudden rise in the HC levels. These levels were far higher than the base diesel values. Including this, the flame quenching and incomplete combustion also led to high HC levels. At 100% load, the maximum HC level with diesel mode was 74 ppm as against 140 ppm and 174 ppm with diesel and bio-diesel ignited dual fuel modes respectively.

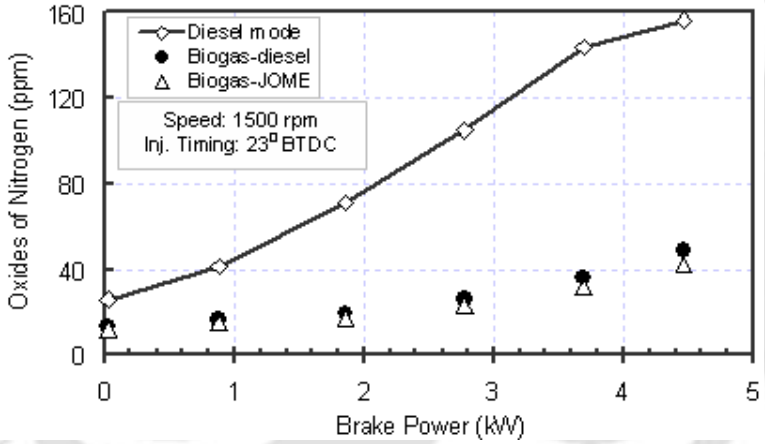

Figure 4.19 Variation of oxides of nitrogen emission with power output
[Uncertainty: 5 %]

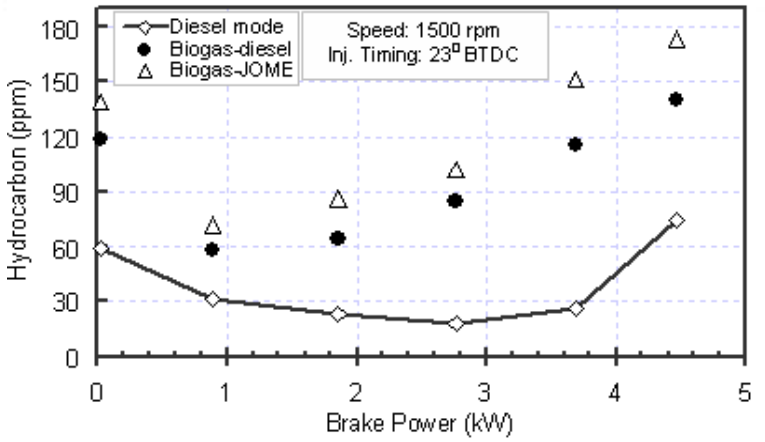

Figure 4.20 Variation of hydrocarbon emission with power output
[Uncertainty: 5 %]

At most of loading conditions, the combination of NO_x and HC emissions for the dual fuel operations were higher than that of the diesel mode. However, they still satisfy regulated emission limits of USA–Environmental Protection Agency (EPA) non-road regulations (http://www.dieselnet.com/standards/) as shown in Fig. 4.21.

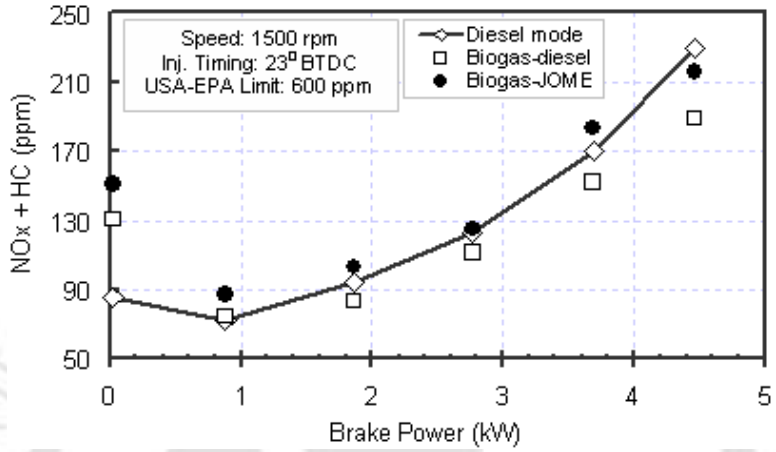

Figure 4.21 Variation of NO_x+HC emission with power output [Uncertainty: 5 %]

4.5 Summary

The results of biogas fuelled dual fuel operations in a single cylinder DI diesel engine by using diesel and jatropha bio-diesel pilot ignition under independent dual fuel mode are presented in this chapter. The outcome of dual fuel modes are compared to a baseline test conducted with standard diesel fuel at varying loads. Biogas-diesel mode managed an effective diesel replacement level, whereas, biogas-JOME mode was able to save full fossil diesel oil utilization in a diesel engine. The dual fuel operations benefited the environment by reducing the concentrations of CO at medium and high loads and the levels NO_x emissions for the entire load range. The bio-diesel ignited mode consumed less friction power over diesel ignited dual fuel mode. The reduction of maximum pressure rise rate for the dual fuel modes retained the engine architecture safe. There was a reduction in thermal efficiency and cylinder peak pressure for the dual fuel modes as compared to diesel mode due to longer pilot ignition delay. At lower loads, the high self ignition temperature of biogas further reduces the efficiency of dual fuel modes. For an increase in load, the HC and CO_2 levels were significantly increased for a higher biogas energy share under the dual fuel modes as compared to the diesel mode. However, the environment is not affected by the higher CO_2 emissions. Actually, using biogas dual fuel modes, there is a reduction in GHGs by not emitting 48% by volume of CH_4 present in biogas composition.

Chapter – 5

THERMODYNAMIC ANALYSIS OF BIOGAS DUAL FUEL ENGINE OPERATION

Overview

In order to reduce greenhouse gases from diesel engines, biogas has been employed as an alternative fuel under dual fuel approach. The experimental investigations of dual fuel operations reveal reductions in thermal efficiencies as compared to diesel mode. From the dual fuel mode viewpoint, it is very essential to have the knowledge of available fuel energy is losses or destroys whereabouts in the engine operations. Further, it is crucial to know the maximum possible performance of the dual fuel modes which can provide a vital comparison parameter with base engine. In addition, impact of process changes such as, load and pilot fuel quality etc. in the system in terms of system losses is also to be assessed. These findings will help in reducing the available energy loss to improve the overall engine performance. Towards this, this chapter discusses both the energy and exergy balance of the diesel and dual fuel operations. The first and second law analysis are coupled together in order to complete the theoretical treatment of an engine operation. The present work is applied the thermo-mechanical availability analysis by retrieving data of the biogas dual fuel experiments presented in Chapter 4. This chapter discusses the energy and exergy balances of dual fuel mode operations fuelled with biogas. It provides both the general performance calculations and the details of the overall thermodynamics aspects of the engine operation. In this work, the effects of pilot fuel quality, diesel/ jatropha bio-diesel (JOME), on dual fuel operations are examined from the second law perspective. Finally, the thermo-mechanical availability analysis outcomes of the dual fuel modes are compared to that of the diesel mode. Specifically, the effects of pilot fuel type on all existing availability terms such as, brake power output, coolant heat transfer, exhaust losses, exergy efficiency, and irreversibility are explored by combining both the first and second laws of thermodynamics.

5.1 Availability Analysis

The knowledge of 'how the energy is lost' will help in finding means to reduce the same to improve the performance of the engine in terms of power output and efficiency (Kumar et al., 2004). This seems to be the main reason behind most energy studies performed on ICEs. The energy balance studies are also done to optimize engine settings or system settings. Depending on the application, it is very important to have the knowledge of an engine run time period and its loading condition for efficient operation of an engine (Kopac and Kokturk, 2005). In this section, the impact of variations of engine load and pilot fuel quality in the energy and exergy balances of the dual fuel operations are evaluated, and compared to that of the baseline diesel mode. The experimental observation data are retrieved from Chapter 4 for the first and second law analysis purpose as per the Eq. (D1) to (D13) described in *Appendix D*. The various calculated energy and exergy terms are calculated in Table 5.1 and 5.2 respectively. The typical variations of the exergy terms during various tested fuel modes are shown individually in Figs. 5.1 through 5.3.

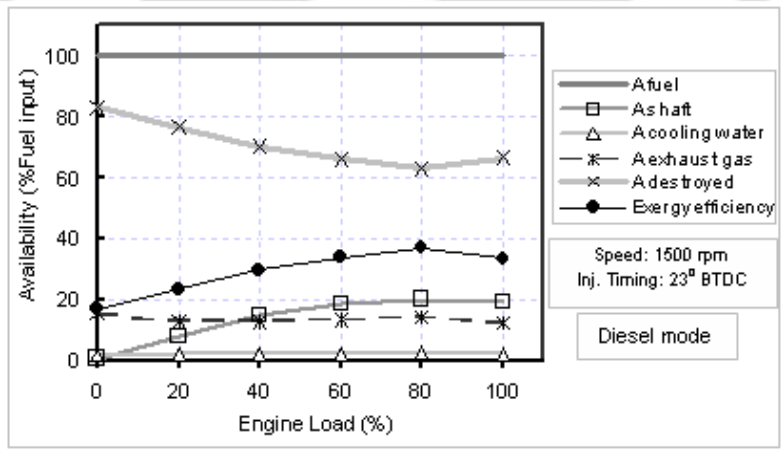

Figure 5.1 Availability distribution with fuel input as function of load (Diesel mode)

During an engine operation, as load increased, the richer fuel-air mixture increased the combustion temperature. Therefore, increased work availability and reduced heat transfer availability losses were obtained, as percentages of the fuel chemical availability. For this, an increase in the exergy efficiency resulted at higher loads for all the tested fuels. The dual fuel operations are favored thermodynamically at higher loads since their exergy efficiencies improve significantly as compared to low load conditions. Because of the improved combustion of biogas at higher loads, the exhaust gas availability was increased. In addition, the shaft availability of the fuels was higher for an increased load. The exergy efficiency was decreased slightly after 80% load due to the poor combustion of fuels where the oxygen availability diminished.

Table 5.1 Energy analysis of diesel and biogas dual fuel mode of operations at various engine loads

Load (%)	Fuel Type	Q_{in}		W_{shaft}		$Q_{cooling}$		$Q_{exhaust}$		$Q_{uncounted}$	
		kW	*%*	*kW*	*%*	*kW*	*%*	*kW*	*%*	*kW*	*%*
0%	Diesel mode	9.68	100	0.03	0.31	3.453	35.67	1.967	20.32	4.554	45.54
	Biogas-diesel	15.79			0.19	2.512	15.91	2.91	18.43	10.338	65.47
	Biogas-JOME	16.67			0.18	2.512	15.07	2.865	17.18	11.263	67.56
20%	Diesel mode	10.42	100	0.88	8.44	4.71	45.2	2.152	20.65	2.678	25.7
	Biogas-diesel	16.76			5.25	3.453	20.6	3.086	18.41	9.341	55.73
	Biogas-JOME	17.18			5.12	3.139	18.27	3.237	18.84	9.924	57.76
40%	Diesel mode	12.17	100	1.86	15.28	5.024	41.28	2.622	21.54	2.664	21.89
	Biogas-diesel	17.64			10.54	4.081	23.13	3.537	20.05	8.162	46.27
	Biogas-JOME	18.18			10.23	3.453	18.99	3.792	20.86	9.075	49.92
60%	Diesel mode	14.57	100	2.77	19.01	5.96	40.9	3.2	21.96	2.64	18.12
	Biogas-diesel	19.21			14.42	4.395	22.88	4.099	21.34	7.946	41.36
	Biogas-JOME	20.52			13.5	3.767	18.36	4.47	21.78	9.513	46.36
80%	Diesel mode	17.64	100	3.69	20.92	6.91	39.17	4.447	25.21	2.593	14.7
	Biogas-diesel	21.94			16.82	5.337	24.32	5.235	23.86	7.678	34.99
	Biogas-JOME	22.93			16.09	5.023	21.9	5.656	24.66	8.561	37.33
100%	Diesel mode	22.88	100	4.46	19.49	7.85	34.31	5.39	23.56	5.18	22.64
	Biogas-diesel	28.21			15.81	5.965	21.14	6.097	21.61	11.688	41.43
	Biogas-JOME	32.67			13.65	5.561	17.02	6.861	21.00	15.698	48.05

Table 5.2 Exergy analysis of diesel and biogas dual fuel mode of operations at various engine loads

Load (%)	Fuel Type	A_{in}		A_{shaft}		$A_{cooling}$		$A_{exhaust}$		$A_{destroyed}$		Exergy Efficiency
		kW	*%*	*kW*	*%*	*kW*	*%*	*kW*	*%*	*kW*	*%*	*%*
0%	Diesel mode	10	100	0.03	0.3	0.166	1.66	1.508	15.08	8.296	82.96	17.04
	Biogas-diesel	18.12			0.17	0.017	0.1	2.004	11.06	16.069	88.68	11.32
	Biogas-JOME	19.25			0.16	0.019	0.1	2.019	10.49	17.182	89.26	10.74
20%	Diesel mode	10.77	100	.0.88	8.17	0.242	2.24	1.396	12.94	8.252	76.62	23.38
	Biogas-diesel	19.6			4.49	0.039	0.2	2.015	10.28	16.665	85.03	14.97
	Biogas-JOME	20.18			4.36	0.036	0.18	2.025	10.03	17.239	85.43	14.57
40%	Diesel mode	12.58	100	1.86	14.78	0.265	2.11	1.6	12.72	8.855	70.39	29.61
	Biogas-diesel	20.7			8.99	0.06	0.29	2.245	10.84	16.535	79.88	20.12
	Biogas-JOME	21.39			8.69	0.045	0.21	2.367	11.06	17.118	80.03	19.97
60%	Diesel mode	15.06	100	2.77	18.39	0.355	2.36	1.954	12.97	9.981	66.27	33.73
	Biogas-diesel	22.68			12.21	0.071	0.31	2.477	10.92	17.36	76.55	23.45
	Biogas-JOME	24.3			11.4	0.066	0.27	2.672	10.99	18.792	77.33	22.67
80%	Diesel mode	18.23	100	3.69	20.24	0.451	2.47	2.579	14.15	11.51	63.14	36.86
	Biogas-diesel	25.97			14.21	0.112	0.43	3.016	11.61	19.152	73.74	26.25
	Biogas-JOME	27.32			13.51	0.108	0.39	3.232	11.83	20.29	74.27	25.73
100%	Diesel mode	23.65	100	4.46	18.86	0.545	2.31	2.854	12.07	15.791	66.77	33.23
	Biogas-diesel	33.71			13.23	0.144	0.43	3.528	10.46	25.578	75.88	24.12
	Biogas-JOME	39.31			11.35	0.139	0.38	4.095	11.13	28.1	76.36	23.64

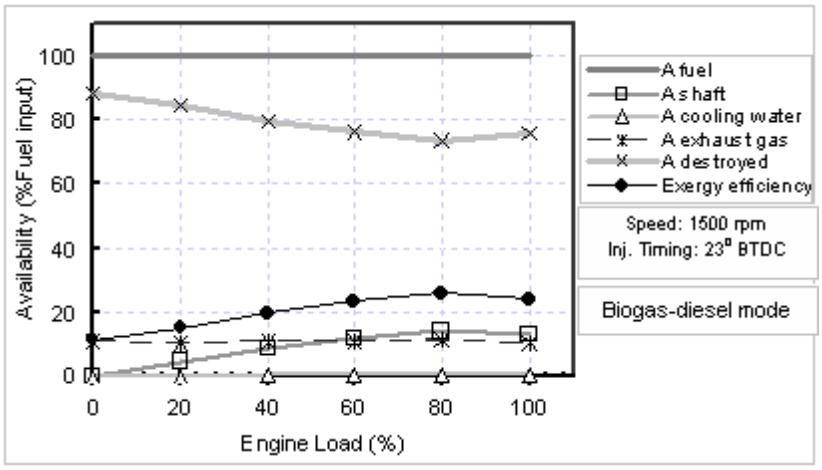

Figure 5.2 Availability distribution with fuel input as function of load (Biogas-diesel mode)

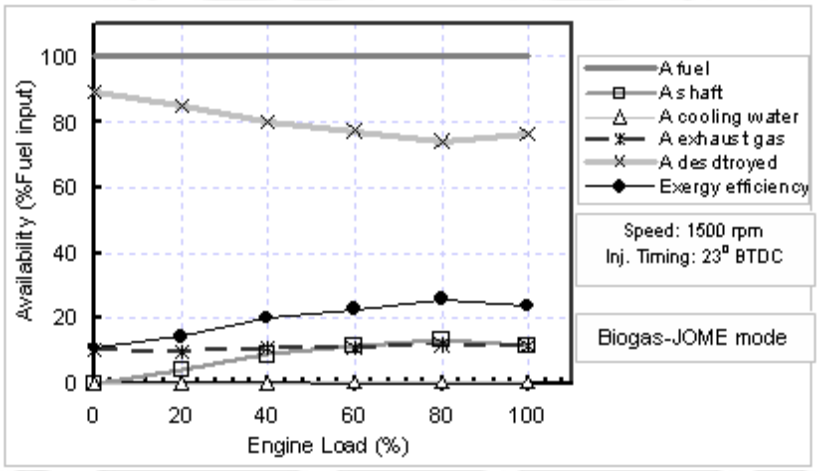

Figure 5.3 Availability distribution with fuel input as function of load (Biogas-JOME mode)

Figure 5.4 shows the percentage of fuel availability exchanged through destroyed availabilities (irreversibilities) versus load for the tested fuel modes. The availability destruction decreased with the increase of load. This is because of the increase in combustion temperatures, decrease in combustion duration, and decrease in entropy generation during oxidation. At low loads (up to 40%), poor combustion of biogas fuels caused less cooling water and exhaust gas availabilities i.e., higher destroyed availability. at maximum efficiency condition (80% load), the minimum destroyed availability was found as 73.7 and 74.3% for diesel and JOME ignited dual fuel modes respectively. While at the same condition, this value was found as 63.1% for diesel mode. Due to presence of a significant part of chemically inert CO_2 in biogas, the combustion temperature of dual fuel modes reduced. This caused a reduction in both the fuel availability and work output of the dual fuel modes. It affects the decrease of second law efficiency and an increase in the percentage of fuel availability destroyed in the form of irreversibility.

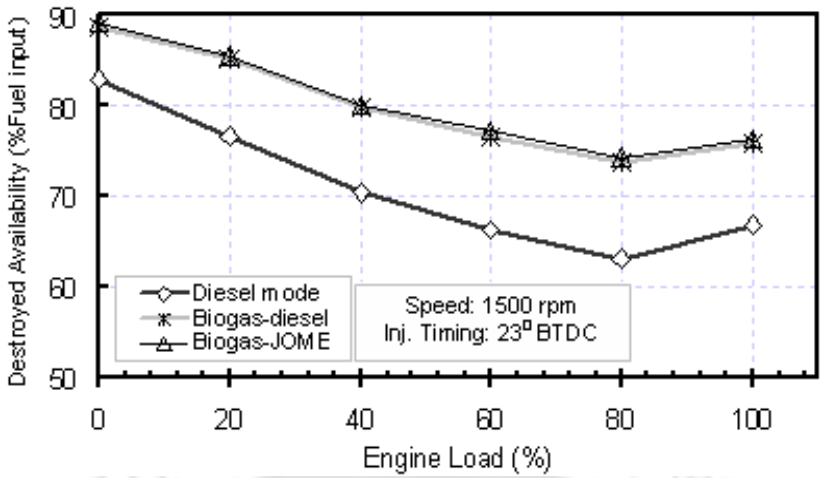

Figure 5.4 Destroyed availability distribution at different engine load

Figure 5.5 shows the kW fuel availability distribution of the diesel and dual fuel mode operations. The results showed that, at lower loads, the lean air-fuel mixture decrease the fuel availability. When load was increased, to produce higher shaft output at respective loads, the enhanced rate of fuel energy increased the amount of kW available fuel input. In the process, a higher kW shaft availability was resulted at higher engine loads. To maintain an equal power output as of diesel mode, dual fuel modes required higher chemical fuel exergy than the diesel mode due to the poor combustion and low energetic biogas fuel. The trend of the supply of fuel exergy under dual fuel modes converged to that of diesel mode for an increase in load up to the overall air-fuel ratio condition of 1.2. This is due to the better combustion of biogas at higher temperature loads.

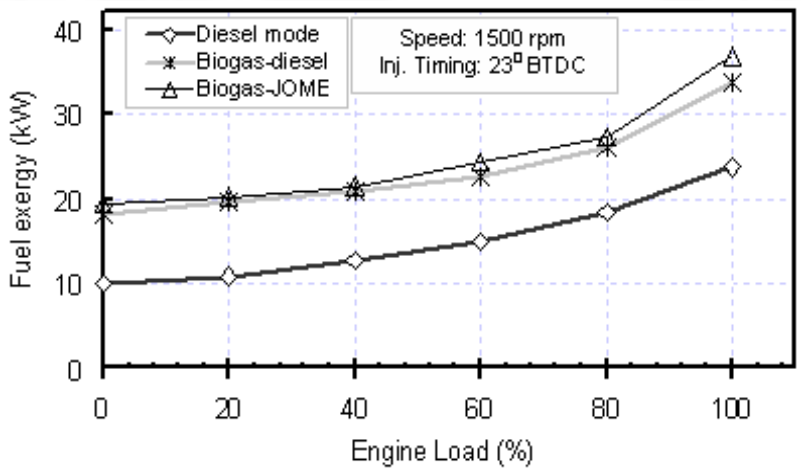

Figure 5.5 Chemical fuel exergy versus load

Figures 5.6 and 5.7 show the exergy transfer through cooling water and exhaust gas versus load respectively, for various modes of operation. The biogas dual fuel operations produced higher exhaust gas temperature as compared to diesel mode for the entire range of load (Fig. 4.5). This leads to higher exhaust gas availability for the dual fuel modes. The biogas-JOME mode produced maximum exhaust gas availability as this operation recorded maximum temperature in its exhaust. At 100% load, the maximum exhaust gas availability was found as 4 kW for biogas-JOME mode as compared to that of 2.8 kW of diesel mode. At the same load, the maximum of this value found as 3.5 kW for biogas-diesel mode. The cooling availability of dual fuel operations was very little due to the intensive cylinder wall loss. Only a maximum of about 0.14 kW cooling availability was accessible from the dual fuel operations as compared to about 0.2 to 0.5 kW to that of diesel mode. At low loads of 0 to 40%, poor combustion of air-biogas mixture caused less cooling water and exhaust gas availability, and hence, resulted higher destroyed availability.

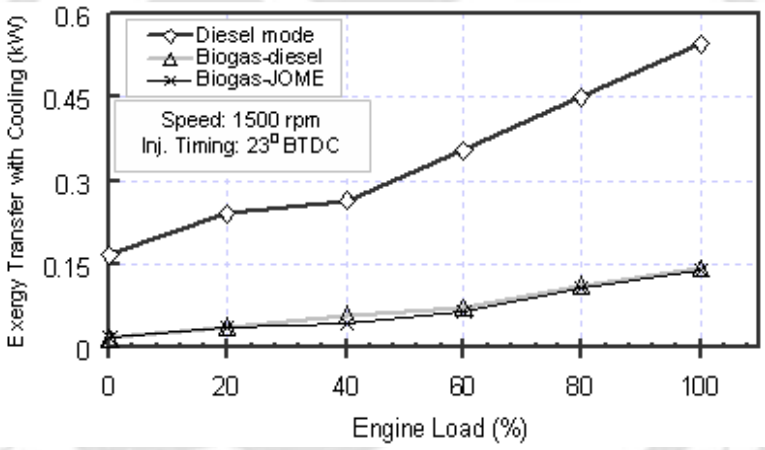

Figure 5.6 Availability transfer by cooling water versus load

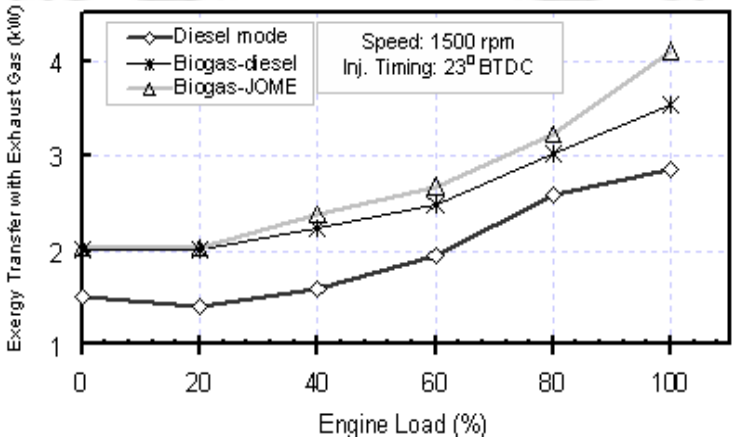

Figure 5.7 Availability transfer by exhaust gas versus load

Figure 5.8 shows the availability transfer by work (kW) as a function of load. Including this, the increase in work availability from both the exhaust gas and cooling water from the diesel and dual fuel modes were illustrated. When load increased, the availability transfer by work increased. This is due to the increase in the energy input into the cylinder and decrease in combustion duration. The availability results showed that, when load was increased, the dual fuel operations generated more increase in the cumulative exhaust gas and cooling water availabilities. This allowed the more of the availability accessible for conversion to work availability. This resulted improvement in the dual fuel exergy efficiency at higher loads. The dual fuel modes produced little higher accessible work availability (about 2 to 4 kW) as compared to diesel mode (about 1.5 to 3.5 kW). This is due to the higher exhaust gas availability loss of the dual fuel operations.

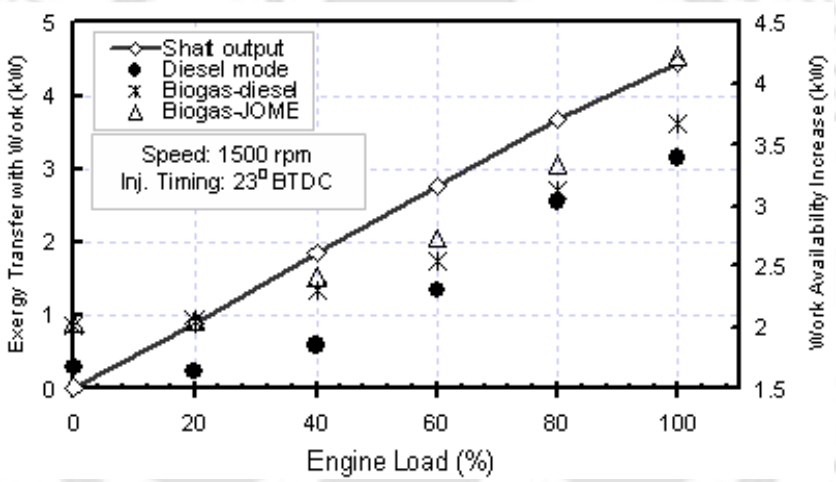

Figure 5.8 Availability transfer by work versus load

Figure 5.9 shows the second-law efficiency versus load for diesel and dual fuel modes. The second law efficiency increased to a load of 80% and then decreased due to the reduction in the combustion speed. As the load increased, the cumulative work, exhaust gas and cooling water availabilities were increased. The increase in the gross work output availability increased the corresponding exergy efficiency. The second law efficiency was observed highest in case of diesel mode and recorded a maximum of 37% at 80% load. At higher loads, the energy input into the cylinder increased and as a consequence the corresponding the cumulative work availability increased. Moreover, increase in load resulted in an improvement of the combustion process from the second law viewpoint. Both the increase in the combustion temperatures and the decrease in the combustion duration with increasing load decrease the combustion irreversibilities. The lower is the irreversibility, the higher is

the exergy efficiency and vice versa. There was a marginal difference in exergy efficiency between the dual fuel modes. The comparison of energy and exergy efficiency of tested fuel modes is shown in Fig. 5.10. It can be noticed that the maximum exergy efficiency of dual fuel modes (about 26%) are higher than the energy efficiency of base diesel engine (about 21%). This suggests that by retrieving the exhaust gas availability losses, the dual fuel modes can achieve even higher efficiencies than that of base diesel mode of operation.

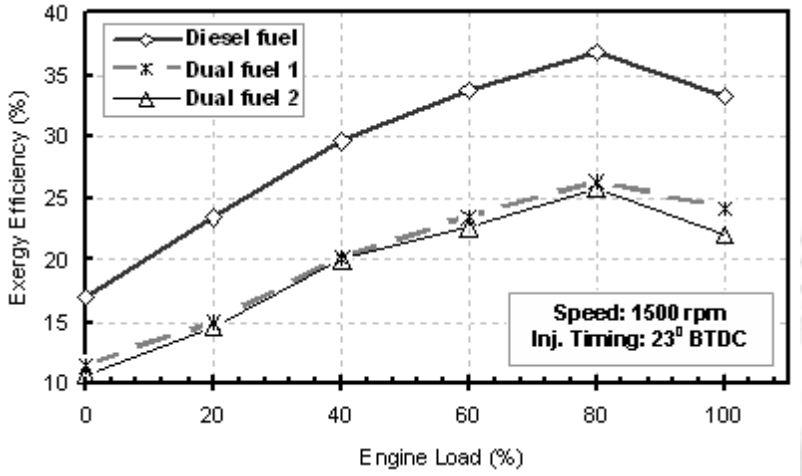

Figure 5.9 Second law efficiency versus load

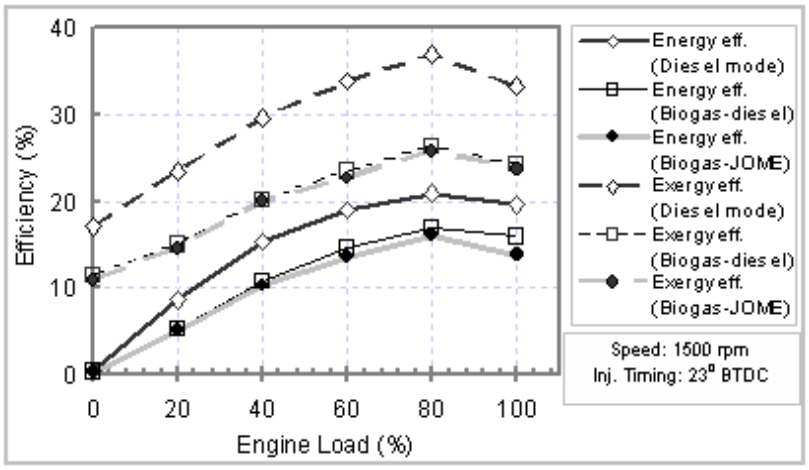

Figure 5.10 Comparison of energy and exergy efficiency versus load

The availability balance affected very little by the pilot fuel quality as shown in Fig. 5.11. The percentage of fuel availability that destroyed was reduced for both pilot fuel cases. This decrease was due to better air-fuel mixture combustion. However, for the diesel ignited dual fuel mode, the destroyed availability was noticed least as compared to other dual fuel mode. Contrary to the trend of destroyed availability, the second law efficiency increased under the

biogas-diesel mode. This is a combined effect of reduction of combustion irreversibility and increase in the maximum temperature of the cycle, which caused the efficiency gains. At 80% load, the maximum exergy efficiencies found were 26.3% and 25.7% for diesel and bio-diesel ignited dual fuel modes. Although bio-diesel has lower energy capacity than diesel, the presence of oxygen content improved the combustion at higher loads. Hence, there was only a 2% decrease in maximum exergy efficiency for bio-diesel pilot than the diesel case.

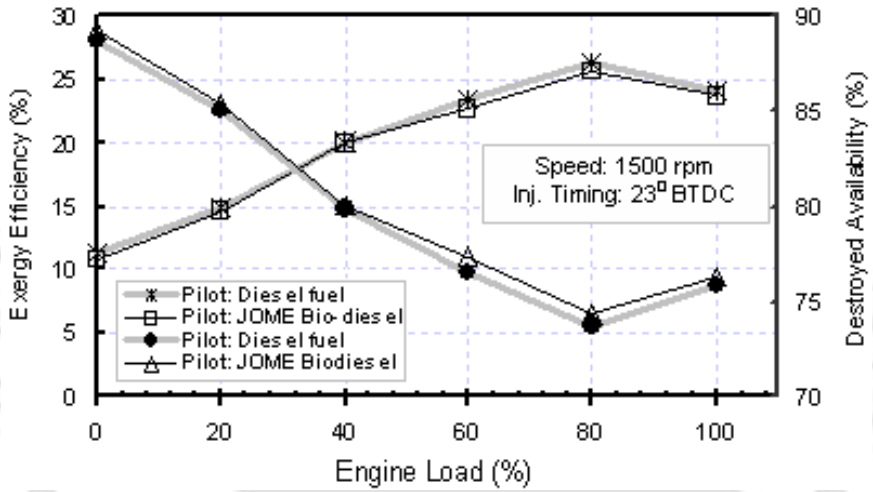

Figure 5.11 Effect of pilot quality on exergy efficiency and destroyed availability

5.2 Summary

A thermodynamic analysis was performed on a single-cylinder, constant-speed and direct-injection diesel engine. The engine was tested under biogas dual fuel operations with diesel and jatropha bio-diesel as pilot fuel ignition. Availability equations were applied to both diesel and dual fuel modes at varying engine loads. The various kinds of exergy terms such as, brake work, cooling water, exhaust gas, and irreversibility) were compared and discussed. There was an increase in exergy efficiency with an increase in load for all the tested fuel modes. However, due to the lower cumulative work output, dual fuel modes have resulted lower exergy efficiency. The results suggest that, due to a marginal difference in exergy efficiency, jatropha bio-diesel can be an effective substitute to the fossil diesel as pilot ignition source. Due to poor fuel-air mixture combustion and lower energy content of biogas fuel, dual fuel modes compelled to expend higher fuel chemical exergy than that of diesel mode. This analysis confirmed that the dual fuel efficiencies can be improved beyond base diesel engine thermal efficiency by accessing the cumulative exergy transfer with exhaust gas and cooling water.

Chapter – 6

SYNGAS–DIESEL DUAL FUEL ENGINE EXPERIMENTS

Overview

Biogas is an attractive energy source because of its decentralized power generation in remote rural areas including its generation from the waste materials like cow dung, and other animal and plant waste matter. Using diesel or bio-diesel pilot ignition as described in Chapters 4 and 5 have shown that biogas, as a primary fuel, can be effectively used in diesel engines under dual fuel mode. Although, the dual fuel modes have produced lower thermal efficiency, this can be offset by large replacement of fossil diesel, and also, lower production of NO_x and CO emissions. Apart from methane based biogas, hydrogen (H_2) is a strong contender as an environment friendly fuel for IC engines because when it burns, only water vapours are released into the atmosphere. Further, IC engines are also capable of burning the carbon monoxide (CO) gas as it is not contaminated. Syngas is mainly a mixture of two energy content molecules, H_2 and CO. It can be manufactured from natural gas, coal, petroleum, biomass, and organic wastes etc. Various researchers have tried to explore the application of this environmentally clean and low cost fuel in gas turbines and reciprocating engines to produce electricity. The present work is an attempt to use a combination of diesel fuel and H_2/CO rich gases under dual fuel operation in a single-cylinder diesel engine. The experiments have been conducted at different operating conditions by varying of engine load and gaseous fuel type. The performance results include brake thermal efficiency, brake specific fuel consumption, diesel substitution rate, exhaust gas temperature and volumetric efficiency. The combustion analysis includes parameters like maximum cylinder pressure, $P-\theta$ diagram, heat release analysis, engine knocking behavior and ignition delay. The main emphasis is put on the standard emissions such as CO, CO_2, NO_x, and HC. The variations of each dry exhaust concentration with engine operating conditions have been plotted. The results of dual fuel engine performance have been compared to that of baseline results obtained with diesel fuel.

6.1 Experimental Design

In this experimental work, a total of four different types of syngas fuels were tested in dual fuel mode. The type of syngas fuel was determined by varying volumetric ratio of H_2 and CO content. The volumetric fraction of H_2 content in fuel-gas was varied to 100, 75, 50 and 0% of the total H_2 and CO contained syngas. Hence, the balance is the CO content in syngas. The previous biogas dual fuel operations have already confirmed the capability of bio-diesel being a pilot fuel for their matching dual fuel engine performance as that of diesel fuel. Therefore, in this syngas dual fuel operations only diesel as pilot ignition is investigated. Table 6.1 summarizes important properties of fuels utilized in the experiments. The lower heating value, density and flame velocity of syngas were calculated theoretically from the each elementary gas composition values. In order to establish the basis for comparison of dual fuel results, a baseline test with 100% diesel fuel was also conducted. To ensure the consistency of the observations, engine tests were conducted as per experimental design as given in Table 6.2. For a safe operation, the engine was run to a maximum of 90% of its power rating and the corresponding load is considered as the 100% benchmark for the experimental design. The engine was operated at different load levels ranges from 0% (idle or no-load condition) to a maximum of 100% load in steps of 20% for baseline test. However, during the dual fuel experiments, at no-load condition, the operation showed a harsh engine running including severe misfire and also, resulted very little diesel replacement rate. Hence, the dual fuel experiments were executed only at 20% engine load to full load. The mass flow rate of diesel and syngas consumed during diesel and dual fuel modes are presented in Table 6.3.

Table 6.1 Important fuel properties used in syngas-diesel operations

Properties	**Diesel**	**Syngas**			
Chemical composition	$C_{12}H_{26}$	100% H_2+ 0% CO	75% H_2+ 25% CO	50% H_2+ 50% CO	0% H_2+ 100% CO
Density (kg/m^3)	850	0.085	0.38*	0.67*	1.9
Lower heating value (MJ/kg)	42	119.81	23.09*	14.81*	10.112
Flame velocity (m/s) (Kumar *et al*., 2003b) (Dong *et al*., 2009)	0.3	2.7	1.9*	1.8*	0.19
Cetane number	45-55	---	---	---	---
Auto-igntion temp. (K) (Kumar *et al*., 2003b)	553	858	---	---	882
Stoichiometric A/F ratio (kg/kg)	14.92*	34.3*	8.075*	4.58*	2.45*
Energy density (MJ/Nm^3)	2.82*	2.87*	2.38*	2.70*	3.79*

* calculated value

Table 6.2 Experimental design for syngas-diesel mode data collection

Mode of operation	System components	Designation of operation	Engine operation
Diesel	Fuel: 100% Standard diesel	Baseline test (or) Diesel mode	Speed: 1500 ± 50 rpm Load: 0, 20, 40, 60, 80, 100% Injection timing: 23^0 BTDC
Dual fuel (Pilot: Diesel)	Primary: Syngas (H_2:CO::100:0)	Dual fuel 1	Speed: 1500 ± 50 rpm Load: 20, 40, 60, 80, 100% Injection timing: 23^0 BTDC
	Primary: Syngas (H_2:CO::75:25)	Dual fuel 2	
	Primary: Syngas (H_2:CO::50:50)	Dual fuel 3	
	Primary: Syngas (H_2:CO::0:100)	Dual fuel 4	

Table 6.3 Fuel consumption data for various engine operations

Engine load (%)	Mass flow rate of diesel (kg/hr)	Mass flow rate of syngas (kg/hr)
	Diesel mode	
0	0.83	---
20	0.91	---
40	1.06	---
60	1.26	---
80	1.53	---
100	1.98	---
	Dual fuel 1	
20	0.65	0.25
40	0.62	0.25
60	0.56	0.3
80	0.51	0.34
100	1.17	0.38
	Dual fuel 2	
20	0.68	1.33
40	0.65	1.33
60	0.63	1.52
80	0.68	1.9
100	1.22	2.09
	Dual fuel 3	
20	0.74	2.01
40	0.72	2.34
60	0.69	3
80	0.66	3.7
100	1.3	5
	Dual fuel 4	
20	0.73	3.8
40	0.73	3.8
60	0.66	4.75
80	0.64	5.7
100	0.87	8.55

6.2 Performance Results

The performance measurements have been made in order to define the characteristics of engine operation on both the diesel and dual fuel modes. Figures 6.1 to 6.7 show the performance parameters, brake thermal efficiency, specific energy consumption, volumetric efficiency, exhaust gas temperature, diesel replacement level and gas flow rate as a function of engine load level as per the test matrix. The performance measurements were made in order to define the characteristics of engine operation under diesel and dual fuel modes. It is to recall here that, the brake power and torque output at different engine loads were kept constant during diesel (baseline) and dual fuel operations (Fig.6.1). For a safe operation, the diesel engine was run to a power output of 4.46 kW and torque of 2.96 kg-m which were about 90% of maximum engine rating. The brake specific energy consumption (BSEC) was increased for dual fuel operations as compared to diesel mode as shown in Fig. 6.1. At low load of 20%, the differences in BSEC between diesel and dual fuel modes were higher. This is due to the incomplete combustion and lower flame velocity of syngas fuels. However, when load increased the BSEC of dual fuel modes improved although always higher than that of diesel mode. Because, to produce same power output as of diesel case, the low energy density syngas fuels need more fuelling than diesel mode. Although 100% CO syngas possess higher energy density, the insufficient oxygen availability led to poor combustion and hence, its dual fuel operation was resulted higher BSEC. Among syngas fuels, the 100% H_2 fuel produced a lower BSEC due to faster combustion rates of hydrogen.

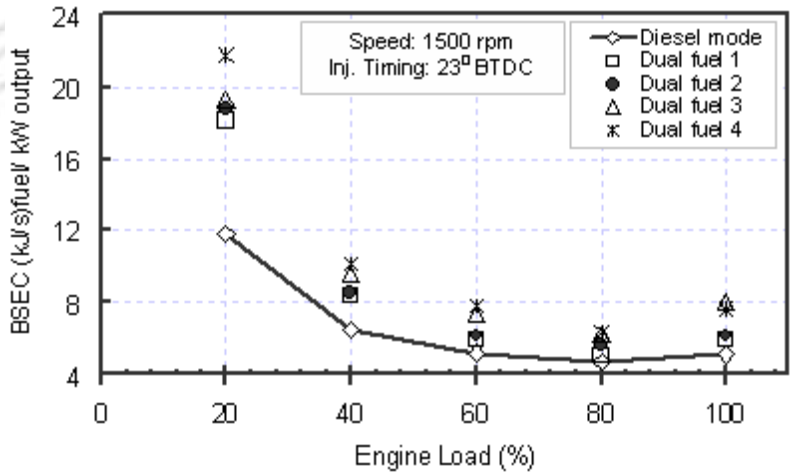

Figure 6.1 Variation of brake specific energy consumption with engine load

The higher BSEC dual fuel modes produced lower thermal efficiency than that of diesel mode for the entire load range (Fig. 6.2). At light loads (20 and 40%) the dual fuel operations

showed a much inferior efficiency as compared to diesel mode. This is due to the poor combustion efficiency caused by a high CO content of the syngas fuels under part load conditions. Again, at these loads, injection of a small pilot quantity has led to a poor ignition and combustion of lean air-gas mixture. Therefore, there is a minor influence of H_2/CO composition on the thermal efficiency at part-loads. However, beyond half-load, the efficiency of dual fuel operations improved. Increasing hydrogen fraction as well as increasing the H_2/CO ratio in the fuel effectively improved the thermal efficiency. This is due to the faster combustion rate of H_2 and CO, and higher level of premixing. At 80% load, the dual fuel operation with 100% H_2 syngas (Dual fuel 1) delivered a maximum efficiency of 20% compared to 21% with the diesel mode. The efficiency decreased with lower H_2/CO ratio fuels. At 80% load, the maximum thermal efficiencies for syngas fuels with H_2 fraction of 75, 50 and 0% were found as 18, 16 and 15% respectively. The extent of de-rating in maximum efficiency was about 6% for the 100% H_2 syngas and increased to as high as 27% for 100% CO syngas operation as compared to diesel mode. The fuel with H_2:CO of 75:25 syngas (Dual fuel 2) resulted a similar efficiency level to that with 100:0 fuel. This is due to the improved CO oxidation in the combustion chamber at higher loads. Also for this reason, at maximum engine load, 100% CO fuel showed a better thermal efficiency than H_2:CO::50:50 syngas (Dual fuel 3) mode. Overall, the decrease in thermal efficiency is attributed by the lower LHV of syngas fuels. Again, at increased loads, the high rates of H_2 content syngas admission make the combustion process too rapid and hence, the thermal efficiency decreases. In this regard, for a producer gas operation, Sridhar et al. (2001) have suggested for optimizing the ignition timing and fuel-gas mass share as per the H_2 fraction of the fuel-gas to derive maximum shaft output and efficiency for an equal energy input.

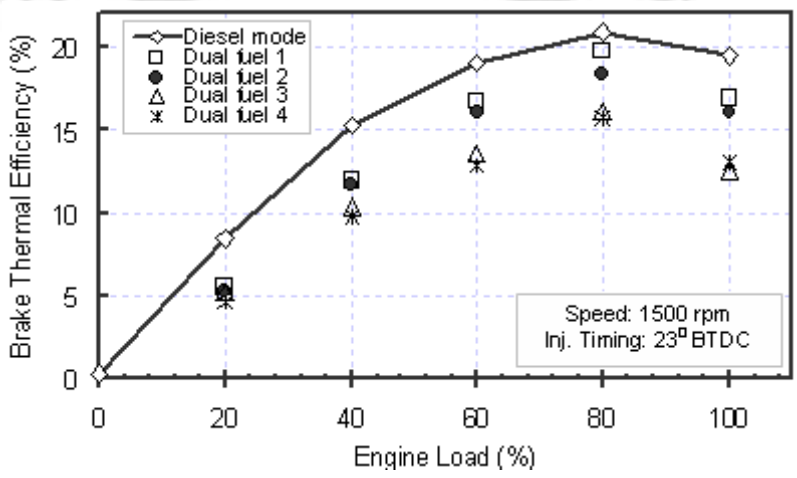

Figure 6.2 Variation of brake thermal efficiency with engine load

The lower thermal efficiency of dual fuel operation is one of the reasons for their higher exhaust temperatures. The variation of exhaust gas temperature with load for syngas-diesel modes is shown in Fig. 6.3. The exhaust gas temperature increased with an increase in load. The reason for the rise in engine exhaust temperature is also due to lack of adequate combustion time between diesel and syngas. The 100% H_2 syngas dual fuel operation recorded highest exhaust temperature for the entire load range due to faster combustion and high cylinder temperature. Among CO content syngas fuels, 100% CO mode showed lowest exhaust gas temperature due to its lower LHV and poor combustion. The maximum exhaust temperatures for 100, 75, 50 and 0% H_2 fraction syngas were found as 982, 951, 942 and 918K respectively, as compared to 846 K of diesel mode.

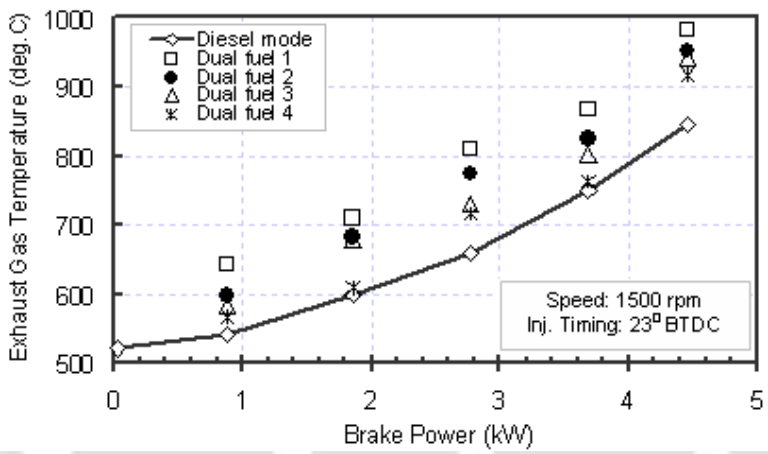

Figure 6.3 Variation of exhaust gas temperature with engine power output

The diesel replacement rate in dual fuel operations under different loading conditions is shown in Fig. 6.4. The replacement of diesel oil by syngas fuels showed a maximum value at their best efficiency loading points. At 80% engine load, the diesel replacement rate has gone up to 72.3% for 100% H_2 syngas mode. The maximum diesel substitution rate diminished for lower H_2 content syngas operations. The maximum diesel replacements were estimated as 60.7, 58.8 and 58.4% for the syngas modes with H_2 fractions of 75, 50 and 0% respectively. Contrary to other dual fuels, 100% CO syngas replaced the diesel fuel to a maximum level of 58.4% at 100% load due to the improved CO oxidation at this condition. The decrease in diesel substitution rate was also found for both low and high load conditions. At low load condition, the syngas-air mixture became too lean so that it was legged the proper ignition quality, and hence, diesel replacement level was lower. However, at full load, the insufficient oxygen availability caused incomplete combustion of syngas, and again, lowered the diesel substitution level.

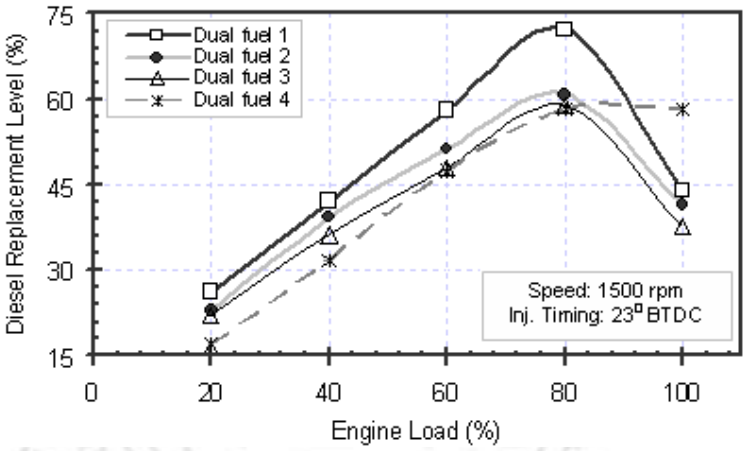

Figure 6.4 Variation of diesel replacement rate with engine load

Figure 6.5 shows the variation of volumetric efficiency with engine loads. Hydrogen, present in syngas, is less dense than air and hence, the light H_2 displaces some air. This resulted a reduction of volumetric efficiency under dual fuel operation at all loads as compared to diesel mode. The volumetric efficiency decreased further by an increase in syngas flow rate.

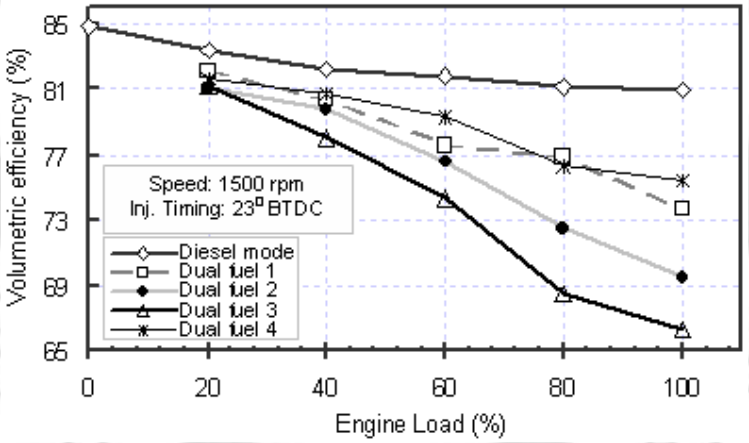

Figure 6.5 Variation of volumetric efficiency with engine load

The gas flow rate increased at higher loads to maintain same power output as of diesel mode (Fig. 6.6). As the gas flow rate is maximum for 50:50 H_2:CO fuel, a lower volumetric efficiency was found as compared to other two H_2 content syngas fuels. At maximum engine load, the lowest volumetric efficiencies were found to be 73.7, 69.5 and 66.2% for H_2 fraction of 100, 75 and 50% in syngas, respectively as compared to 81% of diesel mode. The decrease in volumetric efficiency for 100% CO content syngas was dominated by the gas flow only. Therefore, as the load increased, the rate of decrease in volumetric efficiency was

comparatively lesser than that of syngas with 25 and 50% CO fraction. At 100% load, the lowest volumetric efficiency for 100% CO syngas mode was found to be 75.4%.

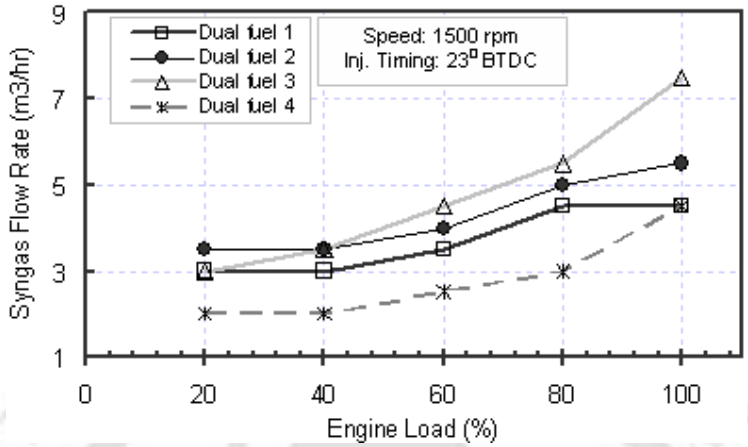

Figure 6.6 Variation of syngas flow rate with engine load

6.3 Combustion Characteristics

The measurement of ignition delay of the tested fuels is based on the duration between pilot injection (23°BTDC) and first positive heat release rate on the heat release diagram (Fig. 6.7). The ignition delay period of the pilot fuel in a dual fuel operation is generally higher than in diesel mode. The ignition delay of pilot diesel increased in the presence of syngas. In a dual fuel combustion system, the pilot spray is surrounded by air-gas mixture and the reaction with this mixture affects the ignition of pilot fuel. From Fig. 6.7, it can be seen that increasing the amount of H_2 content in syngas increased the ignition delay. This is due to the decrease in the amount of pilot diesel surrounded by more air. Therefore, higher H_2 content syngas operations showed higher ignition delays. However, this occurred to a limited extent of H_2 increase only, and thereafter, the ignition delay remained unaffected. Due to this reason 100% and 75% H_2 content syngas combustion showed nearly equal ignition delay duration. The 100% CO mode showed the lowest ignition delays among the dual fuel operations.

In case of a compression ignition mode, combustion occurs in a diffusion mode where fine droplets combustion occurs in an atmosphere of vitiated air. Therefore, the pressure rise is usually rapid. In addition, there are substantial differences in the cylinder peak pressure as the engine load is increased. The peak cylinder pressure started to increase for an increase in engine load (Fig. 6.8).

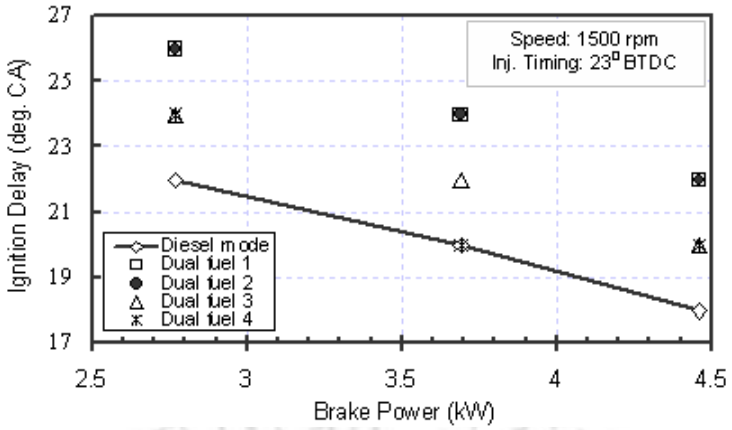

Figure 6.7 Variation of ignition delay with engine power output

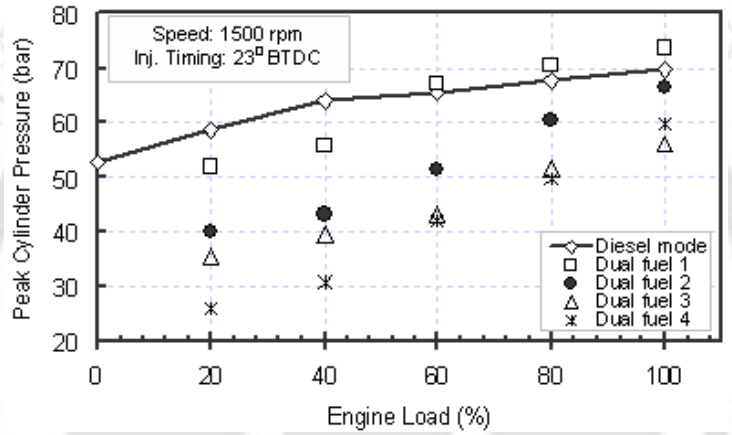

Figure 6.8 Variation of peak cylinder pressure with engine load

For diesel mode, at maximum load (100%), the peak cylinder pressure was found to be highest (69.5 bar) within the entire load range. The peak cylinder pressure were also observed maximum at 100% load for dual fuel operations, and found to be 73.6, 66.5, 56.2 and 59.7bar for syngas fuels with H_2 fraction of 100, 75, 50 and 0%, respectively. For syngas dual fuel operations, shorter combustion duration and an increased ignition delay shifted the overall combustion to expansion stroke, and hence, a reduction of cylinder pressure was resulted. After 40% load, the increase in peak cylinder pressure was observed more intense for the dual fuel modes due to their better combustion at higher temperature zones. Therefore, for the dual fuel modes, the trends of increase in peak pressure prior to 40% load were noticed different than that of after the same load. Among all dual fuel operations, 100% H_2 syngas mode resulted a higher cylinder pressure at all loads because of its shortest combustion duration and highest LHV. Again, at medium and high loads, the peak cylinder pressure of 100% H_2 fraction syngas mode was higher than that of diesel mode due to its high energy release rate.

The syngas fuels which contain H_2 and CO i.e., 75 and 50% H_2 fraction fuels, the combustion retarded further and the cylinder pressure reduced as compared to 100% H_2 fraction syngas mode. Compared to the 100% H_2 case, beyond 60% load, the combustion of 75% H_2 syngas was slightly longer; however, the ignition delay was not affected significantly (Fig. 6.7). Thus, at medium and high loads, a higher increase rate of cylinder pressures for 75% H_2 operation was observed. The peak cylinder pressure of 100% CO syngas was lowest among all tested syngas fuels. This is due to the poor combustion and low energy release rate of fuel. However, for the better combustion of CO gas at maximum temperature region of 100% load, the lower heat content 100% CO syngas mode produced higher peak cylinder pressure than the 50:50 H_2:CO syngas mode.

The trend of maximum rate of pressure rise (MRPR) or combustion noise was similar to that of peak cylinder pressure as shown in Fig. 6.9. At lower engine loads, the cylinder pressure and temperature of dual fuel modes were reduced due to retarded combustion and inefficient oxidation of the gaseous fuels. As the pilot quantity was low, the lean gas-air mixture and thereby, a weak ignition source resulted slower combustion rates. This dropped the peak cylinder pressure and the MRPR. This may be one of the reasons for the reduced thermal efficiency under dual fuel operations at lower loads. Except for 100% H_2 syngas mode (beyond 60% load), all other tested dual fuel modes the MRPR were lower than that of diesel mode for the entire load range. Similar to biogas operations, the syngas dual fuel operations are also established safe operation in the base engine due to their lower MRPR.

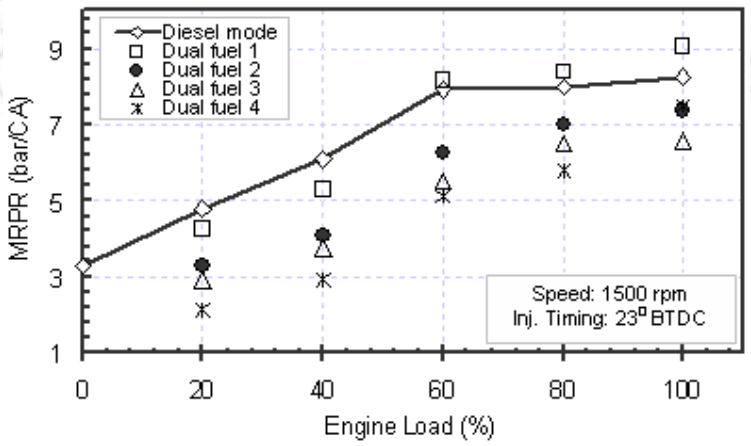

Figure 6.9 Variation of MRPR with engine load

The average data of pressure-crank angle (P-θ) recording at different portion of engine loads is shown in Figs. 6.10 through 6.12. For the entire range of load, there were smooth and

normal combustion curves occurred for the dual fuel modes. This was because of the limited syngas flow (up to the engine misfire condition) for the dual fuel combustion. The rise in the peak pressure depends on the energy release rate of fuels. Due to this, the peak pressure was very high for 100% H_2 syngas mode, and also, occurred earlier irrespective of increased ignition delay as compared to other syngas fuels. This is because of higher flame velocity of H_2 gas (2.7 m/s). It was observed from P-θ diagrams that the attainment of dual fuel peak pressures lag by 6 to15°CA as compared to diesel mode. This is due to the release of syngas energy in the expansion stroke which also lowers peak pressure for dual fuel modes as compared to that of diesel mode. At higher loads of 80 and 100%, the attainment of peak pressure for higher H_2 content syngas (100 and 75%) operations were observed to be minimum of about 6 to 8° CA. Where as, for other dual fuel modes, this value was increased to about 10 to 15° CA due to their lower flame velocity and poor combustion rate.

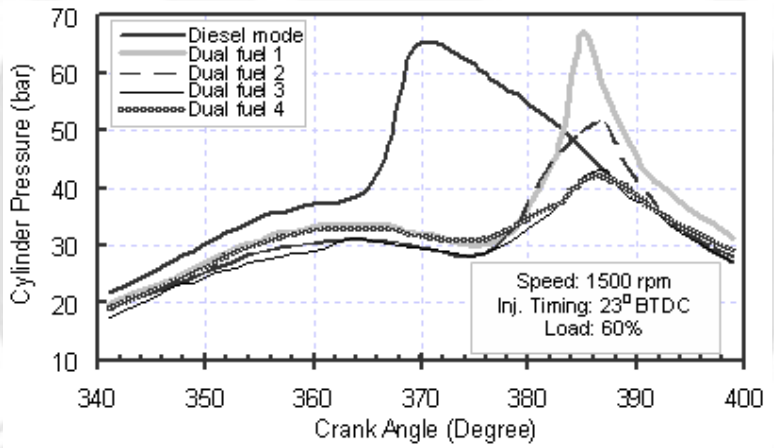

Figure 6.10 Variation of cylinder pressure with crank angle at 60% engine load

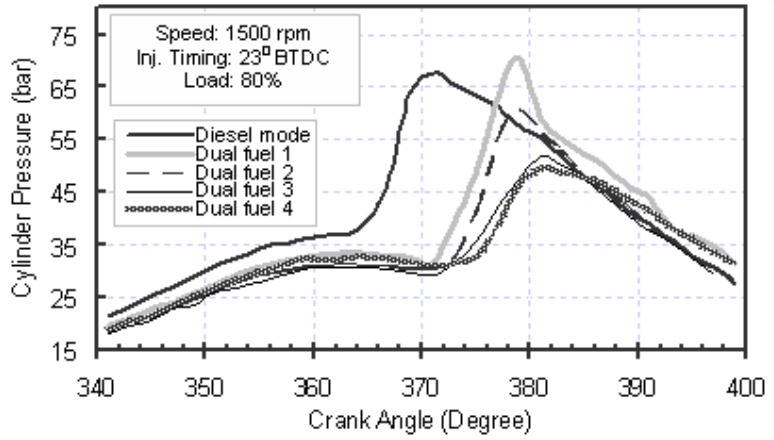

Figure 6.11 Variation of cylinder pressure with crank angle at 80% engine load

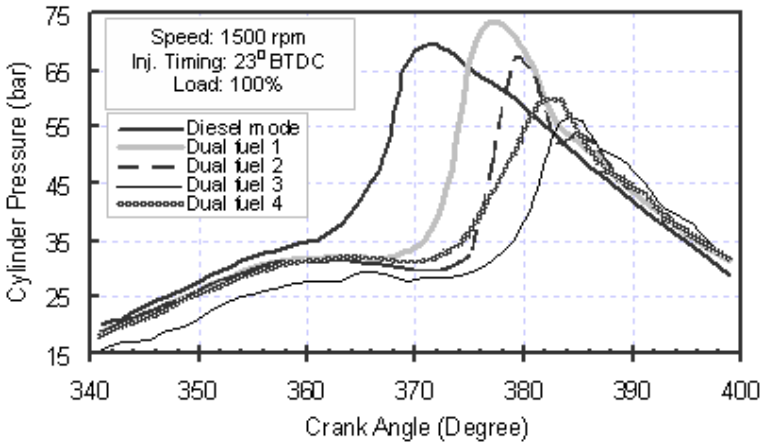

Figure 6.12 Variation of cylinder pressure with crank angle at 100% engine load

The corresponding heat release rate diagrams of pressure crank-angle data are indicated in Figs. 6.13 to 6.15. In general, during a dual fuel operation, the initial heat release is due to the combustion of pilot fuel and then inducted syngas dominates the combustion phase. It can be seen from the figures that there are two pressure peaks for the tested dual fuel modes, one for pilot fuel (diesel) combustion, and the other for the primary (syngas) combustion. It was observed that the peak heat release reaches high values for the higher energy content fuels. Similar trends were exhibited with the P-θ variations also. The heat release rates of dual fuel modes were higher than that of diesel mode for the entire load range. The magnitude of heat release rates increased for an increase in load due to the combustion of higher amount of syngas at higher loads. At 100% load, the maximum heat release rates were found as 215, 166, 133 and 125 J/ deg.CA for the 100, 75, 50 and 0% H_2 content syngas operations, respectively. However, this value was 111 J/ deg.CA for diesel mode, and it occurred at 80% load. The heat release of H_2 content syngas combustion is completed in a shorter period of time than that of diesel combustion because of the higher burning velocity of hydrogen. Looking at the heat release diagrams, it can be seen that there were negative apparent heat release rates after the end of combustion for all the tested H_2 content syngas operations. This is because of the formation of H_2O molecules or moisture by H_2 gas present in syngas composition. A higher amount of negative heat release rate was observed for high H_2 content syngas. The amounts of negative heat release rate of syngas operations (about 30 J/ deg.CA) are much higher than that of the earlier described biogas operations (about 10 J/ deg.CA). This is due to the presence of huge amount of H_2 content combustion during syngas operations. In the process, the negative heat release have resulted a higher cooling loss during the H_2 content syngas dual fuel operations (Fig. 6.16). It can be seen from the Fig. that the H_2

content syngas dual fuel modes produced about 0.5 to 1.5 kW higher cooling losses to that of diesel mode. However, 100% CO dual fuel mode did not follow this cause because it was free from any H_2 content in its composition, and also, it did not produced any negative heat release rates in its combustion.

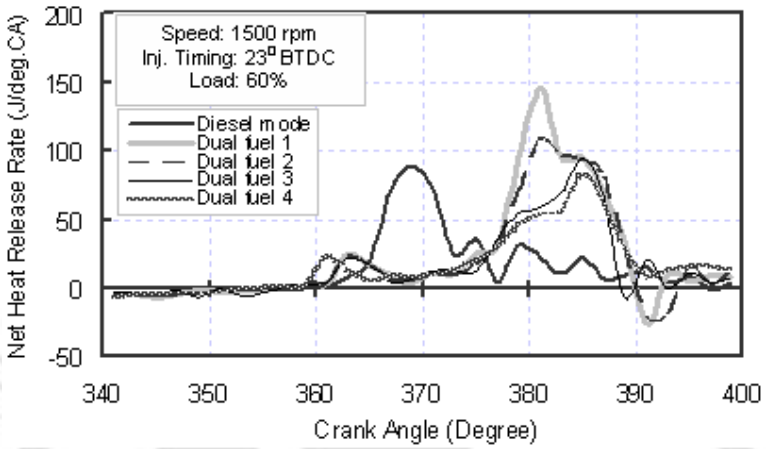

Figure 6.13 Variation of net heat-release rate as a function of crank angle at 60% load

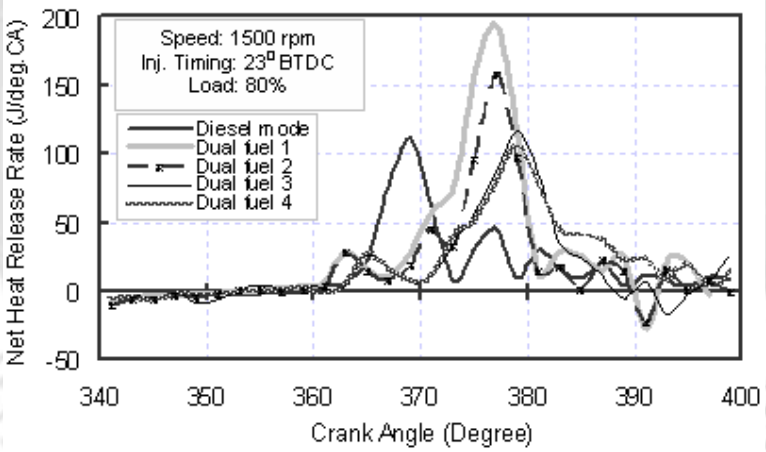

Figure 6.14 Variation of net heat-release rate as a function of crank angle at 80% load

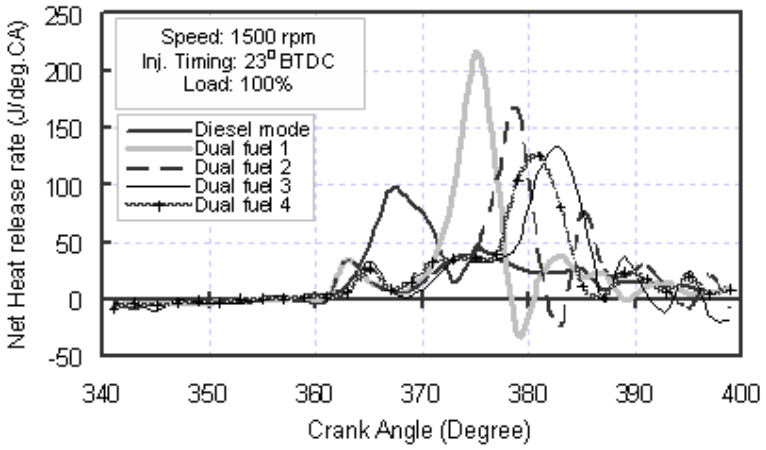

Figure 6.15 Variation of net heat-release rate as a function of crank angle at 100% load

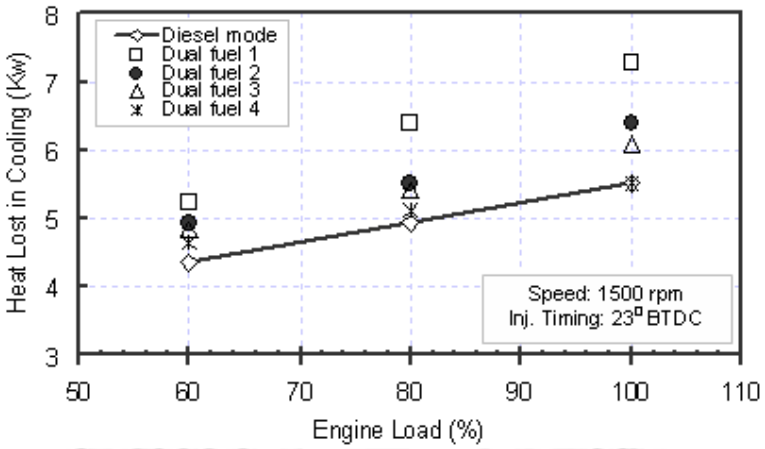

Figure 6.16 Variation of kW cooling loss as a function of engine load

6.4 Emission Characteristics

The higher adiabatic flame temperature of H_2 than that of CO might be a reason for the larger NO_x emission. On the other hand, NO_x emission in the lean combustion is very low. The increase in NO_x levels is a consequence of the higher maximum cylinder pressure and combustion temperature (Heywood, 1988). Due to these factors, the NO_x level increased for an increase in load for the entire load range. At lower engine loads (20% and 40%), the NO_x concentrations were reduced during all the syngas dual fuel operations. This may be due to the poor combustion of gaseous fuel at part-loads which decreases the combustion temperature. At higher engine loads (beyond 60%), a pronounced premixed and advanced combustion have resulted an increased cylinder pressure and temperature. This caused the NO_x concentrations to increase. The highest NO_x emissions were observed for 100% H_2 syngas followed by 75, 50 and 0% as shown in Fig. 6.17. This is because of the achievement of higher combustion pressure and temperature during 100% syngas operation due to their higher heat release rates. The maximum NO_x emissions were found to be 240, 175, 127 and 114 ppm at maximum output condition for 100, 75, 50 and 0% H_2 syngas, respectively as compared to 156 ppm for the diesel mode. In overall, except 100% H_2 fraction syngas mode, all other dual fuel operations produced lower NO_x as compared to diesel mode for the entire load range. Including this, dual fuel operations have also shown a significant reduction in smoke at all loads. The syngas induction reduced the amount of injected diesel fuel and lowers the smoke level. This is clearly evident and visible from the exhaust gas during the dual fuel operation. These are the two main environmental benefits achieved from the operation of syngas dual fuel modes.

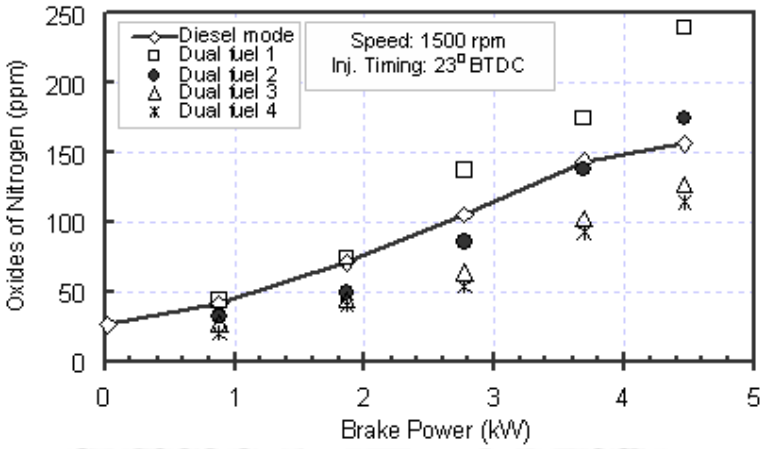

Figure 6.17 Variation of oxides of nitrogen emission with engine power output [Uncertainty: 5 %]

The dual fuel operation with syngas that contained CO resulted in significant increase of the CO emissions due to incomplete CO combustion as compared to diesel mode (Fig. 6.18). Again, the decrease of the combustion temperature and corresponding deterioration of combustion efficiency were held responsible for the increase of CO content in exhaust. Also, syngas that contains CO in its composition, the CO levels seem to be sensitive to the engine load. At low engine loads, the CO emissions were increased significantly. At 20% load, the CO emissions were found as 82, 106 and 186 ppm for 75, 50 and 0% H_2 fraction syngas respectively, whereas it was only 12 ppm for 100% H_2 case. Since 100% H_2 syngas has no carbon, the carbon emissions were lowest for the entire load range. Again, as the load increased, the level of CO emissions started to increase due to insufficient oxygen in combustion. The maximum amount of CO emissions found at 100% load from the dual fuel operation were recorded as 64, 213, 247 and 540 ppm for 100, 75, 50 and 0% H_2 content syngas respectively as compared to 139 ppm for diesel mode. The 100% CO dual fuel mode raised the CO emissions about 2 to 3 times higher than that of diesel mode due to the combustion of only CO gas present its composition. Similarly, the CO_2 concentrations were found to be higher for the syngas dual fuel operations except for the 100% H_2 syngas case (Fig. 6.19). This is due to the huge amount of CO gas combustion present in the fuel-gas composition. Again, during the CO content syngas dual fuel operations, CO oxidized back to CO_2 in the expansion stroke as these operations generated lower combustion temperature. Therefore, the amount of increase in CO emissions was very little when compared to increase in the CO_2 emissions. In overall, all the CO content dual fuel modes produced much higher carbon emissions as compared to the diesel mode.

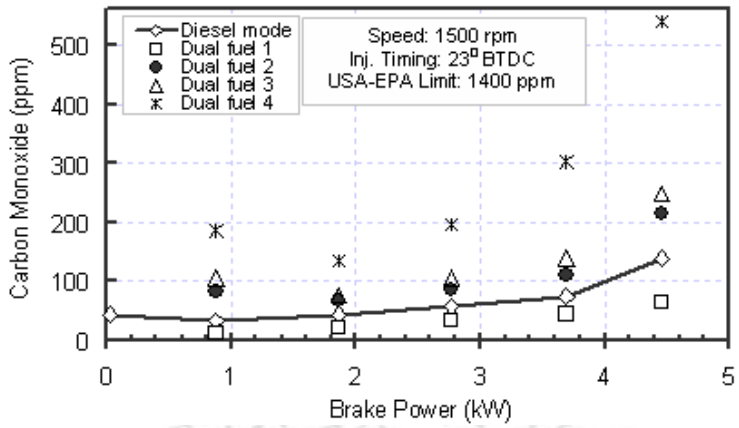

Figure 6.18 Variation of carbon monoxide emission with engine power output [Uncertainty: 5 %]

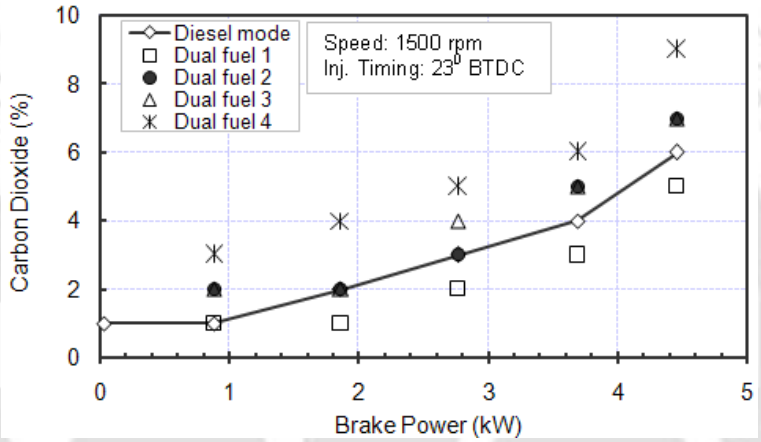

Figure 6.19 Variation of carbon dioxide emission with engine power output [Uncertainty: 5 %]

The unburned hydrocarbon emission variation with engine output for dual fuel operations is shown in Fig. 6.20. The HC emission increased with syngas dual fuel operations as compared to diesel mode due to incomplete combustion of fuel-gas. At low load, poor combustion of syngas with air in the low temperature environment led to higher HC emissions. Further increase of load increased the combustion temperature, and this resulted a more complete combustion of syngas with lower HC emissions. However, after 80% load, the HC emission level started to increase considerably. This is because, the unavailability of adequate oxygen in these rich mixture zones again brought in the poor combustion of syngas-air mixture. At 100% load condition, the maximum HC emissions were found to be 86, 112 and 258 ppm for 75, 50 and 0% H_2 fraction syngas dual fuel modes respectively, as compared to 74 ppm for diesel mode. Whereas, of 100% H_2 syngas combustion produced lowest HC fractions even compared to 100% diesel mode because it does not contain any carbon in the fuel. In addition, this mode consumed less amount of pilot diesel for its dual fuel operation.

Therefore, the CO and HC emission trend of 100% H_2 syngas combustion diverged from all the dual fuel modes including diesel operation. The lowest heating value dual fuel operation with 100% CO content syngas produced highest HC emission level due to their miserable combustion rate and higher pilot diesel combustion. For the entire load range, its HC level was even 2 to 4 times higher than that of diesel mode. Except 100% H_2 dual fuel mode, although the CO and HC emissions for other dual fuel operations were higher, they are still well under the regulated emission limits of USA– Environmental Protection Agency (EPA) non-road regulations (http://www.dieselnet.com/standards/) as shown in Fig. 6.21. However, in order to reduce HC and CO levels further, some researchers have suggested the use of an oxidation catalyst to create favorable exhaust gas temperature and O_2 concentration condition (Roy *et al.,* 2009).

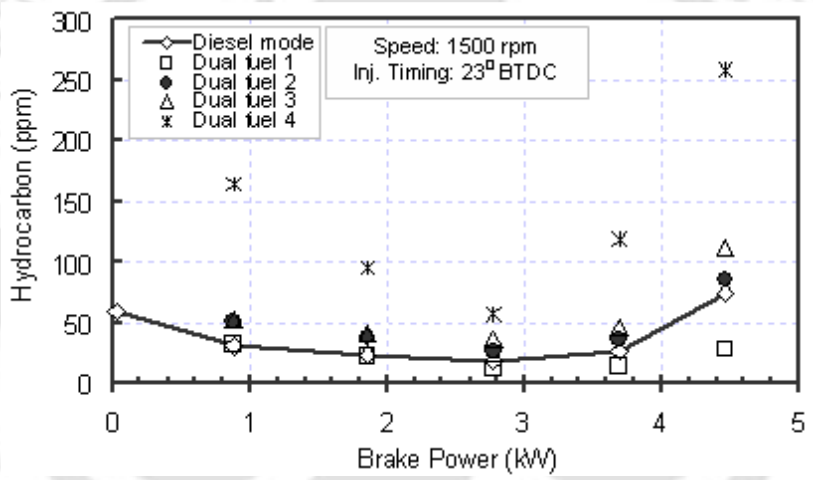

Figure 6.20 Variation of hydrocarbon emission with engine power output [Uncertainty: 5 %]

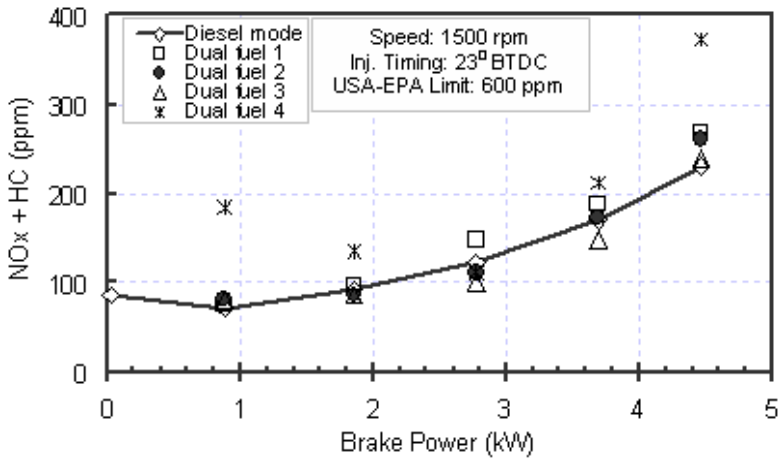

Figure 6.21 Variation of NO_x+ HC emissions with engine power output [Uncertainty: 5 %]

6.5 Summary

The objective of this study is to introduce a new synthetic gaseous fuel, syngas, in a CI diesel engine. The effects of four different kinds of H_2:CO composition syngas fuels 100:0, 75:25, 50:50 and 0:100 are investigated under the dual fuel mode. The experimental results are then compared with the diesel mode on the basis of engine performance, combustion and emission characteristics. The study shows a maximum diesel replacement of about 72% with 100% H_2 syngas mode. While for other dual fuel modes, this value was about 58 to 61% which seem to be reasonable. The drop in the diesel replacement relates to the amount of H_2 content in the syngas composition i.e., energy content of the primary fuel. Except for 100% H_2 syngas mode, the NO_x emissions are found to be lower at the tested loads under dual fuel operations. The combustion of 100% H_2 syngas mode results in lowest CO and HC emissions for the entire power output range. Whereas, 100% CO content syngas mode gives highest level of both CO and HC emissions among other dual fuel combinations as compared to diesel mode. However, these emissions are well within the regulated emission limits of USA–EPA non-road regulations.

At higher loads, the brake thermal efficiency of dual fuel modes rises with an increase in H_2 percentage of syngas composition. At their best efficiency loading point, the efficiency enhances by about 3, 17 and 26% when H_2 content in syngas is substituted by 50, 75 and 100% respectively, to 100% CO syngas composition. However, at the same time, these values are lowered by an extent of about 6 to 27% as compared to diesel mode. Again, the shorter combustion duration and increased ignition delay of dual fuel operations shifts the attainment of peak pressure more towards the expansion stroke, and this reduces the peak cylinder pressure. However, beyond 60% load, the 100% H_2 syngas results a higher peak pressure. The rate of pressure rise can be attributed to its higher energy content and better combustion rate. Due to the presence of H_2 in syngas composition, there is an occurrence of negative heat release after the end of combustion. In general, The CO and CO_2 emission levels seem sensitive to fraction of CO% in syngas. Therefore, a significant rise in these emissions is found with higher CO% syngas dual fuel operations. It can be concluded that syngas promises be a good alternative fuel for a CI diesel engine under dual fuel mode. It gives a significant environmental benefit of keeping the emissions within the limits of environmental regulation. However, at lower outputs, it is not advantageous to use syngas induction due to its poor performance.

Chapter – 7

THERMODYNAMIC ANALYSIS OF SYNGAS–DIESEL ENGINE OPERATION

Overview

The experimental investigations presented in Chapter 6 revealed that the syngas fuelled dual fuel modes resulted in about 6 to 27% lower brake thermal efficiency as compared to diesel mode. In the process, they also produced higher exhaust gas temperatures. Thus, it is very important to have the knowledge of when and where the available fuel energy is lost or destroyed in the engine system. Further, it is crucial to know the maximum possible performance of the dual fuel modes which can provide a vital comparison parameter with base engine. In addition, impact of process change (such as, load, gaseous fuel type etc.) in the system in terms of system losses has to be assessed. These findings would help in reducing the available energy loss to improve the overall engine performance. This chapter discusses both the energy and exergy balance of the diesel and dual fuel operations. The first and second law analysis are coupled together in order to complete the theoretical treatment of an engine operation. In this way, the thermodynamic analysis provides both general performance calculations with the details of the overall thermodynamics of engine operation. The present work is applied the thermo-mechanical availability analysis by retrieving data of the experiments that are presented in Chapter 6. In this work, the effects of various combinations of H_2/CO volumetric ratio rich syngas on the dual fuel engine performance are examined from the second law perspective. Finally, the outcomes of dual fuel modes are compared to that of diesel mode. Specifically, the effects of fuel type on all existing availability terms: brake power output, coolant heat transfer, exhaust gas losses, exergy efficiency, and irreversibility, are explored by both first and second law of thermodynamics.

7.1 Availability Analysis

The knowledge of 'how the energy is lost' will help in finding means to reduce the same to improve the performance of the engine in terms of efficiency and power output (Kumar *et al.,* 2004). This seems to be the main reason behind most energy studies performed on engines. The energy balance studies are also done to optimize engine settings or system settings. Depending on the application, it may be important to have an engine run for long periods of time under a single loading condition. For this reason, it is desired to know the range of engine parameters for most efficient operation (Kopac and Kokturk, 2005). The impact of variations of engine load in the energy and exergy of the baseline test and dual fuel operations are compared in this section. The experimental observation data are retrieved from Chapter 6 here for the first and second law analysis purpose as per the Eq. (D1) to (D13) described in *Appendix D*. The computed energy and exergy analysis data of the various tested fuel types for the entire load range are shown in Table 7.1 and 7.2 respectively.

The availability balance for the individual fuel type as mentioned in experimental matrix of syngas dual fuel operations (Table 6.2) as a function of engine load are presented in Figs. 7.1 to 7.5. This is a balance between the various terms of the second law analysis described by Eq. (D7) to Eq. (D13) in Appendix C, namely, fuel availability input, work output availability, availability exchange through cooling water and exhaust gas, availability destroyed, and exergy efficiency. During an engine operation, as load increased, the richer fuel-air mixture increased the combustion temperature. Therefore, increased work availability and reduced heat transfer availability losses, as percentages of the fuel chemical availability, were obtained. For this reason, an increase in the exergy efficiency was resulted at higher loads for all the tested fuel modes. Specifically, the dual fuel operations were favored thermodynamically at higher loads since their exergy efficiencies improve significantly as compared to low load conditions. Because of the improved combustion syngas at higher loads, (mainly) exhaust gas availability and cooling availability (although of small quantity) were increased. In addition, the shaft availability of the engine operation was increased for an increased load. Therefore, when load was increased, the added cumulative availabilities increased the exergy efficiency. However, this efficiency was decreased slightly after the 80% load due to poor combustion of fuels where insufficient oxygen availability condition was occurred. On the contrary to exergy efficiency trend, after the 80% load, the destroyed availability or irreversibility was increased due to the raised heat transfer from the engine.

Table 7.1 Energy analysis of syngas-diesel dual fuel operation at different engine loads

Load (%)	Fuel Type	Q_{in}		W_{shaft}		$Q_{cooling}$		$Q_{exhaust}$		$Q_{uncounted}$	
		kW	*%*	*kW*	*%*	*kW*	*%*	*kW*	*%*	*kW*	*%*
20 %	Diesel mode	10.43	100	0.88	8.44	3.49	31.48	2.15	20.66	3.90	37.35
	Dual fuel 1	15.90			5.53	4.07	25.43	3.13	19.66	7.82	49.18
	Dual fuel 2	16.10			5.34	5.23	31.73	2.67	16.20	7.70	46.72
	Dual fuel 3	16.89			5.21	5.52	32.68	2.56	15.16	7.93	46.95
	Dual fuel 4	19.17			4.59	4.65	24.25	2.4	12.53	11.24	58.63
40 %	Diesel mode	12.17	100	1.86	15.28	4.36	33.43	2.62	21.49	3.34	27.40
	Dual fuel 1	16.05			11.96	4.94	31.42	3.75	23.37	5.50	34.27
	Dual fuel 2	16.48			11.67	6.10	37.89	3.47	21.53	4.67	29.00
	Dual fuel 3	18.04			10.42	6.39	35.42	3.36	18.63	6.43	35.64
	Dual fuel 4	19.18			9.8	5.52	28.78	2.83	14.73	8.98	46.79
60 %	Diesel mode	14.57	100	2.77	19.01	4.36	28.16	3.35	23.01	4.09	28.05
	Dual fuel 1	16.52			16.71	5.23	31.66	4.82	29.19	3.70	22.40
	Dual fuel 2	17.10			16.14	4.94	28.89	4.42	25.84	4.97	29.06
	Dual fuel 3	20.40			13.53	5.23	25.64	3.85	18.88	8.55	41.91
	Dual fuel 4	21.11			13.12	4.94	23.4	3.91	18.54	9.49	44.95
80 %	Diesel mode	17.64	100	3.69	20.92	4.94	26.33	4.46	25.28	4.55	25.78
	Dual fuel 1	18.68			19.75	6.39	34.23	5.46	29.23	3.14	16.80
	Dual fuel 2	20.87			18.34	5.52	26.54	4.79	23.81	6.12	30.42
	Dual fuel 3	22.92			16.1	5.81	25.35	4.3	18.77	9.12	39.79
	Dual fuel 4	23.49			15.71	5.52	23.5	3.94	16.76	10.34	44.02
100 %	Diesel mode	22.88	100	4.46	19.49	5.52	22.68	5.40	23.61	7.49	32.76
	Dual fuel 1	26.39			16.9	7.27	27.54	6.59	24.97	8.07	30.58
	Dual fuel 2	27.63			16.14	6.39	23.15	5.91	21.38	10.87	39.34
	Dual fuel 3	35.74			12.48	6.10	17.08	5.50	15.39	19.68	55.06
	Dual fuel 4	34.17			13.05	5.52	16.15	5.84	17.09	18.35	53.70

Table 7.2 Exergy analysis of syngas-diesel dual fuel operation at different engine loads

Load (%)	**Fuel Type**	**A_{in}**		**A_{shaft}**		**$A_{cooling}$**		**$A_{exhaust}$**		**$A_{destroyed}$**		**Exergy Efficiency**
		kW	*%*	*kW*	*%*	*kW*	*%*	*kW*	*%*	*kW*	*%*	*%*
20 %	Diesel mode	10.78	100	.0.88	8.16	0.317	2.77	1.373	12.74	8.21	76.16	23.84
	Dual fuel 1	16.13			5.45	0.094	0.58	1.95	12.07	13.26	81.88	18.12
	Dual fuel 2	17.22			5.11	0.082	0.48	1.816	10.54	14.442	83.87	16.13
	Dual fuel 3	17.28			5.09	0.08	0.46	1.69	9.78	14.615	84.49	15.51
	Dual fuel 4	18.94			4.65	0.06	0.32	1.574	8.31	16.426	86.73	13.27
40 %	Diesel mode	12.58	100	1.86	14.78	0.353	2.81	1.598	12.7	8.78	69.51	30.49
	Dual fuel 1	15.83			11.75	0.12	0.76	2.263	14.29	11.637	73.19	26.81
	Dual fuel 2	16.86			11.03	0.123	0.73	2.215	13.14	12.662	75.1	24.9
	Dual fuel 3	18.43			10.09	0.13	0.70	2	10.85	14.431	78.25	21.75
	Dual fuel 4	18.94			9.82	0.095	0.5	1.77	9.33	15.215	80.33	19.67
60 %	Diesel mode	15.06	100	2.77	18.39	0.443	2.94	2.09	13.88	9.86	64.65	35.35
	Dual fuel 1	16.59			16.7	0.14	0.84	2.84	17.1	10.9	65.34	34.66
	Dual fuel 2	17.9			15.47	0.14	0.79	2.74	15.31	12.32	68.43	31.57
	Dual fuel 3	20.79			13.32	0.152	0.73	2.248	10.81	15.69	75.21	24.79
	Dual fuel 4	21.3			13.00	0.134	0.63	2.276	10.69	16.184	75.68	24.32
80 %	Diesel mode	18.23	100	3.69	20.24	0.642	3.52	2.59	14.21	11.3	61.79	38.21
	Dual fuel 1	18.61			19.83	0.177	0.95	3.21	17.25	11.57	61.97	38.03
	Dual fuel 2	21.09			17.5	0.179	0.85	3.438	16.3	13.572	64.35	35.64
	Dual fuel 3	23.34			15.81	0.18	0.77	2.47	10.58	17.07	72.84	27.16
	Dual fuel 4	23.73			15.55	0.164	0.69	2.03	8.55	17.751	74.8	25.2
100 %	Diesel mode	23.65	100	4.46	18.86	0.669	2.66	2.83	11.98	15.69	66.32	33.67
	Dual fuel 1	26.57			16.78	0.239	0.9	3.94	14.83	17.97	67.48	32.52
	Dual fuel 2	28.88			15.44	0.219	0.76	3.484	12.07	20.716	71.73	28.27
	Dual fuel 3	36.46			12.23	0.262	0.72	3.244	8.9	28.336	78.15	21.85
	Dual fuel 4	33.31			13.39	0.246	0.74	3.253	9.76	25.484	76.1	23.9

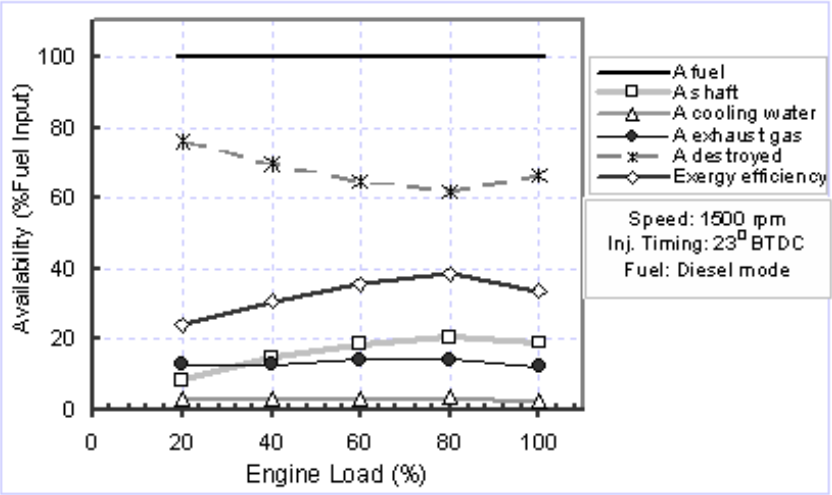

Figure 7.1 Availability distribution with varying fuel input as function of load (Diesel mode)

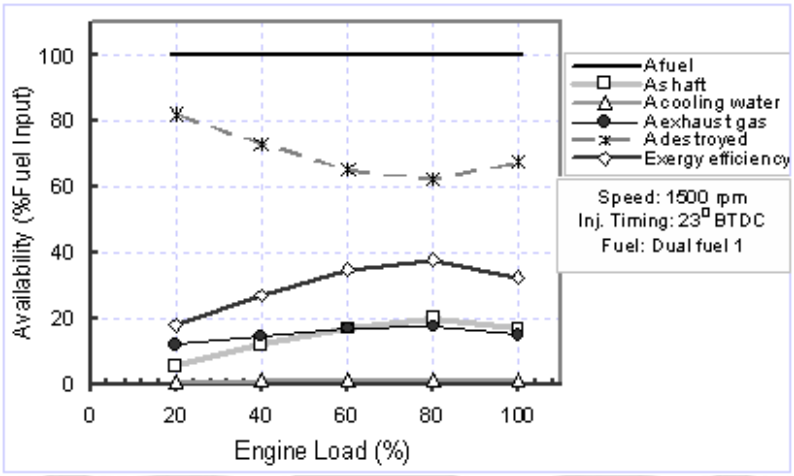

Figure 7.2 Availability distribution with varying fuel input as function of load (Dual fuel 1)

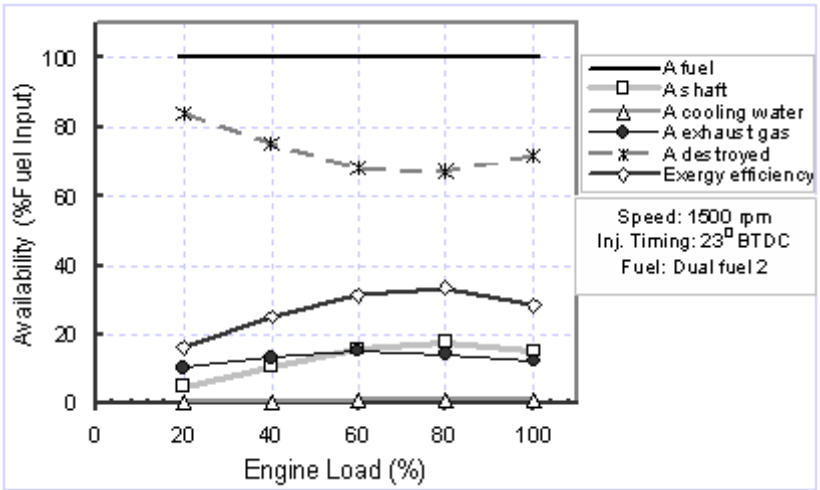

Figure 7.3 Availability distribution with varying fuel input as function of load (Dual fuel 2)

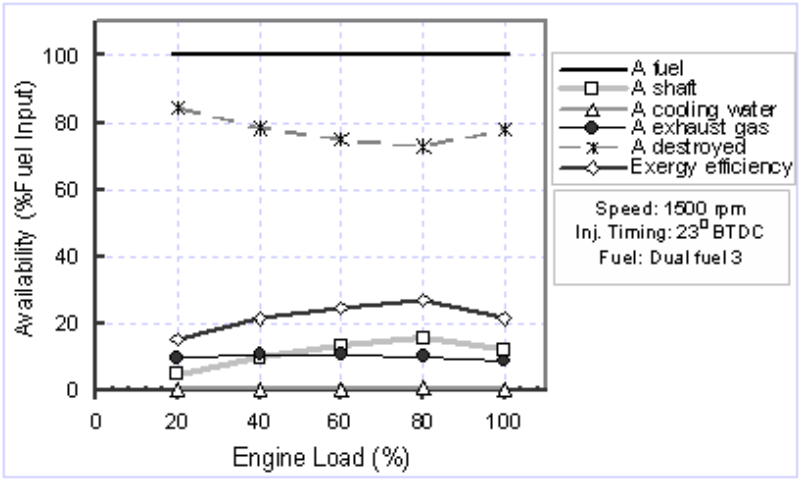

Figure 7.4 Availability distribution with varying fuel input as function of load (Dual fuel 3)

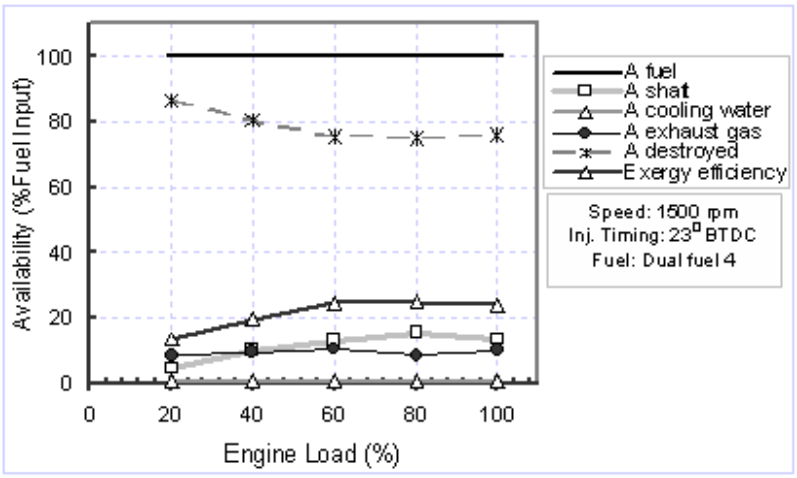

Figure 7.5 Availability distribution with varying fuel input as function of load (Dual fuel 4)

Figure 7.6 depicts the availability distribution on the basis of available energy input to the diesel and dual fuel operations. When load was raised, to maintain higher power output at higher loads, the supply of fuel chemical energy in to the engine cylinder was increased. In the process, at higher engine loads, the shaft availability was calculated against the amount fuel exergy input. The quantity of fuel exergy input for the engine operation at a given load mostly depends on the energy content of the fuel type and effective combustion of the fuel-air mixture. Although some tested gaseous fuels seem to have higher energy content than diesel fuel, however, at lower loads of 20 to 40%, all the tested dual fuel operations required higher fuel exergy input as compared to diesel mode. This is because of their poor combustion characteristics in the low temperature environment. As the load was increased, the differences in fuel exergy input reduced for dual fuel modes as compared to diesel mode for their improved combustion. Again, at high temperature zone of 100% load, the chemical energy

requirement increased for the dual fuel operations due to the diminishing of oxygen availability needed for the complete combustion.

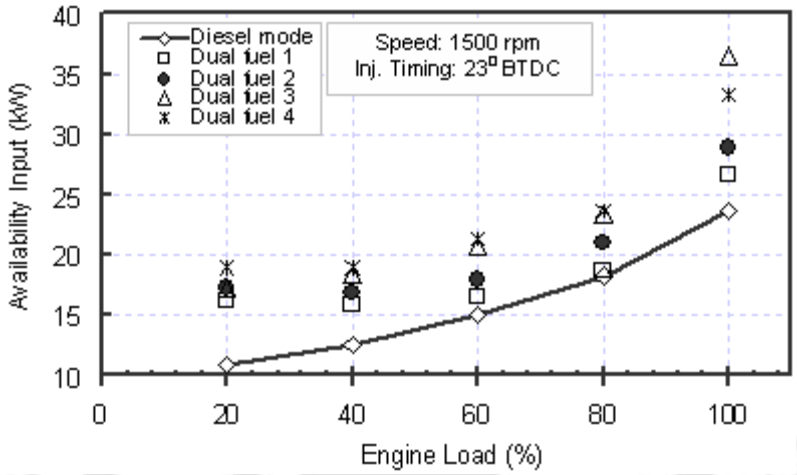

Figure 7.6 Availability (kW) input distribution at different engine load

Figures 7.7 to 7.10 present the individual comparison of shaft output, cooling water, exhaust gas, and destroyed availabilities of various tested modes with load with respect to their respective chemical fuel exergy input. As discussed in earlier Chapters, at an applied load, the kW shaft work produced for both diesel and dual fuel modes were kept same. However, the shaft availability of the various tested fuels as a percentage of fuel input were different due to the difference in their input chemical fuel availability as shown in Fig. 7.6. At low loads (20% and 40%), the shaft availability of dual fuel mode were very miserable as compared to diesel mode (Fig. 7.7). But, this value improved as the load is increased. Generally, increase in the load results the enhancement of the combustion process, increasing the combustion temperatures and the peak cylinder pressure and reducing the combustion duration. The maximum shaft availability recorded at best thermal efficiency point (Fig. 6.2) of 80% load and thereafter, it reduced slightly up to 100% load. The highest shaft availability was found in case of diesel mode as compared to all the tested dual fuel modes for the entire load range. For diesel mode, at 80% load, the shaft availability was found as 20.2%. Whereas, at same loading, this value was figured as 19.8, 17.5, 15.8 and 15.6% for the 100, 75, 50 and 0% H_2 syngas dual fuel operations, respectively. The cooling availability of dual fuel operations was very little due to the intensive cylinder wall loss as shown in Fig. 7.8. Only a maximum of about 1% fuel input cooling availability was accessible from dual fuel operations as compared to about 2 to 3% to that of diesel mode. This is because, the increase in engine cooling water temperature of dual fuel modes were less than that of diesel mode.

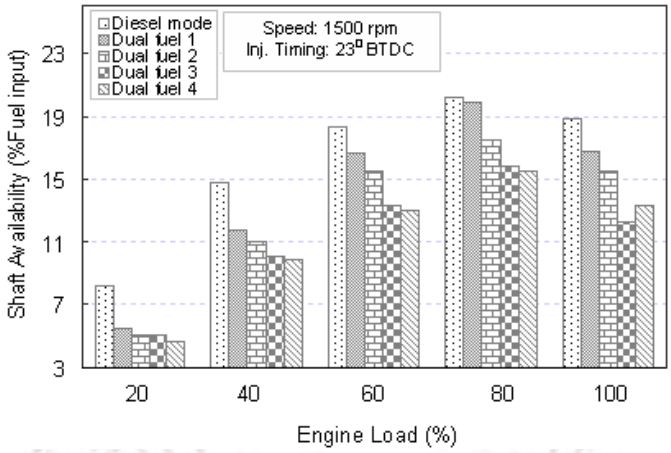

Figure 7.7 Shaft availability distribution at different engine load

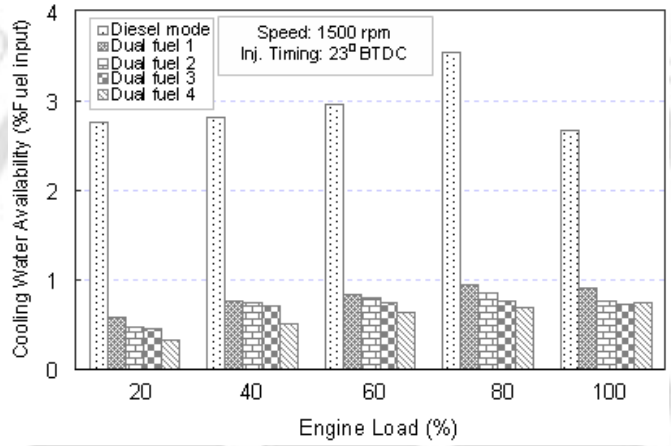

Figure 7.8 Cooling water availability distribution at different engine load

It was reported in Chapter 6 that the syngas dual fuel operations produced higher exhaust gas temperature as compared to diesel mode for the entire load range (Fig. 6.3). This led to higher exhaust gas availability loss for the dual fuel modes (Fig. 7.9). The variation of exhaust gas availability with respect to load is similar to the exhaust gas temperature case for the tested fuel modes. The 100% H_2 syngas dual fuel mode produced highest exhaust gas availability as this operation recorded maximum temperature in its exhaust. At best efficiency point, the maximum exhaust gas availability was found as 17.2% for 100% H_2 syngas mode as compared 14.2% of diesel mode. While for 75 and 50% H_2 syngas modes, at the same working condition, the maximum value was found to be 14.3 and 10.6% respectively. However, the maximum exhaust gas availability for 100% CO syngas mode was observed as 9.8% but at 100% load. This is because better combustion of CO gas at this higher temperature zone developed maximum cylinder temperature for the operation. Due to these huge availability losses through exhaust gas, the efficiencies of dual fuel operations were

lower than that of diesel mode. Therefore, it can be concluded that the exhaust gas available energy loss must be reduced to improve dual fuel engine performance,

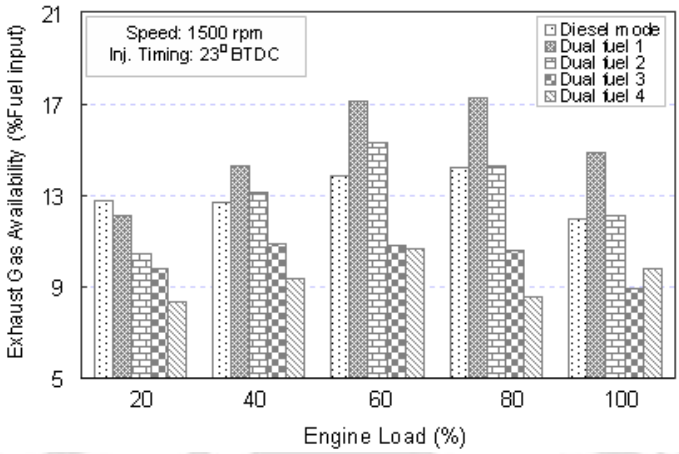

Figure 7.9 Exhaust gas availability distribution at different engine load

At low loads of 20% and 40%, poor combustion of syngas fuels caused less cooling water and exhaust gas availabilities i.e., higher availability was destroyed. The amount of destroyed availability (as a percentage of fuel input) was decreased with increasing load (Fig. 7.10). This is due to the fact that, as load increased, greater values of fuel-air equivalence ratio cause greater temperatures inside the cylinder, and it resulted better combustion of gaseous fuels. The destroyed availability was found minimum at the maximum efficiency condition of 80% engine load. Diesel mode showed the minimum destroyed availability loss (61.8%) among all the tested fuel modes. While at the same loading condition, the minimum of this value was found to be 62, 67.4, 72.3 and 74.8% for the 100, 75, 50 and 0% H_2 content syngas operations respectively.

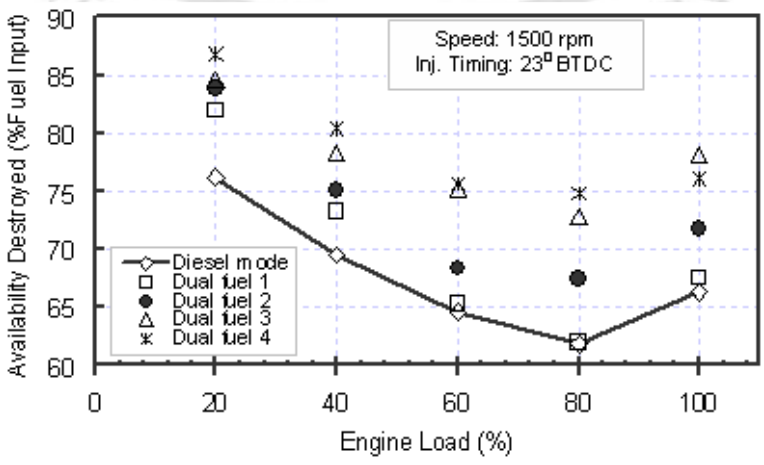

Figure 7.10 Destroyed availability distribution at different engine load

The availability balance is affected by the compositions of the syngas fuel under the dual fuel operation as shown in Fig. 7.11. The percentage of destroyed fuel availability was reduced with the increase in the H_2 content of the syngas composition for the entire load range. This decrease with increasing H_2 content was due to the entropy generation (Dunbar and Lior, 1994), and more specifically, for better air-fuel mixture combustion (Rakopoulos and Kyritsis, 2001; 2006). For the 100% H_2 syngas mode, the destroyed availability was found least as compared to other syngas fuel modes. Contrary to the tendency of destroyed availability, the second law (exergy) efficiency increased with increase of H_2 content. This is a combined effect of reduction of combustion irreversibility and increase in the maximum temperature of the cycle, which caused efficiency gains during the engine operation.

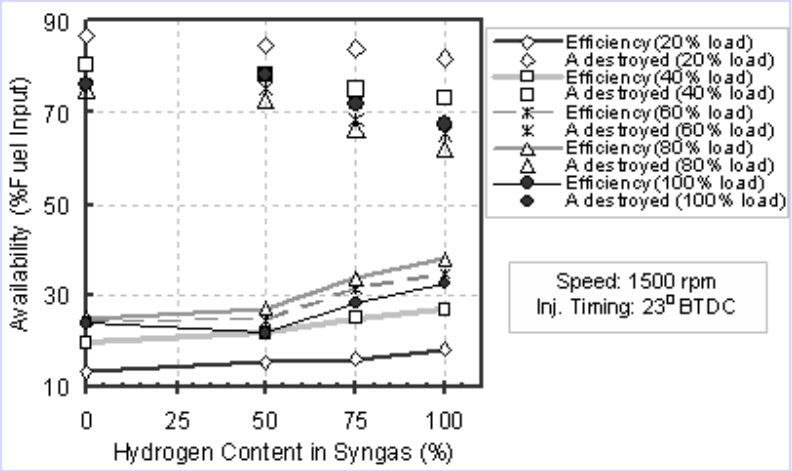

Figure 7.11 Exergy efficiency and destroyed availability as function of hydrogen content

Figure 7.12 shows the shaft availability (kW) as a function of load, along with the accessible cumulative increase in the work availability from both the exhaust gas and cooling water losses for all the tested fuel modes. The availability results showed that, as the load was increased, the dual fuel operations generated more increase in the cumulative exhaust gas and cooling water availabilities. This allowed the more of the availability accessible for conversion to work availability. The drawback of dual fuel operations due to its poor efficiency can be resolved by accessing about 1.5 to 4 kW of work availability losses through an effective exhaust gas heat recovery system. The increase in the gross work output availability increased the corresponding exergy efficiency (Fig. 7.13). At 80% load, the second law efficiency was observed highest in case of diesel mode and recorded a maximum of 38.2%. While at same loading condition, when the volumetric fraction of H_2 in syngas increased from 0% to 50, 75 and 100%, the maximum second law efficiency enhanced from

25.2% to 27.2, 33.6 and 38%, respectively accompanied by a simultaneous reduction in the destroyed availability. For higher H_2 content syngas, the energy input into the cylinder increased, and as a consequence, the corresponding cumulative work availability also increased. Moreover, increase in the H_2 content in syngas resulted an improvement of the combustion process from the second law viewpoint. Therefore, at higher loads, it can be seen that 75% and 100% syngas combustion give comparative exergy efficiency as compared to that of diesel mode. From this thermodynamic analysis, we found that the exergy efficiencies of dual fuel modes are higher than the actual efficiency of base diesel engine (20.92%). This demonstrates that dual fuel engine operations can not be ignored on the basis of their lower efficiency in a diesel engine which was actually designed for the standard diesel fuel. Therefore, a dual fuel engine must be provided with its exhaust gas heat recovery system for a better efficiency figure along with other benefits.

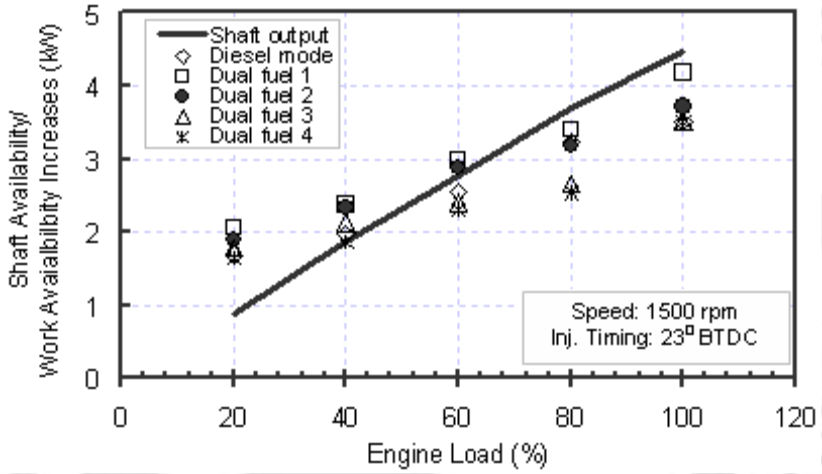

Figure 7.12 Effect of engine load on total raised work availability

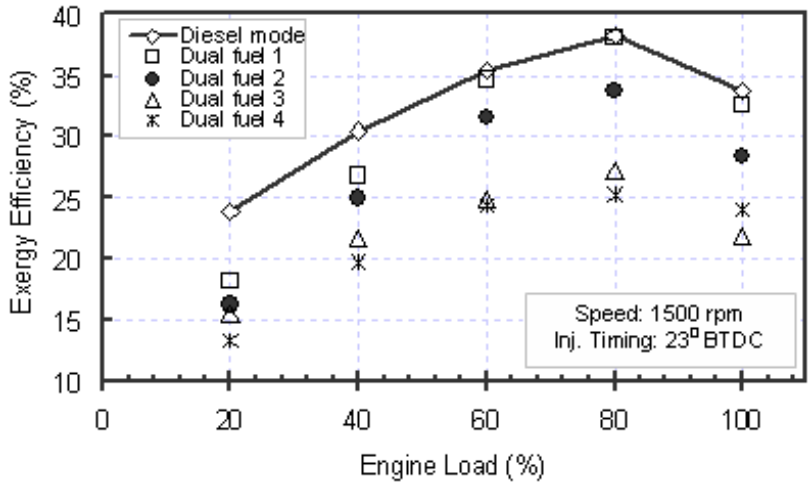

Figure 7.13 Comparison of exergy efficiency as a function of engine load

7.2 Summary

A thermodynamic analysis was executed to find out the energy losses and maximum permissible performance of various syngas dual fuel operations. The energy and availability equations were applied together to the experimental results of a compression ignition diesel engine operated under both diesel and dual fuel modes. The type of dual fuel mode was decided by varying composition of syngas fuel. At different loading conditions, various kinds of availability terms such as, shaft, cooling water, exhaust gas and destroyed availability were analyzed and compared. The added chemical energy from the fuels at higher loads increased the shaft availability (as a percentage fuel input) of all the tested fuels. At higher loads, the syngas dual fuel operations are advantageous from the second law perspective. With increasing load, the destroyed availability is decreased due to higher combustion temperature and pressure, and therefore, the exergy efficiency increased. At maximum efficiency point, the exergy efficiency of 100% H_2 syngas mode, differed by an amount below 0.5% only as compared to that of diesel mode. This demonstrates that hydrogen is an effective gaseous fuel for a diesel engine under dual fuel mode. Similarly, by accessing about 8 to 17% of fuel input from their exhaust gas availability loss, the other dual fuel operations can also increase their work availability. In the process, their maximum permissible efficiency can even go beyond the maximum efficiency of the base diesel engine. In addition, the second law efficiency of low energy content syngas operations can be improved by increasing the volumetric fraction of H_2 in syngas. This increase is accompanied by an increase in the work availability from exhaust gas and cooling water.

Chapter – 8

CLEAN DEVELOPMENT MECHANISM POTENTIAL INVESTIGATION OF THE DUAL FUEL OPERATIONS

Overview

The reductions of greenhouse gases (GHG) from elsewhere can be materialized through several mechanisms of the Kyoto Protocol: the Emission Trade, Joint Implementation and Clean Development Mechanisms (CDM). The CDM allows net global GHG to be reduced at a much lower global cost by financing emission reduction projects in developing countries. The major six GHGs are – CO_2; methane; nitrous oxide; hydrofluorocarbons (HFCs); perfluorocarbons (PFCs); and sulfur hexafluoride (SF). Internal combustion engines (ICE) are a major consumer of fossil fuels, and combustion of fossil fuels inevitably produces emissions of the GHG carbon dioxide (CO_2). The diesel engines which use diesel fuel for their combustion contribute a significant amount of the total GHGs generated from the transport sectors. In general, there are three approaches for reducing transportation emissions: improvements in vehicle technology, a switch to lower-carbon fuels, and travel demand management (EPA, 2007). 'Switch mode of fuel' is an approach i.e., switch from diesel/ petrol to lower-carbon renewable fuels, for reducing CO_2 emissions from ICEs. Towards this, a carbon-neutral fuel, biogas, and a lower-carbon fuel, syngas, have tried in a single-cylinder, constant-speed, direct-injection and compression-ignition diesel engine under dual fuel mode of operation to check their potential in the direction of CDM. The biogas dual fuel operation was assisted with two different pilot quality, diesel and jatropha bio-diesel whereas, syngas dual fuel operation was conducted with various gaseous fuel types achieved by varying H_2 content of the total H_2 and CO fuel composition. Both the dual fuel operations were carried out at different engine loads. In this Chapter, the practical CDM potential of these two dual fuel operations in a diesel engine is assessed.

8.1 The Clean Development Mechanism

The Clean Development Mechanism (CDM) is one of the greenhouse gas (GHG) reduction mechanisms brought up by the Kyoto Protocol. The CDM aims to reduce produced net global GHG from elsewhere. The reciprocating type diesel engines produce the GHG carbon dioxide emissions from the combustion of fossil diesel fuel. The decrease in the diesel fuel usage needed for diesel engine combustion can improve the GHG reductions and benefits the CDM. The use of alternative clean burning fuels in place of diesel fuel in diesel engines can aid to the task of CDM. Adopting this technology, the present work employed two gaseous fuels to investigate their potential towards CDM. The two gaseous fuels, a carbon-neutral fuel, biogas, and a lower-carbon fuel, syngas, were applied in a single-cylinder, constant-speed, direct-injection and compression-ignition diesel engine under dual fuel mode of operation. The biogas dual fuel operation was assisted with two different pilot quality, diesel and jatropha bio-diesel. Whereas, syngas dual fuel operation was conducted with various gaseous fuel types achieved by varying H_2 content of the total H_2 and CO fuel composition. Both the dual fuel operations were carried out at different engine loads. The practical CDM potential of these two dual fuel operations in a diesel engine is assessed after retrieving their average experimental data of the investigations.

8.2 CDM Analysis of Biogas Dual Fuel Operations

Biogas is produced by 'anaerobic digestion' process where, the organic materials such as, cow dung and other animal waste, leaves and water hyacinth etc. break down by bacteria under lesser air environments. A major part of biogas composition contains two main contributors to GHG production, methane (CH_4) and carbon dioxide (CO_2). However, the anaerobic digestion system limits the emission of carbon dioxide and methane into the environment since the digestion takes place in a closed environment. The type of biogas used in this experiment was generated by using cow dung and cook wastes as feed materials. About 48% CH_4 and 42% CO_2 was available in its fuel composition. Methane is about 21 times more powerful greenhouse gas than CO_2, with greater potential for increasing global warming effects (IPCC, 1996). During combustion of biogas, in addition to release of heat energy, methane converts itself into CO_2 as engine exhaust. In this way, methane neutralizes its effect on global warming. Again, during burning via biogas combustion, CO_2 returned to the atmosphere at approximately the same rate it is taken up during photosynthesis. Therefore, biogas is generally considered to be carbon neutral fuel.

The biogas fuelled dual fuel operations produced higher concentrations of CO_2 emissions as compared to diesel mode for the entire load range (Fig. 4.18). This is because, the 42% CO_2 by volume present in biogas composition exit from the engine cylinder without burning due to the inert properties. Again, some additional CO_2 emissions are expected due to the conversion of methane into CO_2 during the combustion. However, the increases in CO_2 emissions are negligible when compared to the release of CH_4 and CO_2 emissions from the decomposition of organic wastes in an oxygen-deprived environment. So, strictly speaking, no more CO_2 is being released to the atmosphere than was initially present. Therefore, in the biogas dual fuel mode CDM analysis, the effects of increased CO_2 emissions are not considered. Carbon monoxide is only a very weak direct GHG, but has important indirect effects on global warming. CO reacts with hydroxyl (OH) radicals in the atmosphere, reducing their abundance. CO in the atmosphere can also lead to the formation of the tropospheric GHG 'ozone'. Hence, only the increases in CO emissions during the biogas dual fuel operations to that of diesel mode are taken into account for the CDM analysis.

The earlier emission analysis of biogas dual fuel operations showed about 20 to 120% higher CO emissions up to half load as compared to the diesel mode (Fig. 4.17). These higher CO emissions are produced by using both diesel and syngas fuel. At a given engine load, diesel and syngas have different energy share to produce the equal shaft output as that of diesel mode. It can be seen that biogas energy share was increased with rise in load i.e. the pilot energy share decreased as shown in Fig. 8.1. This is due to the improved combustion of high self ignition temperature property bearer biogas at higher temperature conditions. Therefore, as a primary fuel substitution, the CDM potential of biogas was tested as a function of the percentage of energy replaced. A sample calculation of this investigation is presented in Table 8.1. Thus, when we consider a total of CO emissions per kW hour, a key advantage of the dual fuel engine was achieved. Figure 8.2 is a plot of CO emissions for each biogas fuel tested as a function of the percentage of energy replaced. For biogas-JOME mode, at 0 and 20% loads, the CO emissions produced per kW hour were higher than diesel mode. While for biogas-diesel mode, this value was higher only at no-load (0% load) condition. Beyond these loads both biogas dual fuel operations showed relatively lower CO emissions than diesel mode. For these dual fuel operations, after 20% load, about 10 to 60% reductions of CO emissions based on ppm per kilowatt hour were achieved. Again, as stated earlier, both dual fuel operations also reduced NO_x emissions for the entire load range. Hence, we can conclude that, after 20% load, both combination of dual fuels have achieved the required reduction of greenhouse gases and satisfied the CDM potential.

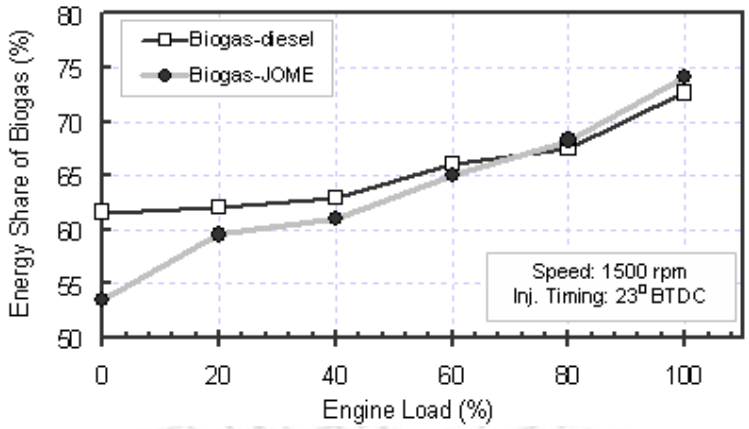

Figure 8.1 Comparison of biogas energy share during dual fuel operations

Table 8.1: Sample calculation for CDM potential check for biogas operation (diesel as pilot)

Load (%)	CO emissions (ppm/ kW)		Energy share (%)		CO emissions from biogas (ppm/ kW)	Relative emission of biogas to diesel mode
	Diesel	*Dual*	*Diesel*	*Dual*		
0	1467	2333	38.43	61.57	1769	1.21
20	39	51	37.97	62.03	36	0.93

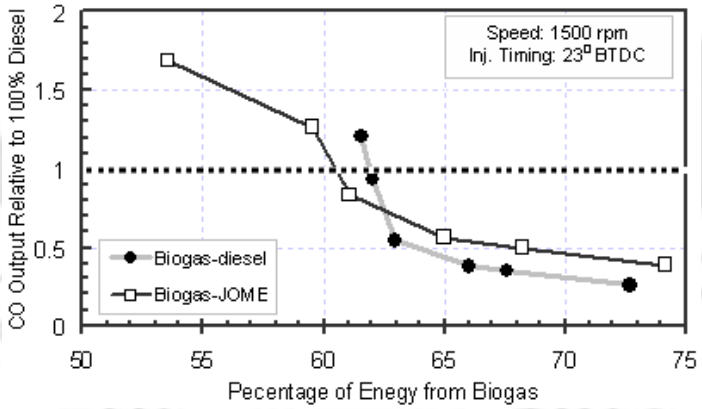

Figure 8.2 Comparison of CO emissions of biogas operations relative to diesel mode

8.3 CDM Analysis of Syngas Dual Fuel Operations

Syngas contains two energy carrier gases in its fuel composition, hydrogen (H_2) and carbon monoxide (CO). Hence, for syngas dual fuel mode CDM analysis purpose, the effects of cumulative increase in the carbon emissions, CO and CO_2, are weighed. From the syngas dual fuel operations, except 100% H_2 mode, it was found that both CO and CO_2 emissions were increased as compared to diesel mode for the entire load range (Fig. 6.18 and 6.19). However, when these total carbon concentrations were calculated based on ppm emissions

per kW hour, a key advantage of the dual fuel engine was achieved. Table 8.2 represents a sample of this calculation by taking H_2:CO::75:25 as an example. It may be recalled here that, similar to that of biogas, syngas and diesel also have different energy share during their dual fuel operations as shown in Fig. 8.3. When the load was increased during a dual fuel operation, the primary fuel share is increased due to the better combustion of the gaseous fuel. As the 100% H_2 syngas mode produced lower carbon emissions than the diesel mode, it obviously satisfies the CDM potential, and hence, the case is not taken into account. Figure 8.4 shows the cumulative CO and CO_2 emissions for each of the tested syngas mode as a function of the percentage of energy replaced. After 20% load, syngas modes having 75% and 50% H_2 content have shown relatively lower carbon emissions than the diesel mode. For these fuels, as the primary fuel for substitution, about 5 to 45% reduction of carbon emissions on ppm per kilowatt hour was achieved. However, the 100% CO syngas mode produced a higher total carbon emission levels than the diesel mode for the entire load range. This suggests that this dual fuel mode disqualifies its operation in a diesel engine from the CDM viewpoint. In overall, it can be concluded that the 100% H_2, 75% and 50% H_2 content syngas modes have achieved the required reduction of greenhouse gases and benefits the CDM.

Table 8.2: Sample calculation for CDM potential check of syngas operation (H_2:CO::75:25)

Load (%)	**Carbon emissions (ppm/ kW)**		**Energy share (%)**		**Carbon emissions from syngas (ppm/ kW)**	**Relative carbon emissions of syngas to diesel mode**
	Diesel	*Dual*	*Diesel*	*Dual*		
20	11402	22820	48.19	51.81	17325	1.52
80	10860	13580	39.43	60.57	9298	0.86

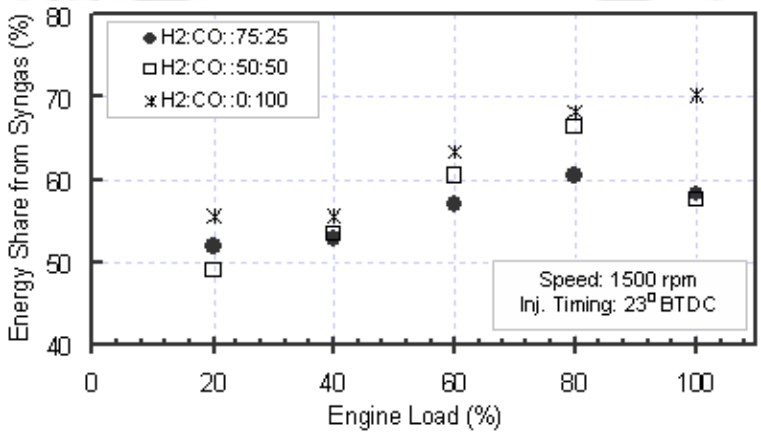

Figure 8.3 Comparison of syngas energy share during dual fuel operations

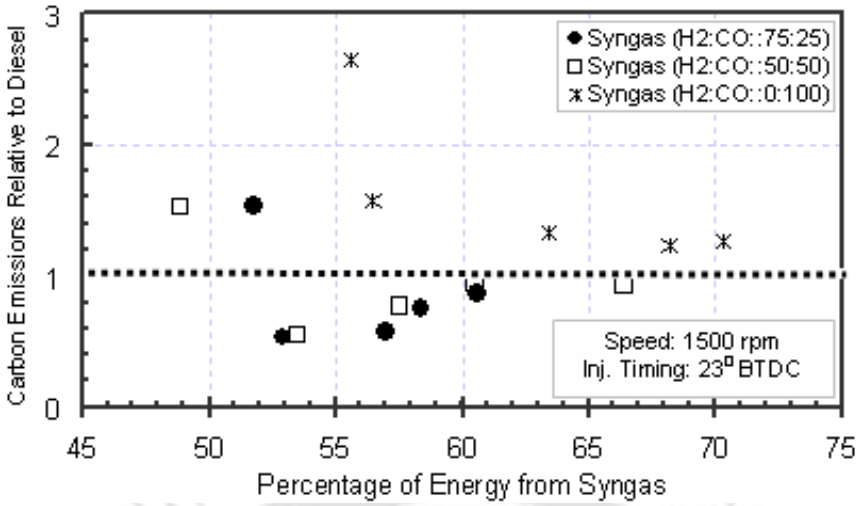

Figure 8.4 Comparison of carbon emissions of syngas operations relative to diesel mode

8.4 Summary

This chapter has investigated the CDM potential of two alternative gaseous fuels, biogas and syngas, for use in a CI diesel engine under dual fuel mode. The total carbon concentrations from the tested dual fuel modes were calculated based on ppm emissions per kW hour and compared relative to the diesel mode to check their potential towards CDM. Up to 20% engine load, the dual fuel operations showed about a 50% increase in carbon emissions relative to diesel mode. In overall, it can be concluded that, except 100% CO syngas mode, all the tested dual fuel operations clearly showed the benefits of reduced carbon emissions (an overall 5 to 60%) relative to the diesel mode. Therefore, to achieve the required reductions of greenhouse gases from diesel engines, the 'dual fuel' engine must be considered.

Adopting the dual fuel technology in an existing diesel engine and achieving CDM potential is a not a major problem because it requires almost no modifications. However, to achieve an equal performance of dual fuel mode with the diesel mode the diesel engine has to be designed according to the optimized injection timing, should incorporate some additional ignition devices mainly for the lower load application etc. For vehicular applications, the fuel storage problem can be avoided by storing the gaseous fuels like other gaseous fuels such as CNG, LPG etc. and its safety conditions are to be done strictly. Furthermore, fundamental problems associated with CDM projects need to be addressed.

Chapter – 9

CONCLUSIONS AND FUTURE SCOPE

Diesel engines are established as a unique combination of energy efficiency, power, reliability, and durability. They play a vital role in transport sectors, farm and construction purpose, power generation, etc. Because these engines adopt fossil diesel fuel-based technology, they contribute to GHG by producing CO and CO_2 emissions. In order to reduce these carbon emissions, there are possible and available clean diesel technologies viz., alternative fuels, hybrid-electric power and fuel cell etc. Use of clean gaseous fuel, alternative to diesel, is one of the techniques which have the potential for reducing GHG emissions. Aspiring to this technology, the present work examines two gaseous fuels, viz., biogas and syngas, in a CI diesel engine under dual fuel operation. Comprehensive literature review suggests that the engine operating and design parameters namely, load, speed, compression ratio, pilot fuel injection timing, pilot fuel mass, intake manifold conditions, and type of gaseous fuel, have effects on the performance, combustion, and emission characteristics of dual fuel diesel engines. As a first step, optimization of engine parameters such as, load, pilot quality and gaseous fuel type are performed in this study. Including this, dependence on petroleum fossil diesel is omitted completely by replacing a non-edible and low emissions bio-fuel, namely jatropha bio-diesel, as pilot ignition source. The whole experiments are conducted on a single-cylinder, four-stroke, constant-speed, and direct-injection CI diesel engine. To begin with, the base engine is slightly modified so as to allow it to operate under dual fuel mode for biogas and syngas operations. In this connection, a gas circuit to be added with the base diesel setup for dual fuel operations is developed and the necessary equipments are fabricated. The diesel engine is then run with 100% standard diesel as baseline tests for reference results. This diesel mode is operated for the entire load range (0 to 100% in steps of 20%), and the outcome of efficiency, combustion and emission characteristics are analyzed and discussed elaborately. At equal power output condition, both the dual fuel engine performances (biogas and syngas) are compared to that of baseline case. Additionally, to explore the energy losses whereabouts, the entire experimental results are analyzed thermodynamically and compared. Finally, the CDM potential of both dual fuel operations is analyzed and discussed. The principal contributions of the present work and further research range have also been highlighted.

9.1 Contribution of the Present Work

9.1.1 Biogas dual fuel operations

The principal contribution of the biogas operations is the revelation of greenhouse gas reductions from wastes. Carbon dioxide and methane emissions result when the wastes either burn or decompose in an oxygen-deprived environment. However, the anaerobic digestion process which generates biogas limits the CO_2 and CH_4 emission from wastes into the environment since the digestion takes place in a closed environment. During combustion of biogas in a diesel engine, the more powerful GHG methane converts itself into CO_2, and hence, it neutralizes its effect on global warming. Again, the GHG emissions from a diesel engine can be effectively reduced by consuming less fossil diesel oil for the combustion. Toward this, two types of biogas dual fuel investigations are carried out experimentally in a CI diesel engine at varying engine loads. The type of dual fuel mode is decided by the pilot ignition source, using either standard diesel or jatropha bio-diesel (JOME). A newly designed and fabricated gas carburetor with necessary measuring equipments is added to the inlet manifold of the base engine setup to work under dual fuel mode. In order to have a quality comparison of the diesel and dual fuel mode outcomes, the power outputs at corresponding tested loads are kept constant. To execute this, the constant diesel fuel supply control lever is redesigned to a variable one. Further, for the thermodynamic analysis of the experimental results, the energy and availability equations are applied to the diesel and dual fuel modes. The important CDM potentials of both biogas and syngas are also analyzed under dual fuel operations.

Experimental investigations on the performance of the biogas dual fuel operations have shown that:

- The experimental investigations of biogas-diesel mode ascertained a maximum diesel replacement of 69% during operation, whereas, biogas-JOME mode managed a maximum replacement level of 66% bio-diesel or 100% fossil diesel fuel.
- The dual fuel operations were benefited by consuming lesser friction power as compared to diesel mode. Specifically, the overall lubricity of bio-diesel over diesel fuel helped to consume lower friction power for its dual fuel operation. In overall, dual fuel operations are able to save friction power than that of diesel mode.
- The presence of CO_2 in the biogas reduced the burning velocity, and thereby, resulted incomplete combustion that increased the BSEC and exhaust gas temperature of dual

fuel modes. In addition, the heat release rate of dual fuel modes is lowered compared to the diesel mode. Including this, the longer pilot ignition delay and high self ignition temperature of biogas helped delaying the dual fuel combustion process more into the expansion stroke. All these factors lowered the peak pressure of dual fuel operation and thus, thermal efficiency reduced. Therefore, at best efficiency loading point, about 19 to 23 % reduction in thermal efficiency was found for dual fuel modes as compared to diesel mode. At this loading condition, this value was differed only a little in between the dual fuel modes. However, the reduction of maximum pressure rise rate under dual fuel modes retained the engine architecture safe.

Emission measurements of the biogas dual fuel operations have shown that:

- The dual fuel operations benefited the environment by reducing emissions of both CO (after 40% load) and NO_x (entire load range) levels. However, the CO_2 emissions from the biogas dual fuel operations are increased about 1 to 1.75 times to that of diesel mode for the entire load range. But, the increase in CO_2 emissions are negligible when compared to the release of CH_4 and CO_2 emissions from the decomposition or burning of wastes in an oxygen-deprived environment. So, no more CO_2 is being added to the atmosphere than was initially present.
- At 80% engine load, the best energy ratio of biogas is about 65% for both the dual fuel operations. When the biogas energy share is increased for an increase in engine output, the dual fuel mode produced higher HC levels are significantly as compared to the diesel mode.
- CDM potential calculation based on increase in CO emissions produced per kW hour, after 20% load, both combination of dual fuel modes have achieved the required reduction of greenhouse gases.

Analysis of the exergy terms for the biogas dual fuel operations by applying thermodynamic laws to experimental data showed that:

- The increase in load resulted an increase in exergy efficiency for all the tested fuel mode conditions. For the dual fuel operations, beyond 20% load, exergy efficiency was increased significantly due to improved combustion of biogas at high temperature zones. However, due to presence of about 42% CO_2 by volume in biogas, the

cumulative work output of the dual fuel modes have been lower, and hence, this resulted lower exergy efficiency for dual fuel modes.

- The maximum possible efficiencies of dual fuel modes can able to exceed the maximum efficiency of the base diesel engine. This can be achieved by accessing the cumulative exergy transfer with exhaust gas and cooling water for conversion to work exergy.
- Using bio-diesel in place of diesel as pilot source reduced the maximum exergy efficiency to only about 2%. This suggests that bio-diesel can substitute the fossil diesel efficiently as pilot ignition.
- It is noticed that dual fuel modes require higher fuel exergy (due to their poor combustion of fuel-air mixture and lower fuel energy content) for producing same amount of shaft output compared to its diesel mode counterparts.
- The exergy transfer with exhaust gases is found to be higher for dual fuel modes as compared to diesel mode. This is due to the higher exhaust gas temperatures generation from the poor dual fuel combustion process. On contrary, exergy transfers with cooling water for both the dual fuel modes are lower than diesel mode.

The dual fuel modes managed an effective diesel replacement level, whereas, biogas-JOME mode was able to save full fossil diesel oil utilization in a diesel engine. The dual fuel operations benefited the environment by reducing the concentrations of CO at medium and high loads and the levels NO_x emissions for the entire load range. The dual fuel modes consumed less friction power over diesel mode. The reduction of maximum pressure rise rate for the dual fuel modes retained the engine architecture safe. The results of thermodynamic analysis suggest that, due to a marginal difference in exergy efficiency, jatropha bio-diesel can be an effective substitute to the fossil diesel as pilot ignition source. The CDM analysis demonstrates that, except 100% CO syngas mode, all the tested dual fuel operations clearly have the benefits of reduced carbon emission relative to the diesel mode. In overall, this research shows that the 'dual fuel' engines can be considered to achieve the required reductions of greenhouse gases from diesel engines.

9.1.2 Syngas dual fuel operations

Both oil companies and automobile manufacturers claim "hydrogen" as future generation fuel. Hydrogen gas is a combustible fuel just like oil or natural gas, but it is ubiquitous, inexhaustible and clean. It can be made either by extracting it from a conventional hydrocarbon fuel, or by splitting water into its component elements: hydrogen and oxygen.

Carbon monoxide (CO), also called carbonous oxide is a major atmospheric pollutant, chiefly from the exhaust of IC engines (including vehicles, portable and back-up generators, lawn mowers, power washers, etc.), but also from improper burning of various other fuels (including wood, coal, charcoal, oil, paraffin, propane, natural gas, and trash). The gas-phase CO emission from ICE exhaust adsorbs, interacts with oxygen in the atmosphere, and finally desorbs as a CO_2 molecule. Emissions of CO_2 from IC engines are stoking the greenhouse effect faster than anything else. However, a research team at Sandia National Laboratories in Albuquerque, New Mexico, has shown in their experiments that the reactors can absorb green house gas CO_2 and turn it into CO. The IC engines are also capable of burning the CO gas as it is not contaminated. This was explored during World War II when CO was used to keep motor vehicles running in some parts of the world where gasoline was scarce. Carbon monoxide as an ICE fuel does not have the high energy content to substitute for hydrogen or methane in the present gas network. However, because the present use of these gases mostly used in industrial or electricity use, it can be used for homes or other non-industrial usage. A major industrial source of CO is producer gas, water gas and other similar synthetic gases.

The main contribution of this study is to introduce the new synthetic gaseous fuel, syngas, including the possible use of CO gas, an alternative diesel engine fuel. The effects of four different kinds of H_2:CO composition syngas fuels 100:0, 75:25, 50:50 and 0:100 were investigated experimentally under the dual fuel mode of operation. The gas circuit consists of a gas mixture and gas carburetor (the one used for biogas operation) with necessary equipments is developed, fabricated and added to the base diesel setup for dual fuel operations. The modified design of variable liquid fuel supply control lever is also used in this case. Similar to biogas analysis, experimental data of syngas dual fuel operations are investigated for thermodynamic analysis and CDM potential. The analysis of whole dual fuel mode results are compared to the reference results of diesel mode.

Experimental investigations on the performance of the syngas dual fuel operations have been summarized as follows;

- The study shows a maximum diesel replacement of above 72% for 100% H_2 syngas at 80% load. At same loading point, it was dropped to 61% and 59% with 75% and 50% H_2 syngas, modes respectively. More interestingly, using only CO as primary gaseous fuel, the maximum diesel replacement is found as 58.4% which is little lower than

that of 50% H_2 syngas case. But, this replacement occurred at 100% load due better combustion of CO gas at higher temperature conditions. This clearly indicates the suitability of CO gas as an alternative fuel in diesel engines.

- Due to shorter combustion duration and increased ignition delay of dual fuel operations, the attainment of peak pressure for dual fuel modes lags about 6 to 15°CA to that of diesel mode. Again, the heat release rate under dual fuel operation is reduced due to poor combustion. In addition, due to the presence of H_2 in syngas composition, there is an occurrence of negative heat release after the end of combustion. For the entire load range, these factors have led to the lower peak cylinder pressure and temperature, higher BSEC and lower thermal efficiency for dual fuel modes as compared to the diesel mode.
- At higher loads, the thermal efficiency of dual fuel modes raised with an increase in H_2% of syngas composition. At best efficiency loading, this value is enhanced by about 3, 17 and 26% when H_2 content in syngas is substituted by 50, 75 and 100% respectively, to 100% CO syngas composition. In overall, at 80% load, the dual fuel operations produced lower efficiency to an extent of about 6 to 27% as compared to diesel mode.

Following inferences can be made from extensive emission measurements of the syngas dual fuel operations.

- The emission analysis revealed that, except for 100% H_2 syngas mode, the NO_x emissions are found to be lower at the tested loads under dual fuel operations. The combustion of 100% H_2 syngas gives a faster and a clean combustion, and thus resulting in lowest CO and HC emissions with a different trend than other syngas modes for the entire range of power outputs. Whereas, 100% CO content syngas produced highest level of both CO and HC emissions among other gaseous fuels as compared to diesel mode.
- The CO emission levels, in general, are sensitive to fraction of CO% in syngas. There is a significant rise in CO and CO_2 emission levels for the CO content syngas fuel modes. However, these emissions are well within the regulated emission limits of USA – EPA non-road regulations.
- The CDM potential investigation disclosed that the 100%, 75% and 50% H_2 content syngas fuels have achieved the required reduction of greenhouse gases. With 100% CO syngas mode, it is unable to meet the CDM requirement as it produced higher

total carbon emission levels than the diesel mode. However, after 60% load, this mode emits only 20 to 30% higher GHG to diesel mode despite a huge amount of CO gas usage as fuel input. In addition, any power generating uses gas as fuel could be switched to CO gas mode without great problems. Therefore, during high load end use, considering the CO gas as an alternative fuel in diesel engines would conserve the other short-supplied gaseous fuels.

Analysis of the exergy terms for the syngas dual fuel operations by applying thermodynamic laws to experimental data have shown the following information.

- When load is increased, the amount of kW fuel input availability of engine increased throughout the tested load range.
- At higher loads, the syngas dual fuel modes are observed advantageous from the second law perspective. With increasing load, the destroyed availability decreased due to higher combustion temperature and pressure, and therefore, the exergy efficiency increased.
- The exergy efficiency of 100% H_2 syngas differs by an amount below 0.5% only to that of diesel mode at maximum efficiency point. This demonstrates that hydrogen is an effective gaseous fuel in a diesel engine under dual fuel operation. The maximum thermal efficiency of 100, 75, 50 and 0% H_2 content syngas dual fuel modes are found as 19.8, 18.3, 16.1 and 15.7% respectively. However, at this best efficiency loading point, the maximum exergy efficiencies are found as 38, 33.6, 27.2 and 25.2% for the same syngas modes respectively. These values are even higher than the maximum efficiency of the base diesel engine (21%). It can be achieved for the syngas dual fuel modes through accessing, mainly, about 8 to 17% of fuel input exhaust gas availability loss.

9.2 Application Potential

Diesel is the most efficient of all internal combustion power systems because of the superior engine efficiency and higher energy content of the fuel. Most of these diesel engines utilized in commercial trucks and buses, all farm and construction equipments, all freight locomotives, river barges and other marine work vessels. In addition, diesel engines also power electric generators used for distributed generation or as emergency back-up power

such as those used by hospitals. The results of present study outline the potential of dual fuel diesel engines in various applications are as follows:

- From the experimental and thermodynamic analyses it was noticed that dual fuel operations showed a comparative performance at medium and higher engine loads without any base diesel engine parameters modifications. Hence, the biogas and syngas dual fuel modes can be employed for stationary diesel engine applications like farm and construction use, power generation and back-up power production, and combined heat and power applications.
- Improving the part-load performance with suitable modifications in pilot injection timing and inlet manifold operating conditions, using gaseous fuels in high compressed cylinders like NG and LPG cases and establishing gas filling points etc., the dual fuel modes can be used for diesel mobile applications.
- Biogas is a readily available and affordable gaseous fuel for people around the world. For the cultivation and farming purpose, rural people mostly use small or low-power single-cylinder diesel engines. However, they encounter problems of liquid fuels shortage due to living in remote locations. The biogas-JOME mode diesel engine operation can fit best for this type of problems for the rural need.
- It is well known that the present gas network operated with methane or other gaseous fuels are used mainly for industrial and electricity purpose. There is a limited use of these fuels for the homes or other non-industrial usage. However, industrial and electrical generating uses can be switched from methane to biogas/ syngas dual fuel modes without great problems. This would reduce methane and other gaseous fuel supply which could be assured to continue for other applications like home heating.

9.3 Scope for Future Work

In this investigation, the independence to foreign petroleum diesel fuel is demonstrated by using two alternative gaseous fuels, biogas and syngas, in a compression-ignition diesel engine under dual fuel mode. Also, the important CDM potential of these fuels has been verified. Most of the important findings have been highlighted in the section 9.1. However, the shortcoming of dual fuel operations can be mastered by for further developments in this area. In this connection, some scope and suggestions for further studies are discussed here.

- Dual fuel mode showed poor thermal efficiency due to (mainly) less energy conversion during the operation. Thus, a waste exhaust gas heat recovery system can be added with the dual fuel engine operation. In this way, a dual fuel mode converts to a combined heat and production (CHP) mode (also called cogeneration) where the recovered heat may be used for the heating purpose. The dual fuel operations produced higher heat losses because the bowl-in combustion chamber which is originally meant for diesel operation with inherent swirl. Hence, the engine combustion chamber modifications can be looked upon to reduce the heat losses.
- At low loads, dual fuel operations revealed a maximum reduction in efficiency as compared to diesel mode. This is because of the poor combustion of high self ignition temperature bearer gaseous fuel under low temperature domain. Hence, a gas to gas heat exchanger may be incorporated in between exhaust gas muffler and inlet manifold where the required heat transfers to the sucked inlet air-gas mixture to provide the high temperature environment for an improved combustion of fuel-gas. In a different way to heat exchanger system, a spark plug or a glow plug may be merged with the inbuilt fuel injection system in which some extra ignition energy can assist the combustion of gaseous fuels.
- The biogas dual fuel modes reached their cycle peak pressure shifted by about 14^0 CA further towards expansion stroke than the diesel mode. While, the attainment peak pressures lag by about 6 to 8° CA for 100 and 75% H_2 content syngas modes, and about 10 to 15°CA for other modes as compared to diesel mode. This affects lower peak cylinder pressure and temperature, and hence, resulted poor performance of dual fuel operations. Therefore, the ignition timing of dual fuel modes should be adjusted as per the primary fuel-gas composition and fuel-gas mass share to derive maximum shaft output and efficiency for an equal energy input.
- The lower calorific value and the lower (less than one) product to reactant mole ratio for gaseous fuels contribute to de-rating of dual fuel engine output. in addition, the poor combustion of gaseous fuels under low temperature domain leads to poor thermal efficiency at part-loads. However, it might be possible to reduce the de-rating of dual fuel modes by working with even higher compression ratio (CR) to that with base diesel engine. The engine CR for dual fuel gas operation can be limited by presuming the knock occurred during the higher CR operation.

- During dual fuel combustion, a smaller amount of pilot fuel is surrounded by much more volume of air-gas mixture, and hence, ignition delay is increased for the pilot fuel and the dual fuel mode as well. Therefore, some ignition improvers like amyl nitrate and iso-propyl nitrate can added to the pilot diesel which has the effect of further lowering the self-ignition temperature of the fuel but more importantly reducing the lag time for ignition to commence once this temperature is reached. In another means, some oxygenated compounds such as, diethyl maleate, dibutyl maleate and diglyme can be blended with pilot fuel which enhances the oxygen concentration for a better combustion environment.
- For the biogas dual fuel modes, in particular, the presence of high volume of CO_2 in the fuel composition reduces the engine performance along-with higher emissions of CO, CO_2 and HC levels. An online technology like CO_2 sequestration from the pre-combustion biogas can be fit to this problem. In this method, the biogas may be passed through CO_2 absorbing elements like; 4A (pore size 4 angstroms (0.4nm)) molecular sieves, potassium hydroxide (KOH) solution or calcium hydroxide ($Ca(OH)_2$) solution before supplying to the gas carburetor for mixing with sucked air.
- The syngas used in this work is simulated by adding H_2 and CO from two individual high pressure gas cylinders. Still, using real syngas as primary fuel, the dual fuel operations may be tried in diesel engines for the comparison of its engine performance behavior to that of simulated syngas case. Again, during the dual fuel operations, the measurement and control of syngas was performed by flow meters of rotameter type. Although this was done very precisely and carefully, still there may be chances of H_2 leakage. Hence, mass flow controller may be used in place of rotameter for a better measurement and control of syngas, and accurate estimation of flow data.
- It has been seen that higher H_2 content dual fuel operations produce higher NO_x levels as compared to diesel mode. Reformed exhaust gas recirculation (REGR) is a technique in which of a catalytic fuel reformer is incorporated in the EGR loop to produce energy-rich gaseous fuels such as H_2, CO and CH_4 in addition to CO_2 gas. It can be achieved by reacting engine fuel with engine exhaust gas in the presence of solid catalyst. This type of dual fuel operation can improve the engine performance and fuel economy from energy-rich gases. In addition, there will be lower NO_x values due to feeding of CO_2 gas through REGR process.
- The most critical emissions from diesel engines are particulate matter and smoke. In this work, the measurements of these emissions could not be performed due to

unavailability of equipments. Therefore, these two all important emissions should be considered between diesel and dual fuel modes for a complete emission comparison.

- In this present experimental investigation, all the completed dual fuel operations performed well in short-term tests. However, the problems are anticipated when these engines operations are performed for long term commercial scale. These problems may include corrosion of engine components, carbon deposits on engine surfaces, engine lubrication, and excessive wear etc. Thus, before adopting usage of biogas and syngas in diesel engines under dual fuel mode as successful technology, long-term dual fuel tests of these fuels are essential.
- In order to promote the application of biogas and syngas as the alternative fuels for diesel engines, a comprehensive analysis of the economic assessment of their dual fuel operations is required from a social viewpoint. Therefore, a cost analysis of the dual fuel operations can be executed by considering various economic terms such as, the fuel cost per kW power production, environmental externalities and other costs. The performance and emissions study merged with the economic assessment can provide a perfect competitive characteristic of the dual fuel modes as the alternative fuels for diesel engines.

REFERENCES

Abu-Jrai, A., Tsolakis, A. and **Megaritis, A.** (2007) 'The Influence of H_2 and CO on Diesel Engine Combustion Characteristics, Exhaust Gas Emissions, and After Treatment Selective Catalytic NO_x Reduction'. *International Journal of Hydrogen Energy*, Vol. 32, No. 15, pp. 3565–3571

Abu-Jrai, A., Rodriguez-Fernandez, J., Tsolakis, A., Megaritis, A., Theinnoi, K., Cracknell, R.F. and Clark, R.H. (2009) 'Performance, Combustion and Emissions of a Diesel Engine Operated with Reformed EGR. Comparison of Diesel and GTL fuelling'. *Fuel*, Vol. 88, pp. 1031–1041

Abd Alla, G.H., Soliman, H.A., Badr, O.A. and **Abd Rabbo, M.F.** (1999) 'Effect of pilot fuel quantity on the performance of a dual fuel engine'. *SAE* Paper 1999-01-3597

Abd Alla, G.H., Soliman, H.A., Badr, O.A. and **Abd Rabbo, M.F.** (2000) 'Effect of pilot fuel quantity on the performance of a dual fuel engine'. *Energy Conversion and Management*, Vol. 41, No. 6, pp. 559–572

Abd Alla, G.H., Soliman, H.A., Badr, O.A. and **Abd Rabbo, M.F.** (2002) 'Effect of injection timing on the performance of a dual fuel engine'. *Energy Conversion and Management*, Vol. 43, No. 2, pp. 269–277

Agarwal, A.K. (2007) 'Biofuels (alcohols and biodiesel) applications as fuels for internal combustion engines'. *Progress in Energy and Combustion Science*, Vol. 33, pp. 233–271

Agarwal, A. and **Assanis, D.N.** (1998) 'Multidimensional modelling of natural gas ignition under compression ignition conditions using detailed chemistry'. *SAE* Paper 980136

Ajav, E.A., Singh, B. and **Bhattacharya, T.K.** (1998) 'Performance of a stationary diesel engine using vapourized ethanol as supplementary fuel'. *Biomass and Bioenergy*, Vol. 15, No. 6, pp. 493–502

Alkidas, A.C. (1988) 'The application of availability and energy balances to a diesel engine'. *ASME Journal of Engineering Gas Turbines and Power*, Vol. 110, pp. 462–469

Al-Najem, N.M. and **Diab, J.M.** (1992) 'Energy – exergy analysis of a diesel engine'. *Heat Recovery Systems and CHP*, Vol. 12, No. 6, pp. 525–529

Badr, O., Karim, G.A. and **Liu, B.** (1999) 'An examination of the fame spread limits in a dual fuel Engine'. *Applied Thermal Engineering*, Vol. 19, pp. 1071–1080

Banapurmath, N.R., Tewari, P.G. and **Hosmath, R.S.** (2008) 'Experimental investigations of a four-stroke single cylinder direct injection diesel engine operated on dual fuel mode with producer gas as inducted fuel and Honge oil and its methyl ester (HOME) as injected fuels'. *Renewable Energy*, Vol. 33; pp 2008–2018

Banapurmath, N.R., Tewari, P.G., Yaliwal, V.S., Kambalimath, S. and **Basavarajappa, Y.H.** (2009) 'Combustion characteristics of a 4-stroke CI engine operated on Honge oil, Neem and Rice Bran oils when directly injected and dual fuelled with producer gas induction'. *Renewable Energy*, Vol. 34, pp 1877–1884

Bari, S. (1996) 'Effect of carbon dioxide on the performance of biogas/diesel duel-fuel engine'. *Renewable Energy*, Vol. 9, No. (1–4), pp. 1007–1010

Bedoya, I.D., Amell, A.A. and **Cadavid, F.J.** (2009) 'Effects of mixing system and pilot fuel quality on diesel–biogas dual fuel engine performance'. *Bioresource Technology*, Vol. 100, pp. 6624–6629

Benson, R.S. and **Whitehouse, N.D.** (1973) *Internal Combustion Engines*, Oxford: Pergamon Press

Bhale, P.V., Despande, N.V. and **Thombre, S.B.** (2008) 'Simulation of wear characteristics of cylinder liner –ring combination with diesel and biodiesel'. *Society of Automotive Engineers*, Paper No. 2008-28-0107

Boehman, A.L. and **Le Corre, O.** (2008) 'Combustion of syngas in internal combustion engines'. *Combustion Science and Technology*, Vol. 180, pp. 1193–1206

Bruges, E.A. (1959) *Available Energy and the Second Law Analysis*, London: Butterworths Scientific Publications

Brzustowski, T.A. and **Golem, P.J.** (1976–77) 'Second law analysis of energy processes part I: Exergy – An introduction'. *Transactions of the Canadian Society for Mechanical Engineering*, Vol. 4, pp. 209–218

Calais, P. and **Sims, R**. (2000) 'A comparison of life-cycle emissions of liquid biofuels and gaseous fossil fuels in the transport sector'. *Proceedings of Solar 2000 Conference. From Fossils to Photons*. June 16-21, 2000. Brisbane

Caton, J.A. (2000a) 'On the destruction of availability (exergy) due to combustion process – with specific application to internal-combustion engines'. *Energy*, Vol. 25, pp. 1097–1117

Caton, J.A. (2000b) 'Operating characteristics of a spark-ignition engine using the second law of thermodynamics: Effects of speed and load'. *Society of Automotive Engineers,* Paper No. 2000-01-0952

Caton, J.A. (2007) 'The effects of compression ratio and expansion ratio on engine performance including the second law of thermodynamics: Results from a cycle simulation'. *Proceedings of the 2007 Fall Conference of the ASME Internal Combustion Engine Division*. October 14–17, 2007. Charleston, SC

Caton, J.A. (2008) 'Results from an engine cycle simulation of compression ratio and expansion ratio effects on engine performance'. *Journal of Engineering for Gas Turbines and Power*, Vol. 130, 052809 (7 pages)

Chavannavar, P.S. and **Caton, J.A.** (2006) 'Destruction of availability (exergy) due to combustion processes: a parametric study'. *Proceedings of the IMechE, Part A: Journal of Power and Energy*, Vol. 220, No. 7, pp. 655–668

Chigier, N. (1981) *Energy, Combustion, and Environment*. USA: McGraw Hill Company

Dunbar, W.R. and **Lior, N.** (1994) 'Sources of combustion irreversibility'. *Combustion Science and Technology*, Vol. 103, No. (1–6), pp. 41–61

Duc, P.M. and **Wattanavichien, K.** (2007) 'Study on biogas premixed charge diesel dual fuelled engine'. *Energy Conversion and Management*, Vol. 48, pp. 2286–2308

Emission Standards. Obtained through the Internet: http://www.dieselnet.com/standards/, [accessed 03/03/2008 at 15:40 hrs]

EPA (2007) 'A Wedge Analysis of the U.S. Transportation Sector. Environmental Protection Agency'. Accessed at http://www.epa.gov/otaq/climate/420r07007.pdf on November 18, 2007

Flynn, P.F., Hoag, K.L., Kamel, M.M. and **Primus, R.J.** (1984) 'A new perspective on diesel engine evaluation based on second law analysis'. *Society of Automotive Engineers,* Paper No. 840032

Fraser, R.A., Siebers, D.L. and **Edwards, C.F.** (1991) 'Autoignition of methane and natural gas in a simulated diesel environment'. *Society of Automotive Engineers,* Paper No. 910227

Garnier, C., Bilcan, A., Le Corre, O. and **Rahmouni, C.** (2005) 'Characterisation of a syngas-diesel fuelled CI engine'. *Society of Automotive Engineers,* Paper No. 2005-01-1731

Goldemberga, J. and **Coelhob, S.T.** (2004) 'Renewable energy-traditional biomass vs. modern biomass'. *Energy Policy*, Vol. 32, pp. 711–714

Henham, A. and **Makkar, M.K.** (1998) 'Combustion of simulated biogas in a dual-fuel diesel engine'. *Energy Conversion and Management*, Vol. 39, No. 16–18, pp. 2001–2009

Heywood, J.B. (1988) *Internal Combustion Engine Fundamentals*. New York; McGraw-Hill Book Company

Hill, P.G. and **Douville, B.** (2000) 'Analysis of combustion in diesel engines fueled by directly injected natural gas'. *ASME Journal of Engineering for Gas Turbines and Power*, Vol. 122, pp. 141–149

Hodgins, K.B., Hill, P.G., Ouellette, P. and **Hung, P.** (1996) 'Directly injected natural gas fuelling of diesel engines'. *Society of Automotive Engineers,* Paper No. 961671

Hosseinzadeh, A. and Khoshbakhi Saray, R. (2009) 'An availability analysis of dual-fuel engines at part loads: the effects of pilot fuel quantity on availability terms'. *Proceedings of the Institution of Mechanical Engineers, Part A: Journal of Power and Energy*, Vol. 223, No. 8, pp. 903–912

Hountalas, D.T. (1994) 'The effect of operating parameters on the net and gross heat release rates of a direct injection diesel engine'. *Proceeding of the Second Biennial ASME-ESDA International Conference on Design of Energy Systems*, 63 (3)

Hountalas, D.T. (2000) 'Available strategies for improving the efficiency of DI diesel engines - a theoretical investigation'. *Society of Automotive Engineers,* Paper No. 2000-01-1176

Hountalas, D.T. and **Papagiannakis, R.G.** (2000) 'Development of a simulation model for direct injection dual fuel diesel-natural gas engines'. *Society of Automotive Engineers,* Paper No. 2000-01-0286

Huang, J. and **Crookes, R.J.** (1998) 'Assessment of simulated biogas as a fuel for the spark ignition engine'. *Fuel*, Vol. 77, No. 15, pp. 1793–1801

Hyvarinen, J. (2000) *In defence of the Kyoto Protocol*. Institute for European Environmental Policy (IEEP), London

Imoto, K., Sugiyama, S. and **Fukuzawa, Y.** (1997) 'Reduction of combustion-induced noise in IDI diesel engine (1st report, target of cycle and low-noise combustion)'. *Transactions of Japan Society of Mechanical Engineers*, Part B, Vol. 63, No. 605, pp. 329–335

IPCC. (1996) 'Inter-Governmental Panel on Climate Change, Greenhouse Gas Inventory'. Reference Manual; Revised 1996 IPCC Guidelines for National Greenhouse Gas Inventories, Vol. 3 (Paris, France, 1997). Web site www.ipcc.ch/pub/guide.htm

Jiang, C., J, Liu, T., and **Zhong, J.** (1989) 'A study on compressed biogas and its application to the compression ignition dual-fuel engine'. *Biomass*, Vol. 20, pp. 53–59

Karim, G.A. (1980) 'A review of combustion processes in the dual fuel engine-the gas diesel engine'. *Progress in Energy and Combustion Science*, Vol. 6, No. 3, pp. 277–285

Karim, G.A. (1987) *The dual fuel engine*. In: Evans RL, editor. Automotive engine alternatives. New York: Plenum Press

Kline, S.J. and **McClintock, F.A.** (1953) 'Describing uncertainties in single-sample experiments'. *Mechanical Engineering*, Vol. 75, pp. 3–8

Kopac, M. and **Kokturk, L.** (2005) 'Determination of optimum speed of an internal combustion engine by exergy analysis'. *International Journal of Exergy*, Vol. 2, No. 1, pp. 40–54

Kouremenos, D.A., Rakopoulos, C.D. and **Hountalas, D.T.** (1997) 'Experimental investigation of the performance and exhaust emissions of a swirl chamber diesel engine using JP-8 aviation fuel'. *International Journal of Energy Research*, Vol. 21, No. 12, pp. 1173–1185

Kouremenos, D.A., Hountalas, D.T., and **Kouremenos, A.D.** (1999) 'Experimental investigation of the effect of fuel composition on the formation of pollutants in direct injection diesel engines'. *Society of Automotive Engineers,* Paper No. 1999-01-0527

Kotas, T.J. (1985) *The exergy method of thermal plant analysis*. London, UK: Butterworths

Krishnan, S.R., Srinivasan, K.K., Singh, S., Bell, S.R., Midkiff, K.C., Gong, W., Fiveland, S.B. and Willi, M. (2004) 'Strategies for reduced NOx emissions in pilot-ignited natural gas engines'. *ASME Journal of Engineering for Gas Turbines and Power*, Vol. 126, pp. 665–671

Kumar, M.S., Ramesh, A. and **Nagalingam, B.** (2001) 'Experimental Investigations on a Jatropha Oil Methanol Dual Fuel Engine'. *Society of Automotive Engineers*, Paper No. 2001-01-0153

Kumar, M.S., Ramesh, A and **Nagalingam, B.** (2003a) 'An experimental comparison of methods to use methanol and jatropha oil in a compression ignition engine'. *Biomass and Bioenergy*, Vol. 25, pp. 309–318

Kumar, M.S., Ramesh, A. and **Nagalingam, B**. (2003b) 'Use of hydrogen to enhance the performance of a vegetable oil fuelled compression ignition engine'. *International Journal of Hydrogen Energy*, Vol. 28, No. 10, pp. 1143–1154

Kumar, P.R., Srinivas, P.N., Nelson, J.E.B. and **Rao, S.S**. (2004) 'Experimental Studies on Energy Appropriation in a Single Cylinder Diesel Engine'. *Institution of Engineers (India) Journal-MC*, Vol. 85, July, pp. 45–49

Kumar, M.S., Ramesh, A. and **Nagalingam, B.** (2010) 'A comparison of the different methods of using jatropha oil as fuel in a compression ignition engine'. *ASME Journal of Engineering for Gas Turbines and Power*, Vol. 132, No. 3, 032801 (10 pages)

Kusaka, J., Okamoto, T., Daisho, Y., Kihara, R. and **Saito, T.** (2000) 'Combustion and exhaust gas emission characteristics of a diesel engine dual-fueled with natural gas'. *Society of Automotive Engineers of Japan Review*, Vol. 21, No. 4, pp. 489–496

Lapidus, A.I., Krylov, I.F. and **Tonkonogov, B.P.** (2005) 'Natural gas motor fuel'. *Chemistry and Technology of Fuels and Oils*, Vol. 41, No. 3, pp. 165–174

Lavoie, G.A., Heywood, J.B. and **Keck, J.C.** (1970) 'Experimental and theoretical study of nitric oxide formation in internal combustion engines'. *Combustion Science and Technology*, Vol. 1, pp. 313–326

Lekpradit, T., Tongorn, S., Nipattummakul, N. and **Kerdsuwan, S.** (2008) 'Study on advanced injection timing on a dual-fuel diesel engine with producer gas from a down-draft gasifier for power generaton'. *Journal of Metals, Materials and Minerals*, Vol. 18, No. 2, pp. 169–173

Li, H. and **Karim, G.A.** (2005) 'Exhaust emissions from an SI engine operating on gaseous fuel mixtures containing hydrogen'. *International Journal of Hydrogen Energy*, Vol. 30, pp. 1491–1499

Liu, Z. and **Karim, G.A.** (1995) 'Knock characteristics of dual-fuel engines fuelled with hydrogen fuel'. *International Journal of Hydrogen Energy*, Vol. 20, No. 11, pp. 919–924

Liu, Z. (1995) *An examination of the combustion characteristics of compression ignition engines fuelled with gaseous fuels*. Ph.D. thesis, Department of Mechanical Engineering, University of Calgary, Canada

Liu, Z. and **Karim, G.A.** (1997) 'Simulation of combustion processes in gas-fuelled diesel engines'. *Proceedings of Institution of Mechanical Engineers, Part A: Journal of Power and Energy*, Vol. 211, pp. 159–169

MacLean, H.L. and **Lave, L.B.** (2003) 'Evaluating automobile fuel/propulsion system technologies'. *Progress in Energy and Combustion Science*, Vol. 29, pp. 1–69

McKinley, T.L. and **Primus, R.J.** (1988) 'An assessment of turbocharging systems for diesel engines from first and second law perspectives'. *Society of Automotive Engineers,* Paper No. 880598

Mansour, C., Bounif, A., Aris, A. and **Gaillard, F.** (2001) 'Gas-diesel (dual-fuel) modelling in diesel engine environment'. *International Journal of Thermal Science*, Vol. 40, No. 4, pp. 409–424

Masjuki, H.H., Maleque, M.A., Kubo, A. and **Nonaka, T.** (1999) 'Palm oil and mineral oil based lubricants–their tribological and emission performance'. *Tribology International*, Vol. 32, pp. 305–314

Masood, M, Ishrat, M.M. and **Reddy, A.S.** (2007) 'Computational combustion and emission analysis of hydrogen–diesel blends with experimental verification'. *International Journal of Hydrogen Energy*, Vol. 32, pp. 2539–2547

Milton, B.E. (2001) *Thermodynamics, combustion and engines*. School of Mechanical Engineering and Manufacturing Engineering, UNSW, Australia

Mohammadi, A., Shioji, M., Ishiyama, T. and **Kitazaki, M.** (2006) 'Utilization of low-calorific gaseous fuel in a direct-injection diesel engine'. *ASME Journal of Engineering for Gas Turbines and Power*, Vol. 128, pp. 915–920

Moran, M.J. (1982) *Availability Analysis: A Guide to Efficient Energy Use*. Prentice Hall, New Jersey

Moffat, R.J. (1982) 'Contributions to the theory of single-sample uncertainty analysis'. *ASME Journal of Fluids Engineering*, Vol. 104, pp. 250–260

Naber, J.D., Siebers, D.L., Westbrook, C.K., Caton, J.A. and **di Julio, S.S.** (1994) 'Natural gas autoignition under diesel conditions: experiments and chemical kinetic modelling'. *Society of Automotive Engineers,* Paper No. 942034

Nakanishi, T., Shimoda, S., Yamasaki, N., Inokuchi, Y., Takemoto, T., Okazawa, H. and **Namba, M.** (2000) 'Numerical and experimental methods to investigate cooling air flow in the construction machinery's engine compartment'. *Society of Automotive Engineers*, Paper No. 2000-01-2577

Nielsen, O.B., Qvale, B. and **Sorenson, S.** (1987) 'Ignition delay in the dual fuel engine'. *Society of Automotive Engineers,* Paper No. 870589

Noguchi, N., Terao, H. and **Sakata, C.** (1996) 'Performance improvement by control of flow rates and diesel injection timing on dual-fuel engine with ethanol'. *Bioresource Technology*, Vol. 56, pp. 35–39

Nwafor, O.M.I. (2000a) 'Effect of advanced injection timing on the performance of natural gas in diesel engine'. *Sadhana*, Vol. 25, No. 1, pp. 11–20

Nwafor, O.M.I. (2000b) 'Effect of choice of pilot fuel on the performance of natural gas in diesel engines'. *Renewable Energy*, Vol. 21, pp. 495–504

Nwafor, O.M.I. (2002) 'Knock characteristics of dual-fuel combustion in diesel engines using natural gas as primary fuel'. *Sadhana*, Vol. 27, No. 3, pp. 375–382

Nwafor, O.M.I. (2007) 'Effect of advanced injection timing on emission characteristics of diesel engine running on natural gas'. *Renewable Energy*, Vol. 32, pp. 2361–2368

Nwafor, O.M.I. and **Rice, G.** (1994) 'Combustion characteristics and performance of natural gas in high speed indirect injection diesel engine'. *Renewable Energy*, Vol. 5, No. 5–8, pp. 841–848

Otera, J. (1993) 'Transesterification'. *Journal of Chemical Reviews*, Vol. 93, No. 4, pp. 1449–1470

Ozcan, H. (2010) 'Hydrogen enrichment effects on the second law analysis of a lean burn natural gas engine', *International Journal of Hydrogen Energy*, Vol. 35, pp. 1443–1452

Papagiannakis, R.G. and **Hountalas, D.T.** (2003) 'Experimental investigation concerning the effect of natural gas percentage on performance and emissions of a DI dual fuel diesel engine'. *Applied Thermal Engineering*, Vol. 23, pp. 353–365

Papagiannakis, R.G. and **Hountalas, D.T.** (2004) 'Combustion and exhaust emission characteristics of a dual fuel compression ignition engine operated with pilot diesel fuel and natural gas'. *Energy Conversion and Management*, Vol. 45, pp. 2971–2987

Parikh, P.P., Bhave, A.G., Kapse, D.V. and **Shashikantha.** (1989) 'Study of thermal and emission performance of small gasifier–dual-fuel engine systems'. *Biomass*, Vol. 19, 75–97

Park, S.S., Kim, Y.J. and **Kang, C.H.** (2002) 'Atmospheric polycyclic aromatic hydrocarbons in Seoul, Korea'. *Atmospheric Environment,* Vol. 36, pp. 2917–2924

Porpatham, E., Ramesh, A. and **Nagalingam, B.** (2007) 'Effect of hydrogen addition on the performance of a biogas fuelled spark ignition engine'. *International Journal of Hydrogen Energy*, Vol. 32, pp. 2057–2065

Porpatham, E., Ramesh, A. and **Nagalingam, B.** (2008) 'Investigation on the effect of concentration of methane in biogas when used as a fuel for a spark ignition engine'. *Fuel*, Vol. 87, pp. 1651–1659

Prakash, G. (2001) *Investigations on a biogas diesel dual fuel engine*. MS thesis. Internal Combustion Engines Laboratory, Indian Institute of Technology Madras, Chennai, India.

Primus, R.J. (1984) 'A second law approach to exhaust system optimization'. *Society of Automotive Engineers,* Paper No. 840033

Primus, R.J. and **Flynn, P.F.** (1985) 'Diagnosing the Real Performance Impact of Diesel Engine Design Parameter Variation (A Primer in the Use of Second Law Analysis)'. *International Symposium on Diagnostics and Modeling of Combustion in Reciprocating Engines*. Tokyo, Japan, pp. 529–538

Primus, R.J., Hoag, K.L., Flynn, P.F. and **Brands, M.C.** (1984) 'An appraisal of advanced engine concepts using second law analysis techniques'. *Society of Automotive Engineers,* Paper No. 841287

Pundir, B. P. (2010) *IC Engines Combustion and Emissions*. Narosa Publishing House Private Limited. New Delhi

Rakopoulos, C.D. and **Giakoumis, E.G.** (1997) 'Speed and load effects on the availability balances and irreversibilities production in a multi-cylinder turbocharged diesel engine'. *Applied Thermal Engineering*, Vol. 17, No. 3, pp. 299–313

Rakopoulos, C.D. and **Giakoumis, E.G.** (2006) 'Second-law analyses applied to internal combustion engines operation'. *Progress in Energy and Combustion Science*, Vol. 32, No. 1, pp. 2–47

Rakopoulos, C.D., Hountalas, D.T., Taklis, G.N. and **Tzanos, E.I.** (1995) 'Analysis of combustion and pollutants formation in a direct injection diesel engine using a multi-zone model'. *International Journal of Energy Research*, Vol. 19, No. 1, pp. 63–88

Rakopoulos, C.D. and **Kyritsis, D.C.** (2001) 'Comparative second-law analysis of internal combustion engine operation for methane, methanol and dodecane fuels'. *Energy*, Vol. 26, pp. 705–722

Rakopoulos, C.D. and **Kyritsis, D.C.** (2006) 'Hydrogen enrichment effects on the second-law analysis of natural and landfill gas in engine cylinders'. *International Journal of Hydrogen Energy*, Vol. 31, pp. 1384–1393

Rakopoulos, C.D. and **Michos, C.N.** (2008) 'Development and validation of a multi-zone combustion model for performance and nitric oxide formation in syngas fueled spark ignition engine'. *Energy Conversion and Management*, Vol. 49, pp. 2924–2238

Rakopoulos, C.D., Michos, C.N. and **Giakoumis, E.G.** (2008) 'Availability analysis of a syngas fueled spark ignition engine using a multi-zone combustion model'. *Energy*, Vol. 33, pp. 1378–1398

Ramadhas, A.S., Jayaraj, S. and **Muraleedharan, C.** (2006) 'Power generation using coir-pith and wood derived producer gas in diesel engines'. *Fuel Processing Technology*, Vol. 87, pp 849–853

Ramadhas, A.S., Jayaraj, S. and **Muraleedharan, C.** (2008) 'Dual fuel mode operation in diesel engines using renewable fuels: rubber seed oil and coir-pith producer gas'. *Renewable Energy*, Vol. 33, No. 9, 2077–2083

Roy, M.M., Tomita, E., Kawahara, N., Harada, Y. and **Sakane, A.** (2009) 'Performance and Emission Comparison of a Supercharged Dual Fuel Engine Fueled by Producer Gases with Varying Hydrogen Content'. *International Journal of Hydrogen Energy*, Vol. 34, pp. 7811–7822

Sahoo, P.K. and **Das, L.M.** (2009) 'Combustion analysis of jatropha, karanja and polanga based biodiesel as fuel in a diesel engine'. *Fuel*, Vol. 88, pp. 994–999

Sahoo, B.B., Sahoo, N. and **Saha, U.K.** (2009a) 'Effect of engine parameters and type of gaseous fuel on the performance of dual-fuel gas diesel engines–A critical review'. *Renewable and Sustainable Energy Reviews*, Vol. 13, pp. 1151–1184

Sahoo, B.B., Saha, U.K., Sahoo, N. and **Prusty, P.** (2009b) 'Analysis of throttle opening variation impact on a diesel engine performance using second law of thermodynamics'. *ASME Internal Combustion Engine Division 2009 Spring Technical Conference*. May 3–6, 2009. Milwaukee, Wisconsin, USA

Selim, M.Y.E. (2001) 'Pressure-time characteristics in diesel engine fuelled with natural gas'. *Renewable Energy*, Vol. 22, No. 4, pp. 473–489

Selim, M.Y.E. (2004) 'Sensitivity of dual fuel engine combustion and knocking limits to gaseous fuel composition'. *Energy Conversion and Management*, Vol. 45, No. 3, pp. 411–425

Selim, M.Y.E. (2005) 'Effect of engine parameters and gaseous fuel type on the cyclic variability of dual fuel engines'. *Fuel*, Vol. 84, No. 7-8, pp. 961–971

Selim, M.Y.E., Radwan, M.S. and **Saleh, H.E.** (2008) 'Improving the performance of dual fuel engines running on natural gas/ LPG by using pilot fuel derived from jojoba seeds'. *Renewable Energy*, Vol. 33, pp. 1173–1185

Shapiro, H.N. and **Kuehn, T.H.** (1980) 'Second law analysis of the Ames solid waste recovery systems'. *Energy*, Vol. 5, No. 8–9, August/ September, pp. 985–991

Sharma, Y. C. and **Singh, B.** (2008) 'Development of biodiesel from karanja, a tree found in rural India'. *Fuel*, Vol. 87, pp.1740–1742

Shudo, T. and **Takahashi, T. (2004)** 'Influence of reformed gas composition on HCCI combustion engine system fueled with DME and H_2-CO-CO_2 which are onboard-reformed from methanol utilizing engine exhaust heat'. *Transactions of Japan Society of Mechanical Engineering*, Part B, Vol. 70, No. 698, pp. 2663–2669

Shudo, T. (2006) 'An HCCI combustion engine system using on-board reformed gases of methanol with waste heat recovery: ignition control by hydrogen'. *International Journal of Vehicle Design*, Vol. 41, pp. 206–226

Singh, R.N., Singh, S.P. and **Pathak, B.S.** (2007a) 'Investigations on operation of CI engine using producer gas and rice bran oil in mixed fuel mode'. *Renewable Energy*, Vol. 32, No. 9, pp. 1565–1580

Singh, R.N., Singh, S.P. and **Pathak, B.S.** (2007b) 'Performance of renewable fuel based CI engine'. *Agricultural Engineering International: the CIGR E-journal*, Manuscript EE 0014, Vol. IX.

Spath, P.L. and **Dayton, D.C.** (2003) 'Preliminary Screening-Technical and Economic Assessment of Synthesis Gas to Fuels and Chemicals with Emphasis on the Potential for Biomass-Derived Syngas'. National Renewable Energy Laboratory (NREL), Report No. TP–510–34929

Sridhar, G., Paul, P.J. and **Mukunda, H.S.** (2001) 'Biomass derived producer gas as a reciprocating engine fuel–an experimental analysis'. *Biomass and Bioenergy*, Vol. 21, pp. 61–72

Sridhar, G. (2003) *Experimental and Modelling studies of producer gas based spark-ignited reciprocating engines*. Ph.D. thesis, Indian Institute of Science, Bangalore, India

Sridhar, G., Dasappa, S., Sridhar, H.V., Paul, P.G. and **Rajan, N.K.S.** (2005) 'Gaseous emissions using producer gas as fuel in reciprocating engine'. *Society of Automotive Engineers,* Paper No. 2005-01-1732

Sonntag, R.E. and **van Wylen, G.J.** (1991) *Introduction to thermodynamics*. Third edition, John Wiley & Sons

Stepanov, V.S. (1995) 'Chemical energies and exergies of fuels'. *Energy*, Vol. 20, No. 3, pp. 235–242

Stewart, J., Clarke, A. and **Chen, R.** (2007) 'An experimental study of the dual-fuel performance of a small compression ignition diesel engine operating with three gaseous fuels'. *Proceedings of Institute of Mechanical Engineers Part D: Journal of Automobile Engineering*, Vol. 221, pp. 943–956

Sudheesh, K. and **Mallikarjuna, J.M.** (2010) 'Diethyl ether as an ignition improver for biogas homogeneous charge compression ignition (HCCI) operation– an experimental investigation'. *Energy*, Vol. 35 (9), pp. 3614–3622

Swami Nathan, S., Mallikarjuna, J.M. and **Ramesh, A.** (2010) 'An experimental study of the biogas–diesel HCCI mode of engine operation'. *Energy Conversion and Management*, Vol. 51, pp. 1347–1353

Tat, M.E. (2003) Investigation of oxides of nitrogen emissions from biodiesel fueled engines. *PhD Thesis*. Iowa State University, Ames, IA

Thyagarajan, V. and **Babu, M.K.G.** (1985) 'A combustion model for a dual fuel direct injection diesel engine, Diagnostics and modelling of combustion in reciprocating engine'. *Proceedings of Comodia Symposium*, Tokyo; 607

Tippayawong, N., Promwungkwa, A. and **Rerkkriangkrai, P.** (2007) 'Long-term operation of a small biogas/diesel dual-fuel engine for on-farm electricity generation'. *Biosystems Engineering*, Vol. 98, No. 1, pp. 26–32

Tsolakis, A., Megaritis, A. Yap, D. and **Abu-Jrai, A.** (2005) 'Combustion Characteristics and Exhaust Gas Emissions of a Diesel Engine Supplied with Reformed EGR'. *Society of Automotive Engineers,* Paper No. 2005-01-2087

Uma, R., Kandpal, T.C. and **Kishore, V.V.N.** (2004) 'Emission characteristics of an electricity generation system in diesel alone and dual fuel modes'. *Biomass and Bioenergy*, Vol. 27, No. 2, pp. 195–203

UN Framework Convention on Climate Change Site. Obtained through the Internet: http://www.unfccc.de/, [accessed 23/12/2007 at 10:05 hrs]

VanGerpen, J.H. and **Shapiro, H.H.** (1990) 'Second law analysis of diesel engine combustion'. *ASME Journal for Engineering Gas Turbines and Power*, Vol. 112, pp. 129–137

von Mitzlaff, K. (1988) 'Engines for biogas'. A publication of Deutsches Zentrum fur Entwicklungstecknologien, GATE

Zhanghou, J. (1990) *Utilization and distribution of biogas*. (Memeograph), Tongi University, China

Appendix – A

Engine Performance Analysis Procedure

I. Efficiency Calculation:

(i) Brake power (*BP*): $$BP = \frac{2\times 3.142\times N\times W\times R}{60\times 1000}\ ,\ kW \quad \text{(A1)}$$

(ii) Brake mean effective pressure (*BMEP*):

$$BMEP = \frac{BP\times 60}{(\pi/4)\times D^2\times L\times(N/n)\times K\times 100}\ ,\ bar \quad \text{(A2)}$$

(iii) Indicated power (*IP*):

Work done per cycle per cylinder =

$$Area\ of\ P\text{-}V\ diagram \times X\ scale\ factor \times Y\ scale\ factor \times 100000,\ N\text{-}m$$

$$IP = \frac{Work\ done\ per\ cycle\ per\ cylinder \times(N/n)\times K}{60\times 1000}\ ,\ kW \quad \text{(A3)}$$

(iv) Indicated mean effective pressure (*IMEP*):

$$IMEP = \frac{IP\times 60}{(\pi/4)\times D^2\times L\times(N/n)\times K\times 100}\ ,\ bar \quad \text{(A4)}$$

(v) Frictional power (*FP*): $$FP = IP - BP\ ,\ kW \quad \text{(A5)}$$

(vi) Fuel flow (*F1*): $$F1 = \left(X\times 60\times \rho_{Lf}/10^6\right)\ ,\ kg/hr \quad \text{(A6)}$$

where, X is the cc liquid fuel consumption of engine in 1 min (cc/ min) and ρ_{Lf} is the liquid fuel density in kg/m^3.

(vii) Brake specific fuel consumption (*bsfc*): $$bsfc = F1/BP\ ,\ kg/BP\text{-}hr \quad \text{(A7)}$$

(viii) Brake thermal efficiency (η_{bth}):

For a case 100% diesel fuel operation, $$\eta_{bth} = \frac{BP\times 3600}{\dot{m}_d\times LHV_d}\times 100\ ,\ \% \quad \text{(A8)}$$

For a case of dual fuel operation, $$\eta_{bth} = \frac{BP}{\dot{m}_{pf}LHV_{pf} + \dot{m}_g LHV_g}\times 100\ ,\ \% \quad \text{(A9)}$$

where, $\dot{m}_{pf}$ (kg/s) and $\dot{m}_g$ (kg/s) are the pilot fuel and gas mass flow rate respectively, and LHV_{pf} (kJ/kg) and LHV_g (kJ/kg) are the pilot fuel and gas lower heating value respectively.

(ix) Indicated thermal efficiency (η_{ith}): $\eta_{ith} = \dfrac{IP \times 3600}{F1 \times C_v} \times 100\ ,\ \%$ (A10)

(x) Mechanical efficiency (η_{mech}): $\eta_{mech} = BP / IP \times 100\ ,\ \%$ (A11)

(xi) Air-fuel ratio (*A/F*):

Air flow, $F2 = C_d \times (\pi/4) \times d^2 \times \sqrt{\dfrac{2gh \times W_{den}}{A_{den}}} \times 3600 \times A_{den}\ ,\ kg/hr$

Volumetric efficiency, $\eta_{vol} = \dfrac{F2}{(\pi/4) \times D^2 \times L \times (N/n) \times 60 \times K \times A_{den}} \times 100\ ,\ \%$

$$A/F = \frac{Air\ flow}{Fuel\ flow} = \frac{F2}{F1} \quad \text{(A12)}$$

(xii) Brake specific energy consumption (*BSEC*):

It is defined as the fuel energy required (kJ/s) to produce unit kW shaft output.

$$BSEC = \frac{\sum (\dot{m}_{fuel} \times LHV_{fuel})}{BP}\ ,\ (kJ/s)_{fuel} / kW_{output} \quad \text{(A13)}$$

(xiii) Liquid fuel replacement rate (Z):

It determined by using the liquid fuel mass flow rate in liquid fuel mode $\dot{m}_{Lf}$ (kg/s) and pilot fuel mass flow rate in dual fuel mode $\dot{m}_{pf}$ (kg/s).

$$Z = \frac{\dot{m}_{Lf} - \dot{m}_{pf}}{\dot{m}_{Lf}} \times 100\ ,\ \% \quad \text{(A14)}$$

(xiv) Stoichiometric air-fuel ratio (λ):

A stoichiometric mixture has just enough air to completely burn the available fuel to CO_2 and H_2O. The relative amounts of oxygen enrichment and fuel dilution can be quantified by the stoichiometric mixture fraction.

For a typical hydrocarbon we have,

$$CH_n + \left(1 + \frac{n}{4}\right)\left(O_2 + \frac{79}{21}N_2\right) \rightarrow CO_2 + \frac{n}{2}H_2O + \left(1 + \frac{n}{4}\right)N_2 \quad \text{(A15)}$$

A hydrocarbon fuel leads to stoichiometric air-fuel ratio,

$$\lambda = \left\{(32 + 3.76 \times 28)\left(1 + \frac{n}{4}\right)\right\} / (12 + n)$$

The diesel used in this work have chemical formula as $C_{12}H_{26}$ i.e., $n = 2.167$

Hence, for diesel fuel, $\lambda = 14.92$

(xv) Energy Density (MJ/m^3):

The energy density or energy content in the engine cylinder determines the power developed in that cylinder. It depends upon the calorific value of fuel used and the stoichiometric air requirement for its combustion. Taking diesel as fuel in a diesel engine, the calculation of its energy density is obtained as indicated below.

Stoichiometric A/F for diesel = 14.92

With an excess air factor of 20%, the airflow per unit weight of the diesel = 17.9 kg.

Density of air = 1.2 kg/m^3, and density of diesel = 850 kg/m^3

Total volume in cylinder = volume occupied by air + fuel =

$$(17.9/1.2)+(1/850)=14.92\ m^3$$

Lower calorific value of diesel = 42 MJ/kg

Hence, the energy density of cylinder for diesel fuel at the nominal rating of the engine mixture = $(42/14.92)=2.82\ MJ/m^3$

II. Combustion Analysis:

(a) Heat Release Analysis:

The apparent net heat-release rate was calculated by making a first law analysis of the average pressure versus crank angle variation using the equation given below:

$$\frac{dQ_n}{dt}=\left(\frac{\gamma}{\gamma-1}\times P\times\frac{dV}{dt}\right)+\left(\frac{1}{\gamma-1}\times V\times\frac{dP}{dt}\right) \quad \text{(A16)}$$

where Q_n is the apparent net heat-release rate, γ the ratio of specific heats, V the instantaneous volume of the cylinder, P the cylinder pressure. An appropriate range of γ for diesel heat-release analysis is 1.3 to 1.35 (Heywood, 1988; Pundir, 2010).

(b) Ignition Delay Period (θ_R):

Ignition delay (θ_R) is defined as the crank angle difference between start of liquid fuel injection into the combustion chamber and the start of combustion, as follows:

$$\theta_R=\theta_{IGN}-\theta_{INJ}\ ,\ ^\circ CA \quad \text{(A17)}$$

where θ_{IGN} $(^\circ CA\ BTDC)$ is the crank angle at ignition and θ_{INJ} $(^\circ CA\ BTDC)$ is the crank angle at dynamic injection. The standard start of the pilot fuel injection was obtained from the manufacturer specifications, 23^0 BTDC. The start of combustion crank angle was determined from the $dP/d\theta$ diagram as it changes its concavity when combustion starts.

Nomenclature		
Observations		
F1	Fuel flow	kg/hr
F2	Air flow	kg/hr
W	Dynamometer load	Newton
N	Speed of the engine	rpm
System constants		
D	Engine cylinder diameter	meter
L	Engine stroke length	meter
K	Number of cylinders	---
n	Number of revolutions per cycle	1 for two stroke 2 for four stroke
R	Dynamometer lever arm for loading	meter
LHV	Lower heating value of fuel	kJ/kg
d	Orifice diameter (air flow)	meter
C_d	Coefficient of discharge	---
A_{den}	Air density	kg/m^3
W_{den}	Water density	kg/m^3
h	Manometer reading across orifice meter	meters of water

Appendix – B

Design and Dimensioning of Gas Carburetor

A 'gas carburetor' (also called gas mixer) is of a tube or flow channel type shape with separate inlets, one for air connects to air filter and other one for fuel-gas. The single air-gas mixture outlet is connected to engine intake manifold. The homogeneous mixture is then supplied to the engine combustion chamber for ignition through the injection of the pilot fuel in the usual way. In addition to low cost, this simple design gas carburetor is integrated into a normal diesel engine with little efforts. In this present work, the dimensions of a T-joint tube type gas carburetor are designed according to recommendations of von Mitzlaff (1988). The engine input design data required for this design and dimensioning are presented in Table B1.

Table B1: Engine input design data for the gas carburetor design

Maximum rated power (*P*), kW	5.2
Engine speed (*N*), rpm	1500
Bore (*D*), mm	87.5
Stroke (*L*), mm	110
Type of operation: 2-Stroke/ 4-Stroke	4-Stroke
Number of cylinders (*K*)	1
Volumetric efficiency (η_{vol}), %	90
Manifold connection diameter (d_{im}), mm	40
Substitution of diesel by biogas fuel (S), %	90
Air filter connection diameter, mm	40

Dimension of gas carburetor inlet = dimension of air filter (B1)

Dimension of gas carburetor outlet = dimension of inlet manifold (B2)

Dimension 1:

Distance between the gas inlet and the inlet to the engine manifold $\geq 2 \times d_{im}$ (B3)

Dimension 2: $V_{gc} = V_s = \left(\pi / 4 \times D^2 \times L \times K / 10^9\right)$, m^3 (B4)

Dimension 3: $A_{gc} = A_{im} = \left(\pi / 4 \times d^2{}_{im} / 10^6\right)\ ,\ m^2$ (B5)

Dimension 4: $L_{gc} = \left(V_{gc} / A_{gc}\right)\ ,\ m$ (B6)

The following assumption parameters serve for the dimensioning of the gas nozzle:

i. The active pressure difference between the gas nozzle before the carburetor and the airflow in the carburetor = 0.02 bar (20 cm water head).

ii. Velocity at gas nozzle, C_{gn} = 20 m/s

iii. Low volumetric calorific value of fuel gas, kJ/m^3

iv. Specific fuel consumption of the engine, $sfc = 0.8\ m^3 / kW \cdot h$

The following steps are followed to find out dimensions of gas nozzle:

Volumetric air intake,

$$V_{air} = \left(\eta_{vol} / 100\right) \times \left(V_s \times n / 60\right)\ ,\ m^3 / s \quad \begin{matrix} n = N\ (2\text{-}S\ engine) \\ n = N/2\ (4\text{-}S\ engine) \end{matrix} \tag{B7}$$

Manifold intake velocity, $C_{im} = \left(V_{air} / A_{im}\right)\ ,\ m/s$

$$\text{i.e. } C_{in} = \left(\eta_{vol} / 100\right) \times \left(V_s \times n / 60\right) \times \left(1 / A_{im}\right)\ ,\ m/s \tag{B8}$$

Check: $C_{in} < C_{gn}$

Volume flow of gaseous fuel consumption at rated power,

$$f_c = \left(sfc \times P / 3600\right)\ ,\ m^3 / s \tag{B9}$$

For dual-fuel operation: $f_{cd} = \left(S \times f_c / 100\right)\ ,\ m^3 / s$ (B10)

Dimension 5: Cross-sectional area of nozzle, $A_{gn} = \left(f_{cd} / C_{gn}\right)\ ,\ m^2$

$$\text{i.e. } A_{gn} = \left(S / 100\right) \times \left(sfc \times P / 3600\right) \times \left(1 / C_{gn}\right)\ ,\ m^2 \tag{B11}$$

Dimension 6: Diameter of the nozzle, $d_{gn} = \sqrt{\left(4 \times A_{gn} / \pi\right)} \times 1000\ ,\ mm$ (B12)

A 10% over sizing of the gas nozzle diameter is allowable for all possible ranges of engine operation.

Dimension 7: Safer nozzle diameter, $\left(d_{gn}\right)_{safe} = 110\ \%\ d_{gn}\ ,\ mm$ (B13)

The shape of the nozzle and the way it is connected or introduced into the mixing device is important for a good mixture of air and gas. The method designed here is T-joint with the gas nozzle protruding into the gas carburetor (Figure B1). The gas nozzle is cut oblique (30^0–45^0) with the opening facing the engine inlet. The protruding gas nozzle slightly decreases the cross-sectional area for the airflow and causes a slight depression, thus increases the active pressure drop for the gas to flow into the carburetor. The pressure drop rises with engine suction (engine speed), and hence sucks more gas.

The dimensions found for designed gas carburetor for the diesel engine are as follows:

Diameter of gas carburetor inlet (air filter side) = 40 mm.

Diameter of gas carburetor outlet (inlet manifold side) = 40 mm.

Check: $C_{im} = 5.92,\ m/s\ <\ C_{gn}\left(20,\ m/s\right)$ - OK

To ensure complete mixing of air and fuel gas, the gas mixer valve is installed at a distance of ten pipe diameters (i.e. $10\ d_{im}$) upstream of the inlet manifold (Stewart *et al*., 2007).

Dimension 1: Distance between gas inlet and the inlet to the engine manifold = 400 mm

Dimension 2: $V_{gc} = 0.661\times10^{-3},\ m^3$

Dimension 3: $A_{gc} = 1.256\times10^{-3},\ m^2$

Dimension 4: $L_{gc} = 0\cdot55,\ m = 550,\ mm$

Dimension 5: $A_{gn} = 0.518\times10^{-4},\ m^2$

Dimension 6: $d_{gn} = 8.12,\ mm$

Dimension 7: $\left(d_{gn}\right)_{safe} = 8.93,\ mm \approx 10,\ mm$

The designed T-joint with the gas nozzle protruding into the gas carburetor as per the base engine input data is presented in Figure B1 with its complete dimensions. The carburetor is finally fabricated and added to the diesel engine for the conversion into dual fuel operation.

Notation			
A_{im}	Cross-sectional area of inlet manifold, m^2	A_{gn}	Cross-sectional area of nozzle, m^2
A_{gc}	Cross-sectional area of gas carburetor, m^2	C_{im}	Manifold intake velocity
C_{gn}	Velocity at gas nozzle, m/s	d_{im}	Inlet manifold diameter, mm
d_{gn}	Diameter of fuel-gas nozzle, mm	L_{gc}	Length of the gas carburetor, m
n	Number of cycles per minute	V_{air}	Volumetric air intake, m^3/s
V_s	Cubic capacity of engine, m^3	V_{gc}	Volume of gas carburetor, m^3
Nomenclature			
Subscripts			
im	Inlet Manifold	*gn*	Gas Nozzle
gc	Gas Carburetor		

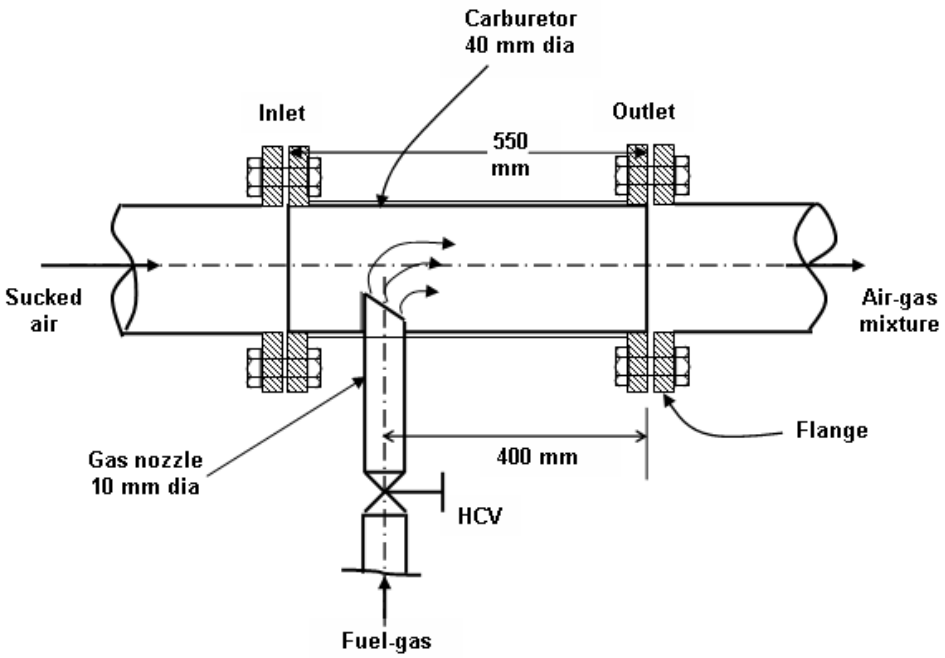

Figure B1: T-joint with the gas nozzle protruding type gas carburetor with designed dimensions

Appendix – C

Measurement Uncertainty Analysis

The uncertainty (also called, error) in measurement of various quantities and propagation of these errors are discussed in this section. A more precise method of estimating uncertainty in experimental results has been presented by Kline and McClintok (1953). The method is based on a careful specification of the uncertainties in the various primary experimental measurements. These are systematic errors which are dependent on the resolution of the measuring device. Consider an experimental result, N, is a given function of the independent variables $x_1, x_2, x_3, \cdots, x_n$. Thus,

$$N = N\left(x_1, x_2, x_3, \cdots, x_n\right) \tag{C1}$$

Let, ΔN be the uncertainty in the result and $\Delta N_1, \Delta N_2, \Delta N_3, \cdots, \Delta N_n$ be the uncertainties in the independent variables. If the uncertainties in the independent variables are all given with the same odds, then the uncertainty in the result having these odds is given as,

$$\Delta N = \left[\left(\frac{\partial N}{\partial x_1}\Delta N_1\right)^2 + \left(\frac{\partial N}{\partial x_2}\Delta N_2\right)^2 + \cdots + \left(\frac{\partial N}{\partial x_n}\Delta N_n\right)^2\right]^{1/2} \tag{C2}$$

The estimated relative errors of each measured independent parameter for both diesel and dual fuel modes are summarized in Table D1. For each performance parameter the overall relative measurement error is established in Table D2. The overall measurement uncertainties of thermodynamic analysis parameters are given in Table D3. For some measurements error is obtained from the manual from the equipment and for others it is estimation.

A sample calculation is presented here for the uncertainty associated with the case-by-case measurement of brake thermal efficiency with diesel and dual fuel mode operations.

We know that, irrespective of fuel mode, brake power output from engine is given by,

$$BP = \frac{2\times 3.142\times N\times W\times R}{60\times 1000}\ ,\ kW$$

The independent variables accompanying measurement of BP are N and W, as R is a system constant.

For a case diesel mode operation, $\eta_{bth} = \frac{BP \times 3600}{\dot{m}_d \times LHV_d} \times 100$, %

Here, the independent variables are: $N, W, \dot{m}_d, LHV_d$

The error in measurement of $N, W, \dot{m}_d, LHV_d$ are $0.5\%, 0.5\%, 1\%, 1\%$ respectively.

The uncertainty in measurement of thermal efficiency of diesel mode is estimated to be

$$\Delta\eta_{bth} = \left(0.005^2 + 0.005^2 + 0.01^2 + 0.01^2\right) = 0.015 = 1.5\%$$

For a case of dual fuel mode operation, $\eta_{bth} = \frac{BP}{\dot{m}_{pf} LHV_{pf} + \dot{m}_g LHV_g} \times 100$, %

Here, the independent variables are: $N, W, \dot{m}_{pf}, LHV_{pf}, \dot{m}_g, LHV_g$

The error in measurement of $N, W, \dot{m}_{pf}, LHV_{pf}, \dot{m}_g, LHV_g$ are $0.5\%, 0.5\%, 1\%, 1\%, 2\%, 1\%$ respectively.

The uncertainty in measurement of thermal efficiency of dual fuel mode is estimated to be

$$\Delta\eta_{bth} = \left(0.005^2 + 0.005^2 + 0.01^2 + 0.01^2 + 0.02^2 + 0.01^2\right) = 0.027 = 2.7\%$$

Table C1: Relative errors of independent variables

Independent variable	Relative error
Engine speed	0.5 %
Engine load	0.5 %
Liquid fuel flow rate	1 %
Gas flow rate	2 %
Water flow rate	2 %
LHV of liquid fuel	1 %
LHV of gaseous fuel	1 %
Temperature	3^0 C
Cylinder pressure	2 %
Cylinder volume	0.1 %
Specific heat of exhaust gas	0.5 %
Ratio of specific heat	0.5 %
CO, CO_2, NO_x, HC emissions	5 %
Height of liquid in air column	0.5 %

Table C2: Overall measurement errors for performance parameters

Performance parameter	**Diesel mode error**	**Dual fuel mode error**
Brake power	0.7 %	0.7 %
BMEP	0.86 %	0.86 %
BSEC	1.5 %	1.5 %
Brake thermal efficiency	1.5 %	2.7 %
Volumetric efficiency	0.7 %	0.7 %
Air flow rate	0.5 %	0.5 %
Air-fuel ratio	1 %	2.3 %
Equivalence ratio	1.1 %	2.3 %
Liquid fuel substitution level	N/A	1.4 %
Net heat release rate	2 %	2 %
Ignition delay	0.1 %	0.1 %

Table C3: Overall measurement errors for thermodynamic parameters

Thermodynamic parameter	**Diesel mode error**	**Dual fuel mode error**
Heat input	1.1 %	2.3 %
Shaft output	0.7 %	0.7 %
Heat lost in cooling water	2.1 %	2.1 %
Heat lost in exhaust gas	1.3 %	2.4 %
Availability input	1.1 %	2.3 %
Shaft availability	0.7 %	0.7 %
Cooling water availability	2.1 %	2.1 %
Exhaust gas availability	1.3 %	2.4 %
Exergy efficiency	2.8 %	4 %

Appendix – D

Thermodynamic Analysis Calculation

I. Energy Analysis

The first law of thermodynamics states that energy is conserved in every device and process. Thus, energy may exist in many different forms and may be converted from one form to another within a thermodynamic system (Heywood, 1988). The energy input (Q_{in}) in any IC engine is contained in its fuel. This amount of input energy is then converted into other forms (Al-Najem and Diab, 1992). In a diesel engine, the input energy contained in the supplied diesel fuel is converted to the following forms (Sahoo *et al*., 2009b):

i. Useful brake output or shaft power (P_{shaft});
ii. Energy transferred to cooling water (Q_{cw});
iii. Energy transferred to the exhaust gases (Q_{eg});
iv. Uncounted losses $(Q_{uncounted})$ due to friction, radiation, heat transfer to surroundings, operating auxiliary equipment, etc.

The amount of each of these energies stated above evaluated on the basis of the first law of thermodynamics is now described. The input energy (Q_{in}) to the diesel engine is the amount of fuel energy content in the supplied diesel fuel and it is given by,

For a diesel mode, $$Q_{in} = \left[\left(\dot{m}_d / 3600\right) \times LHV_d\right],\ kW \qquad \text{(D1)}$$

For a dual fuel mode,

$$Q_{in} = \left[\left(\dot{m}_{Lf} / 3600\right) \times LHV_{Lf}\right] + \left[\left(\dot{m}_g / 3600\right) \times LHV_g\right],\ kW \qquad \text{(D2)}$$

The energy converted to shaft output, $P_{shaft} = Brake\ power\ output,\ kW$ (D3)

The heat loss from the engine block to the cooling water is given by,

$$Q_{cw} = \left[\left(\dot{m}_w / 3600\right) \times C_{pw} \times \left(T_2 - T_1\right)\right],\ kW \qquad \text{(D4)}$$

The energy wasted in form of exhaust gas losses is evaluated by,

$$Q_{eg} = \left[\left(\dot{m}_{eg} / 3600\right) \times C_{peg} \times \left(T_5 - T_6\right)\right],\ kW \qquad \text{(D5)}$$

The physical property of the exhaust gas (C_{peg}) is determined from the energy balance of exhaust gas calorimeter. The variation of C_{peg} with exhaust gas temperature is considered here for the more accurate analysis.

The amount of the uncounted losses is determined by performing an energy balance and is given by,

$$Q_{uncounted} = \left[Q_{in} - \left(P_{shaft} + Q_{cw} + Q_{eg} \right) \right], \; kW \tag{D6}$$

II. Availability Analysis

The second law analysis (also called, exergy or availability analysis) indicates various forms of energy that have different levels of ability to do useful mechanical work. This ability to perform useful mechanical work is defined as availability (Heywood, 1988). In an IC engine, the availability input (A_{in}) which contained in its chemical availability of fuel is converted into other exergy forms (Al-Najem and Diab, 1992). In a diesel engine, the input availability in diesel fuel is converted to the following forms (Sahoo *et al*., 2009b):

a) Useful brake output or shaft availability (A_{shaft});

b) Availability transferred to cooling water (A_{cw});

c) Availability transferred to the exhaust gases (A_{eg});

d) Uncounted availability destructions $(A_{destroyed})$ due to friction, radiation, heat transfer to surroundings, operating auxiliary equipment, etc.

The amount of each of these availability transfers evaluated on the basis of the second law of thermodynamics is now explained as cited by Flynn *et al.* (1984), Kotas (1985) and Stepanov (1995). Chemical exergy of fuel or input availability,

$$(A_{in})_{Diesel} = \left[1.0338 \times (\dot{m}_d / 3600) \times LHV_d \right], \; kW \tag{D7}$$

$$(A_{in})_{Dual} = \left[A_{pf} + A_g \right], \; kW \tag{D8}$$

where,

$$(A_{pf})_{Diesel} = \left[1.0338 \times (\dot{m}_{pf} / 3600) \times LHV_d \right], \; kW$$

$$(A_{pf})_{Bio\text{-}diesel} = \left[0.975 \times (\dot{m}_{pf} / 3600) \times HHV_{BD} \right], \; kW$$

and,

$$A_g = \left[0.985 \times \left(\dot{m}_g / 3600\right) \times LHV_g\right],\ kW \quad \text{(For the only } H_2 \text{ content gaseous fuels)}$$

$$A_g = \left[0.95 \times \left(\dot{m}_g / 3600\right) \times HHV_g\right],\ kW \quad \text{(For complicated structure gaseous fuels)}$$

The availability associated with the shaft work,

$$A_{shaft} = Brake\ power\ output,\ kW \tag{D9}$$

The availability associated with the cooling water,

$$A_{cw} = Q_{cw} - \left[\left(\dot{m}_w / 3600\right) \times C_{pw} \times T_0 \times \ln\left(T_2 / T_1\right)\right],\ kW \tag{D10}$$

The availability associated with the exhaust gas is given by,

$$A_{eg} = Q_{eg} + \left[\left(\dot{m}_{eg} / 3600\right) \times T_0 \times \left(C_{peg} \ln\left\{T_0 / T_5\right\} - R_{eg} \ln\left\{P_0 / P_{eg}\right\}\right)\right],\ kW \tag{D11}$$

The physical property of the exhaust gas $\left(R_{eg}\right)$ is determined from the energy balance of exhaust gas calorimeter and products of a complete combustion of the diesel fuel.

The uncounted availability destruction is determined from the availability balance as,

$$A_{destroyed} = \left[A_{in} - \left(A_{shaft} + A_{cw} + A_{eg}\right)\right],\ kW \tag{D12}$$

The exergy efficiency $\left(\eta_{II}\right)$ is the ratio of total availability recovered from the system to the total availability input into the system. The recovered availability includes A_{shaft}, A_{eg} and A_{cw}.

$$\eta_{II} = \left(Availability\ recovered / Availability\ input\right) = 1 - \left(A_{destroyed} / A_{in}\right) \tag{D13}$$

Nomenclature

Abbreviations	
A	Availability, kW
HHV	Higher heating value, kJ/kg
LHV	Lower heating value, kJ/kg
Notations	
C_p	Specific heat, kJ/kg-K
$\dot{m}$	Mass flow rate, kg/hr
P_0	Ambient pressure, bar
P_{eg}	Exhaust gas pressure out from engine, bar
R_{eg}	Exhaust gas constant, kJ/kg-K
T_0	Ambient temperature, K
T_1	Cooling water inlet temperature to engine, K
T_2	Cooling water outlet temperature from engine, K
T_3	Calorimeter water inlet temperature, K
T_4	Calorimeter water outlet temperature, K
T_5	Exhaust gas temperature from engine, K (or) Calorimeter exhaust gas inlet temperature), K
T_6	Calorimeter exhaust gas outlet temperature, K
Symbols	
BD	Bio-diesel
d	Diesel
pf	Pilot fuel
g	Gaseous fuel
eg	Exhaust gas
w	Water
cw	Cooling water
in	Input
Lf	Liquid fuel

LIST OF PUBLICATIONS

Journals:

1. Sahoo BB, Sahoo N, and Saha UK, (2009), Effect of Engine Parameters and Type of Gaseous Fuel on the Performance of Dual Fuel Gas Diesel Engines - A Critical Review, ***Renewable and Sustainable Energy Reviews*****,** Vol. 13, pp. 1151-1184.

2. Sahoo BB, Saha UK, and Sahoo N (2011), Effect of Load Level on the Performance of a Dual Fuel Compression Ignition Engine Operating on Syngas Fuels With Varying H_2/CO Content, ***ASME Journal of Engineering for Gas Turbines and Power*** **(in press)**

3. Sahoo BB, Saha UK, and Sahoo N, (2011), Determination of Performance Limits for a Syngas–Diesel Fueled Compression Ignition Engine by Second Law Analysis, ***Energy*****,** Vol. 36, pp. 760–769.

Conferences:

4. Sahoo BB, Saha UK, Sahoo N, and Prusty P, (2009), Analysis of Throttle Opening Variation Impact on a Diesel Engine Performance Using Second–Law of Thermodynamics, ***ASME Internal Combustion Engine Division 2009 Spring Technical Conference***, May 3–6, 2009, Milwaukee, Wisconsin, USA.

5. Sahoo BB, Sahoo N, and Saha UK, (2010), Effect of H_2:CO Ratio in Syngas For a Dual Fuel Engine Operation, ***ASME-ATI-UIT Conference on Thermal and Environmental Issues in Energy Systems***, May 16–19, Sorrento, Italy, pp. 249 – 254.

6. Sahoo BB, Sahoo N, and Saha UK, (2010), Assessment of a Syngas Diesel Dual-Fuelled Compression Ignition Engine, ***ASME 4th International Conference on Energy Sustainability,*** May 17–22, Phoenix, Arizona, USA.

7. Debnath BK, Sahoo BB, Saha UK, and Sahoo N, (2010), Simulation of Combustion and Emission Characteristics in a Duel Fuelled Diesel Engine, ***ASME 2010 Internal Combustion Engine Division Fall Technical Conference***, September 12–15, San Antonio, Texas, USA.

8. Sahoo BB, Sahoo N, and Saha UK, (2010), Effect of Load Level on the Performance of a Biogas–Diesel Dual Fuel Compression Ignition Engine, ***National Seminar on Renewable Energy Technology: Issues and Prospects***, September 24–25, NERIST, Itanagar, India.

9. Sahoo BB, Sahoo N, and Saha UK, (2011), Dual Fuel Mode Performance Studies of a Small Diesel Engine Using Green Fuels, ***2nd International Conference on Mechanical, Industrial and Manufacturing Technologies***, February 26–28, Singapore.